When is it appropriate to take off the mask? Regulation of ß(1,3)-glucan exposure in *Candida albicans* and its impact on virulence.

A Dissertation Presented for the
Doctor of Philosophy
Degree
The University of Tennessee, Knoxville

Andrew S. Wagner
December 2022

Copyright © 2022 by Andrew S. Wagner
All rights reserved.

ACKNOWLEDGEMENTS

There are many people that have helped me get to this point in my graduate career, and I would like to take the time to highlight a few that I am especially grateful for their support. First and foremost, I would like to thank my advisor, Dr. Todd Reynolds. From an academic perspective, Dr. Reynolds has been a phenomenal mentor. His excitement for science and passion for mentoring has made my experience in graduate school enjoyable, even in the moments where my experiments or hypotheses had me frustrated to no end. I've grown tremendously as a scientist under his guidance and have thoroughly enjoyed the opportunity to learn from him. However, in addition to his contributions to my academic progression, Dr. Reynolds has served as an excellent role model for what a mentor should be. His humble attitude, sense of humor and ease with which he communicates in an open and comforting manner to all students and people he encounters is a regular reminder of how to truly lead. I'm grateful to have met such a kind and caring person, and am extremely fortunate that he also happened to be my boss!

In addition to my advisor, I would like to thank my doctorate committee (Drs. Liz Fozo, Tim Sparer and Francisco Barrera) for all the help that they have given me over the years. I have encountered numerous obstacles, like all scientists, during my time in graduate school, and their feedback has been invaluable in helping me get to where I am now. I would also like to give a special thanks to Dr. Fozo, who has always been there to help discuss ideas, problems, and successes that I've had over the years. She has also done an excellent job of keeping me focused and grounded, and for that I am thankful.

I have been fortunate in making many friends during my time in graduate school that both helped me succeed academically, and that have kept me sane when things in the lab were not going well. For starters, I would like to thank my current and former lab mates (Eric Gann, Bob Tams, Kyle Bonifer, Tian Chen, Jordan Cannon, Elise Phillips, Stephen Lumsdaine, Aeric Zhou, Mikayla Mangrum, Ainsley King, Jemma Mcleish and Wes Goltry) for all their support both inside and outside of the lab. Each of you challenge me daily to think through my work and help trouble shoot ideas, and are always willing to get a beer when the time calls. I would also like to give a special thanks to Trevor Hancock,

Bridget O’Banion, Rachel Johnston and Bikash Bogati. Each of these individuals were foundational support systems for me to get outside perspectives on my science, but were excellent friends as well. Furthermore, I would like to thank all my friends of from jiu jitsu that provided an escape from work and science when I needed it.

Finally, I would like to thank my entire support system back in Ohio. First, my family has always been there for me when I wanted to burn down science or was just homesick. You all constantly support me, while also keeping my head from getting too big. I wouldn’t have made it through the last 5+ years without them, and I’m thankful and lucky that I have such an amazing family that I can always count on. I would also like to thank Drs. Paul Morris and George Bullerjahn at Bowling Green State University. It is because of them that I developed my passion for science, and I would likely not be here today if I had not gotten the opportunity to learn from them in undergrad.

ABSTRACT

Mucosal and nosocomial bloodstream infections by fungal pathogens are a recurring problem in public health. *Candida spp.*, including *C. albicans*, are the leading causes of fungal infections, and have an attributable mortality rate of up to 50% for bloodstream infections. Unfortunately, increasing drug resistance and cytotoxic side effects of some leading antifungals has put a strain on disease control strategies. Thus, the identification of novel drug targets is needed. One attractive class of targets for adjunctive drug development are proteins that impact the ability of fungi to evade the host immune system. One way that *C. albicans* evades immune detection is by masking the immunogenic cell wall epitope ß[beta](1,3)-glucan under an outer layer of mannosylated glycoproteins. Accordingly, dysregulation of proteins important for ß(1,3)-glucan masking more readily exposes *C. albicans* to host pathogen recognition receptors and enhances fungal clearance. Yet, our understanding of the regulatory pathways that mediate ß(1,3)-glucan exposure (unmasking) and how the host immune system responds to this phenotype are poorly understood.

We have previously shown that hyperactivation of the Cek1 mitogen activated protein kinase (MAPK) pathway induces unmasking and attenuates virulence during systemic infection in mice. In this dissertation, we expand on these findings and show that virulence attenuation is host immune system dependent, and that neutrophils are key mediators in unmasked fungal cell clearance. Furthermore, we show that hyperactive Cek1 induces unmasking via the transcription factor Cph1, which then activates the calcineurin pathway to further increase ß-glucan exposure. Importantly, we find that calcineurin plays a more general role in mediating unmasking. In response to Cek1 hyperactivation or caspofungin treatment, calcineurin induces unmasking. However, in response to exogenous calcium, calcineurin reduces ß-glucan exposure. To elucidate the mechanism driving these changes, we show that two putative outer cell wall proteins within the calcineurin regulon (*FGR41* and *CWP419*) are important regulators of unmasking, and that calcineurin can further alter ß(1,3)-glucan exposure during caspofungin treatment by regulating chitin synthesis. Finally, we show that the impact of unmasking on disease progression is niche

specific, as both systemic and oral infections with unmasked fungal cells attenuates virulence, while vulvovaginal infection increases immunopathogenesis markers.

TABLE OF CONTENTS

CHAPTER 1 - INTRODUCTION 1
Abstract 2
Introduction 3
Immunogenic properties of the *C. albicans* cell wall. 4
ß*(1,3)-glucan*. 4
Mannosylated cell wall components 6
Chitin 7
Environmental signals that decrease *C. albicans* ß(1,3)-glucan exposure 8
Hypoxia-Induced Masking. 8
Lactate-Induced Masking 9
Iron Limitation-Induced Masking. 12
Environmental signals that increase *C. albicans* ß(1,3)-glucan exposure (unmasking). 12
Acidic pH. 13
Host Immune Response-Induced Unmasking 13
Drug-Induced Unmasking 14
MAPK pathways mediating ß(1,3)-glucan exposure. 16
The Cek1 MAPK Pathway. 17
The Mkc1 MAPK Pathway. 19
Relevance of ß-glucan exposure to pathogenesis and disease control. 20
Summary 22
References 24
CHAPTER 2 - ACTIVATION OF CPH1 CAUSES UNMASKING IN *CANDIDA ALBICANS* AND ATTENUATES VIRULENCE IN MICE IN A NEUTROPHIL-DEPENDENT MANNER 46
Abstract 47
Introduction 48
Results 50
Discussion 70

Materials and Methods 76
References 87
Appendix 97
CHAPTER 3 - CEK1 REGULATES ß(1,3)-GLUCAN EXPOSURE THROUGHT CALCINEURIN EFFECTORS IN *CANDIDA ALBICANS* 116
Abstract 117
Introduction 118
Results 120
Discussion 133
Materials and Methods 137
References 144
Appendix 156
CHAPTER 4 - CHITIN LEVELS IMPACT CASPOFUNGIN-INDUCED ß(1,3)-GLUCAN UNMASKING IN *CANDIDA ALBICANS* 175
Abstract 176
Introduction 177
Results 179
Discussion 194
Materials and Methods 196
References 200
Appendix 211
CHAPTER 5 - MUCOSAL INFECTION WITH UNMASKED *CANDIDA ALBICANS* CELLS IMPACTS DISEASE PROGRESSION IN A HOST NICHE SPECIFIC MANNER 222
Abstract 223
Introduction 224
Results 226
Discussion 235
Materials and Methods 238
References 243

Appendix 252
CHAPTER 6 - CONCLUSIONS AND FUTURE DIRECTIONS 256
Regulation of ß(1,3)-glucan exposure in *C. albicans*. 257
What are Cph1 effector proteins that mediate ß(1,3)-glucan unmasking? 257
How is signal transduction decision making achieved?. 258
What directs chitin synthesis and unmasking in response to caspofungin exposure?. 260
Host responses to infection with unmasked fungal cells. 262
What are the impacts that the various host PRRs have in response to infection?.. 262
W*hat are the roles of other myeloid derived immune cells?*. 264
What host responses are specific to ß(1,3)-glucan exposure? 265
References 267
VITA 274

LIST OF TABLES

S2.1 Table: Plasmids used in this study. 97
S2.2 Table: Primers used in this study. 99
S2.3 Table: Strains used in this study. 106
S3.1 Table: Plasmids used in this study. 156
S3.2 Table: Primers used in this study. 158
S3.3 Table: Strains used in this study. 164
S4.1 Table: Plasmids used in this study. 211
S4.2 Table: Primers used in this study. 213
S4.3 Table: Strains used in this study. 216
S5.1 Table: Strains used in this study. 252

LIST OF FIGURES

Fig 1.1: Wild-type and perturbed *Candida albicans* cell wall organization. 5
Fig 1.2: Signal transduction pathways within *Candida albicans* that regulate ß(1,3)-glucan exposure. 10
Fig 2.1: Systemic infection with a hyperactive Ste11$^{\Delta N467}$ mutant attenuates fungal colonization in multiple niches within a mouse host. 52
Fig 2.2: Virulence attenuation during systemic infection by the hyperactive Ste11$^{\Delta N467}$ mutant is host immune system dependent. 54
Fig 2.3: Hyperactive *STE11*$^{\Delta N467}$ expression induces changes in cell wall components of yeast, but not hyphal cells of *C. albicans*. 57
Fig 2.4: Disruption of downstream components in the Cek1 MAPK pathway blocks ß(1,3)-glucan unmasking by hyperactive *STE11*$^{\Delta N467}$ 60
Fig 2.5: *CPH1* deletion reduces *STE11*$^{\Delta N467}$ induced macrophage TNFα secretion and partially restores virulence during systemic infection in mice. 64
Fig 2.6: Cph1 mediates activation of its upstream MAPK, Cek1. 66
Fig 2.7: *DFI1* expression levels partially mediate ß(1,3)-glucan unmasking and macrophage TNFα secretion induced by hyperactive *STE11*$^{\Delta N467}$ expression. 68
Fig 2.8: Dfi1 does not mediates activation of the MAPK Cek1. 71
Fig 2.9: Proposed model for hyperactive *STE11*$^{\Delta N467}$ induced unmasking. 77
S2.1 Fig: Characterization of serum cytokines during systemic infection with a hyperactive *STE11* mutant. 109
S2.2 Fig: Representative Staining of Peripheral Blood during immunosuppression by cyclophosphamide. 110
S2.3 Fig: Representative scatter plots of leukocyte populations during 1A8 neutrophil depletion. 111
S2.4 Fig: Kidney fungal burden in 1A8 control mice treated with PBS and infected with 1x10^4 cells of the *STE11/P*$_{tet\text{-}off}$-*STE11*$^{\Delta N467}$ or wild-type strains. 112
S2.5 Fig: Gating strategy for yeast cell population of *C. albicans.* 113
S2.6 Fig: *CEK1* deletion in the CAI4 wild-type background does not induce unmasking. 114

S2.7 Fig: The *hst7*ΔΔ mutation blocks ß(1,3)-glucan unmasking by hyperactive *STE11*$^{\Delta N467}$. 115
Fig 3.1: Calcineurin mediates hyperactive Ste11$^{\Delta N467}$-induced and caspofungin-induced unmasking in *C. albicans.* 122
Fig 3.2: Crz1 mediates masking in response to exogenous calcium. 124
Fig 3.3: Proposed model for calcineurin-regulated ß(1,3)-glucan exposure. 126
Fig 3.4: Key cell wall proteins mediate ß(1,3)-glucan exposure in *C. albicans.* 128
Fig 3.5: *FGR41* overexpression and deletion modulates Ste11$^{\Delta N467}$-induced, but not caspofungin-induced, ß(1,3)-glucan unmasking. 130
Fig 3.6: Loss of *FGR41* attenuates virulence in a host immune system dependent manner. 132
S3.1 Fig: Gating strategy for yeast cell population of *C. albicans.* 166
S3.2 Fig: Loss of FGR41 induces changes in total chitin and mannan levels in C. albicans. 167
S3.3 Fig: Overexpression of calcineurin effector genes does not restore calcium-induced masking in a *crz1Δ/Δ* mutant. 168
S3.4 Fig: Loss of *FGR41* or *CWP419* does not attenuate fungal growth *in vitro*. 169
S3.5 Fig: Characterization of serum cytokines during systemic infection with an *fgr41Δ/Δ* mutant. 170
S3.6 Fig: *FGR41* overexpression does not impact fungal burden 4 days post infection. 171
S3.7 Fig: Loss of *FGR41* modestly delays hyphal development *in vitro*. 172
S3.8 Fig: Loss of *FGR41* or *CWP419* does not impact susceptibility to cell wall stressors. 173
S3.9 Fig: Cyclophosphamide treatment globally diminishes immune cells at early timepoints. 174
Fig 4.1: Areas of increased chitin co-localize with unmasked foci in response to caspofungin. 180
Fig 4.2: Calcineurin inhibition attenuates both unmasking and chitin synthesis in response to caspofungin exposure. 182

Fig 4.3: Chitin levels correlate with ß(1,3)-glucan exposure following caspofungin treatment in calcineurin-inhibited cells. 184
Fig 4.4: Loss of *MKC1* attenuates caspofungin-driven unmasking and chitin synthesis. 186
Fig 4.5: Calcineurin and Mkc1 work in parallel to mediate caspofungin-induced chitin synthesis and unmasking. 188
Fig 4.6: Calcineurin inhibition does not impact caspofungin-induced activation of Mkc1. 189
Fig 4.7: Caspfungin exposure increases Chs3 levels. 191
Fig 4.8: Chs3 levels correlate with total chitin content during caspofungin addition to calcineurin-inhibited cells. 192
S4.1 Fig: Gating strategy for single yeast cells. 218
S4.2 Fig: Calcineurin inhibition does not impact cell survival following caspofungin exposure. 219
S4.3 Fig: Propidium iodide staining does not correlate with chitin content following caspofungin exposure to calcineurin-inhibited cells. 220
S4.4 Fig: Caspofungin-induced unmasking requires drug-mediated inhibition of Fks1. 221
Fig 5.1: Oropharyngeal infection with an unmasked *STE11*$^{\Delta N467}$ mutant attenuates tongue fungal burden at 5 days post infection. 227
Fig 5.2: *STE11*$^{\Delta N467}$ oral isolates collected at 5 days post infection show wild-type levels of ß(1,3)-glucan exposure. 229
Fig 5.3: *STE11*$^{\Delta N467}$ oral isolates collected at 5 days post infection show reduced levels of Cek1 activation. 230
Fig 5.4: Virulence attenuation of the unmasked *STE11*$^{\Delta N467}$ mutant is more pronounced early into oropharyngeal infection. 232
Fig 5.5: Infection with an unmasked *STE11*$^{\Delta N467}$ mutant increases immunopathogenesis markers during a murine model of vulvovaginal candidiasis. 234
Fig 6.1: Cph1 and Ace2 regulate specific nodes within the Cek1 MAPK Pathway. 259

CHAPTER 1 - INTRODUCTION

This work was performed by: Andrew S. Wagner, Tian Chen and Todd B. Reynolds

Author Contributions: Conceptualization, ASW, TC and TBR; Writing–original draft preparation, ASW and TC (Both contributed equally and are co-first authors); Writing–review and editing, ASW, TC and TBR; Visualization, ASW and TC; Funding Acquisition, TBR.

This chapter has been published in Frontiers in Fungal Biology and was slightly modified for this dissertation:

- Chen T*, Wagner AS*, Reynolds TB. When Is It Appropriate to Take Off the Mask? Signaling Pathways That Regulate ß(1,3)-Glucan Exposure in Candida albicans. Frontiers in Fungal Biology. 2022;3. doi: 10.3389/ffunb.2022.842501.

*Denotes co-first authorship

Abstract

Candida spp. are an important source of systemic and mucosal infections in immune compromised populations. However, drug resistance or toxicity has put limits on the efficacy of current antifungals. The *C. albicans* cell wall is considered a good therapeutic target due to its roles in viability and fungal pathogenicity. One potential method for improving antifungal strategies could be to enhance the detection of fungal cell wall antigens by host immune cells. ß(1,3)-glucan, which is an important component of fungal cell walls, is a highly immunogenic epitope. Consequently, multiple host pattern recognition receptors, such as dectin-1, complement receptor 3 (CR3), and the ephrin type A receptor A (EphA2) are capable of recognizing exposed (unmasked) ß(1,3)-glucan moieties on the cell surface to initiate an anti-fungal immune response. However, ß(1,3)-glucan is normally covered (masked) by a layer of glycosylated proteins on the outer surface of the cell wall, hiding it from immune detection. In order to better understand possible mechanisms of unmasking ß(1,3)-glucan, we must develop a deeper comprehension of the pathways driving this phenotype. In this review, we describe the medical importance of ß(1,3)-glucan exposure in anti-fungal immunity, and highlight environmental stimuli and stressors encountered within the host that are capable of inducing changes in the levels of surface exposed ß(1,3)-glucan. Furthermore, particular focus is placed on how signal transduction cascades regulate changes in

ß(1,3)-glucan exposure, as understanding the role that these pathways have in mediating this phenotype will be critical for future therapeutic development.

Introduction

Candida species are the most common human fungal pathogens and are also ranked as the fourth most frequent cause of hospital-acquired bloodstream infections, with up to 40% mortality in epidemiological studies [1, 2]. *Candida* species colonize the human gastrointestinal tract and skin asymptomatically in many immunocompetent individuals. However, under certain conditions, *Candida* species can cause mucosal or systemic infections. Risk factors for each infection type vary, with risk factors for systemic infections including central venous catheter implants, major surgeries such as organ transplants, neutropenia, and cancer therapy [3-6]. Risk factors for oropharyngeal mucosal infections include dentures, premature birth, and HIV infection, while hormone replacement therapy and diabetes are associated with increased risk of acquiring vulvovaginal infections [7-9]. Current anti-fungal drugs for systemic *Candida* infections include three major classes - azoles, polyenes, and echinocandins, each of which target a specific aspect of the cell envelope (plasma membrane-cell wall complex) [10, 11]. However, a combination of drug toxicity, drug resistance and poor oral availability [12-14] have limited the efficacy of these options.

The majority of life-threatening fungal infections are opportunistic in nature, and a novel approach that may be necessary to complement current antifungals will be to simultaneously improve host immune efficacy. This can include cytokine therapy and other adjunctive therapeutic approaches [15, 16]. A related strategy to improve adjunctive therapy that specifically targets the fungi themselves is to make fungal cells more recognizable to the host immune effector cells. A better understanding of the interaction of *Candida* species with their cognate host receptors, particularly for how different cell wall components are recognized by their receptors on immune cells, will provide new insights that will facilitate such an approach, while also improving our understanding of the process of fungal pathogenesis.

The recognition of fungal pathogens is the first step in coordination of the host's response to fungal infections, and appears to play an important role in shaping fungal colonization of the host by commensal fungi like the *Candida spp*. [17-19]. Fungal cell wall composition and architecture are therefore critical in modulating the host immune response. Consequently, *Candida spp.* have developed strategies for sensing environmental signals encountered within the host in

order to regulate the exposure of immunogenic epitopes located within their cell wall. This review will summarize the various conditions leading to the modification of cell wall structure and epitope exposure in *C. albicans*, including the internal regulatory pathways that are responsible for sensing and inducing these changes, and will highlight their immune-modulatory significance.

Immunogenic properties of the *C. albicans* cell wall.

The *C. albicans* cell wall is a firm, but dynamic structure that is essential for fungal viability since it serves as a tough, but malleable barrier that sustains cell shape and prevents osmotic lysis [20, 21]. The cell wall of *C. albicans* is a layered structure, consisting of an outer mannan layer that covers a central layer of the core structural polysaccharides ß(1,3)-glucan and ß(1,6)-glucan, as well as a basal chitin layer (Fig. 1.1). The structural synthesis of the cell wall and each of its cognate components has been reviewed extensively and will not be discussed here [20, 22-25]. However, each individual component of the *C. albicans* cell wall has been shown to have immunomodulatory properties, and therefore highlights the significance of this structure in mediating host-pathogen interactions.

ß(1,3)-glucan

ß(1,3)-glucan accounts for ~40% of the total mass of the *C. albicans* cell wall [26], and has been found to induce a strong pro-inflammatory immune response upon recognition by host pattern recognition receptors (PRRs) such as dectin-1 [26-31], complement receptor 3 (CR3) [32, 33] and the ephrin type A receptor 2 (EphA2) [34, 35]. As a central component of the cell wall, and as a consequence of the pro-inflammatory nature of this epitope, ß(1,3)-glucan exposure (referred to as unmasking) is highly regulated to ensure successful host immune system evasion during infection. This is highlighted by virulence defects during systemic infection with mutants that have increased ß(1,3)-glucan unmasking, such as deletions in the phosphatidylserine synthase gene *CHO1* [36], the glycosyltransferase gene *KRE5* [37], the yeast cell wall protein *YWP1* [38] and the exo-1,3 and endo-1,3-glucanses *XOG1* and *ENG1*, respectively [38, 39]. Additionally, loss of host ß(1,3)-glucan PRRs has been shown to increase disease severity during both systemic infection (in dectin1$^{-/-}$ and CR3$^{-/-}$ mice) [33, 40, 41] and mucosal infections (in dectin1$^{-/-}$ and epha2$^{-/-}$ mice) [34, 35, 42, 43], further highlighting the importance of ß(1,3)-glucan recognition in disease control.

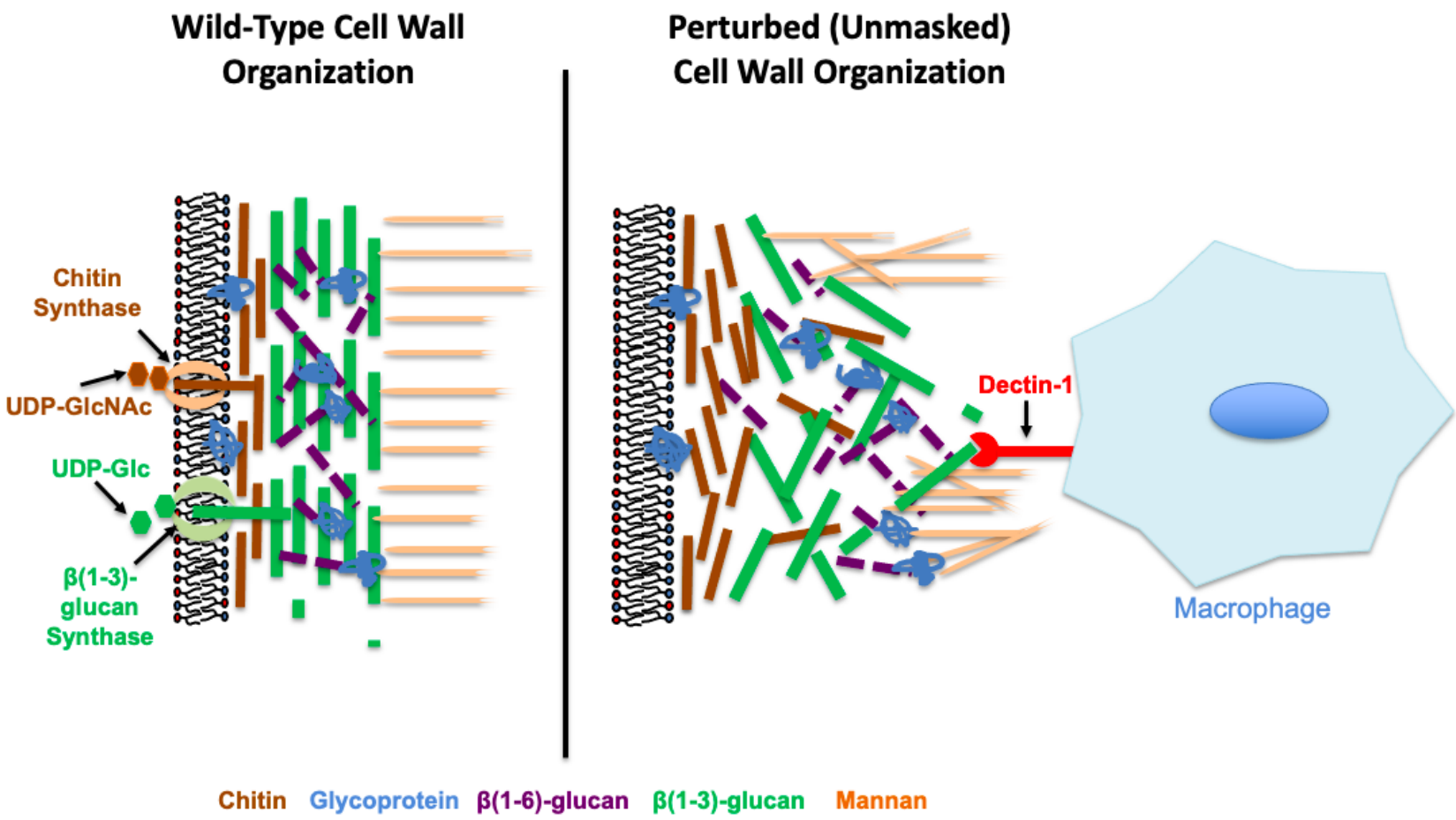


Fig 1.1: **Wild-type and perturbed *Candida albicans* cell wall organization.**

However, it is important to note that dectin-1 mediated clearance was found to be strain specific to *C. albicans* [44, 45], and appears to be impacted by basal chitin levels within the cell wall of different isolates. Therefore, cell wall architecture is an important mediator in facilitating the dectin-1 immune response.

Mannosylated cell wall components

The outer layer of the fungal cell wall is largely composed of heavily glycosylated proteins and lipids, and serves as the first interface between fungal cells and the host. Mannan is the most prevalent carbohydrate decorating these outer cell wall proteins, accounting for ~80-90% of all attached sugar moieties [46]. As a consequence of the high abundance of mannosylated cell wall structures and their exposure to the host environment, there are several PRRs capable of recognizing mannosylated residues decorating the outer cell wall. These include dectin-2 (α-mannan) [47, 48], dendritic cell-specific intracellular adhesion molecule-3-grabbing non-integrin (DC-SIGN) (*N*-mannan) [49], mannose receptor (MR) (*N*-mannan) [49, 50], galectin-3 (ß(1,2)-mannosides) [51-53], and the Toll-like receptors TLR4 (*O*-mannan) [50] and TLR2 (phospholipomannan) [54].

The impact that mannose-binding PRRs have on disease progression has been studied *in vitro* and *in vivo*, and each receptor has been shown to impact disease either directly or in combination with additional host PRRs. For example, dectin-$2^{-/-}$ mice systemically infected with *C. albicans* display reduced survival and increased fungal burden [48], and this phenotype is further exacerbated during systemic infection in dectin-1 and dectin-2 double knockout mice (dectin-$1^{-/-}$dectin-$2^{-/-}$) [41], suggesting a synergistic role for these receptors in mediating disease control. Similarly, galectin-$3^{-/-}$ mice are more susceptible to systemic infection with *C. albicans* and display higher levels of kidney fungal burden than immunocompetent wild-type mice [55]. This receptor is also required for full activation of TNFα expression when dectin-1 is activated by ß(1,3)-glucan *in vitro* [56], further highlighting the interactions between host PRRs. TLR2 receptors have also been shown to synergize with dectin-1 signaling in responses to zymosan (autoclaved yeast cells that expose ß(1,3)-glucan) by increasing pro-inflammatory cytokine production *in vitro*, in spite of the fact that TLR2 alone does not directly recognize zymosan nor activate immune responses sufficiently when stimulated by zymosan preparations [57]. However, *in vivo* studies on the impact that TLR2 has during systemic infection have been confounding in nature, with contradictory reports demonstrating increased survival during systemic infection with

C. albicans in TLR2$^{-/-}$ mice [58], while other reports have demonstrated reduced survival during systemic infection and increased dissemination during intraperitoneal infection in TLR2$^{-/-}$ mice [59, 60]. Systemic infection in TLR4$^{-/-}$ mice has also been shown to increase susceptibility to *C. albicans* in a strain specific manner, and is marked by increased fungal burden and impaired neutrophil recruitment in isolates recognized by TLR4 [61, 62]. Finally, intraperitoneal infection in MR$^{-/-}$ mice does not appear to impact survival rates when compared to infected wild-type mice [63]. Yet, loss of MR does have a role in regulating fungal burden, as increased fungal burden in the lungs and brain at 7 days post infection (d.p.i.) and in the spleen and lungs at 21 d.p.i. has been observed in MR$^{-/-}$ mice.

In addition to their ability to stimulate the immune system directly, mannosylated proteins in the outer cell wall have also been proposed to serve a protective role for *C. albicans* during infection by covering (masking) immunogenic ß(1,3)-glucan epitopes within the central layer of the cell wall. This is supported by the observation that mutations in genes of the *MNN2* α(1,2)-mannosyltransferase family, components of the *N*-glycosylation pathway, significantly reduce mannan levels in the outer cell wall, while also increasing the levels of exposed ß(1,3)-glucan [64]. Likewise, loss of glycosylphosphatidylinositol (GPI)-anchored proteins, a major constituent of the outer cell wall [20, 23], have also been shown to increase ß-glucan exposure. Genetic deletion of *GPI7*, an essential protein in GPI anchor synthesis, blocks the decoration of the second mannose in the glycan with phosphoethanolamine and subsequently unmasks ß(1,3)-glucan [65]. Additionally, chemical inhibition of GPI anchor synthesis with gepinacin, which inhibits the activity of a critical acyltransferase Gwt1, or with the 2-aminonicitinomide derivative 11g, increased ß(1,3)-glucan exposure in the cell wall and resulted in increased cytokine production from murine macrophages [66-69]. In the case of 11g treatment, this also corresponded with increased survival and reduced kidney fungal burden during systemic infection in mice [68].

Chitin

As the most basal component of the *C. albicans* cell wall, chitin represents ~10% of the total cell wall weight [23]. The direct role that chitin plays as an immunogen during *C. albicans* infection is still largely unknown. However, Wagener *et al.* have shown that purified chitin particles are capable of eliciting both a pro-inflammatory response (TNFα secretion) by murine macrophages exposed to high concentrations of purified chitin and an anti-inflammatory response (IL-10 secretion) at low concentrations, demonstrating a concentration dependent impact for chitin on

immune stimulation [70]. This anti-inflammatory response was also found to be dependent on the presence of the intracellular nucleotide binding oligomerization domain containing 2 (NOD2) and TLR9 receptors, implicating these host PRRs in the chitin induced IL-10 response. Furthermore, the extracellular receptor LYSMD3 on lung epithelia was recently reported to recognize chitin [71].

In addition to its ability to regulate immune system activation, chitin levels have also been indirectly associated with ß(1,3)-glucan exposure. Although it is usually considered to be more basal, large additions of chitin seem to cause substantial unmasking. This has been observed for regions damaged on hyphae by neutrophils, cell wall changes induced by caspofungin treatment, clinical isolates from symptomatic vulvovaginal candidiasis patients, and mutants like a hyperactive *STE11*$^{\Delta N467}$ mutant (a MAP3K of the Cek1 MAPK pathway) and a *cho1*Δ/Δ mutant [72-76]. This latter mutant is of particular interest, as the cell wall in the *cho1*Δ/Δ mutant is accompanied by a loss of the smooth outer structure of the cell and an increase in surface rigidity [77]. Thus, a model to explain this is that the chitin is deposited in such a way that it disrupts the architectural substructure of the cell wall, and cause significant exposure of ß(1,3)-glucan (Fig. 1.1).

Environmental signals that decrease *C. albicans* ß(1,3)-glucan exposure.

As a consequence of the immunogenic nature of fungal cell wall epitopes, fungal pathogens have developed mechanisms for immune avoidance that involve concealing (masking) ß(1,3)-glucan [23, 74, 78-80]. In *C. albicans*, ß(1,3)-glucan is buried underneath an outer layer of glycosylated proteins in the cell wall in a phenomenon referred to as masking [23, 74, 78]. The process of concealing ß(1,3)-glucan is largely impacted by exogenous signals encountered by fungal cells, and represents an adaptive feature deployed by *C. albicans* in response to the diverse niches that it may encounter.

Hypoxia-Induced Masking

Low oxygen abundance is a common stressor encountered by *C. albicans* in both its commensal and pathogenic states. As a commensal organism, hypoxia toleration must be achieved to permit colonization of the lower gastrointestinal tract [81, 82] and is regularly encountered once pathogenesis ensues in inflamed and necrotic tissue [83, 84]. Consequently, *C. albicans* induces robust changes in both its metabolism and cell wall organization/composition to adapt to hypoxic

conditions [85-87]. Pradhan *et al.* have observed that one such change induced by hypoxia is a reduction in the levels of exposed ß(1,3)-glucan moieties in the cell wall [88, 89]. This is accompanied by reduced phagocytosis of hypoxia exposed *C. albicans* cells by murine macrophages and decreased cytokine production (specifically IL-10 and CCL5) by human peripheral blood mononuclear cells (hPBMCs).

The mechanism driving hypoxia-induced masking was found to depend on proper mitochondrial functioning, as mutations in *C. albicans* genes that are important for mitochondrial respiration (*GOA1* and *UPC2*) and reactive oxygen species (ROS) processing (specifically by the alternative oxidase *AOX1* and the mitochondrial localized superoxide dismutase *SOD1*) impacted ß(1,3)-glucan masking [88]. Furthermore, the cAMP-Protein Kinase A (cAMP-PKA) pathway was also necessary to reduce ß(1,3)-glucan exposure. The cAMP-PKA pathway has been implicated in regulating yeast-to-hyphae and white-to-opaque morphogenic switching, as well as virulence of *C. albicans* [90-93]. The canonical pathway consists of two upstream GTPases (Ras1 and Ras2), an adenylyl cyclase (Cyr1) that is necessary for producing cAMP, and the downstream protein kinase A (PKA) that is composed of catalytic (Tpk1 and Tpk2) and regulatory (Bcy1) subunits that respond to cAMP production (Fig. 1.2) [94]. Within the cAMP-PKA pathway, deletions of *CYR1* or simultaneous deletions of both PKA catalytic subunits (*tpk1*Δ/Δ*tpk2*Δ/Δ) blocked masking caused by hypoxia exposure. The cAMP-PKA pathway was proposed to be regulated by proper ROS processing to hydrogen peroxide within the mitochondria, thus linking these processes together.

Lactate-Induced Masking

In addition to changes in oxygen levels within different niches of the host, the major carbon sources within different anatomical locations also vary. For example, glucose levels are high in the blood and relatively low in the lower gastrointestinal tract [95], where alternative carbon sources such as short chain fatty acids and lactic acid are more readily present [96, 97]. In order to adapt to these diverse conditions, *C. albicans* induces metabolic changes to better utilize the exogenous carbon sources in its immediate environment [98-100]. Carbon source availability has also been shown to

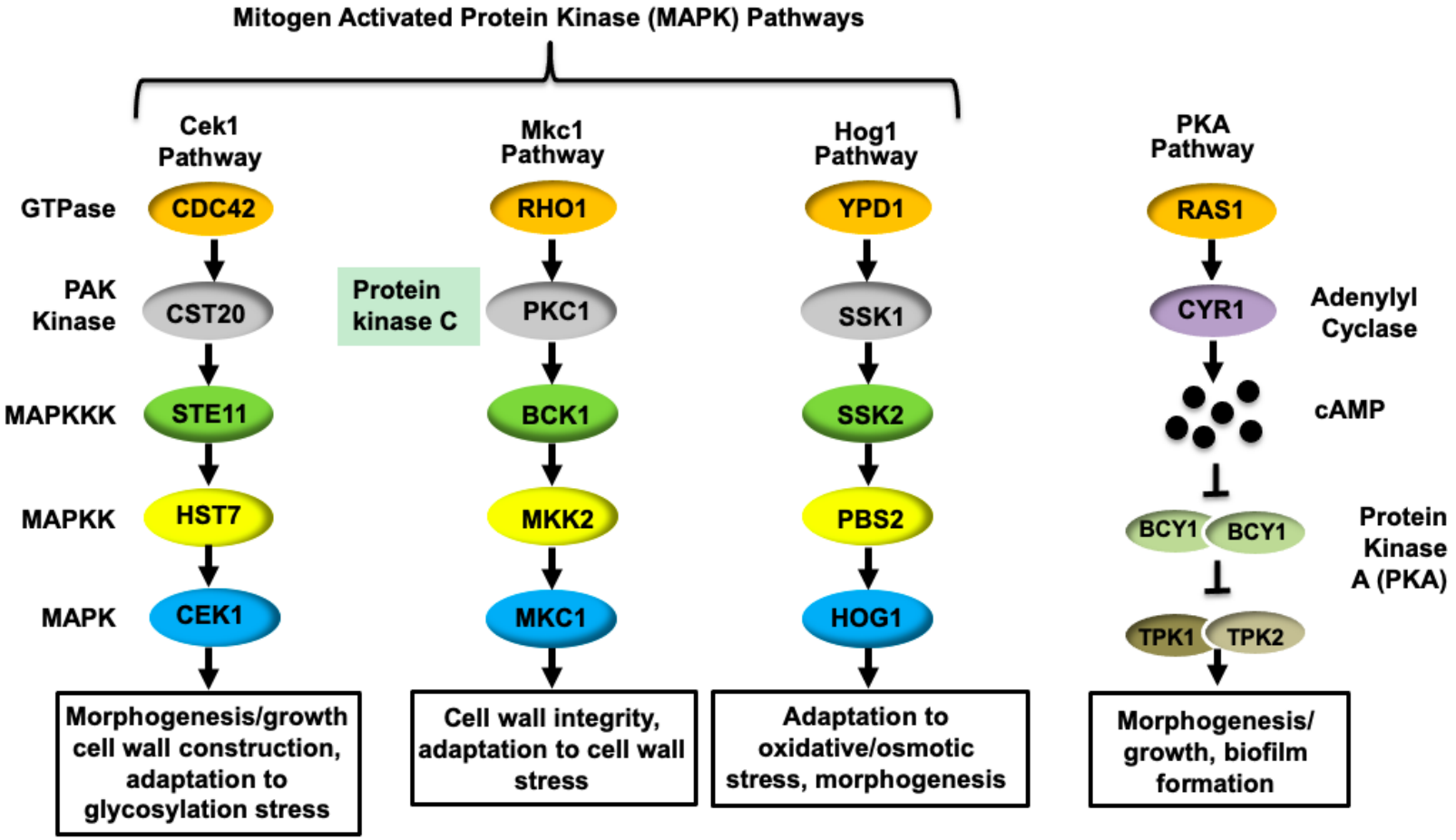


Fig 1.2: **Signal transduction pathways within *Candida albicans* that regulate ß(1,3)-glucan exposure.**

impact cell wall architecture and epitope exposure in a carbon-source dependent manner. Namely, exposure to L-lactate or glycerol have been found to induce ß(1,3)-glucan masking in *C. albicans* when compared to glucose grown cells (the most prominently used carbon source for *in vitro Candida* growth) [89, 101], while exposure to the short chain fatty acids acetate or butyrate inversely increased ß(1,3)-glucan unmasking [89]. With respect to L-lactate exposed cells, epitope masking correlated with decreased production of pro-inflammatory cytokines, including TNFα and MIP1, by murine macrophages *in vitro* as well as reduced phagocytosis [101, 102]. This further highlights the immunomodulatory impact that ß(1,3)-glucan exposure has on virulence-related phenotypes.

The mechanism driving L-lactate-induced masking has been explored, and two signal transduction pathways have been found to be essential in this response. Ballou *et al.* have shown that masking induced by L-lactate is mediated via a signal transduction pathway that requires the G-protein coupled receptor Gpr1 and the downstream transcription factor Crz1 [101]. Pradhan *et al.* then elaborated on this work and showed that the cAMP-PKA pathway is also needed to induce masking in response to lactate exposure, as deletions of both *CYR1* and *TPK1* both blocked ß(1,3)-glucan masking [89]. Gpr1 has also been shown to interact with the cAMP-PKA pathway to mediate hyphal formation [103, 104]. In response to L-lactate-driven masking, Gpr1 may serve as a receptor. The observation that the cAMP-PKA pathway is necessary for L-lactate-induced masking, as well as hypoxia-driven masking (see section above)[88], implicates this pathway as a conserved regulator for ß(1,3)-glucan masking. However, Crz1 is a well-known effector of calcineurin when stimulated by exogenous Ca^{2+} [105]. As deletion of the structural subunits of calcineurin did not impact L-lactate-induced masking [101], the observation that Crz1 mediates this phenotype represents a non-canonical pathway for Crz1 activation. Childers *et al.* reported that Crz1 and Gpr1 are both needed to induce expression of the exo-1,3-ß-glucanase Xog1 in response to L-lactate [39]. Xog1 cleaves exposed ß(1,3)-glucan moieties in the cell wall to cause masking, and thus represents an effector gene mediated by this pathway in response to lactate exposure. However, Crz1 regulation of this pathway may not be entirely direct, as it regulates expression of the transcription factor *ACE2* as well. *ACE2* is also

required for lactate-induced masking [101], but a direct role of Ace2 in regulating *XOG1* expression in response to $_{L}$lactate has not been assessed.

Iron Limitation-Induced Masking

Nutrient sequestration (in a process referred to as nutritional immunity) is an additional host stressor that *C. albicans* must overcome in order to successfully induce disease [106, 107]. One such stressor of nutritional immunity that is capable of inducing metabolic and architectural changes in the cell wall of *C. albicans* is a reduction of trace metals in the surrounding environment [108-110]. Pradhan *et al.* have reported that specific depletion of copper and iron were sufficient to induce changes in the cell wall of *C. albicans* and induce masking of immunogenic ß(1,3)-glucan moieties, while the loss of zinc and manganese inversely increase ß(1,3)-glucan exposure [89]. With respect to iron limitation, which induced the strongest change in ß(1,3)-glucan exposure levels of these metals, the observed masking was also associated with decreased phagocytosis by bone marrow derived macrophages (BMDMs) and reduced secretion of the pro-inflammatory cytokines TNFα, IL-6 and MIP-s1α by hPBMCs. Iron-induced masking was found to be regulated by two parallel signal transduction pathways, one that is again mediated by PKA and another that consists of the iron transceptor Ftr1 and the iron-responsive transcription factor Sfr1. However, it is important to note that iron-depletion-induced masking was not dependent on Cyr1, as was observed for hypoxia and $_{L}$-lactate induced masking. Thus, although PKA is involved in iron depletion-induced, hypoxia-induced, and lactate-induced masking, the mechanism by which it is activated in response to iron-reduction is non-canonical.

Environmental signals that increase *C. albicans* ß(1,3)-glucan exposure (unmasking).

In addition to host stimuli that induce masking of ß(1,3)-glucan, fungal pathogens also encounter stressors that alter the normal architecture of the cell wall to further increase immunogenic epitope exposure (Fig. 1.1). These changes come in multiple forms, and can be induced by both environmental signals sensed by *C. albicans*, or mechanical and physical perturbances encountered *in vivo* that impact cell wall integrity and synthesis.

Acidic pH

Changes in host pH levels vary drastically between the various niches that *C. albicans* can inhabit. This is apparent in the strongly acidic pH's encountered in the stomach and vaginal lumen (pH ~2 and 4-5, respectively), as opposed to the range of pH's (~4-7.4 in the gastrointestinal tract) in the lower gastrointestinal tract [111-113]. In response to alterations in environmental pH, Sherrington *et al.* have revealed that *C. albicans* adaptation to an acidic pH of 4.0 or below promotes cell wall remodeling, increases exposure of both chitin and ß(1,3)-glucan, and reduces thickness of the outer mannan layer [114]. These changes also correspond with enhanced immune recognition, leading to increased phagocytosis by macrophages and neutrophils and increased pro-inflammatory cytokine production (TNFα, IL-6, IL-1ß) by PBMCs.

The mechanism by which ß(1,3)-glucan exposure is induced by acidic pH remains to be fully defined, but chitin exposure was found to be regulated by the transcription factors Bcr1 and Rim101 and was dependent on the repression of the fungal chitinase Cht2 [114]. In this model, *CHT2* expression is promoted in alkaline environments by both Bcr1 and Rim101, but in acidic environments the Rim101 pathway is repressed and *CHT2* expression is decreased. This change is proposed to lead to longer chitin fibrils due to decreased microfibril processing by Cht2, thus impairing efficient remodeling of the inner cell wall layer and enhancing exposure of chitin at the cell surface. Interestingly, after about 2-4 hours at pH 4.0, glucan and chitin are remasked [115]. The process of ß-glucan remasking, but not remasking of chitin, can be blocked by treatment with the *C.albicans* quorum-sensing molecule farnesol, suggesting a role for the farnesol response pathway in mediating these changes. Moreover, loss of the transcription factor Efg1 reduced the levels of exposed chitin, but not of ß-glucan. Loss of *EFG1* was found to derepress *CHT2* expression at an acidic pH of 4, which was proposed to be the mechanism driving these changes.

Host Immune Response-Induced Unmasking

During infection, unmasking can occur in response to the host environment. Wheeler *et al.* described a time-course of ß(1,3)-glucan exposure during disseminated infection in mice by *C. albicans* [74]. The polymer is masked by the outer layer of

glycoproteins at the beginning of infection, with ~20% of fungal cells showing exposed ß(1,3)-glucan foci at 16 hours post-infection, and by 7 d.p.i. the percentage of cells showing unmasking increased to 80%. The exact mechanism by which unmasking occurs *in vivo* is not fully understood, but it has been observed that when *C. albicans* hyphae are exposed to neutrophils *in vitro*, that these immune cells damage the cell wall via neutrophil extracellular trap (NET) production and cause ß(1,3)-glucan unmasking [72]. Neutrophil-damage of hyphae results in cell wall remodeling, during which the outer layer of glycosylated proteins is damaged within seconds upon neutrophil attack, followed by chitin deposition 30 mins post-insult and then β-glucan unmasking. This process was found to depend on the mitogen activated protein kinase (MAPK) Hog1, as *hog1ΔΔ* hyphal cells failed to show unmasking upon NET exposure. Hog1 is a known regulator of morphogenesis, and has been extensively implicated in mediating stress responses to both osmotic and oxidative insults (Fig. 1.2) [116-118]. However, a *hog1ΔΔ* mutant does not exhibit any changes in ß(1,3)-glucan exposure during growth as yeast form cells in culture [119]. Thus, this study highlights a stimulus-dependent role for Hog1 in mediating unmasking, and it is possible that this relationship holds true for some other MAPKs of *C. albicans* as well. In addition to inducing ß(1,3)-glucan exposure, the Hog1-mediated NET response also increased production of chitin via the chitin synthase Chs3, the major chitin synthase of *C. albicans* [72, 120]. Although a causative role for chitin deposition in increasing ß(1,3)-glucan exposure has yet to be empirically demonstrated, the observation that chitin levels are increased following NET insult before ß(1,3)-glucan unmasking occurs further strengthens the correlative evidence that chitin plays a role in impacting ß-glucan epitope exposure.

Drug-induced Exposure

Three main classes of antifungals are currently used in the treatment of candidiasis [10, 11] and the impact that each of them has on immunogenic epitope exposure has been studied both *in vitro* and *in vivo*. Amongst all antifungals, the impact that the echinocandin caspofungin has on ß(1,3)-glucan exposure in *C. albicans* is the most well studied [74, 121, 122]. Wheeler *et al.* reported that sub-lethal dosages of caspofungin upset the intricate cell

wall structure of *C. albicans* and causes ß(1,3)-glucan exposure without killing the fungi *in vitro* [121]. This increased exposure in turn elicits more potent pro-inflammatory responses, including TNFα secretion, from macrophages through dectin-1 binding. Furthermore, caspofungin treatment in mice prior to systemic infection maintains the ability to induce unmasking of fungal cells, and therefore demonstrates that this phenotype is maintained *in vivo* [74]. Amphotericin B, a member of the polyene drug class, has also been shown to induce unmasking upon exposure *in vitro* [89], although the impact that amphotericin-induced unmasking has on immune stimulation is thus far understudied. Treatment with fluconazole, a member of the azole drug class, has been found to induce unmasking upon exposure to yeast cells *in vitro* [89]. However, unlike caspofungin, this phenotype did not translate *in vivo*, as fungal isolates from mice that had been previously treated with fluconazole prior to infection did not show a difference in ß-glucan exposure when compared to fungal cells from untreated mice [74]. Thus, more work is needed to better understand the role that fluconazole may play in eliciting ß-glucan exposure in a clinical setting.

In an attempt to better understand how caspofungin induces cell wall changes in *C. albicans*, Badrane *et al.* showed that rapid responses at the plasma membrane in components related to the actin cytoskeleton also occurred in addition to caspofungin-induced cell wall rearrangements [123]. This includes redistribution of both phosphatidylinositol-(4,5)-bisphosphate (PI (4,5) P_2), a signaling phospholipid, and septins, which serve as scaffolds for cytokinesis events [123]. PI (4,5) P_2 and septins are re-localized 5 minutes after exposure to caspofungin, which represents an early event in response to drug treatment, and further re-directs chitin and cell wall proteins to deposit at the site of co-localization [123]. This response might be important for membrane localized cell wall repair proteins like chitin synthases to fix the damage caused by ß(1,3)-glucan biosynthesis inhibition. In fact, chitin production increases in response to caspofungin treatment [73, 77, 123]. As increased chitin levels have been correlated with increased ß(1,3)-glucan unmasking (see above), the septins may play an upstream role in unmasking as well [72-77, 124].

MAPK pathways mediating ß(1,3)-glucan exposure.

It is well established that both canonical and non-canonical signaling pathways are responsible for inducing changes in the *C. albicans* cell wall in response to environmental stimuli, and that this in turn impacts the levels of ß(1,3)-glucan epitopes exposed to the host environment. In addition to stimulus-mediated activation of these pathways, direct interrogation of additional signal transduction pathways via genetic manipulation of their cognate components has also been found to mediate ß-glucan exposure. This is particularly apparent for genetic modifications within the mitogen activated protein kinase (MAPK) pathways of *C. albicans*, which have already been heavily implicated in a wide range of stimuli responses, including osmotic stress, oxidative stress, cell wall damage, α-factor pheromone signaling, and changes in glycosylation [72, 116, 125-129].

MAPK pathways are well-conserved signaling cascades in eukaryotes, and are composed of a conserved module of three kinases: a MAP kinase kinase kinase (MAP3K), a MAP kinase kinase (MAP2K) and a MAP kinase (MAPK) [130]. Activation of the MAP3K induces a phosphorelay system, in which it phosphorylates (activates) the MAP2K, which then phosphorylates and activates the MAPK to transmit signaling. Once phosphorylated, the MAPK activates, via phosphorylation, the appropriate transcription factor to respond to the initial stimulus. *C. albicans* possess three such MAPK pathways: the Cek1, Mkc1 and Hog1 MAPK pathways (Fig. 1.2). Information pertaining to the role of the Hog1 pathway in mediating ß-glucan unmasking has already been discussed (see "Host Immune Response-Induced Unmasking" above), but the impact that both the Cek1 and Mkc1 MAPK pathways have on regulating ß-glucan exposure in *C. albicans* will be elaborated below.

All three of these MAPKs are upregulated in response to caspofungin treatment [127, 131], and both the Cek1 and Mkc1 pathways are upregulated in the *cho1*ΔΔ mutant [132, 133]. Since unmasking occurs in both of these conditions, the Cek1 and Mkc1 pathways were analyzed to determine if either could drive unmasking by being activated alone. This revealed that the Cek1 pathway had a clear ability to cause unmasking when activated in the absence of other stimuli. This has been a useful tool to study unmasking as is simplifies the system and is less pleiotropic than more complex stimuli like stress or

the *cho1*ΔΔ mutation. We describe the reported roles of the Cek1 and Mkc1 pathways in unmasking below.

The Cek1 MAPK Pathway

The canonical Cek1 MAPK pathway consists of a core kinase cascade of Ste11-Hst7-Cek1/Cek2 (Fig. 1.2) that regulates the activation of the downstream transcription factors Cph1 and Ace2 [76, 129, 134-136]. This pathway is heavily involved in mediating cell wall organization, and has consequently been shown to play an active role in inducing morphogenic changes from yeast to hyphae (through Cph1) [134, 135], from white to opaque phase in mating-competent *C. albicans* strains (through Cph1) [129], mating signaling itself [137], and in responding to glycostructure damage in the cell wall (through Ace2) [127, 136, 138]. Due to the direct impact that the Cek1 MAPK pathway plays in regulating cell wall architecture, it is unsurprising that genetic alterations within the pathway also induce changes in immunogenic epitope exposure. The impact that deletion of *CEK1* itself has on unmasking has been the subject of conflicting reports, with some analyses showing increased unmasking upon deletion of *CEK1* [119, 126] and others showing no impact on epitope exposure [76]. However, it has been shown that expression of a single hyperactive allele of the MAP3K *STE11*, in which the N-terminal 467 amino acid autoinhibitory domain has been deleted (*STE11*$^{\Delta N467}$), causes hyperactivation of the downstream MAPK Cek1 and induces increased ß(1,3)-glucan unmasking, as well as increases in both total and exposed chitin levels within the cell wall [76, 132, 133]. Hyperactive *STE11*$^{\Delta N467}$ expression in turn enhances survival in mice and attenuates fungal colonization in the kidneys, spleen and brain [76, 132]. Importantly, immunosuppression via cyclophosphamide treatment was able to restore both survival rates and kidney fungal burden to near wild-type levels [76]. Thus, the observed virulence defect is largely host immune system driven, and attenuation is likely the consequence of the increased epitope exposure observed during hyperactive *STE11*$^{\Delta N467}$ expression *in vitro*.

Ste11$^{\Delta N467}$-induced unmasking was further found to be mediated through the downstream transcription Cph1, as deletion of *CPH1* in a hyperactive *STE11*$^{\Delta N467}$ mutant restored ß(1,3)-glucan and chitin exposure to wild-type levels. *CPH1* deletion was also

able to suppress the kidney fungal burden defect caused by the *STE11*$^{\Delta N467}$ allele in systemic infections [76]. Interestingly, *STE11*$^{\Delta N467}$ expression also induced activation of an unidentified parallel signaling pathway that is mediated through the putative cell wall sensor Dfi1. The Dfi1 protein is a 2 transmembrane protein that has been implicated in Cek1 activation and hyphal formation [139, 140]. Although deletion of *DFI1* in a *STE11*$^{\Delta N467}$ mutant background partially suppressed unmasking toward wild-type levels, it did not appear to impact the activation status of Cek1 itself, suggesting that Dfi1 signaling is transmitted elsewhere. Thus, similar to what has been observed for hypoxia-induced [88] and iron-induced [89] unmasking, multiple pathways appear to function in unison to elicit the full levels of ß(1,3)-glucan exposure observed during *STE11*$^{\Delta N467}$ expression. Although the mechanism driving unmasking in a *STE11*$^{\Delta N467}$ mutant is unknown, RNA sequencing revealed an enrichment in structural cell wall genes (such as GPI-anchored proteins) and those involved in cell wall synthesis and repair (such as chitin synthase, chitinase, transglucosylase, and ß-glucanase genes) [132], and it is likely that these changes work synergistically to increase ß(1,3)-glucan exposure during *STE11*$^{\Delta N467}$ expression.

Ace2, another transcription factor downstream of Cek1, has been shown to play an important role in sustaining cell wall structure in *C. albicans*. The *ace2*ΔΔ mutant displays severe ß(1,3)-glucan exposure, and transcripts induced by Ace2 upregulation are thought to be partially responsible for ß(1,3)-glucan masking induced by lactate treatment [101, 135, 141]. This may be due to the ability of Ace2 to control the degradation of ß(1,3)-glucan (possibly via Xog1), or it may be the consequence of Ace2 regulation of either mannan or chitin synthesis within the cell. The expression of another glucanase, the exo-1,3-ß-glucanase *ENG1*, has been implicated in regulating ß(1,3)-glucan exposure in yeast cells by directly degrading exposed ß(1,3)-glucan moieties in the outer cell wall [38]. Loss of *ENG1* induces strong unmasking during exponential growth of yeast cells *in vitro* [38]. *ENG1* has been shown to sit within the Ace2 regulon [142], and it may be possible that Ace2 regulates masking via this enzyme. However, Ace2-mediated changes in epitope exposure may be related to the role that Ace2 plays in controlling cell wall glycostructure [136]. Damage of *N*-glycans is sensed by the cell wall proteins Msb2 and Sho1, and results

in the activation of Cek1, which in turn activates cell wall repair activities mediated by Ace2 transcriptionally [127, 143]. In addition, Ace2 controls the expression of *O*-glycosylation genes in an isoform-specific manner [136]. Under unstressed condition, Ace2 represses Pmt1 expression via the transcription factor Zcf21, and de-represses it in response to tunicamycin [143]. Ace2 also has the ability to regulate basal chitin levels by influencing the expression of the chitinase gene *CHT3* [142, 144], which is the major chitinase responsible for homeostatic cell wall architecture and cell separation in yeast cells [145]. Therefore, it may be possible that any one of these functions, and more than likely many of them, impact epitope exposure during *ACE2* deletion and in response to lactate exposure.

The Mkc1 MAPK Pathway

In *C. albicans*, the Mkc1 MAPK cascade, consisting of Bck1-Mkk2-Mkc1 (Fig. 1.2), is activated in response to exogenous cell wall stress, oxidative stimuli, antifungal drugs, and low-temperature shocks [146]. Mkc1 is also important for fungal pathogenesis, as loss of *MKC1* reduces fungal virulence in the mouse systemic infection model [147]. Individually, neither a *mkk2*ΔΔ nor a *mkc1*ΔΔ mutation induces changes in ß-glucan exposure in yeast cells [119, 133, 148]. However, Mkc1 does appear to impact ß(1,3)-glucan exposure levels when *de novo* phospholipid biosynthesis is interrupted by loss of the phosphatidylserine synthase gene *CHO1*. A *cho1*ΔΔ shows increased activation of Mkc1, and disruption of this MAPK in *cho1*Δ/Δ (*cho1*Δ/Δ *mkc1*Δ/Δ double mutant) leads to a further increase of ß(1,3)-glucan exposure when compared to its already unmasked *cho1*Δ/Δ parent strain [133]. Thus, it appears that Mkc1 may, in fact, play a role in minimizing unmasking induced by the *cho1*Δ/Δ mutation by restoring cell wall integrity. Finally, a hyperactive GTP-bound form of Rho1 ($RHO1^{Q67L}$), located upstream of Mkc1, displays increased ß(1,3)-glucan exposure compared to wild-type. However, it also exhibits increased phosphorylation of Cek1 along with Mkc1 [133]. This suggests that components within the signal transduction pathway can also directly impact unmasking, but it is unclear if the increased ß-glucan exposure from the hyperactive $RHO1^{Q67L}$ mutant

is caused by upregulation of Mkc1 or Cek1, which is a known inducer of unmasking [76, 132, 133].

Relevance of ß-glucan exposure to pathogenesis and disease control.

This review has extensively highlighted environmental signals that either increase or decrease cell wall immunogen exposure, with particular focus on the core cell wall polysaccharide ß(1,3)-glucan, and how *C. albicans* actively perceives these signals to induce cell wall changes. The immunomodulatory impact that these changes have on the immune response has been highlighted as well. However, while this review has focused on individual stimuli that regulate epitope exposure, often the host environment is an amalgamation of host stressors that must be simultaneously accounted for in order to successfully induce disease. For example, hypoxia encountered during disease progression is also often associated with inflammation processes [84], and thus a large number of host immune cells are also actively present within these environments. As previously discussed, NET formation *in vitro* is sufficient to induce unmasking [72], and it is presumed that this also occurs during *in vivo* infection. Yet, the hypoxic environment in which this response is occurring is capable of initiating a response pathway to reduce ß(1,3)-glucan exposure [88]. Furthermore, neutrophils within a hypoxic/anoxic environment also actively produce and release large amounts of lactate *in vitro*, and this has been proposed to work synergistically with the hypoxic response to further induce masking in *C. albicans* [149]. Thus, one can easily envision the arms race between fungal pathogen and the host to influence ß-glucan exposure levels to favor a given side, and highlights the interplay that these systems likely have during disease progression *in vivo*. Yet, this fine balance provides an attractive target to leverage for disease control in order to provide a favorable outcome for the host.

Concealing immunogenic epitopes, and specifically ß(1,3)-glucan, is a conserved strategy utilized by pathogenic fungi during disease progression, and as such the disruption of these processes may prove useful as a broad targeting approach for fungal disease control. In addition to *C. albicans*, in *Histoplasma capsulatum*, α-glucan and the glycosylhydrolyase Eng1 are important for minimizing β-glucan exposure [79, 150], and

in *Aspergillus fumigatus* biosynthesis of galactosaminogalactan by Uge3 masks hyphal β-glucan from immune detection [80]. In both *C. albicans* and *H. capsulatum*, mutants have been identified that induce unmasking without strongly changing the overall fitness of the fungal pathogen *in vivo*, and attenuate virulence in a manner that depends on a functional host immune response [76, 150]. These observations consequently show that inappropriately increasing exposure of immunogenic ß(1,3)-glucan moieties in the cell wall is indeed an effective strategy to attenuate virulence, and further supports the idea that we can leverage this process as a therapeutic approach. There is also evidence to suggest that the mechanism of clearance for echinocandins *in vivo* also relies on cell wall remodeling and epitope exposure in addition to their fungicidal effects. It has been shown that systemic infection in dectin1$^{-/-}$ mice diminishes the antifungal activities of caspofungin treatment seen in immunocompetent mice [45]. Here, kidney fungal burden was not significantly different in *C. albicans* infected dectin1$^{-/-}$ mice that were given caspofungin or the drug vehicle control, in contrast to wild-type mice where caspofungin did significantly reduce kidney fungal burden. A similar observation was also seen in *C. albicans* infected neutropenic mice receiving anidulafungin treatment [151]. All the immunocompetent mice that were systemically infected with *C. albicans* and received anidulafungin survived, while ~50-60% of neutropenic mice receiving anidulafungin succumbed to infection. Thus, *in vivo* evidence strongly supports the claim that unmasked fungal cells are more readily recognized and cleared by the host.

Although support exists for utilizing fungal unmasking to facilitate host pathogen clearance, attention must be paid to the infection site for which this strategy is deployed. Many of these studies have been done in systemic infection models, which is only a single manifestation of candidiasis. The observation that loss of the oral epithelial ß(1,3)-glucan receptor EphA2 further exacerbates oropharyngeal candidiasis in mice suggests that leveraging ß(1,3)-glucan exposure as an immunotherapeutic approach may be beneficial for fungal clearance within the oral cavity as well [35]. This is also supported by the observation that oral infection with an unmasked *cho1Δ/Δ* mutant results in reduced fungal burden on the tongue, although fitness defects caused by loss of *CHO1* also likely contribute to this colonization attenuation [152]. Similarly, the observation that mutants

exhibiting increased ß(1,3)-glucan unmasking have reduced fitness within the murine gastrointestinal tract also suggests that manipulating this phenotype may work as an effective control strategy within the gut [17]. Yet, for any infection site, the basis of this approach is dependent on proper recognition and clearance by immune cells. During vulvovaginal candidiasis, neutrophil mediated clearance in the vaginal lumen of mice has been found to be impaired as a consequence of heparan sulfate within the infection site [75, 153]. The inability to clear fungal cells may therefore result in a situation in which polymorphonuclear cell recruitment is high and immunopathogenesis occurs as a consequence. Indeed, clinical isolates from the vaginal lumen display large amounts of variability in their basal levels of ß(1,3)-glucan exposure, and a correlation between increased fungal unmasking, neutrophil recruitment and symptom development for the patient has been established [75, 154]. Thus, unlike during systemic and oral infections, leveraging unmasking as a therapeutic approach for vulvovaginal candidiasis may have detrimental outcomes for the host. Therefore, more work is needed to better understand infections in which this therapeutic strategy is appropriate.

Summary

The work presented in this dissertation will focus on further elucidating how ß(1,3)-glucan exposure is regulated by *C. albicans*, and how the host subsequently responds to infection with unmasked fungal cells. We have previously shown that hyperactivation of the Cek1 MAPK pathway induces unmasking and attenuates virulence during systemic infection in mice [132, 133]. However, it is unknown what downstream effector proteins mediate this phenotype, nor how the host recognizes and more effectively clears the unmasked fungal cells. In Chapter 2, we show that unmasking is mediated by the transcription factor Cph1, which stimulates a parallel signaling pathway to induce the full levels of ß-glucan exposure observed during hyperactivation of the Cek1 MAPK pathway. We also show that virulence attenuation during systemic infection with the hyperactive Cek1 MAPK mutant is largely dependent on an intact immune response, and that neutrophils play a major role in mediating fungal clearance. In Chapter 3, we expand on

these findings and show that the calcineurin pathway is the parallel signaling pathway activated by Cph1 to induce the full levels of unmasking observed during Cek1 hyperactivation. We also show that calcineurin plays a more general role in unmasking, and is also responsible for regulating ß(1,3)-glucan exposure in response to caspofungin and exogenous calcium. Importantly, we identify two novel downstream effector proteins (Fgr41 and Cwp419) within the calcineurin regulon that mediate this phenotype. In Chapter 4, we show that calcineurin appears to induce unmasking during caspofungin treatment via increased deposition of chitin at the poles of budding daughter cells. Furthermore, we show that the MAPK Mkc1 is also an important regulator of chitin synthesis and unmasking in response to caspofungin, and that it works synergistically with the calcineurin pathway to induce these changes. In Chapter 5, we show that mucosal infection with unmasked fungal cells has a niche specific impact on disease progression. Mice infected with an unmasked hyperactive Cek1 mutant showed attenuated tongue fungal burden in an oropharyngeal infection model in mice but showed markers of immunopathogenesis during vulvovaginal infection. Finally, in Chapter 6, these findings are discussed, and future routes of investigation are proposed.

References

1. Wisplinghoff H, Bischoff T, Tallent SM, Seifert H, Wenzel RP, Edmond MB. Nosocomial bloodstream infections in US hospitals: analysis of 24,179 cases from a prospective nationwide surveillance study. Clinical infectious diseases : an official publication of the Infectious Diseases Society of America. 2004;39(3):309-17. doi: 10.1086/421946. PubMed PMID: 15306996.

2. Horn DL, Neofytos D, Anaissie EJ, Fishman JA, Steinbach WJ, Olyaei AJ, et al. Epidemiology and outcomes of candidemia in 2019 patients: data from the prospective antifungal therapy alliance registry. Clin Infect Dis. 2009;48(12):1695-703. Epub 2009/05/16. doi: 10.1086/599039. PubMed PMID: 19441981.

3. Morrell M, Fraser VJ, Kollef MH. Delaying the empiric treatment of candida bloodstream infection until positive blood culture results are obtained: a potential risk factor for hospital mortality. Antimicrobial agents and chemotherapy. 2005;49(9):3640-5. doi: 10.1128/AAC.49.9.3640-3645.2005. PubMed PMID: 16127033; PubMed Central PMCID: PMC1195428.

4. Karabinis A, Hill C, Leclercq B, Tancrede C, Baume D, Andremont A. Risk factors for candidemia in cancer patients: a case-control study. J Clin Microbiol. 1988;26(3):429-32. PubMed PMID: 3356785; PubMed Central PMCID: PMCPMC266307.

5. Wiley JM, Smith N, Leventhal BG, Graham ML, Strauss LC, Hurwitz CA, et al. Invasive fungal disease in pediatric acute leukemia patients with fever and neutropenia during induction chemotherapy: a multivariate analysis of risk factors. J Clin Oncol. 1990;8(2):280-6. doi: 10.1200/JCO.1990.8.2.280. PubMed PMID: 2299371.

6. Bertagnolio S, de Gaetano Donati K, Tacconelli E, Scoppettuolo G, Posteraro B, Fadda G, et al. Hospital-acquired candidemia in HIV-infected patients. Incidence, risk factors and predictors of outcome. J Chemother. 2004;16(2):172-8. doi: 10.1179/joc.2004.16.2.172. PubMed PMID: 15216953.

7. Peterson DE, Boers-Doets CB, Bensadoun RJ, Herrstedt J, Committee EG. Management of oral and gastrointestinal mucosal injury: ESMO Clinical Practice

Guidelines for diagnosis, treatment, and follow-up. Ann Oncol. 2015;26 Suppl 5:v139-51. doi: 10.1093/annonc/mdv202. PubMed PMID: 26142468.

8. Pienaar ED, Young T, Holmes H. Interventions for the prevention and management of oropharyngeal candidiasis associated with HIV infection in adults and children. Cochrane Database Syst Rev. 2010;(11):CD003940. doi: 10.1002/14651858.CD003940.pub3. PubMed PMID: 21069679; PubMed Central PMCID: PMCPMC7156835.

9. Pankhurst CL. Candidiasis (oropharyngeal). BMJ Clin Evid. 2013;2013:1304. PubMed PMID: 24209593; PubMed Central PMCID: PMCPMC3821534.

10. Bustamante CI. Treatment of Candida infection: a view from the trenches! Curr Opin Infect Dis. 2005;18(6):490-5. PubMed PMID: 16258321.

11. Eggimann P, Garbino J, Pittet D. Management of Candida species infections in critically ill patients. The Lancet Infectious diseases. 2003;3(12):772-85. PubMed PMID: 14652203.

12. Whaley SG, Berkow EL, Rybak JM, Nishimoto AT, Barker KS, Rogers PD. Azole Antifungal Resistance in Candida albicans and Emerging Non-albicans Candida Species. Front Microbiol. 2016;7:2173. Epub 2017/01/28. doi: 10.3389/fmicb.2016.02173. PubMed PMID: 28127295; PubMed Central PMCID: PMCPMC5226953.

13. Perlin DS. Mechanisms of echinocandin antifungal drug resistance. Ann N Y Acad Sci. 2015;1354:1-11. doi: 10.1111/nyas.12831. PubMed PMID: 26190298; PubMed Central PMCID: PMCPMC4626328.

14. Ostrosky-Zeichner L, Marr KA, Rex JH, Cohen SH. Amphotericin B: time for a new "gold standard". Clinical infectious diseases : an official publication of the Infectious Diseases Society of America. 2003;37(3):415-25. Epub 2003/07/29. doi: 10.1086/376634. PubMed PMID: 12884167.

15. Netea MG, Brown GD, Kullberg BJ, Gow NA. An integrated model of the recognition of Candida albicans by the innate immune system. Nat Rev Microbiol. 2008;6(1):67-78. doi: 10.1038/nrmicro1815. PubMed PMID: 18079743.

16. Casadevall A, Pirofski LA. Adjunctive immune therapy for fungal infections. Clin Infect Dis. 2001;33(7):1048-56. Epub 2001/08/31. doi: 10.1086/322710. PubMed PMID: 11528579.

17. Sem X, Le GT, Tan AS, Tso G, Yurieva M, Liao WW, et al. beta-glucan Exposure on the Fungal Cell Wall Tightly Correlates with Competitive Fitness of Candida Species in the Mouse Gastrointestinal Tract. Front Cell Infect Microbiol. 2016;6:186. doi: 10.3389/fcimb.2016.00186. PubMed PMID: 28066722; PubMed Central PMCID: PMCPMC5177745.

18. Taylor PR, Tsoni SV, Willment JA, Dennehy KM, Rosas M, Findon H, et al. Dectin-1 is required for beta-glucan recognition and control of fungal infection. Nat Immunol. 2007;8(1):31-8. doi: DOI 10.1038/ni1408. PubMed PMID: WOS:000242934400011.

19. Gantner BN, Simmons RM, Underhill DM. Dectin-1 mediates macrophage recognition of Candida albicans yeast but not filaments. Embo Journal. 2005;24(6):1277-86. doi: 10.1038/sj.emboj.7600594. PubMed PMID: WOS:000228327000018.

20. Chaffin WL. Candida albicans cell wall proteins. Microbiol Mol Biol Rev. 2008;72(3):495-544. Epub 2008/09/06. doi: 10.1128/MMBR.00032-07. PubMed PMID: 18772287; PubMed Central PMCID: PMCPMC2546859.

21. Free SJ. Fungal cell wall organization and biosynthesis. Adv Genet. 2013;81:33-82. Epub 2013/02/20. doi: 10.1016/B978-0-12-407677-8.00002-6. PubMed PMID: 23419716.

22. Hall RA, Gow NA. Mannosylation in Candida albicans: role in cell wall function and immune recognition. Mol Microbiol. 2013;90(6):1147-61. Epub 2013/10/16. doi: 10.1111/mmi.12426. PubMed PMID: 24125554; PubMed Central PMCID: PMCPMC4112839.

23. Gow NAR, Latge JP, Munro CA. The Fungal Cell Wall: Structure, Biosynthesis, and Function. Microbiology spectrum. 2017;5(3). doi: 10.1128/microbiolspec.FUNK-0035-2016. PubMed PMID: 28513415.

24. Ruiz-Herrera J, Ortiz-Castellanos L. Cell wall glucans of fungi. A review. Cell Surf. 2019;5:100022. Epub 2019/03/21. doi: 10.1016/j.tcsw.2019.100022. PubMed PMID: 32743138; PubMed Central PMCID: PMCPMC7389562.
25. Garcia-Rubio R, de Oliveira HC, Rivera J, Trevijano-Contador N. The Fungal Cell Wall: Candida, Cryptococcus, and Aspergillus Species. Front Microbiol. 2019;10:2993. Epub 2020/01/30. doi: 10.3389/fmicb.2019.02993. PubMed PMID: 31993032; PubMed Central PMCID: PMCPMC6962315.
26. Gow NA, Netea MG, Munro CA, Ferwerda G, Bates S, Mora-Montes HM, et al. Immune recognition of Candida albicans beta-glucan by dectin-1. J Infect Dis. 2007;196(10):1565-71. Epub 2007/11/17. doi: 10.1086/523110. PubMed PMID: 18008237; PubMed Central PMCID: PMCPMC2655640.
27. Taylor PR, Brown GD, Reid DM, Willment JA, Martinez-Pomares L, Gordon S, et al. The beta-glucan receptor, dectin-1, is predominantly expressed on the surface of cells of the monocyte/macrophage and neutrophil lineages. J Immunol. 2002;169(7):3876-82. Epub 2002/09/24. doi: 10.4049/jimmunol.169.7.3876. PubMed PMID: 12244185.
28. Brown GD, Taylor PR, Reid DM, Willment JA, Williams DL, Martinez-Pomares L, et al. Dectin-1 is a major beta-glucan receptor on macrophages. J Exp Med. 2002;196(3):407-12. Epub 2002/08/07. doi: 10.1084/jem.20020470. PubMed PMID: 12163569; PubMed Central PMCID: PMCPMC2193936.
29. Brown GD, Gordon S. Immune recognition. A new receptor for beta-glucans. Nature. 2001;413(6851):36-7. Epub 2001/09/07. doi: 10.1038/35092620. PubMed PMID: 11544516.
30. Kennedy AD, Willment JA, Dorward DW, Williams DL, Brown GD, DeLeo FR. Dectin-1 promotes fungicidal activity of human neutrophils. Eur J Immunol. 2007;37(2):467-78. Epub 2007/01/19. doi: 10.1002/eji.200636653. PubMed PMID: 17230442.
31. Cohen-Kedar S, Baram L, Elad H, Brazowski E, Guzner-Gur H, Dotan I. Human intestinal epithelial cells respond to beta-glucans via Dectin-1 and Syk. Eur J Immunol.

2014;44(12):3729-40. Epub 2014/09/25. doi: 10.1002/eji.201444876. PubMed PMID: 25251945.

32. van Bruggen R, Drewniak A, Jansen M, van Houdt M, Roos D, Chapel H, et al. Complement receptor 3, not Dectin-1, is the major receptor on human neutrophils for beta-glucan-bearing particles. Mol Immunol. 2009;47(2-3):575-81. Epub 2009/10/09. doi: 10.1016/j.molimm.2009.09.018. PubMed PMID: 19811837.

33. Li X, Utomo A, Cullere X, Choi MM, Milner DA, Jr., Venkatesh D, et al. The beta-glucan receptor Dectin-1 activates the integrin Mac-1 in neutrophils via Vav protein signaling to promote Candida albicans clearance. Cell Host Microbe. 2011;10(6):603-15. Epub 2011/12/20. doi: 10.1016/j.chom.2011.10.009. PubMed PMID: 22177564; PubMed Central PMCID: PMCPMC3244687.

34. Swidergall M, Solis NV, Wang Z, Phan QT, Marshall ME, Lionakis MS, et al. EphA2 Is a Neutrophil Receptor for Candida albicans that Stimulates Antifungal Activity during Oropharyngeal Infection. Cell Rep. 2019;28(2):423-33 e5. Epub 2019/07/11. doi: 10.1016/j.celrep.2019.06.020. PubMed PMID: 31291578; PubMed Central PMCID: PMCPMC6638578.

35. Swidergall M, Solis NV, Lionakis MS, Filler SG. EphA2 is an epithelial cell pattern recognition receptor for fungal beta-glucans. Nat Microbiol. 2018;3(1):53-61. Epub 2017/11/15. doi: 10.1038/s41564-017-0059-5. PubMed PMID: 29133884; PubMed Central PMCID: PMCPMC5736406.

36. Chen YL, Montedonico AE, Kauffman S, Dunlap JR, Menn FM, Reynolds TB. Phosphatidylserine synthase and phosphatidylserine decarboxylase are essential for cell wall integrity and virulence in Candida albicans. Mol Microbiol. 2010;75(5):1112-32. Epub 2010/02/06. doi: 10.1111/j.1365-2958.2009.07018.x. PubMed PMID: 20132453.

37. Herrero AB, Magnelli P, Mansour MK, Levitz SM, Bussey H, Abeijon C. KRE5 gene null mutant strains of Candida albicans are avirulent and have altered cell wall composition and hypha formation properties. Eukaryot Cell. 2004;3(6):1423-32. Epub 2004/12/14. doi: 10.1128/EC.3.6.1423-1432.2004. PubMed PMID: 15590817; PubMed Central PMCID: PMCPMC539026.

38. Yang M, Solis NV, Marshall M, Garleb R, Zhou T, Wang D, et al. Control of β-glucan exposure by the endo-1,3-glucanase Eng1 in Candida albicans modulates virulence. bioRxiv. 2020:2020.09.07.285791. doi: 10.1101/2020.09.07.285791.
39. Childers DS, Avelar GM, Bain JM, Pradhan A, Larcombe DE, Netea MG, et al. Epitope Shaving Promotes Fungal Immune Evasion. mBio. 2020;11(4). Epub 2020/07/09. doi: 10.1128/mBio.00984-20. PubMed PMID: 32636248; PubMed Central PMCID: PMCPMC7343991.
40. Taylor PR, Tsoni SV, Willment JA, Dennehy KM, Rosas M, Findon H, et al. Dectin-1 is required for beta-glucan recognition and control of fungal infection. Nat Immunol. 2007;8(1):31-8. Epub 2006/12/13. doi: 10.1038/ni1408. PubMed PMID: 17159984; PubMed Central PMCID: PMCPMC1888731.
41. Thompson A, Davies LC, Liao CT, da Fonseca DM, Griffiths JS, Andrews R, et al. The protective effect of inflammatory monocytes during systemic C. albicans infection is dependent on collaboration between C-type lectin-like receptors. PLoS Pathog. 2019;15(6):e1007850. Epub 2019/06/27. doi: 10.1371/journal.ppat.1007850. PubMed PMID: 31242262; PubMed Central PMCID: PMCPMC6594653.
42. Carvalho A, Giovannini G, De Luca A, D'Angelo C, Casagrande A, Iannitti RG, et al. Dectin-1 isoforms contribute to distinct Th1/Th17 cell activation in mucosal candidiasis. Cell Mol Immunol. 2012;9(3):276-86. Epub 2012/05/01. doi: 10.1038/cmi.2012.1. PubMed PMID: 22543832; PubMed Central PMCID: PMCPMC4012853.
43. Gales A, Conduche A, Bernad J, Lefevre L, Olagnier D, Beraud M, et al. PPARgamma controls Dectin-1 expression required for host antifungal defense against Candida albicans. PLoS Pathog. 2010;6(1):e1000714. Epub 2010/01/12. doi: 10.1371/journal.ppat.1000714. PubMed PMID: 20062524; PubMed Central PMCID: PMCPMC2795865.
44. Saijo S, Fujikado N, Furuta T, Chung SH, Kotaki H, Seki K, et al. Dectin-1 is required for host defense against Pneumocystis carinii but not against Candida albicans.

Nat Immunol. 2007;8(1):39-46. Epub 2006/12/13. doi: 10.1038/ni1425. PubMed PMID: 17159982.

45. Marakalala MJ, Vautier S, Potrykus J, Walker LA, Shepardson KM, Hopke A, et al. Differential adaptation of Candida albicans in vivo modulates immune recognition by dectin-1. PLoS Pathog. 2013;9(4):e1003315. Epub 2013/05/03. doi: 10.1371/journal.ppat.1003315. PubMed PMID: 23637604; PubMed Central PMCID: PMCPMC3630191.

46. Netea MG, Joosten LA, van der Meer JW, Kullberg BJ, van de Veerdonk FL. Immune defence against Candida fungal infections. Nat Rev Immunol. 2015;15(10):630-42. Epub 2015/09/22. doi: 10.1038/nri3897. PubMed PMID: 26388329.

47. McGreal EP, Rosas M, Brown GD, Zamze S, Wong SY, Gordon S, et al. The carbohydrate-recognition domain of Dectin-2 is a C-type lectin with specificity for high mannose. Glycobiology. 2006;16(5):422-30. Epub 2006/01/21. doi: 10.1093/glycob/cwj077. PubMed PMID: 16423983.

48. Saijo S, Ikeda S, Yamabe K, Kakuta S, Ishigame H, Akitsu A, et al. Dectin-2 recognition of alpha-mannans and induction of Th17 cell differentiation is essential for host defense against Candida albicans. Immunity. 2010;32(5):681-91. Epub 2010/05/25. doi: 10.1016/j.immuni.2010.05.001. PubMed PMID: 20493731.

49. Cambi A, Netea MG, Mora-Montes HM, Gow NA, Hato SV, Lowman DW, et al. Dendritic cell interaction with Candida albicans critically depends on N-linked mannan. J Biol Chem. 2008;283(29):20590-9. Epub 2008/05/17. doi: 10.1074/jbc.M709334200. PubMed PMID: 18482990; PubMed Central PMCID: PMCPMC2459306.

50. Netea MG, Gow NA, Munro CA, Bates S, Collins C, Ferwerda G, et al. Immune sensing of Candida albicans requires cooperative recognition of mannans and glucans by lectin and Toll-like receptors. J Clin Invest. 2006;116(6):1642-50. Epub 2006/05/20. doi: 10.1172/JCI27114. PubMed PMID: 16710478; PubMed Central PMCID: PMCPMC1462942.

51. Fradin C, Poulain D, Jouault T. beta-1,2-linked oligomannosides from Candida albicans bind to a 32-kilodalton macrophage membrane protein homologous to the mammalian lectin galectin-3. Infect Immun. 2000;68(8):4391-8. Epub 2000/07/19. doi:

10.1128/IAI.68.8.4391-4398.2000. PubMed PMID: 10899835; PubMed Central PMCID: PMCPMC98331.

52. Kohatsu L, Hsu DK, Jegalian AG, Liu FT, Baum LG. Galectin-3 induces death of Candida species expressing specific beta-1,2-linked mannans. J Immunol. 2006;177(7):4718-26. Epub 2006/09/20. doi: 10.4049/jimmunol.177.7.4718. PubMed PMID: 16982911.

53. Jouault T, El Abed-El Behi M, Martinez-Esparza M, Breuilh L, Trinel PA, Chamaillard M, et al. Specific recognition of Candida albicans by macrophages requires galectin-3 to discriminate Saccharomyces cerevisiae and needs association with TLR2 for signaling. J Immunol. 2006;177(7):4679-87. Epub 2006/09/20. doi: 10.4049/jimmunol.177.7.4679. PubMed PMID: 16982907.

54. Jouault T, Ibata-Ombetta S, Takeuchi O, Trinel PA, Sacchetti P, Lefebvre P, et al. Candida albicans phospholipomannan is sensed through toll-like receptors. J Infect Dis. 2003;188(1):165-72. Epub 2003/06/26. doi: 10.1086/375784. PubMed PMID: 12825186.

55. Linden JR, De Paepe ME, Laforce-Nesbitt SS, Bliss JM. Galectin-3 plays an important role in protection against disseminated candidiasis. Med Mycol. 2013;51(6):641-51. Epub 2013/03/16. doi: 10.3109/13693786.2013.770607. PubMed PMID: 23488971; PubMed Central PMCID: PMCPMC3713172.

56. Esteban A, Popp MW, Vyas VK, Strijbis K, Ploegh HL, Fink GR. Fungal recognition is mediated by the association of dectin-1 and galectin-3 in macrophages. Proceedings of the National Academy of Sciences of the United States of America. 2011;108(34):14270-5. doi: 10.1073/pnas.1111415108. PubMed PMID: 21825168; PubMed Central PMCID: PMC3161568.

57. Gantner BN, Simmons RM, Canavera SJ, Akira S, Underhill DM. Collaborative induction of inflammatory responses by dectin-1 and Toll-like receptor 2. J Exp Med. 2003;197(9):1107-17. doi: 10.1084/jem.20021787. PubMed PMID: 12719479; PubMed Central PMCID: PMCPMC2193968.

58. Netea MG, Sutmuller R, Hermann C, Van der Graaf CA, Van der Meer JW, van Krieken JH, et al. Toll-like receptor 2 suppresses immunity against Candida albicans

through induction of IL-10 and regulatory T cells. J Immunol. 2004;172(6):3712-8. Epub 2004/03/09. doi: 10.4049/jimmunol.172.6.3712. PubMed PMID: 15004175.

59. Villamon E, Gozalbo D, Roig P, O'Connor JE, Fradelizi D, Gil ML. Toll-like receptor-2 is essential in murine defenses against Candida albicans infections. Microbes Infect. 2004;6(1):1-7. Epub 2004/01/24. doi: 10.1016/j.micinf.2003.09.020. PubMed PMID: 14738887.

60. Tessarolli V, Gasparoto TH, Lima HR, Figueira EA, Garlet TP, Torres SA, et al. Absence of TLR2 influences survival of neutrophils after infection with Candida albicans. Med Mycol. 2010;48(1):129-40. Epub 2009/05/27. doi: 10.3109/13693780902964339. PubMed PMID: 19468929.

61. Netea MG, Van Der Graaf CA, Vonk AG, Verschueren I, Van Der Meer JW, Kullberg BJ. The role of toll-like receptor (TLR) 2 and TLR4 in the host defense against disseminated candidiasis. J Infect Dis. 2002;185(10):1483-9. Epub 2002/05/07. doi: 10.1086/340511. PubMed PMID: 11992285.

62. Netea MG, Gow NA, Joosten LA, Verschueren I, van der Meer JW, Kullberg BJ. Variable recognition of Candida albicans strains by TLR4 and lectin recognition receptors. Med Mycol. 2010;48(7):897-903. Epub 2010/02/20. doi: 10.3109/13693781003621575. PubMed PMID: 20166865.

63. Lee SJ, Zheng NY, Clavijo M, Nussenzweig MC. Normal host defense during systemic candidiasis in mannose receptor-deficient mice. Infect Immun. 2003;71(1):437-45. Epub 2002/12/24. doi: 10.1128/IAI.71.1.437-445.2003. PubMed PMID: 12496194; PubMed Central PMCID: PMCPMC143203.

64. Graus MS, Wester MJ, Lowman DW, Williams DL, Kruppa MD, Martinez CM, et al. Mannan Molecular Substructures Control Nanoscale Glucan Exposure in Candida. Cell Rep. 2018;24(9):2432-42 e5. Epub 2018/08/30. doi: 10.1016/j.celrep.2018.07.088. PubMed PMID: 30157435; PubMed Central PMCID: PMCPMC6204226.

65. Shen H, Chen SM, Liu W, Zhu F, He LJ, Zhang JD, et al. Abolishing Cell Wall Glycosylphosphatidylinositol-Anchored Proteins in Candida albicans Enhances Recognition by Host Dectin-1. Infect Immun. 2015;83(7):2694-704. Epub 2015/04/22.

doi: 10.1128/IAI.00097-15. PubMed PMID: 25895969; PubMed Central PMCID: PMCPMC4468527.

66. Umemura M, Okamoto M, Nakayama K, Sagane K, Tsukahara K, Hata K, et al. GWT1 gene is required for inositol acylation of glycosylphosphatidylinositol anchors in yeast. J Biol Chem. 2003;278(26):23639-47. Epub 2003/04/26. doi: 10.1074/jbc.M301044200. PubMed PMID: 12714589.

67. McLellan CA, Whitesell L, King OD, Lancaster AK, Mazitschek R, Lindquist S. Inhibiting GPI anchor biosynthesis in fungi stresses the endoplasmic reticulum and enhances immunogenicity. ACS Chem Biol. 2012;7(9):1520-8. Epub 2012/06/26. doi: 10.1021/cb300235m. PubMed PMID: 22724584.

68. Huang X, Liu Y, Ni T, Li L, Yan L, An M, et al. 11g, a Potent Antifungal Candidate, Enhances Candida albicans Immunogenicity by Unmasking beta-Glucan in Fungal Cell Wall. Front Microbiol. 2020;11:1324. Epub 2020/07/23. doi: 10.3389/fmicb.2020.01324. PubMed PMID: 32695076; PubMed Central PMCID: PMCPMC7338940.

69. Ni T, Li R, Xie F, Zhao J, Huang X, An M, et al. Synthesis and Biological Evaluation of Novel 2-Aminonicotinamide Derivatives as Antifungal Agents. ChemMedChem. 2017;12(4):319-26. Epub 2017/01/11. doi: 10.1002/cmdc.201600545. PubMed PMID: 28071858.

70. Wagener J, Malireddi RK, Lenardon MD, Koberle M, Vautier S, MacCallum DM, et al. Fungal chitin dampens inflammation through IL-10 induction mediated by NOD2 and TLR9 activation. PLoS Pathog. 2014;10(4):e1004050. Epub 2014/04/12. doi: 10.1371/journal.ppat.1004050. PubMed PMID: 24722226; PubMed Central PMCID: PMCPMC3983064.

71. He X, Howard BA, Liu Y, Neumann AK, Li L, Menon N, et al. LYSMD3: A mammalian pattern recognition receptor for chitin. Cell Rep. 2021;36(3):109392. Epub 2021/07/22. doi: 10.1016/j.celrep.2021.109392. PubMed PMID: 34289364; PubMed Central PMCID: PMCPMC8344708.

72. Hopke A, Nicke N, Hidu EE, Degani G, Popolo L, Wheeler RT. Neutrophil Attack Triggers Extracellular Trap-Dependent Candida Cell Wall Remodeling and

Altered Immune Recognition. PLoS pathogens. 2016;12(5):e1005644. doi: 10.1371/journal.ppat.1005644. PubMed PMID: 27223610; PubMed Central PMCID: PMC4880299.

73. Davis SE, Hopke A, Minkin SC, Jr., Montedonico AE, Wheeler RT, Reynolds TB. Masking of beta(1-3)-glucan in the cell wall of Candida albicans from detection by innate immune cells depends on phosphatidylserine. Infection and immunity. 2014. doi: 10.1128/IAI.01612-14. PubMed PMID: 25114110.

74. Wheeler RT, Kombe D, Agarwala SD, Fink GR. Dynamic, morphotype-specific Candida albicans beta-glucan exposure during infection and drug treatment. PLoS Pathog. 2008;4(12):e1000227. Epub 2008/12/06. doi: 10.1371/journal.ppat.1000227. PubMed PMID: 19057660; PubMed Central PMCID: PMCPMC2587227.

75. Pericolini E, Perito S, Castagnoli A, Gabrielli E, Mencacci A, Blasi E, et al. Epitope unmasking in vulvovaginal candidiasis is associated with hyphal growth and neutrophilic infiltration. PLoS One. 2018;13(7):e0201436. Epub 2018/08/01. doi: 10.1371/journal.pone.0201436. PubMed PMID: 30063729; PubMed Central PMCID: PMCPMC6067721.

76. Wagner AS, Hancock TJ, Lumsdaine SW, Kauffman SJ, Mangrum MM, Phillips EK, et al. Activation of Cph1 causes ss(1,3)-glucan unmasking in Candida albicans and attenuates virulence in mice in a neutrophil-dependent manner. PLoS Pathog. 2021;17(8):e1009839. Epub 2021/08/26. doi: 10.1371/journal.ppat.1009839. PubMed PMID: 34432857.

77. Hasim S, Allison DP, Retterer ST, Hopke A, Wheeler RT, Doktycz MJ, et al. beta-(1,3)-Glucan Unmasking in Some Candida albicans Mutants Correlates with Increases in Cell Wall Surface Roughness and Decreases in Cell Wall Elasticity. Infect Immun. 2017;85(1). Epub 2016/11/17. doi: 10.1128/IAI.00601-16. PubMed PMID: 27849179; PubMed Central PMCID: PMCPMC5203643.

78. Wheeler RT, Fink GR. A Drug-Sensitive Genetic Network Masks Fungi from the Immune System. PLoS pathogens. 2006;2(4):e35. doi: 10.1371/journal.ppat.0020035.

79. Rappleye CA, Eissenberg LG, Goldman WE. Histoplasma capsulatum alpha-(1,3)-glucan blocks innate immune recognition by the beta-glucan receptor. Proceedings

of the National Academy of Sciences of the United States of America. 2007;104(4):1366-70. doi: 10.1073/pnas.0609848104. PubMed PMID: 17227865; PubMed Central PMCID: PMCPMC1783108.

80. Gravelat FN, Beauvais A, Liu H, Lee MJ, Snarr BD, Chen D, et al. Aspergillus galactosaminogalactan mediates adherence to host constituents and conceals hyphal beta-glucan from the immune system. PLoS Pathog. 2013;9(8):e1003575. Epub 2013/08/31. doi: 10.1371/journal.ppat.1003575. PubMed PMID: 23990787; PubMed Central PMCID: PMCPMC3749958.

81. He G, Shankar RA, Chzhan M, Samouilov A, Kuppusamy P, Zweier JL. Noninvasive measurement of anatomic structure and intraluminal oxygenation in the gastrointestinal tract of living mice with spatial and spectral EPR imaging. Proc Natl Acad Sci U S A. 1999;96(8):4586-91. Epub 1999/04/14. doi: 10.1073/pnas.96.8.4586. PubMed PMID: 10200306; PubMed Central PMCID: PMCPMC16376.

82. Rosenbach A, Dignard D, Pierce JV, Whiteway M, Kumamoto CA. Adaptations of Candida albicans for growth in the mammalian intestinal tract. Eukaryot Cell. 2010;9(7):1075-86. Epub 2010/05/04. doi: 10.1128/EC.00034-10. PubMed PMID: 20435697; PubMed Central PMCID: PMCPMC2901676.

83. Eltzschig HK, Carmeliet P. Hypoxia and inflammation. N Engl J Med. 2011;364(7):656-65. Epub 2011/02/18. doi: 10.1056/NEJMra0910283. PubMed PMID: 21323543; PubMed Central PMCID: PMCPMC3930928.

84. Grahl N, Shepardson KM, Chung D, Cramer RA. Hypoxia and fungal pathogenesis: to air or not to air? Eukaryot Cell. 2012;11(5):560-70. Epub 2012/03/27. doi: 10.1128/EC.00031-12. PubMed PMID: 22447924; PubMed Central PMCID: PMCPMC3346435.

85. Setiadi ER, Doedt T, Cottier F, Noffz C, Ernst JF. Transcriptional response of Candida albicans to hypoxia: linkage of oxygen sensing and Efg1p-regulatory networks. J Mol Biol. 2006;361(3):399-411. Epub 2006/07/21. doi: 10.1016/j.jmb.2006.06.040. PubMed PMID: 16854431.

86. Sosinska GJ, de Groot PWJ, Teixeira de Mattos MJ, Dekker HL, de Koster CG, Hellingwerf KJ, et al. Hypoxic conditions and iron restriction affect the cell-wall

proteome of Candida albicans grown under vagina-simulative conditions. Microbiology (Reading). 2008;154(Pt 2):510-20. Epub 2008/01/30. doi: 10.1099/mic.0.2007/012617-0. PubMed PMID: 18227255.

87. Burgain A, Tebbji F, Khemiri I, Sellam A. Metabolic Reprogramming in the Opportunistic Yeast Candida albicans in Response to Hypoxia. mSphere. 2020;5(1). Epub 2020/02/28. doi: 10.1128/mSphere.00913-19. PubMed PMID: 32102943; PubMed Central PMCID: PMCPMC7045390.

88. Pradhan A, Avelar GM, Bain JM, Childers DS, Larcombe DE, Netea MG, et al. Hypoxia Promotes Immune Evasion by Triggering beta-Glucan Masking on the Candida albicans Cell Surface via Mitochondrial and cAMP-Protein Kinase A Signaling. mBio. 2018;9(6). Epub 2018/11/08. doi: 10.1128/mBio.01318-18. PubMed PMID: 30401773; PubMed Central PMCID: PMCPMC6222127.

89. Pradhan A, Avelar GM, Bain JM, Childers D, Pelletier C, Larcombe DE, et al. Non-canonical signalling mediates changes in fungal cell wall PAMPs that drive immune evasion. Nat Commun. 2019;10(1):5315. Epub 2019/11/24. doi: 10.1038/s41467-019-13298-9. PubMed PMID: 31757950; PubMed Central PMCID: PMCPMC6876565.

90. Rocha CR, Schroppel K, Harcus D, Marcil A, Dignard D, Taylor BN, et al. Signaling through adenylyl cyclase is essential for hyphal growth and virulence in the pathogenic fungus Candida albicans. Mol Biol Cell. 2001;12(11):3631-43. Epub 2001/11/06. doi: 10.1091/mbc.12.11.3631. PubMed PMID: 11694594; PubMed Central PMCID: PMCPMC60281.

91. Sonneborn A, Bockmuhl DP, Gerads M, Kurpanek K, Sanglard D, Ernst JF. Protein kinase A encoded by TPK2 regulates dimorphism of Candida albicans. Mol Microbiol. 2000;35(2):386-96. Epub 2000/01/29. doi: 10.1046/j.1365-2958.2000.01705.x. PubMed PMID: 10652099.

92. Bockmuhl DP, Krishnamurthy S, Gerads M, Sonneborn A, Ernst JF. Distinct and redundant roles of the two protein kinase A isoforms Tpk1p and Tpk2p in morphogenesis and growth of Candida albicans. Mol Microbiol. 2001;42(5):1243-57. Epub 2002/03/12. doi: 10.1046/j.1365-2958.2001.02688.x. PubMed PMID: 11886556.

93. Ding X, Cao C, Zheng Q, Huang G. The Regulatory Subunit of Protein Kinase A (Bcy1) in Candida albicans Plays Critical Roles in Filamentation and White-Opaque Switching but Is Not Essential for Cell Growth. Front Microbiol. 2016;7:2127. Epub 2017/01/21. doi: 10.3389/fmicb.2016.02127. PubMed PMID: 28105026; PubMed Central PMCID: PMCPMC5215307.

94. Huang G, Huang Q, Wei Y, Wang Y, Du H. Multiple roles and diverse regulation of the Ras/cAMP/protein kinase A pathway in Candida albicans. Mol Microbiol. 2019;111(1):6-16. Epub 2018/10/10. doi: 10.1111/mmi.14148. PubMed PMID: 30299574.

95. Barelle CJ, Priest CL, Maccallum DM, Gow NA, Odds FC, Brown AJ. Niche-specific regulation of central metabolic pathways in a fungal pathogen. Cell Microbiol. 2006;8(6):961-71. Epub 2006/05/10. doi: 10.1111/j.1462-5822.2005.00676.x. PubMed PMID: 16681837; PubMed Central PMCID: PMCPMC1472618.

96. Yamaguchi N, Sonoyama K, Kikuchi H, Nagura T, Aritsuka T, Kawabata J. Gastric colonization of Candida albicans differs in mice fed commercial and purified diets. J Nutr. 2005;135(1):109-15. Epub 2004/12/30. doi: 10.1093/jn/135.1.109. PubMed PMID: 15623841.

97. Rios-Covian D, Ruas-Madiedo P, Margolles A, Gueimonde M, de Los Reyes-Gavilan CG, Salazar N. Intestinal Short Chain Fatty Acids and their Link with Diet and Human Health. Front Microbiol. 2016;7:185. Epub 2016/03/01. doi: 10.3389/fmicb.2016.00185. PubMed PMID: 26925050; PubMed Central PMCID: PMCPMC4756104.

98. Rubin-Bejerano I, Fraser I, Grisafi P, Fink GR. Phagocytosis by neutrophils induces an amino acid deprivation response in Saccharomyces cerevisiae and Candida albicans. Proc Natl Acad Sci U S A. 2003;100(19):11007-12. Epub 2003/09/06. doi: 10.1073/pnas.1834481100. PubMed PMID: 12958213; PubMed Central PMCID: PMCPMC196917.

99. Vieira N, Casal M, Johansson B, MacCallum DM, Brown AJ, Paiva S. Functional specialization and differential regulation of short-chain carboxylic acid transporters in the pathogen Candida albicans. Mol Microbiol. 2010;75(6):1337-54. Epub 2009/12/09. doi:

10.1111/j.1365-2958.2009.07003.x. PubMed PMID: 19968788; PubMed Central PMCID: PMCPMC2859246.

100. Miramon P, Lorenz MC. A feast for Candida: Metabolic plasticity confers an edge for virulence. PLoS Pathog. 2017;13(2):e1006144. Epub 2017/02/10. doi: 10.1371/journal.ppat.1006144. PubMed PMID: 28182769; PubMed Central PMCID: PMCPMC5300112.

101. Ballou ER, Avelar GM, Childers DS, Mackie J, Bain JM, Wagener J, et al. Lactate signalling regulates fungal beta-glucan masking and immune evasion. Nat Microbiol. 2016;2:16238. Epub 2016/12/13. doi: 10.1038/nmicrobiol.2016.238. PubMed PMID: 27941860; PubMed Central PMCID: PMCPMC5704895.

102. Ene IV, Cheng SC, Netea MG, Brown AJ. Growth of Candida albicans cells on the physiologically relevant carbon source lactate affects their recognition and phagocytosis by immune cells. Infect Immun. 2013;81(1):238-48. Epub 2012/11/02. doi: 10.1128/IAI.01092-12. PubMed PMID: 23115042; PubMed Central PMCID: PMCPMC3536122.

103. Miwa T, Takagi Y, Shinozaki M, Yun CW, Schell WA, Perfect JR, et al. Gpr1, a putative G-protein-coupled receptor, regulates morphogenesis and hypha formation in the pathogenic fungus Candida albicans. Eukaryotic cell. 2004;3(4):919-31. doi: 10.1128/EC.3.4.919-931.2004. PubMed PMID: 15302825; PubMed Central PMCID: PMCPMC500877.

104. Maidan MM, De Rop L, Serneels J, Exler S, Rupp S, Tournu H, et al. The G protein-coupled receptor Gpr1 and the Galpha protein Gpa2 act through the cAMP-protein kinase A pathway to induce morphogenesis in Candida albicans. Mol Biol Cell. 2005;16(4):1971-86. Epub 2005/01/28. doi: 10.1091/mbc.e04-09-0780. PubMed PMID: 15673611; PubMed Central PMCID: PMCPMC1073676.

105. Karababa M, Valentino E, Pardini G, Coste AT, Bille J, Sanglard D. CRZ1, a target of the calcineurin pathway in Candida albicans. Molecular microbiology. 2006;59(5):1429-51. doi: 10.1111/j.1365-2958.2005.05037.x.

106. Hood MI, Skaar EP. Nutritional immunity: transition metals at the pathogen-host interface. Nat Rev Microbiol. 2012;10(8):525-37. Epub 2012/07/17. doi:

10.1038/nrmicro2836. PubMed PMID: 22796883; PubMed Central PMCID: PMCPMC3875331.

107. Crawford A, Wilson D. Essential metals at the host-pathogen interface: nutritional immunity and micronutrient assimilation by human fungal pathogens. FEMS Yeast Res. 2015;15(7). Epub 2015/08/06. doi: 10.1093/femsyr/fov071. PubMed PMID: 26242402; PubMed Central PMCID: PMCPMC4629794.

108. Chen C, Pande K, French SD, Tuch BB, Noble SM. An iron homeostasis regulatory circuit with reciprocal roles in Candida albicans commensalism and pathogenesis. Cell Host Microbe. 2011;10(2):118-35. Epub 2011/08/17. doi: 10.1016/j.chom.2011.07.005. PubMed PMID: 21843869; PubMed Central PMCID: PMCPMC3165008.

109. Malavia D, Lehtovirta-Morley LE, Alamir O, Weiss E, Gow NAR, Hube B, et al. Zinc Limitation Induces a Hyper-Adherent Goliath Phenotype in Candida albicans. Front Microbiol. 2017;8:2238. Epub 2017/12/01. doi: 10.3389/fmicb.2017.02238. PubMed PMID: 29184547; PubMed Central PMCID: PMCPMC5694484.

110. Li CX, Gleason JE, Zhang SX, Bruno VM, Cormack BP, Culotta VC. Candida albicans adapts to host copper during infection by swapping metal cofactors for superoxide dismutase. Proc Natl Acad Sci U S A. 2015;112(38):E5336-42. Epub 2015/09/10. doi: 10.1073/pnas.1513447112. PubMed PMID: 26351691; PubMed Central PMCID: PMCPMC4586888.

111. Vylkova S, Carman AJ, Danhof HA, Collette JR, Zhou H, Lorenz MC. The fungal pathogen Candida albicans autoinduces hyphal morphogenesis by raising extracellular pH. mBio. 2011;2(3):e00055-11. Epub 2011/05/19. doi: 10.1128/mBio.00055-11. PubMed PMID: 21586647; PubMed Central PMCID: PMCPMC3101780.

112. Gunther LS, Martins HP, Gimenes F, Abreu AL, Consolaro ME, Svidzinski TI. Prevalence of Candida albicans and non-albicans isolates from vaginal secretions: comparative evaluation of colonization, vaginal candidiasis and recurrent vaginal candidiasis in diabetic and non-diabetic women. Sao Paulo Med J. 2014;132(2):116-20. Epub 2014/04/10. doi: 10.1590/1516-3180.2014.1322640. PubMed PMID: 24714993.

113. Fallingborg J. Intraluminal pH of the human gastrointestinal tract. Dan Med Bull. 1999;46(3):183-96. Epub 1999/07/28. PubMed PMID: 10421978.
114. Sherrington SL, Sorsby E, Mahtey N, Kumwenda P, Lenardon MD, Brown I, et al. Adaptation of Candida albicans to environmental pH induces cell wall remodelling and enhances innate immune recognition. PLoS Pathog. 2017;13(5):e1006403. Epub 2017/05/26. doi: 10.1371/journal.ppat.1006403. PubMed PMID: 28542528; PubMed Central PMCID: PMCPMC5456412.
115. Cottier F, Sherrington S, Cockerill S, Del Olmo Toledo V, Kissane S, Tournu H, et al. Remasking of Candida albicans beta-Glucan in Response to Environmental pH Is Regulated by Quorum Sensing. mBio. 2019;10(5). Epub 2019/10/17. doi: 10.1128/mBio.02347-19. PubMed PMID: 31615961; PubMed Central PMCID: PMCPMC6794483.
116. Monge RA, Roman E, Nombela C, Pla J. The MAP kinase signal transduction network in Candida albicans. Microbiology. 2006;152(Pt 4):905-12. doi: 10.1099/mic.0.28616-0. PubMed PMID: 16549655.
117. Alonso-Monge R, Real E, Wojda I, Bebelman JP, Mager WH, Siderius M. Hyperosmotic stress response and regulation of cell wall integrity in Saccharomyces cerevisiae share common functional aspects. Molecular microbiology. 2001;41(3):717-30. PubMed PMID: 11532139.
118. Alonso-Monge R, Navarro-Garcia F, Molero G, Diez-Orejas R, Gustin M, Pla J, et al. Role of the mitogen-activated protein kinase Hog1p in morphogenesis and virulence of Candida albicans. Journal of bacteriology. 1999;181(10):3058-68. PubMed PMID: 10322006; PubMed Central PMCID: PMCPMC93760.
119. Correia I, Prieto D, Roman E, Wilson D, Hube B, Alonso-Monge R, et al. Cooperative Role of MAPK Pathways in the Interaction of Candida albicans with the Host Epithelium. Microorganisms. 2019;8(1). Epub 2019/12/29. doi: 10.3390/microorganisms8010048. PubMed PMID: 31881718; PubMed Central PMCID: PMCPMC7023383.
120. Mio T, Yabe T, Sudoh M, Satoh Y, Nakajima T, Arisawa M, et al. Role of three chitin synthase genes in the growth of Candida albicans. J Bacteriol. 1996;178(8):2416-9.

Epub 1996/04/01. doi: 10.1128/jb.178.8.2416-2419.1996. PubMed PMID: 8636047; PubMed Central PMCID: PMCPMC177954.

121. Wheeler RT, Fink GR. A drug-sensitive genetic network masks fungi from the immune system. PLoS Pathog. 2006;2(4):e35. Epub 2006/05/03. doi: 10.1371/journal.ppat.0020035. PubMed PMID: 16652171; PubMed Central PMCID: PMCPMC1447670.

122. Tams RN, Wagner AS, Jackson JW, Gann ER, Sparer TE, Reynolds TB. Pathways That Synthesize Phosphatidylethanolamine Impact Candida albicans Hyphal Length and Cell Wall Composition through Transcriptional and Posttranscriptional Mechanisms. Infect Immun. 2020;88(3). Epub 2019/12/04. doi: 10.1128/IAI.00480-19. PubMed PMID: 31792076; PubMed Central PMCID: PMCPMC7035933.

123. Badrane H, Nguyen MH, Blankenship JR, Cheng S, Hao B, Mitchell AP, et al. Rapid redistribution of phosphatidylinositol-(4,5)-bisphosphate and septins during the Candida albicans response to caspofungin. Antimicrob Agents Chemother. 2012;56(9):4614-24. Epub 2012/06/13. doi: 10.1128/AAC.00112-12. PubMed PMID: 22687514; PubMed Central PMCID: PMCPMC3421880.

124. Valotteau C, Prystopiuk V, Cormack BP, Dufrene YF. Atomic Force Microscopy Demonstrates that Candida glabrata Uses Three Epa Proteins To Mediate Adhesion to Abiotic Surfaces. mSphere. 2019;4(3). doi: 10.1128/mSphere.00277-19. PubMed PMID: 31043520; PubMed Central PMCID: PMCPMC6495341.

125. Cullen PJ, Edgerton M. Unmasking fungal pathogens by studying MAPK-dependent cell wall regulation in Candida albicans. Virulence. 2016;7(5):502-5. doi: 10.1080/21505594.2016.1177695. PubMed PMID: 27088569; PubMed Central PMCID: PMC5026791.

126. Galan-Diez M, Arana DM, Serrano-Gomez D, Kremer L, Casasnovas JM, Ortega M, et al. Candida albicans beta-glucan exposure is controlled by the fungal CEK1-mediated mitogen-activated protein kinase pathway that modulates immune responses triggered through dectin-1. Infect Immun. 2010;78(4):1426-36. Epub 2010/01/27. doi: 10.1128/IAI.00989-09. PubMed PMID: 20100861; PubMed Central PMCID: PMCPMC2849429.

127. Roman E, Cottier F, Ernst JF, Pla J. Msb2 signaling mucin controls activation of Cek1 mitogen-activated protein kinase in Candida albicans. Eukaryot Cell. 2009;8(8):1235-49. Epub 2009/06/23. doi: 10.1128/EC.00081-09. PubMed PMID: 19542310; PubMed Central PMCID: PMCPMC2725568.

128. Scaduto CM, Kabrawala S, Thomson GJ, Scheving W, Ly A, Anderson MZ, et al. Epigenetic control of pheromone MAPK signaling determines sexual fecundity in Candida albicans. Proc Natl Acad Sci U S A. 2017;114(52):13780-5. Epub 2017/12/20. doi: 10.1073/pnas.1711141115. PubMed PMID: 29255038; PubMed Central PMCID: PMCPMC5748179.

129. Ramirez-Zavala B, Weyler M, Gildor T, Schmauch C, Kornitzer D, Arkowitz R, et al. Activation of the Cph1-dependent MAP kinase signaling pathway induces white-opaque switching in Candida albicans. PLoS Pathog. 2013;9(10):e1003696. Epub 2013/10/17. doi: 10.1371/journal.ppat.1003696. PubMed PMID: 24130492; PubMed Central PMCID: PMCPMC3795047.

130. Gonzalez-Rubio G, Fernandez-Acero T, Martin H, Molina M. Mitogen-Activated Protein Kinase Phosphatases (MKPs) in Fungal Signaling: Conservation, Function, and Regulation. Int J Mol Sci. 2019;20(7). Epub 2019/04/10. doi: 10.3390/ijms20071709. PubMed PMID: 30959830; PubMed Central PMCID: PMCPMC6479966.

131. Munro CA, Selvaggini S, de Bruijn I, Walker L, Lenardon MD, Gerssen B, et al. The PKC, HOG and Ca2+ signalling pathways co-ordinately regulate chitin synthesis in Candida albicans. Mol Microbiol. 2007;63(5):1399-413. Epub 2007/02/17. doi: 10.1111/j.1365-2958.2007.05588.x. PubMed PMID: 17302816; PubMed Central PMCID: PMCPMC2649417.

132. Chen T, Wagner AS, Tams RN, Eyer JE, Kauffman SJ, Gann ER, et al. Lrg1 Regulates beta (1,3)-Glucan Masking in Candida albicans through the Cek1 MAP Kinase Pathway. mBio. 2019;10(5). Epub 2019/09/19. doi: 10.1128/mBio.01767-19. PubMed PMID: 31530671; PubMed Central PMCID: PMCPMC6751057.

133. Chen T, Jackson JW, Tams RN, Davis SE, Sparer TE, Reynolds TB. Exposure of Candida albicans beta (1,3)-glucan is promoted by activation of the Cek1 pathway. PLoS

Genet. 2019;15(1):e1007892. Epub 2019/02/01. doi: 10.1371/journal.pgen.1007892. PubMed PMID: 30703081; PubMed Central PMCID: PMCPMC6372213.

134. Csank C, Schroppel K, Leberer E, Harcus D, Mohamed O, Meloche S, et al. Roles of the Candida albicans mitogen-activated protein kinase homolog, Cek1p, in hyphal development and systemic candidiasis. Infect Immun. 1998;66(6):2713-21. Epub 1998/05/29. doi: 10.1128/IAI.66.6.2713-2721.1998. PubMed PMID: 9596738; PubMed Central PMCID: PMCPMC108260.

135. Liu H, Kohler J, Fink GR. Suppression of hyphal formation in Candida albicans by mutation of a STE12 homolog. Science. 1994;266(5191):1723-6. Epub 1994/12/09. doi: 10.1126/science.7992058. PubMed PMID: 7992058.

136. van Wijlick L, Swidergall M, Brandt P, Ernst JF. Candida albicans responds to glycostructure damage by Ace2-mediated feedback regulation of Cek1 signaling. Molecular microbiology. 2016;102(5):827-49. doi: 10.1111/mmi.13494. PubMed PMID: 27589033.

137. Chen J, Chen J, Lane S, Liu H. A conserved mitogen-activated protein kinase pathway is required for mating in Candida albicans. Mol Microbiol. 2002;46(5):1335-44. Epub 2002/11/28. doi: 10.1046/j.1365-2958.2002.03249.x. PubMed PMID: 12453219.

138. Cantero PD, Lengsfeld C, Prill SK, Subanovic M, Roman E, Pla J, et al. Transcriptional and physiological adaptation to defective protein-O-mannosylation in Candida albicans. Mol Microbiol. 2007;64(4):1115-28. Epub 2007/05/16. doi: 10.1111/j.1365-2958.2007.05723.x. PubMed PMID: 17501932.

139. Zucchi PC, Davis TR, Kumamoto CA. A Candida albicans cell wall-linked protein promotes invasive filamentation into semi-solid medium. Mol Microbiol. 2010;76(3):733-48. Epub 2010/04/14. doi: 10.1111/j.1365-2958.2010.07137.x. PubMed PMID: 20384695; PubMed Central PMCID: PMCPMC3163599.

140. Herwald SE, Zucchi PC, Tan S, Kumamoto CA. The two transmembrane regions of Candida albicans Dfi1 contribute to its biogenesis. Biochem Biophys Res Commun. 2017;488(1):153-8. Epub 2017/05/10. doi: 10.1016/j.bbrc.2017.04.158. PubMed PMID: 28483525; PubMed Central PMCID: PMCPMC5521179.

141. Roman E, Correia I, Salazin A, Fradin C, Jouault T, Poulain D, et al. The Cek1-mediated MAP kinase pathway regulates exposure of-1,2 and-1,2-mannosides in the cell wall of Candida albicans modulating immune recognition. Virulence. 2016;7(5):558-77. doi: 10.1080/21505594.2016.1163458. PubMed PMID: WOS:000380007500011.
142. Mulhern SM, Logue ME, Butler G. Candida albicans transcription factor Ace2 regulates metabolism and is required for filamentation in hypoxic conditions. Eukaryot Cell. 2006;5(12):2001-13. Epub 2006/09/26. doi: 10.1128/EC.00155-06. PubMed PMID: 16998073; PubMed Central PMCID: PMCPMC1694816.
143. Cantero PD, Ernst JF. Damage to the glycoshield activates PMT-directed O-mannosylation via the Msb2-Cek1 pathway in Candida albicans. Molecular microbiology. 2011;80(3):715-25. doi: 10.1111/j.1365-2958.2011.07604.x. PubMed PMID: 21375589.
144. Kelly MT, MacCallum DM, Clancy SD, Odds FC, Brown AJ, Butler G. The Candida albicans CaACE2 gene affects morphogenesis, adherence and virulence. Mol Microbiol. 2004;53(3):969-83. Epub 2004/07/17. doi: 10.1111/j.1365-2958.2004.04185.x. PubMed PMID: 15255906.
145. Dunkler A, Walther A, Specht CA, Wendland J. Candida albicans CHT3 encodes the functional homolog of the Cts1 chitinase of Saccharomyces cerevisiae. Fungal genetics and biology : FG & B. 2005;42(11):935-47. doi: 10.1016/j.fgb.2005.08.001. PubMed PMID: 16214381.
146. Kamada Y, Qadota H, Python CP, Anraku Y, Ohya Y, Levin DE. Activation of yeast protein kinase C by Rho1 GTPase. The Journal of biological chemistry. 1996;271(16):9193-6. PubMed PMID: 8621575.
147. Diez-Orejas R, Molero G, Navarro-Garcia F, Pla J, Nombela C, Sanchez-Perez M. Reduced virulence of Candida albicans MKC1 mutants: a role for mitogen-activated protein kinase in pathogenesis. Infection and immunity. 1997;65(2):833-7. PubMed PMID: 9009353; PubMed Central PMCID: PMCPMC176136.
148. Roman E, Alonso-Monge R, Miranda A, Pla J. The Mkk2 MAPKK Regulates Cell Wall Biogenesis in Cooperation with the Cek1-Pathway in Candida albicans. PloS

one. 2015;10(7):e0133476. doi: 10.1371/journal.pone.0133476. PubMed PMID: 26197240; PubMed Central PMCID: PMC4509911.

149. Lopes JP, Stylianou M, Backman E, Holmberg S, Jass J, Claesson R, et al. Evasion of Immune Surveillance in Low Oxygen Environments Enhances Candida albicans Virulence. mBio. 2018;9(6). Epub 2018/11/08. doi: 10.1128/mBio.02120-18. PubMed PMID: 30401781; PubMed Central PMCID: PMCPMC6222133.

150. Garfoot AL, Shen Q, Wuthrich M, Klein BS, Rappleye CA. The Eng1 beta-Glucanase Enhances Histoplasma Virulence by Reducing beta-Glucan Exposure. mBio. 2016;7(2):e01388-15. Epub 2016/04/21. doi: 10.1128/mBio.01388-15. PubMed PMID: 27094334; PubMed Central PMCID: PMCPMC4850272.

151. Wiederhold NP, Najvar LK, Bocanegra R, Kirkpatrick WR, Patterson TF. Comparison of anidulafungin's and fluconazole's in vivo activity in neutropenic and non-neutropenic models of invasive candidiasis. Clin Microbiol Infect. 2012;18(2):E20-3. Epub 2011/12/02. doi: 10.1111/j.1469-0691.2011.03712.x. PubMed PMID: 22128831.

152. Davis SE, Tams RN, Solis NV, Wagner AS, Chen T, Jackson JW, et al. Candida albicans Cannot Acquire Sufficient Ethanolamine from the Host To Support Virulence in the Absence of De Novo Phosphatidylethanolamine Synthesis. Infect Immun. 2018;86(8). Epub 2018/06/06. doi: 10.1128/IAI.00815-17. PubMed PMID: 29866908; PubMed Central PMCID: PMCPMC6056879.

153. Yano J, Noverr MC, Fidel PL, Jr. Vaginal Heparan Sulfate Linked to Neutrophil Dysfunction in the Acute Inflammatory Response Associated with Experimental Vulvovaginal Candidiasis. mBio. 2017;8(2). Epub 2017/03/16. doi: 10.1128/mBio.00211-17. PubMed PMID: 28292981; PubMed Central PMCID: PMCPMC5350465.

154. Gerwien F, Dunker C, Brandt P, Garbe E, Jacobsen ID, Vylkova S. Clinical Candida albicans Vaginal Isolates and a Laboratory Strain Show Divergent Behaviors during Macrophage Interactions. mSphere. 2020;5(4). Epub 2020/08/21. doi: 10.1128/mSphere.00393-20. PubMed PMID: 32817377; PubMed Central PMCID: PMCPMC7407065.

CHAPTER 2 - ACTIVATION OF CPH1 CAUSES UNMASKING IN *CANDIDA ALBICANS* AND ATTENUATES VIRULENCE IN MICE IN A NEUTROPHIL-DEPENDENT MANNER

This work was performed by: Andrew S. Wagner, Trevor J. Hancock, Stephen W. Lumsdaine, Sarah J. Kauffman, Mikayla M. Mangrum, Elise K. Phillips, Timothy E. Sparer and Todd B. Reynolds

Author Contributions: Conceptualization, ASW and TBR; Methodology, ASW, TJH and TES.; Formal analysis, ASW and TBR; Investigation, ASW, TJH (Developed panel and helped in the analysis for immunosuppression checks), SJK (Helped with animal injections), SWL (Helped with animal injections and CFU plating), MMM (Helped with CFU plating) and EKP (helped with CFU plating); Writing–original draft preparation, ASW; Writing–review and editing, ASW and TBR; Visualization, ASW; Funding Acquisition, TBR and TES.

This work has been published in PLoS Pathogens:
-Wagner AS, Hancock TJ, Lumsdaine SW, Kauffman SJ, Mangrum MM, Phillips EK, et al. Activation of Cph1 causes ss(1,3)-glucan unmasking in Candida albicans and attenuates virulence in mice in a neutrophil-dependent manner. PLoS Pathog. 2021;17(8):e1009839. Epub 2021/08/26. doi: 10.1371/journal.ppat.1009839. PubMed PMID: 34432857.

Abstract

Masking the immunogenic cell wall epitope ß(1,3)-glucan under an outer layer of mannosylated glycoproteins is an important virulence factor deployed by *Candida albicans* during infection. Consequently, increased ß(1,3)-glucan exposure (unmasking) reveals *C. albicans* to the host's immune system and attenuates its virulence. We have previously shown that activation of the Cek1 MAPK pathway via expression of a hyperactive allele of an upstream kinase (*STE11*$^{\Delta N467}$) induces unmasking. It also increases survival of mice in a murine disseminated candidiasis model and attenuated kidney fungal burden by ≥33 fold. In this communication, we utilized cyclophosphamide-induced immunosuppression to test if the clearance of the unmasked *STE11*$^{\Delta N467}$ mutant was dependent on the host immune system. Suppression of the immune response by cyclophosphamide reduced the attenuation in fungal burden caused by the. *STE11*$^{\Delta N467}$ allele. Moreover, specific depletion

of neutrophils via 1A8 antibody treatment also reduced *STE11*$^{\Delta N467}$-dependent fungal burden attenuation, but to a lesser extent than cyclophosphamide, demonstrating an important role for neutrophils in mediating fungal clearance of unmasked *STE11*$^{\Delta N467}$ cells. In an effort to understand the mechanism by which Ste11$^{\Delta N467}$ causes unmasking, transcriptomics were used to reveal that several components in the Cek1 MAPK pathway were upregulated, including the transcription factor *CPH1* and the cell wall sensor *DFI1*. In this report we show that a *cph1*ΔΔ mutation restored ß(1,3)-glucan exposure to wild-type levels in the *STE11*$^{\Delta N467}$ strain, confirming that Cph1 is the transcription factor mediating Ste11$^{\Delta N467}$-induced unmasking. Furthermore, Cph1 is shown to induce a positive feedback loop that increases Cek1 activation. In addition, full unmasking by *STE11*$^{\Delta N467}$ is dependent on the upstream cell wall sensor *DFI1*. However, while deletion of *DFI1* significantly reduced Ste11$^{\Delta N467}$-induced unmasking, it did not impact activation of the downstream kinase Cek1. Thus, it appears that once stimulated by Ste11$^{\Delta N467}$, Dfi1 activates a parallel signaling pathway that is involved in Ste11$^{\Delta N467}$-induced unmasking.

Introduction

Pathogenic fungi are a significant burden to public health, accounting for up to 1.5 million deaths annually worldwide [1]. Within all infected individuals, the health status of the host and the ability of the pathogen to successfully evade host immune system detection are closely related to the severity of the resulting infection. In a healthy host, the immune system is equipped with numerous pattern recognition receptors (PRRs) that are capable of recognizing and mounting an immune response to pathogen associated molecular patterns (PAMPs) located on the fungi [2]. The cell wall is a major source of fungal associated PAMPs, and therefore acts a vital junction in this host immune system-pathogen interaction [3, 4]. Consequently, fungal pathogens have evolved regulatory systems to dictate the level of exposure of these immunogenic epitopes located within their cell wall as a means to mediate host immune system evasion.

Fungal pathogens deploy various mechanisms to successfully evade their host. Several pathogens utilize thick outer proteinaceous or carbohydrate layers to cover immunogenic epitopes within their cell walls. For example, wild-type *Candida albicans*

covers (masks) immunogenic ß(1,3)-glucan, located within the central layer of its cell wall, with a dense outer layer of mannosylated proteins [5, 6]. This masking in turn shields immunogenic ß(1,3)-glucan epitopes from host PRRs, such as dectin-1, compliment receptor 3, and EphA2 located on macrophages [7-11], neutrophils [10, 12, 13] and host epithelia [14], to facilitate immune system evasion. *Aspergillus fumigatus* covers immunogenic epitopes with hydrophobins or galactosaminogalactan on its conidia and hyphae, respectively, to similarly impair dectin-1 binding [15, 16]. Alternatively, pathogens may also utilize extracellular enzymes that are capable of reducing the levels of exposed antigens in their cell wall. This can be observed in both *C. albicans* and *Histoplasma capsulatum*, which utilize the endo-1,3-ß-glucanase Eng1 to degrade exposed ß(1,3)-glucan [17, 18]. *C. albicans* can additionally deploy the exo-1,3-ß-glucanase Xog1 to induce masking in response to lactate exposure [19].

Due to the vital interface that the cell wall plays in regulating successful immune system evasion by pathogenic fungi, disruption of antigen masking is beginning to gain attention as an alternative therapeutic approach to treating disease progression [19-21]. In this strategy, the host immune system can be leveraged to facilitate enhanced fungal clearance. With respect to *Candidiasis*, the applicability of this approach will benefit from an understanding of how *C. albicans* actively regulates its levels of exposed immunogenic epitopes, such as ß(1,3)-glucan and chitin, and how the host immune system subsequently responds to infection by the unmasked fungus. Such information could be used to attenuate the ability of *C. albicans* to evade host immune system detection and further enhance clearance. Recent findings are beginning to highlight the applicability of regulated activation of signal cascades to address the aforementioned questions. *C. albicans* has been shown to regulate its levels of ß(1,3)-glucan exposure in response to various environmental stimuli, including acidic pH, hypoxia and lactate exposure [22-24]. This change in cell wall architecture is facilitated through appropriate signal transduction cascades that are induced in response to the environmental stimulus. For example, in response to lactate exposure, *C. albicans* induces masking via a non-canonical signal cascade between the G-coupled-protein-receptor Gpr1 and the transcription factor Crz1 [24]. This cascade in turn influences the expression of the exo-1,3-ß-glucanase Xog1 to regulate masking [19]. Thus,

regulated activation of signal cascades that mediate unmasking can serve as a model to study how *C. albicans* regulates its homeostatic levels of exposed ß(1,3)-glucan. Furthermore, these pathways may also serve as inducible systems to study how the host immune system responds to infection with unmasked *C. albicans* cells *in vivo*. Similarly, our lab has shown that hyperactivation of the Cek1 Mitogen Activated Protein Kinase (MAPK) pathway, consisting of a Ste11-Hst7-Cek1 signal cascade, is also capable of activating ß(1,3)-glucan exposure [25, 26]. We have shown that regulated hyperactivation of the pathway via expression of a hyperactive allele of the upstream MAP3 kinase (*STE11*$^{\Delta N467}$) under the control of a tetracycline (*tet*)-repressible promoter causes increased ß(1,3)-glucan unmasking that elicits activation of macrophages (cytokine secretion) *in vitro* [25]. Furthermore, we have shown that activation of this pathway can be regulated *in vivo* and that mice infected with the *STE11*$^{\Delta N467}$ strain show prolonged survival and a ≥33-fold reduction in kidney fungal burden compared to the wild-type during systemic infection.

In this report, we utilize the controlled activation of the Cek1 MAPK pathway to assess the impact that the host immune system has on clearance of an unmasked *STE11*$^{\Delta N467}$ mutant during systemic infection, and further elucidate how *STE11*$^{\Delta N467}$ expression induces ß(1,3)-glucan unmasking in *C. albicans*. We found that clearance of unmasked *STE11*$^{\Delta N467}$ cells is largely host immune system dependent, and relies on multiple immune cells aside from just neutrophils for proper clearance. We also present data showing that *STE11*$^{\Delta N467}$-induced unmasking of both ß(1,3)-glucan and chitin is mediated through the transcription factor Cph1 and that activated Cph1 induces overexpression of the cell wall sensor *DFI1*, which stimulates an unidentified parallel signaling pathway that further influences ß(1,3)-glucan exposure.

Results

Systemic infection with a hyperactive Ste11$^{\Delta N467}$ mutant decreases organ colonization and circulatory cytokine levels in mice.

We have previously shown that overexpression of a single allele of a hyperactive *STE11* mutant gene (*STE11*$^{\Delta N467}$) induces increased ß(1,3)-glucan unmasking and attenuates

virulence in a mouse model of systemic candidiasis [25, 26]. However, although we have shown that hyperactive *STE11*$^{\Delta N467}$ prolongs survival and significantly reduces kidney fungal burden in mice during systemic infection, its impact on colonization in other host organs is unknown. Thus, to develop a more holistic understanding of the impact that hyperactive *STE11*$^{\Delta N467}$ expression has on systemic disease progression, we intravenously infected mice with either wild-type *C. albicans* or a strain carrying a normal *STE11* allele on one chromosome and a hyperactive *STE11*$^{\Delta N467}$ allele under the control of a tetracycline (*tet*)-repressible promoter on the other (*STE11/P*$_{tet\text{-}off}$*-STE11*$^{\Delta N467}$) [25, 27]. The use of the *tet*-repressible promoter allows for controlled regulation of the hyperactive *STE11*$^{\Delta N467}$ allele. The addition of doxycycline causes the strain to act similar to the wild-type because the *STE11*$^{\Delta N467}$ allele is repressed, but the remaining wild-type copy of *STE11* is still expressed. In contrast, in the absence of doxycycline the *P*$_{tet\text{-}off}$ promoter overexpresses the hyperactive *STE11*$^{\Delta N467}$ allele and induces unmasking. Thus, if we infect mice with the *STE11/P*$_{tet\text{-}off}$*-STE11*$^{\Delta N467}$ strain without giving the mice doxycycline in their drinking water, then the strain will be unmasked. To ensure that unmasking occurred only during infection, overnight cultures of the wild-type and *STE11/P*$_{tet\text{-}off}$*-STE11*$^{\Delta N467}$ were grown in YPD with doxycycline to repress premature hyperactivation of the Cek1 MAPK pathway [25]. Mice were then intravenously infected with $1x10^6$ CFU/mouse of either the wild-type or *STE11/P*$_{tet\text{-}off}$*-STE11*$^{\Delta N467}$ strain. Doxycycline was either present or absent in the drinking water of mice to regulate *P*$_{tet\text{-}off}$*-STE11*$^{\Delta N467}$ expression. Mice were then sacrificed at 4 days post infection (d.p.i) to assess fungal burden of the kidney, liver, spleen and brain.

In accordance with our previous observation [25], an ~15-33-fold decrease in kidney fungal burden was observed in mice infected with *C. albicans* that overexpressed *STE11*$^{\Delta N467}$ (*STE11/P*$_{tet\text{-}off}$*-STE11*$^{\Delta N467}$ strain without doxycycline) compared to all other conditions (Fig 2.1A). Furthermore, this difference was also apparent in fungal burden trends in both the spleen and brain, suggesting that hyperactive *STE11*$^{\Delta N467}$ expression during systemic infection impacts fungal burden in multiple host niches to which *C. albicans* disseminates. However, liver fungal burden trends only showed a significant

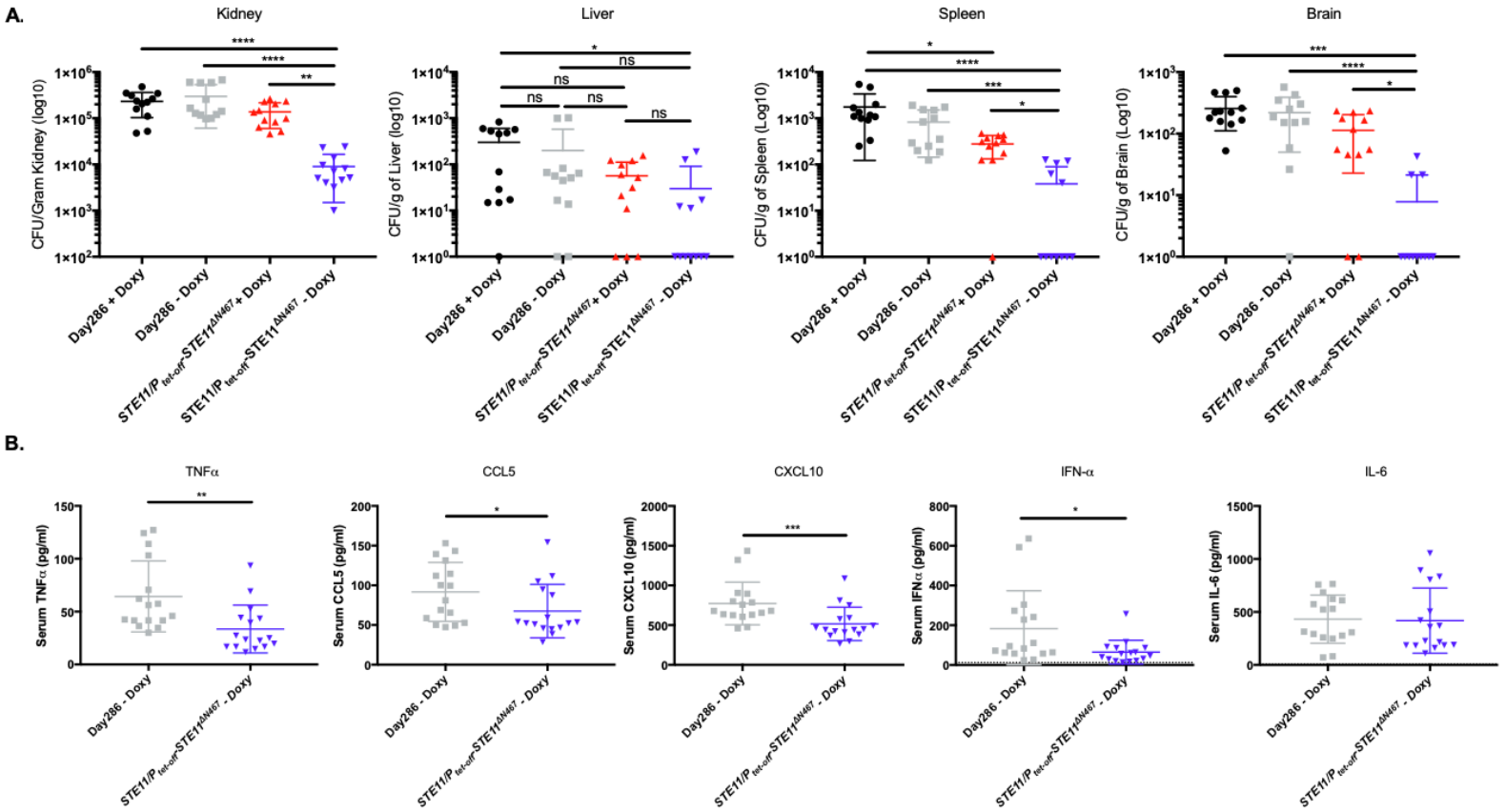


Fig 2.1: Systemic infection with a hyperactive Ste11$^{\Delta N467}$ mutant attenuates fungal colonization in multiple niches within a mouse host.
(A) ICR mice were intravenously infected with 1x10^6 cells of *C. albicans* wild-type (Day286) or the *STE11/P$_{tet-off}$-STE11$^{\Delta N467}$* strain and their kidneys, livers, spleens, and brains were harvested 4 days post infection (d.p.i.) to assess fungal burden. (n = 6 mice)(*p<0.05, **p<0.01, ***p<0.0005, ****p<0.0001, by Kruskal-Wallis test with Dunn's multiple comparisons post-hoc analysis). (B) Serum collected 4 days post infection was assessed to determine the protein concentrations of TNFα, CCL5, CXCL10, IFNα and IL-6 via flow cytometry using the LEGENDplex cytokine bead-based array kit. (n = 8 mice)(*p<0.05, **p<0.005, ***p<0.0005, by Mann-Whitney test).

difference between mice infected with *STE11/P$_{tet\text{-}off}$-STE11$^{\Delta N467}$* without doxycycline and mice infected with wild-type plus doxycycline.

In accordance with the decreased colonization levels observed in the kidneys, brains and spleens of mice infected with the *STE11/P$_{tet\text{-}off}$-STE11$^{\Delta N467}$* strain, there was also a modest reduction in several proinflammatory cytokines within the serum of mice infected the hyperactive *STE11$^{\Delta N467}$* mutant at 4 days post infection. Namely, TNFα ($p<0.005$), CCL5 ($p<0.05$), CXCL10 ($p<0.0005$) and IFNα ($p<0.05$) were found at lower levels within the serum of mice infected with the *STE11/P$_{tet\text{-}off}$-STE11$^{\Delta N467}$* strain when compared to the wild-type control (Fig 2.1B). However, no difference was observed in the serum concentrations of IL-6, CCL2, IL-1ß, IL-12, GM-CSF, CXCL1, IL-10, IFN-ß or IFN-γ (Fig 2.1B, S2.1 Fig). Together, this suggests that systemic infection with a hyperactive *STE11$^{\Delta N467}$* mutant only modestly impacts serum concentrations of select proinflammatory cytokines at 4 days post infection.

Virulence attenuation by hyperactive Ste11$^{\Delta N467}$ is host immune system dependent. Although the data in Fig 2.1A showed a clear impact of hyperactive *STE11$^{\Delta N467}$* expression on fungal burden in multiple organs during systemic infection, the mechanism driving virulence attenuation in mice was unclear. We hypothesized that the observed virulence decrease was driven by enhanced recognition and clearance of *Candida* by the immune system as a consequence of hyperactive Cek1-mediated unmasking. However, decreased growth in the host could be responsible for the phenotype as well. Therefore, to assess whether virulence attenuation by *STE11$^{\Delta N467}$* is dependent on the host's immune system, we immunosuppressed mice with cyclophosphamide prior to infection (Fig 2.2A, S2.2 Fig). This should eliminate any virulence differences that are dependent on the host's immune response. We then inoculated cyclophosphamide-treated mice with $1x10^4$ CFU/mouse of either the wild-type strain as a control or the *STE11/P$_{tet\text{-}off}$-STE11$^{\Delta N467}$* strain. A lower infection dose was used to account for the increased susceptibility of immunosuppressed mice. Mice were not given doxycycline in their drinking water to

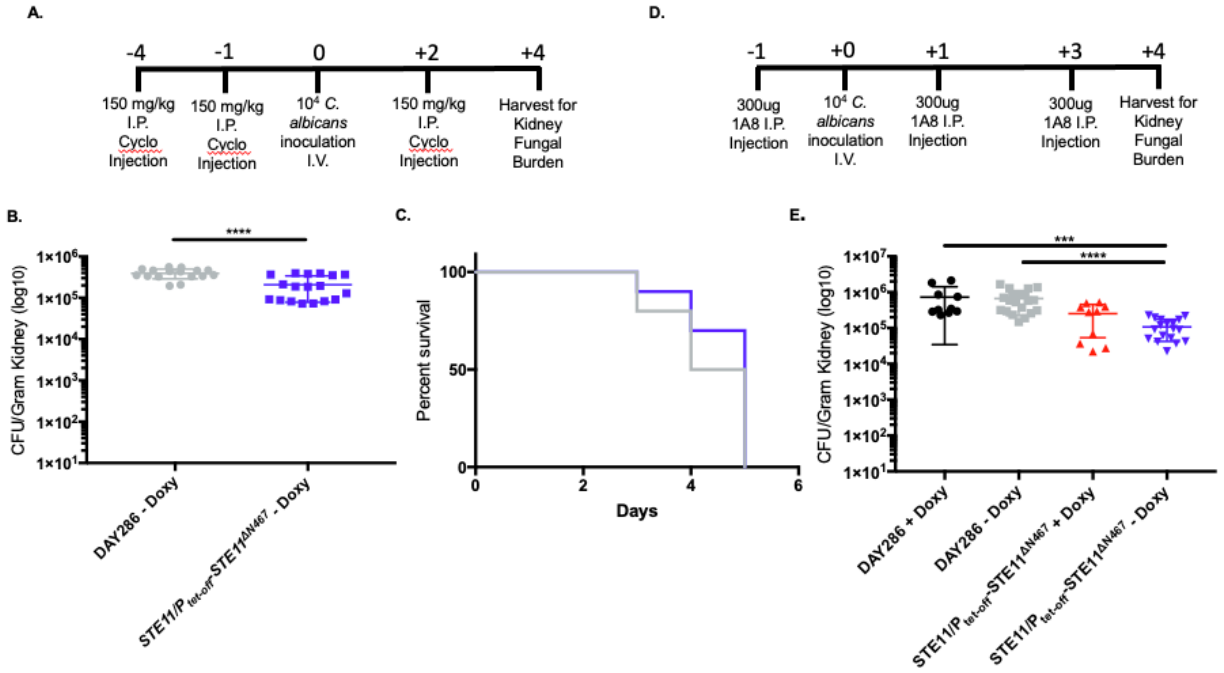


Fig 2.2: Virulence attenuation during systemic infection by the hyperactive Ste11$^{\Delta N467}$ mutant is host immune system dependent.
(A) ICR mice were immunosuppressed with recurring intraperitoneal injections of 150mg/kg of cyclophosphamide every 3 days starting 4 days prior to infection. At day 0, mice were intravenously injected with 1x10^4 cells of *C. albicans* wild-type (Day286) or the *STE11/P$_{tet-off}$-STE11$^{\Delta N467}$* strain that were pregrown in YPD containing doxycycline to repress *STE11$^{\Delta N467}$* expression prior to infection. Kidneys were harvested 4 days post infection (d.p.i.) to assess fungal burden. (B) Kidney fungal burden in mice immunosuppressed with cyclophosphamide 4 d.p.i. (n = 8-9 mice) (*p<0.0001, by student's t-test). (C) Survival curve for cyclophosphamide-immunosuppressed mice that were intravenously injected with 1x10^4 cells of wild-type (Day286) or the *STE11/P$_{tet-off}$-STE11$^{\Delta N467}$* strain. Immunosuppression was maintained via recurring intraperitoneal injections every 3 days with 150mg/kg of cyclophosphamide starting 4 days prior to infection (day -4). (n = 10 mice) (D) Neutrophil depletion was achieved with recurring intraperitoneal injections of 300ug of anti-mouse Ly6G (1A8) antibody every 2 days starting one day prior to infection. At day 0, ICR mice were intravenously injected with 1x10^4 cells of *C. albicans* wild-type (Day286) or the *STE11/P$_{tet-off}$-STE11$^{\Delta N467}$* strain and kidney fungal burden was assessed 4 d.p.i. (E) Kidney fungal burden in neutrophil depleted mice 4 d.p.i. (+/- Doxy = addition or absence of doxycycline) (n = 5 mice for Day286 and *STE11/P$_{tet-off}$-STE11$^{\Delta N467}$* + doxycycline controls, n = 9 mice for *STE11/P$_{tet-off}$-STE11$^{\Delta N467}$* – doxycycline, and n = 10 mice for Day286 – doxycycline) (***p<0.0005 and ****p<0.0001, by Kruskal-Wallis test with Dunn's multiple comparisons post-hoc analysis).

permit hyperactive *STE11*$^{\Delta N467}$ expression and all mice were sacrificed at 4 days post infection (d.p.i) to measure kidney fungal burden.

Mice infected with wild-type *C. albicans* exhibited an average fungal burden of $3.94x10^5$ CFU g^{-1} kidney, while mice infected with the *STE11/P*$_{tet\text{-}off}$-*STE11*$^{\Delta N467}$ strain exhibited an average of $2.08x10^5$ CFU g^{-1} kidney (Fig 2.2B). Thus, there was only an ~2-fold difference between them ($p<0.0001$). This is a >15-fold difference in fungal burden trends when compared to the same infection conditions in immunocompetent mice (Figs 2.1A & 2.2A). Furthermore, survival analysis revealed that mice infected with either strain succumbed to infection at a similar rate (Fig 2.2C), abolishing the prolonged survival previously reported [25]. Collectively, this demonstrates that the host immune system is required for virulence attenuation caused by overexpression of the *STE11*$^{\Delta N467}$ allele.

It is important to note that the ~2-fold decrease in fungal burden in the immunocompromised mice (Fig 2.2A) is consistent with an ~1.68-fold difference that was observed in immunocompetent mice that received doxycycline and were infected with the *STE11/P*$_{tet\text{-}off}$-*STE11*$^{\Delta N467}$ strain compared to wild-type (Fig 2.1A). This consistent difference might be due to other factors unrelated to the host immune system, such as a modest fitness defect.

Although immunosuppression via cyclophosphamide treatment was able to show a reliance on the host immune system for virulence attenuation during infection with an unmasked hyperactive *STE11*$^{\Delta N467}$ mutant, it was still unclear what primary immune cells were contributing to the enhanced fungal clearance. This is due to the broad depletion of different host immune cells induced by cyclophosphamide treatment (S2.2 Fig), including both circulatory monocytes and neutrophils. Neutrophils have been shown to play a major role in fungal clearance and harbor multiple receptors, such as dectin-1, compliment receptor 3 (CR3) and EphA2, that are capable of recognizing exposed ß(1,3)-glucan to facilitate an immune response [10, 12, 13, 28]. We therefore hypothesized that neutrophils would also play a major role in the clearance of an unmasked *STE11/P*$_{tet\text{-}off}$-*STE11*$^{\Delta N467}$ strain. To test this, neutropenia was specifically induced via recurring injections with an anti-Ly6G antibody (1A8) that is specific for depleting host neutrophils (Fig 2.2D, S2.3 Fig) [29, 30]. Mice receiving either the 1A8 treatment or a PBS control injection were

intravenously infected with $1x10^4$ CFU/mouse of either the wild-type or the *STE11/$P_{tet\text{-}off}$-STE11$^{\Delta N467}$* strain and kidney fungal burden was assessed 4 d.p.i.. Control mice that received the PBS drug vehicle control showed very little detectable fungal burden during infection with either strain (S2.4 Fig). However, upon 1A8 depletion, mice that did not receive doxycycline and were infected with the wild-type showed an average fungal burden of $6.63x10^5$ CFU g^{-1} kidney, while mice infected with *STE11/$P_{tet\text{-}off}$-STE11$^{\Delta N467}$* exhibited an average of $1.08x10^5$ CFU g^{-1} kidney (Fig 2.2E). Thus, there was an ~6-fold difference in fungal burden between them ($p<0.0001$). This shows that neutrophils are required for the large(~33-fold) decrease in fungal colonization observed in Fig 1A. However, the depletion of neutrophils alone did not restore fungal colonization as efficiently as was observed with cyclophosphamide treatment (Fig 2.2B), suggesting that loss of additional immune cell types is needed to restore clearance of the unmasked fungi to the levels observed during cyclophosphamide-induced immunosuppression.

Hyperactive *STE11$^{\Delta N467}$* expression induces altered exposure of both ß(1,3)-glucan and chitin in yeast cells.

Hyperactivate *STE11$^{\Delta N467}$* attenuates virulence in a manner that is dependent on the host immune system and this correlates with increased exposure of ß(1,3)-glucan on yeast cells *in vitro* [25, 26]. However, ß(1,3)-glucan is only one of several PAMPs in the fungal cell wall, [25, 31-35] and it is possible that the exposure (or total levels) of other immunogenic cell wall epitopes, such as chitin and mannan, are altered by *STE11$^{\Delta N467}$* expression. To address this, the wild-type and *STE11/$P_{tet\text{-}off}$-STE11$^{\Delta N467}$* strains were stained with calcofluor white, wheat germ agglutinin and concanavalin A to assess the levels of total chitin, exposed chitin and mannan, respectively. Staining and subsequent flow cytometry in conditions that overexpress *STE11$^{\Delta N467}$* (no doxycycline) revealed a significant increase in both total and exposed chitin levels within the cell wall of the *STE11/$P_{tet\text{-}off}$-STE11$^{\Delta N467}$* mutant when compared to the wild-type (Fig 2.3A-B, S2.5 Fig). Furthermore, this was accompanied by a modest decrease in concanavalin A binding in the *STE11/$P_{tet\text{-}off}$-STE11$^{\Delta N467}$* strain, suggesting a slight reduction in mannan levels in the outer

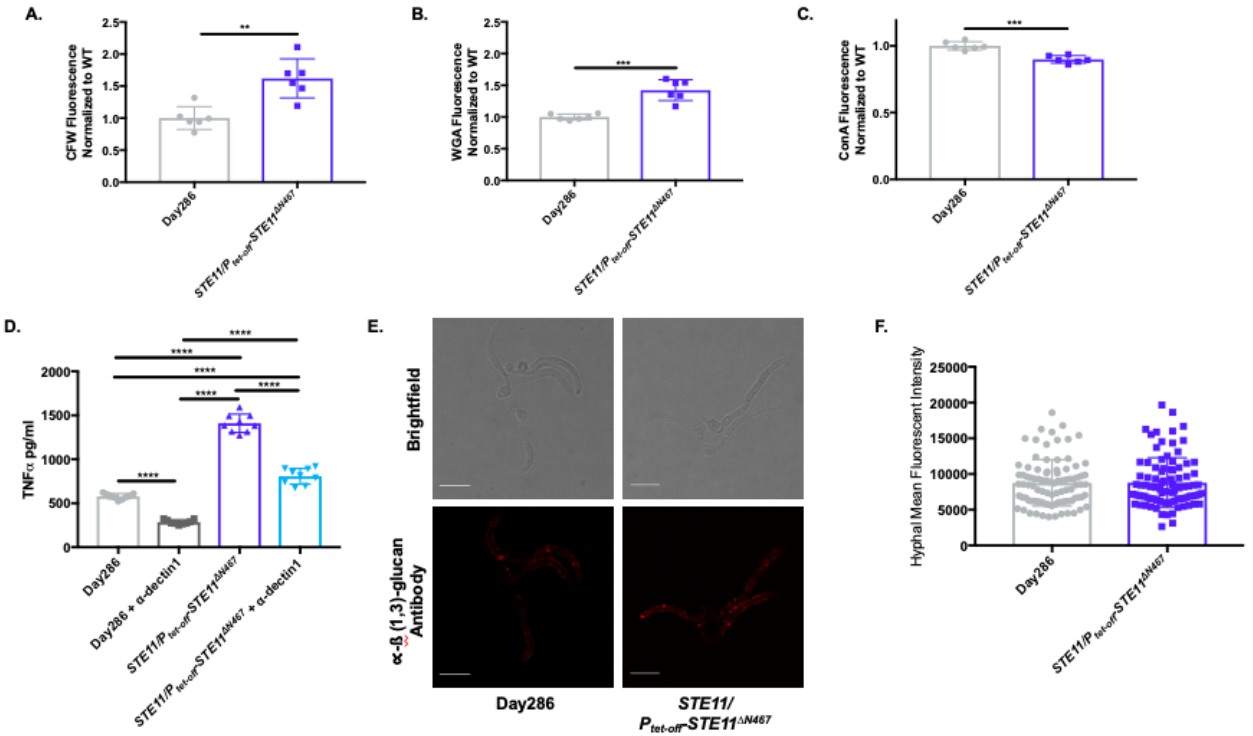


Fig 2.3: Hyperactive *STE11*$^{\Delta N467}$ expression induces changes in cell wall components of yeast, but not hyphal cells of *C. albicans*.
(A-C) Overnight cultures of Day286 wild-type and *STE11/*$P_{tet\text{-}off}$*-STE11*$^{\Delta N467}$ cells grown in YPD without doxycycline were stained with calcofluor white (CFW), fluorescein conjugated wheat germ agglutinin (WGA) and Alexa Fluor 647 conjugated concanavalin A (ConA) to assess total chitin, surface exposed chitin, and mannan, respectively. Three biological replicates with 2 technical replicates were run for each sample. (A) CFW staining, (B) WGA staining and (C) ConA staining. (**p<0.005, p<0.0005, by student's t-test). (D) The impact that dectin-1 recognition of exposed ß(1,3)-glucan has on macrophage immune activation was assessed via antibody blocking using an anti-dectin-1 monoclonal neutralizing antibody. RAW264.7 macrophages and UV-inactivated Day286 wild-type or *STE11/*$P_{tet\text{-}off}$*-STE11*$^{\Delta N467}$ cells were co-incubated for 4 hours at a multiplicity of infection (M.O.I.) of 10. Prior to infection, macrophages were either pretreated with 5ug/ml of the anti-dectin-1 neutralizing antibody or a corresponding volume of tissue culture media lacking the antibody. Following co-incubation with yeast cells, supernatants were collected and filtered through a 0.22µm filter and secreted TNFα levels were determined via an ELISA. (****p<0.0001, by one-way ANOVA). (E-F) Hyphal cells of the Day286 wild-type and *STE11/*$P_{tet\text{-}off}$*-STE11*$^{\Delta N467}$ were stained with anti-ß(1,3)-glucan antibody and a Cy3-conjugated secondary antibody for microscopy analysis of hyphal ß(1,3)-glucan unmasking. (E) Representative confocal microscopy image of stained hyphal cells. The scale bar indicates 10µm. (F) Quantification of hyphal immunofluorescence via ImageJ analysis (n=3 independent stains for each strain with 30 hyphal cells quantified per replicate)(p=0.9258, by student's t-test)

cell wall (Fig 2.3C). Thus, hyperactivation of the Cek1 MAPK pathway induces robust changes in both the exposure and total levels of additional immunogenic cell wall epitopes to ß(1,3)-glucan that may contribute to the observed virulence attenuation.

We have previously reported that co-incubation of RAW264.7 macrophages with the *STE11/$P_{tet\text{-}off}$-STE11$^{\Delta N467}$* mutant causes a significant increase in the levels of TNFα production when compared to the wild-type [25]. As our results in Fig 2.3A-C show altered levels of multiple immunogenic epitopes in the cell wall, we next sought to assess the sole impact that ß(1,3)-glucan unmasking has on the previously observed *in vitro* immune activation of macrophages. Thus, we performed an antibody blocking assay using an anti-dectin-1 antibody to block the dectin-1 receptor, a prominent ß(1,3)-glucan receptor, on RAW264.7 macrophages and subsequently assessed the levels of TNFα production following co-incubation with UV-inactivated wild-type or *STE11/$P_{tet\text{-}off}$-STE11$^{\Delta N467}$* cells. In accordance with our previous findings, co-incubation with RAW264.7 macrophages with *STE11/$P_{tet\text{-}off}$-STE11$^{\Delta N467}$* cells caused a significant increase in TNFα production when compared to cells co-incubated with the wild-type control ($p<0.0001$) (Fig 2.3D). However, in macrophage samples pretreated with the anti-dectin-1 antibody there was a significant reduction in the levels of TNFα production upon co-incubation with the *STE11/$P_{tet\text{-}off}$-STE11$^{\Delta N467}$* strain ($p<0.0001$). Yet, it is important to note that the observed reduction was not a complete restoration to wild-type levels of TNFα production. This shows that although dectin-1 mediated immune signaling is required for TNFα production following co-incubation with unmasked hyperactive *STE11$^{\Delta N467}$* cells, there are also likely independent stimuli aside from exposed ß(1,3)-glucan that are contributing to the increased immune activation induced by the *STE11/$P_{tet\text{-}off}$-STE11$^{\Delta N467}$* mutant. Thus, although this experiment does not rule out an important role for the other PAMPs, it does show that ß(1,3)-glucan exposure is required for hyperactive *STE11$^{\Delta N467}$*-induced TNFα production by macrophages.

Hyperactive *STE11$^{\Delta N467}$* induced ß(1,3)-glucan unmasking is specific to the yeast morphology of *C. albicans*.

It is clear that hyperactive *STE11$^{\Delta N467}$* expression causes ß(1,3)-glucan unmasking in an immunogically relevant manner in yeast cells (Fig 2.3). However, during systemic infection there is a heterogenous population of both yeast and hyphal cells that are necessary for *C. albicans* pathogenesis [36, 37]. Therefore, we tested whether hyperactive *STE11$^{\Delta N467}$* expression caused ß(1,3)-glucan exposure on hyphal cells as well. To achieve this, hyphal formation was induced in wild-type and *STE11/P$_{tet\text{-}off}$-STE11$^{\Delta N467}$* strains, and ß(1,3)-glucan exposure was measured by immunofluorescence microscopy with anti-ß(1,3)-glucan antibody staining (Fig 2.3E&F). Quantification of staining using ImageJ showed no significant difference in the levels of ß(1,3)-glucan exposure between the wild-type and *STE11/P$_{tet\text{-}off}$-STE11$^{\Delta N467}$* strains (Fig 2.3F), demonstrating that the impact that hyperactivate *STE11$^{\Delta N467}$* expression has on unmasking is specific to the yeast morphology of *C. albicans*.

Hyperactive *STE11$^{\Delta N467}$* induces ß(1,3)-glucan unmasking through the canonical Ste11-Hst7-Cek1 signal cascade.

Since hyperactivation of *STE11$^{\Delta N467}$* induces changes in the levels of multiple immunogenic epitopes within the cell wall, we next sought to identify the mechanism driving these changes. We had previously shown that Ste11$^{\Delta N467}$ causes downstream activation of the MAPK Cek1 [25], which led us to hypothesize that signal transduction is propagated through this protein. To test this, we created a *cek1ΔΔ* mutation in a CRISPR-Cas9-competent wild-type strain (SC5314 *LEU2/leu2Δ*) and a *STE11/P$_{tet\text{-}off}$-STE11$^{\Delta N467}$* mutant in the same wild-type background to assess the impact of Cek1 on unmasking. Immunofluorescent staining using an anti-ß(1,3)-glucan antibody and subsequent flow cytometry revealed that a *cek1ΔΔ* mutation in the wild-type background did not impact unmasking (Fig 2.4A). However, a *STE11/P$_{tet\text{-}off}$-STE11$^{\Delta N467}$cek1ΔΔ* double mutant successfully blocked the unmasking induced by hyperactive Ste11$^{\Delta N467}$ alone, which was restored upon reintroduction of a functional *CEK1* gene under the control of the

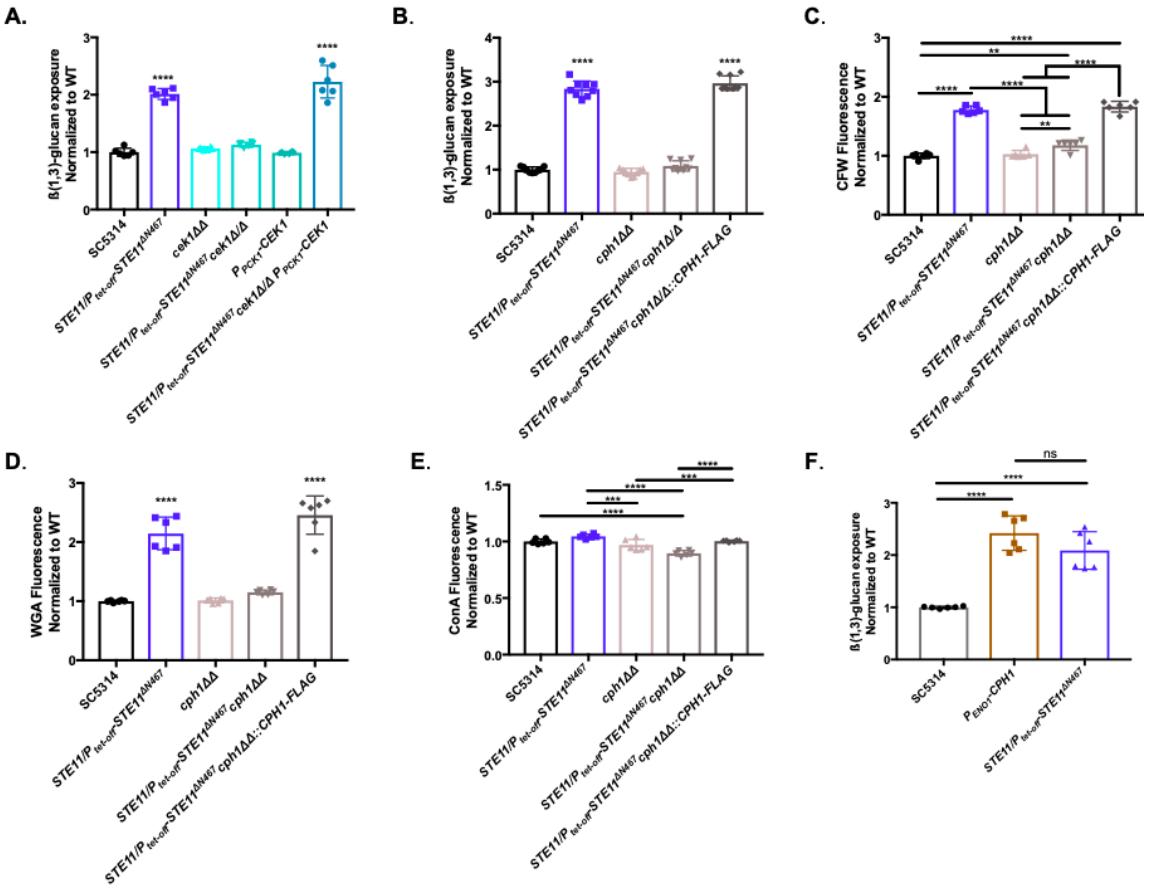


Fig 2.4: Disruption of downstream components in the Cek1 MAPK pathway blocks ß(1,3)-glucan unmasking by hyperactive *STE11*$^{\Delta N467}$.
(A-B) Overnight cultures of cells were stained with anti-ß(1,3)-glucan antibody and a phycoerythrin-conjugated secondary antibody followed by flow cytometry analysis to assess the levels of ß(1,3)-glucan exposure. (A) ß(1,3)-glucan unmasking of *cek1ΔΔ* mutants. (B) ß(1,3)-glucan unmasking of *cph1ΔΔ* mutants. (C-E) Overnight cultures of cells were stained with calcofluor white (CFW), fluorescein conjugated wheat germ agglutinin (WGA) and Alexa Fluor 647 conjugated concanavalin A (ConA) to assess total chitin, surface exposed chitin, and mannan levels, respectively, of *cph1ΔΔ* mutants. (C) CFW staining, (D) WGA staining and (E) ConA staining. (F) Overnight cultures were stained to assess ß(1,3)-glucan unmasking of the P_{ENO1}-*CPH1* overexpression mutant. For all stains, three biological replicates with 2-3 technical replicates were analyzed by flow cytometry for each sample. (**p<0.01, ***p<0.001, ****p<0.0001, by one-way ANOVA).

constitutive phosphoenolpyruvate carboxylase promoter *(P_{PCK1}-CEK1)*. Therefore, hyperactive Ste11$^{\Delta N467}$ induces unmasking through the MAPK Cek1.

Interestingly, while the data presented supports the role of Cek1 in mediating hyperactive Ste11$^{\Delta N467}$ induced unmasking, our findings are in disagreement with other studies in which *CEK1* was deleted. Specifically, it has been shown that a homozygous deletion of *CEK1* in the CAI4 wild-type background is sufficient to induce unmasking on its own [38, 39]. Although the *cek1ΔΔ* mutant used in our study did not induce this same phenotype, it is important to note that it was made in the SC5314 strain background, rather than CAI4. Thus, to determine if the observed differences associated with a *cek1ΔΔ* mutation were due to differences in the wild-type strains used, we created a *cek1ΔΔ* mutant in the CAI4 background using CRISPR-Cas9. Consistent with the phenotype observed during disruption in the SC5314 background, *CEK1* deletion in the CAI4 laboratory strain did not impact unmasking (S2.6 Fig), demonstrating that strain variability (of the strains in our possession) does not account for the reported differences in unmasking caused by *cek1ΔΔ*.

Our data implicate Cek1 as the downstream MAPK mediating hyperactive *STE11$^{\Delta N467}$* induced unmasking, yet it was still unclear if signal transduction to Cek1 was mediated through the canonical Ste11-Hst7-Cek1 signal cascade. To address this, we created a *hst7ΔΔ* mutation in both the wild-type and *STE11/$P_{tet\text{-}off}$-STE11$^{\Delta N467}$* strains. Similar to our observations using *cek1ΔΔ* mutants, deletion of *HST7* in the *STE11/$P_{tet\text{-}off}$-STE11$^{\Delta N467}$* strain (*STE11/$P_{tet\text{-}off}$-STE11$^{\Delta N467}$hst7ΔΔ*) completely restored unmasking to wild-type levels (S2.7 Fig). Thus, hyperactive Ste11$^{\Delta N467}$-induced unmasking is mediated via the canonical Ste11-Hst7-Cek1 signal transduction pathway.

Cek1 induces ß(1,3)-glucan unmasking through the transcription factor Cph1.

Cek1 propagates signal transduction through two main transcription factors, Cph1 and Ace2 [32, 40-43]. Although our findings have shown that Cek1 is acting to cause ß(1,3)-glucan unmasking, it was not clear which downstream transcription factor is required, as both Cph1 and Ace2 activation impact cell wall architecture [24, 32, 42, 44-46]. Our prior

RNA sequencing results revealed that *CPH1*, but not *ACE2*, transcript levels are upregulated in a *STE11/P$_{tet\text{-}off}$-STE11$^{\Delta N467}$* mutant [25]. Therefore, we hypothesized that Cek1 mediates *STE11$^{\Delta N467}$*-induced unmasking through Cph1. To this end, we created a *cph1ΔΔ* mutation in both the wild-type and *STE11/P$_{tet\text{-}off}$-STE11$^{\Delta N467}$* strains to epistatically test the role of Cph1 in unmasking. Immunofluorescent staining for exposed ß(1,3)-glucan and subsequent flow cytometry revealed that a *STE11/P$_{tet\text{-}off}$-STE11$^{\Delta N467}$cph1ΔΔ* double mutant returns ß(1,3)-glucan exposure to wild-type levels, and that unmasking is restored in the double mutant upon complementation with a C-terminally FLAG-tagged *CPH1* gene (Fig 2.4B). Furthermore, staining for other immunogenic epitopes in the cell wall revealed that the *STE11/P$_{tet\text{-}off}$-STE11$^{\Delta N467}$cph1ΔΔ* mutant also restored calcofluor white and wheat germ agglutinin binding to wild-type levels (Fig 2.4C&D), demonstrating that Cph1 is the transcription factor mediating changes for both the ß(1,3)-glucan and chitin exposure observed during *STE11$^{\Delta N467}$* expression. Interestingly, concanavalin A staining of a *STE11/P$_{tet\text{-}off}$-STE11$^{\Delta N467}$* mutant in the SC5314 wild-type background exhibited no changes in mannan levels compared to the wild-type (Fig 2.4E), but did show a modest reduction upon *CPH1* deletion. Altogether, our data demonstrate that hyperactive Ste11$^{\Delta N467}$ functions through Cph1 to mediate both chitin and ß(1,3)-glucan exposure, but it is not clearly involved in inducing changes in cell wall mannan levels.

As it appears that Ste11$^{\Delta N467}$-induced hyperactivation of Cph1 is sufficient to induce unmasking, we further hypothesized that overexpression of *CPH1* on its own would increase ß(1,3)-glucan exposure. To this end, we created a *CPH1* overexpression strain by placing a third allele of *CPH1* under the control of the constitutive enolase (*ENO1*) promoter (*P$_{ENO1}$-CPH1*). Immunofluorescent staining revealed that the *P$_{ENO1}$-CPH1* mutant exhibited a significant increase in ß(1,3)-glucan exposure when compared to the wild-type (Fig 2.4F) ($p<0.0001$) and had similar levels of unmasking to the *STE11/P$_{tet\text{-}off}$-STE11$^{\Delta N467}$* mutant ($p=0.1362$). Therefore, it appears that hyperactivation of *CPH1* alone is sufficient to induce ß(1,3)-glucan unmasking.

Deletion of *CPH1* in a hyperactive *STE11$^{\Delta N467}$* background blocks macrophage immune activation and restores virulence during systemic infection in mice.

Hyperactive *STE11$^{\Delta N467}$* is sufficient to induce unmasking of ß(1,3)-glucan and chitin (Fig 2.4), increase TNFα production by RAW264.7 macrophages *in vitro* (Fig 2.3D), and attenuate virulence during a systemic infection model in mice (Fig 2.1A). As our data have shown that a *cph1ΔΔ* mutation in the *STE11/P$_{tet\text{-}off}$-STE11$^{\Delta N467}$* background is capable of blocking hyperactive Ste11$^{\Delta N467}$ induced exposure of both ß(1,3)-glucan and chitin, we further hypothesized that it will also reduce macrophage immune activation *in vitro*. To test this, *CPH1* knockout mutants were UV-irradiated and co-incubated with RAW264.7 macrophages, and TNFα secretion was assessed by ELISA (Fig 2.5A). This experiment revealed that introduction of the *cph1*ΔΔ mutation into the *STE11/P$_{tet\text{-}off}$-STE11$^{\Delta N467}$* strain reduced TNFα secretion from murine macrophages to wild-type levels. These data suggested that loss of *CPH1* would also be sufficient to restore virulence of the *STE11/P$_{tet\text{-}off}$-STE11$^{\Delta N467}$* strain during systemic infections in mice. To test this, mice were intravenously injected with 1x10^6 CFU of the wild-type, *STE11/P$_{tet\text{-}off}$-STE11$^{\Delta N467}$*, *STE11/P$_{tet\text{-}off}$-STE11$^{\Delta N467}$cph1ΔΔ* or *STE11/P$_{tet\text{-}off}$-STE11$^{\Delta N467}$cph1ΔΔ::CPH1-Flag* reintegrate strains. Kidneys were then harvested 4 d.p.i. to assess fungal burden. As shown in Fig 2.5B, mice infected with the *STE11/P$_{tet\text{-}off}$-STE11$^{\Delta N467}$cph1ΔΔ* double mutant had a significant increase in fungal burden toward wild-type levels when compared to the *STE11/P$_{tet\text{-}off}$-STE11$^{\Delta N467}$* parent strain (p=0.0009). Furthermore, fungal burden attenuation was restored upon complementation with a C-terminally flag-tagged *CPH1* allele. Therefore, *CPH1* deletion in a hyperactive *STE11$^{\Delta N467}$* background is capable of restoring fungal burden toward wild-type levels during a systemic infection in mice.

Cph1 functions in a positive feedback loop to increase hyperactivation of the upstream MAPK Cek1.

RNA sequencing experiments that compared transcriptomes of the *STE11/P$_{tet\text{-}off}$-STE11$^{\Delta N467}$* strain and the wild-type control revealed that during *STE11$^{\Delta N467}$* expression there was increased expression of Cph1, Cek1, and some components of the Cek1 MAPK

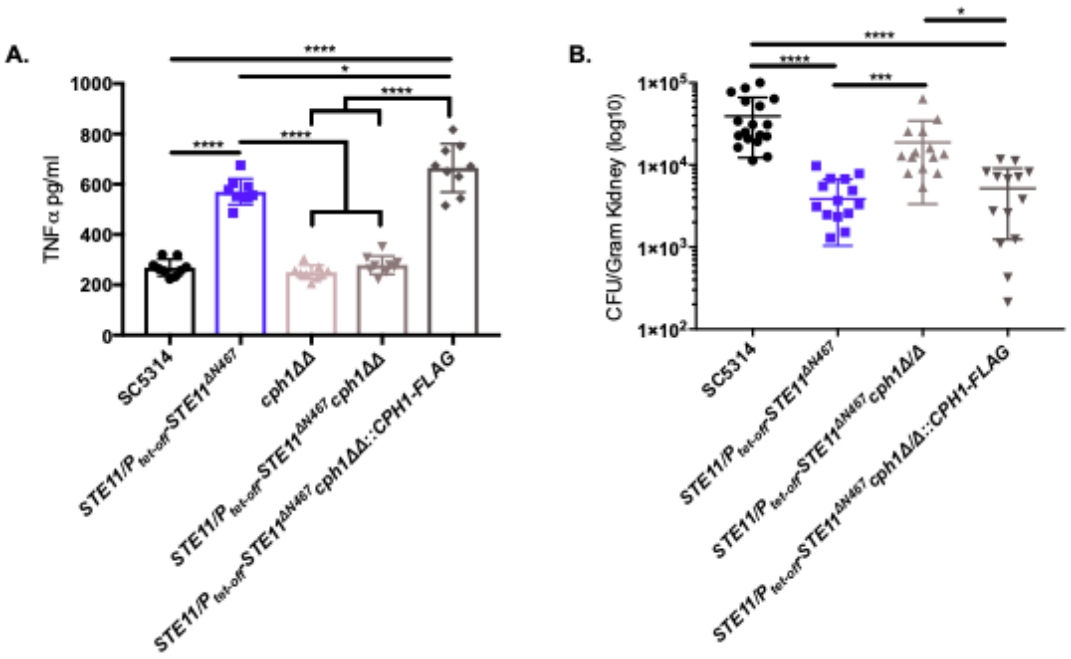


Fig 2.5: *CPH1* deletion reduces *STE11*$^{\Delta N467}$ induced macrophage TNFα secretion and partially restores virulence during systemic infection in mice.

(A) TNFα secretion by RAW264.7 macrophages. RAW264.7 murine macrophages and UV-inactivated *C. albicans* strains were co-incubated for 4 hours at a multiplicity of infection (M.O.I.) of 10. Culture supernatant was subsequently filtered through a 0.22μm filter and assessed via ELISA analysis to determine secreted TNFα levels. (*p = 0.0063, ****p<0.0001, by one-way ANOVA)(n = 3 biological replicates with 3 technical replicates for each sample). (B) Kidney fungal burden 4 d.p.i. during infection with *cph1ΔΔ* mutants. ICR mice were intravenously injected with 1x10^6 cells of *C. albicans* wild-type (SC5314), *STE11/P*$_{tet\text{-}off}$*-STE11*$^{\Delta N467}$, *STE11/P*$_{tet\text{-}off}$*-STE11*$^{\Delta N467}$*cph1ΔΔ* or the *STE11/P*$_{tet\text{-}off}$*-STE11*$^{\Delta N467}$*cph1ΔΔ::CPH1-Flag* strain and kidneys were harvested 4 d.p.i to assess fungal burden. (n = 7-8 mice)(*p<0.05, ***p<0.001, ****p<0.0001, by Kruskal-Wallis test with Dunn's multiple comparisons post-hoc analysis.).

pathway that sit upstream of the transcription factor and kinase [25]. Specifically, the cell wall sensors *OPY2* and *DFI1*, both of which have been shown to impact Cek1 activation [47-49], were upregulated. As our results indicate that Cph1 is driving unmasking of both ß(1,3)-glucan and chitin (Figs 2.4B&D), the increased expression of these upstream components of the signaling pathway, and increased expression of *CPH1* itself, suggests the possibility that Cph1 induces a positive feedback loop to amplify its own transcriptional response. This is further supported by chip-ChIP data showing that Cph1 binds directly to the promoters of *CEK1* and *OPY2*, as well as to its own promoter [50]. We therefore assessed the impact that a *cph1ΔΔ* disruption has on activation of its own upstream MAPK, Cek1. To do this, we measured the levels of the phosphorylated (active) form of Cek1 in the wild-type, *STE11/P$_{tet-off}$-STE11$^{\Delta N467}$*, *cph1ΔΔ, STE11/P$_{tet-off}$-STE11$^{\Delta N467}$cph1ΔΔ* and *STE11/P$_{tet-off}$-STE11$^{\Delta N467}$cph1ΔΔ::CPH1-Flag* reintegrate strains. As shown in Figs 2.6A&B, activation of Cek1 was ~33-fold higher in the *STE11/P$_{tet-off}$-STE11$^{\Delta N467}$* strain during *STE11$^{\Delta N467}$* induction when compared to the wild-type. However, phosphorylated Cek1 levels were significantly reduced in the *STE11/P$_{tet-off}$-STE11$^{\Delta N467}$cph1ΔΔ* double mutant (~5.77-fold over wild-type) compared to its *STE11/P$_{tet-off}$-STE11$^{\Delta N467}$* parent strain ($p<0.0001$). Therefore, it appears that expression of the downstream transcription factor *CPH1* is necessary for full hyperactivation of Cek1 in the *STE11/P$_{tet-off}$-STE11$^{\Delta N467}$* strain and suggests that a loop is necessary for the full activation of the transcriptional circuit. It was of interest to note that the level of total Cek1 did not change, indicating that the increase in phosphorylated Cek1 was not simply a result of increased levels of the Cek1 protein overall. This is further supported by the observation that *CPH1* overexpression on its own is also sufficient for impacting the activation of its upstream MAPK, Cek1, but does not change the total levels of Cek1 observed. Western blot analysis of phosphorylated-Cek1 levels demonstrated a 3.30-fold increase in Cek1 activation in the *P$_{ENO1}$-CPH1* mutant compared to the wild-type (Figs 2.6C & D) ($p<0.0001$). Thus, it appears that Cph1 induces a positive feedback loop to amplify signal transduction and regulate the magnitude of its corresponding phenotypic modifications.

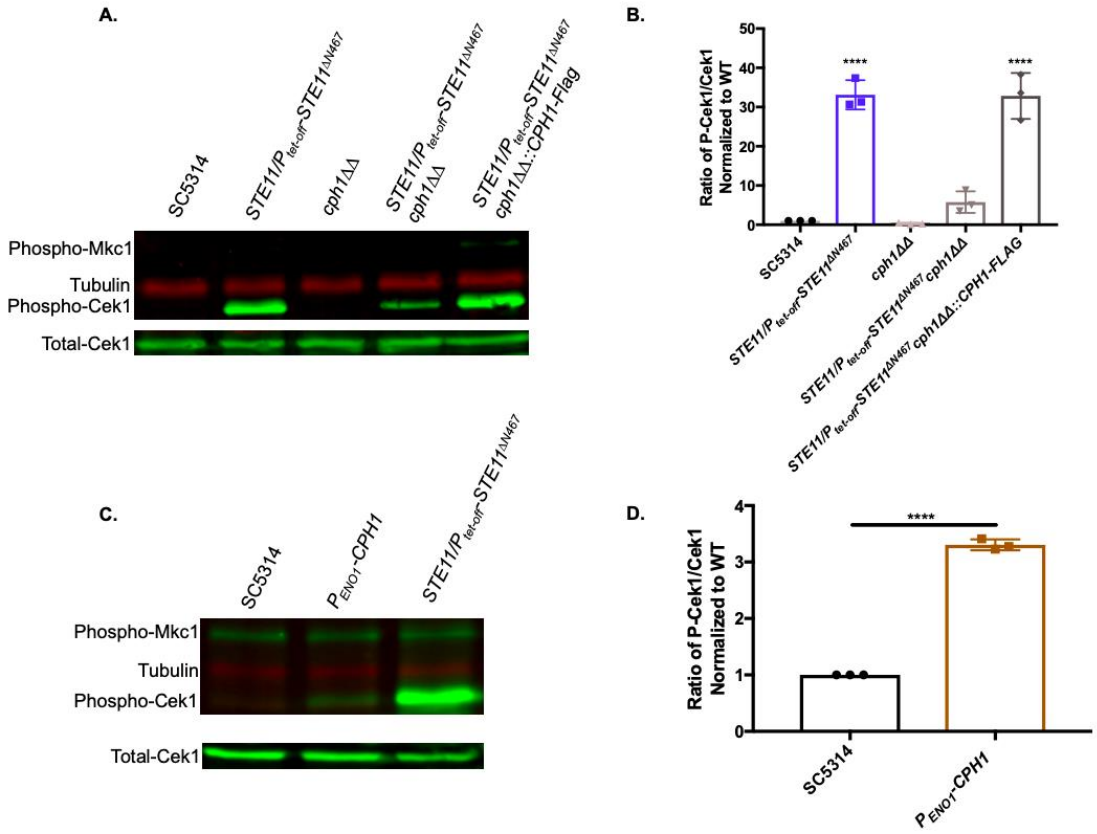


Fig 2.6: Cph1 mediates activation of its upstream MAPK, Cek1.
Proteins were harvested from cells grown to mid-log phase for western blot analysis. Membranes were blotted using an anti-P44/42 antibody for phosphorylated Cek1 detection and an anti-Cek1 antibody for total Cek1 detection. (A) Western blot showing active and total Cek1 levels in *cph1*ΔΔ deletion mutants. (B) Fold change relative to the wild-type in Phosphorylated-Cek1 to total Cek1 levels for all *CPH1* deletion mutants. (n = 3 biological replicates assessed on 3 separate western blots) (****p<0.0001, by one-way ANOVA with Tukey's post hoc analysis). (C) Western blot showing active and total Cek1 levels for the P_{ENO1}-*CPH1* overexpression mutant. (D) Fold change relative to the wild-type in Phosphorylated-Cek1 to total Cek1 levels for the P_{ENO1}-*CPH1* overexpression mutant. (n = 3 biological replicates assessed on 3 separate western blots) (****p<0.0001, by students t-test).

The cell wall sensor Dfi1 is needed for Cph1-mediated ß(1,3)-glucan unmasking.

Cph1 acts in a feedback loop that amplifies activation of Cek1. Our previous RNA sequencing results showed increased transcript levels of two cell wall sensors that have been reported to impact Cek1 activation, *DFI1* and *OPY2,* during hyperactive *STE11*$^{\Delta N467}$ expression [25]. We therefore hypothesized that these cell wall sensors are also needed for full loop stimulation during Cph1 activation. To address this, we created individual *dfi1ΔΔ* and *opy2ΔΔ* mutants in both the wild-type and *STE11/P*$_{tet\text{-}off}$*-STE11*$^{\Delta N467}$ strains. Combinatorial cell wall sensor mutants in both strain backgrounds were also created to account for any redundancy in signal transduction through the pathway. Subsequent immunofluorescent staining and flow cytometry revealed that a *STE11/P*$_{tet\text{-}off}$*-STE11*$^{\Delta N467}$*opy2ΔΔ* double mutant had no impact on unmasking when compared to *STE11/P*$_{tet\text{-}off}$*-STE11*$^{\Delta N467}$ (Fig 2.7A) (p=0.8607). However, a *STE11/P*$_{tet\text{-}off}$*-STE11*$^{\Delta N467}$*dfi1ΔΔ* double mutant was partially suppressed for unmasking compared to the *STE11/P*$_{tet\text{-}off}$*-STE11*$^{\Delta N467}$ strain (Fig 2.7B) (p<0.0001). Furthermore, a *STE11/P*$_{tet\text{-}off}$*-STE11*$^{\Delta N467}$*dfi1ΔΔopy2ΔΔ* triple mutant was not further reduced for unmasking when compared to the *STE11/P*$_{tet\text{-}off}$*-STE11*$^{\Delta N467}$*dfi1ΔΔ* double mutant (p=0.9684), demonstrating that these two cell wall sensors do not play redundant or additive roles in Cph1 mediated feedback into the Cek1 MAPK pathway.

Interestingly, during reintroduction of *DFI1* under the control of the constitutive enolase promoter (*P*$_{ENO1}$*-DFI1*) into the *STE11/P*$_{tet\text{-}off}$*-STE11*$^{\Delta N467}$*dfi1ΔΔopy2ΔΔ* triple mutant, we observed an increase in ß(1,3)-glucan unmasking when compared to *STE11/P*$_{tet\text{-}off}$*-STE11*$^{\Delta N467}$ alone (Fig 2.7B). Thus, we were interested in determining the impact that increased *DFI1* expression may have on unmasking during Cph1 hyperactivation. To this end, we induced *DFI1* overexpression by placing it under the control of the constitutive enolase promoter (*P*$_{ENO1}$*-DFI1*) in both the wild-type and *STE11/P*$_{tet\text{-}off}$*-STE11*$^{\Delta N467}$ background strains. In doing so, these mutants now harbored three alleles of *DFI1* in their genome (both wild-type alleles and the *P*$_{ENO1}$*-DFI1* allele at the enolase locus). Immunofluorescent staining and flow cytometry of these mutants revealed that overexpression of *DFI1* on its own in the wild-type background is insufficient to induce

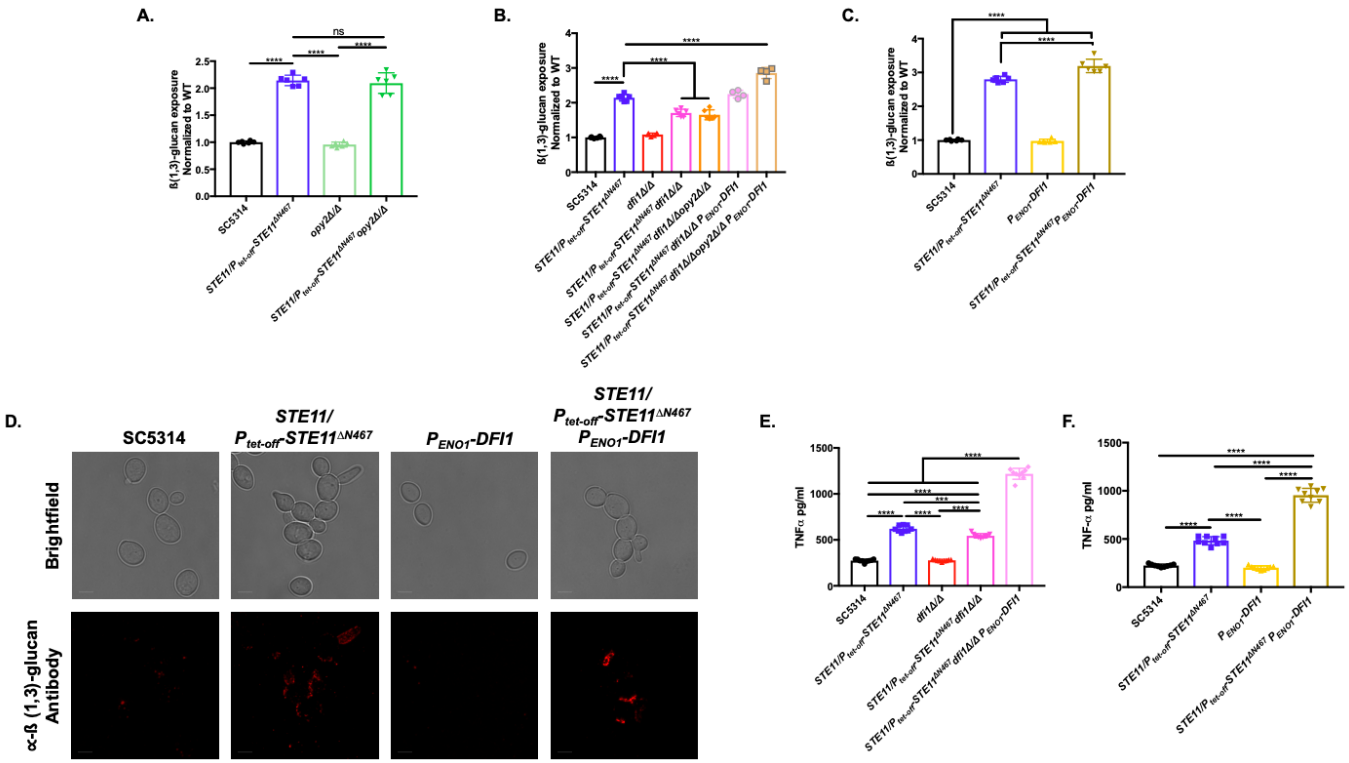


Fig 2.7: *DFI1* expression levels partially mediate ß(1,3)-glucan unmasking and macrophage TNFα secretion induced by hyperactive *STE11*$^{\Delta N467}$ expression.

(A-D) Overnight cultures of cells were stained with anti-ß(1,3)-glucan antibody and a phycoerythrin-conjugated secondary antibody for flow cytometry analysis or a Cy3-conjugated secondary antibody for confocal microscopy to assess the levels of ß(1,3)-glucan exposure. (A) ß(1,3)-glucan unmasking of *opy2ΔΔ* mutants. (B) ß(1,3)-glucan unmasking of *dfi1ΔΔ* mutants. (C) ß(1,3)-glucan unmasking of P_{ENO1}-*DFI1* overexpression mutants. (****p<0.0001, by one-way ANOVA with Tukey's post hoc analysis)(n = 3 biological replicates with 2-3 technical replicates were run for each sample.. (D) Representative microscopy images of ß(1,3)-glucan exposure of *DFI1* overexpression mutants. The scale bar indicates 10μm. (E-F) The impact of altered *DFI1* expression levels on macrophage TNFα secretion was assessed via co-incubation of RAW264.7 murine macrophages with UV-inactivated *DFI1* mutants for 4 hours at a multiplicity of infection (M.O.I.) of 10. Culture supernatant was subsequently filtered through a 0.22um filter and assessed via ELISA analysis to determine secreted TNFα levels. (E) TNFα levels during co-incubation with RAW264.7 and *dfi1ΔΔ* mutants. (F) TNFα levels during co-incubation with RAW264.7 and P_{ENO1}-*DFI1* overexpression mutants. (***p<0.0005, ****p<0.0001, by one-way ANOVA with Tukey's post hoc analysis) (n = 3 biological replicates with 3 technical replicates for each sample).

unmasking (Fig 2.7C)(p=0.9771). However, *DFI1* overexpression in the *STE11/P$_{tet\text{-}off}$-STE11$^{\Delta N467}$* parent strain, when hyperactivation of the Cek1 MAPK pathway is induced, further increased the observed unmasking when compared to the *STE11/P$_{tet\text{-}off}$-STE11$^{\Delta N467}$* mutant that only harbors the wild-type alleles of *DFI1* ($p<0.0001$). It is important to note that we have previously shown that Ste11$^{\Delta N467}$-induced unmasking occurs within cells in the yeast morphology (Fig 2.3F) [26], but a *dfi1ΔΔ* mutation has also been previously shown to impact invasion in embedded agar, a process that is largely mediated by hyphal formation [48, 49]. Therefore, it was important to assess whether overexpression of *DFI1* under stimulating conditions was inducing a morphological transition into hyphae that may account for the observed increase in unmasking. Immunofluorescent staining and subsequent confocal microscopy revealed that this is not the case, and that unmasking is occurring within the yeast population (Fig 2.7D). Thus, it appears that the level of Dfi1 in the cell wall of *C. albicans* yeast cells can impact the subsequent ß(1,3)-glucan unmasking induced by activated Cph1.

DFI1 expression levels impact macrophage TNFα production *in vitro.*

Due to the observed impact that *DFI1* expression has on *STE11$^{\Delta N467}$*-induced unmasking, we next wished to assess its impact on murine macrophage immune activation. Co-incubation with RAW264.7 macrophages and *C. albicans DFI1* mutants showed that, similar to unmasking, a *STE11/P$_{tet\text{-}off}$-STE11$^{\Delta N467}$dfi1ΔΔ* double mutant was able to partially restore TNFα production to wild-type levels (Fig 2.7E). Furthermore, overexpression of *DFI1* on a third allele in the hyperactive *STE11$^{\Delta N467}$* background was also sufficient to significantly increase supernatant TNFα levels when compared to its *STE11/P$_{tet\text{-}off}$-STE11$^{\Delta N467}$* parent strain (Fig 2.7F)($p<0.0001$). Moreover, in contrast to what was observed for ß(1,3)-glucan staining alone, TNFa-secretion was increased in the *STE11/P$_{tet\text{-}off}$-STE11$^{\Delta N467}$* strain when *DFI1* was overexpressed, even when the two native *DFI1* copies were deleted (compare Fig 2.7B to 2.7E).

Dfi1 stimulation impacts ß(1,3)-glucan unmasking through an alternative pathway than the Cek1 MAPK pathway. It is clear that Dfi1 impacts ß(1,3)-glucan unmasking and is needed to achieve the full levels of unmasking observed during expression of a hyperactive *STE11*$^{\Delta N467}$ allele. As Dfi1 has previously been shown to impact activation of the MAPK Cek1, we hypothesized that Dfi1 impacted unmasking levels by serving as a node in the Cph1-mediated positive feedback loop in the Cek1 MAPK pathway. In this model, altered expression levels of *DFI1* would correlate with a corresponding change in the levels of phosphorylated (activated) Cek1. However, neither *DFI1* deletion (Fig 2.8A) nor *DFI1* overexpression (Fig 2.8B) mutants showed any impact on Cek1 activation. Thus, it appears that Dfi1 mediates unmasking via a parallel, unidentified signaling pathway that is activated during hyperactive *STE11*$^{\Delta N467}$ expression.

Discussion

We have previously shown that overexpression of a single allele of a hyperactive *STE11*$^{\Delta N467}$ mutant increases ß(1,3)-glucan exposure and attenuates virulence in a mouse model of systemic candidiasis [25, 26]. In this report we demonstrate that the previously reported virulence attenuation is primarily driven by the host immune response, as cyclophosphamide induced immunosuppression in mice largely negated the previously observed decrease in kidney fungal burden 4 days post infection (Figs 2.1 & 2.2). Furthermore, we found that while neutrophils play a major role in this fungal clearance, other immune cells appear to be involved in recognizing and responding to infection with an unmasked hyperactive *STE11*$^{\Delta N467}$ mutant, as 1A8 neutrophil depletion was unable to completely restore fungal colonization levels to those observed during cyclophosphamide induced immunosuppression. Our previous findings also showed that *STE11*$^{\Delta N467}$ expression leads to increased phosphorylation levels of the MAPK Cek1 [25, 26]. Here, we have expanded on these findings and show that Ste11$^{\Delta N467}$ functions through the transcription factor *CPH1* to increase both ß(1,3)-glucan and chitin exposure (Fig 2.4). *CPH1* disruption reduced Ste11$^{\Delta N467}$ induced unmasking and TNFα secretion by murine macrophages to wild-type levels, as well as partially restored virulence during systemic

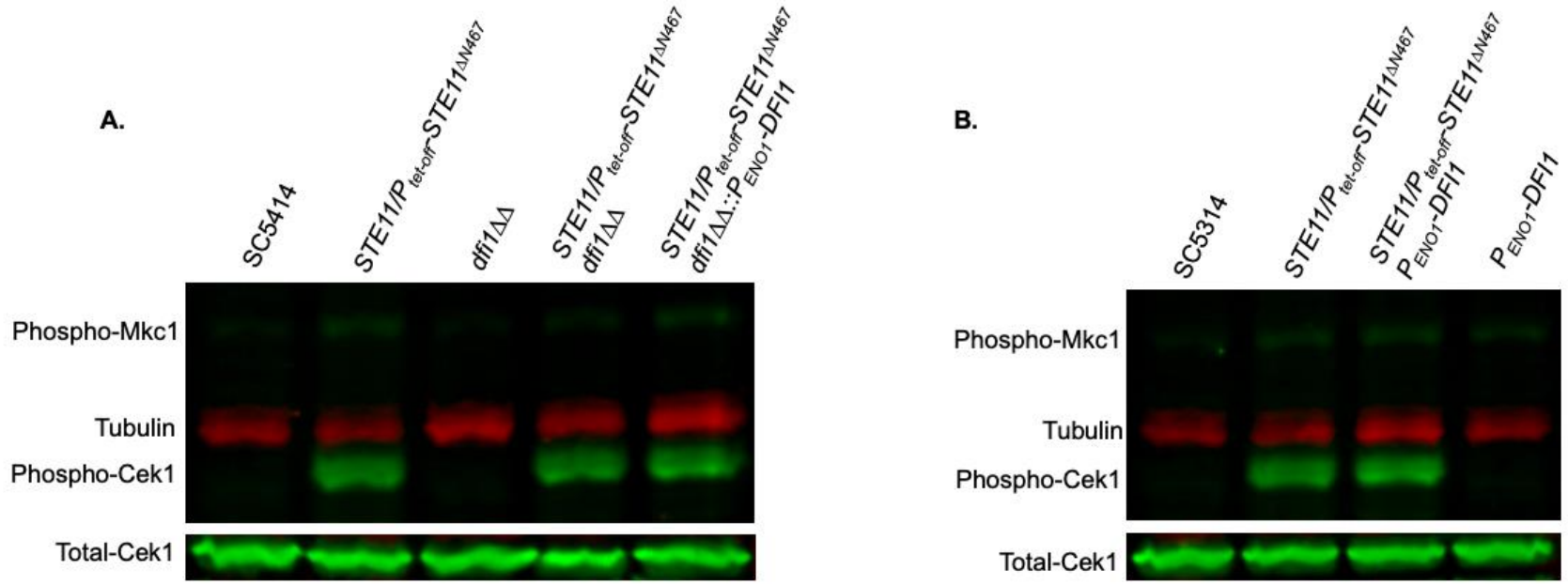


Fig 2.8: Dfi1 does not mediates activation of the MAPK Cek1.
Proteins were harvested from cells grown to mid-log phase for western blot analysis. Membranes were blotted using an anti-P44/42 antibody for phosphorylated Cek1 detection and an anti-Cek1 antibody for total Cek1 detection. (A) Western blot showing active and total Cek1 levels in *DFI1* deletion mutants. (B) Western blot showing active and total Cek1 levels in *DFI1* overexpression mutants.

infection in mice. Moreover, we have found that Cph1 functions in a positive feedback loop that is necessary to achieve the total activation of Cek1 observed during *STE11*$^{\Delta N467}$ expression (Fig 2.6), and that a parallel, as of yet unidentified, pathway is activated via the cell wall sensor Dfi1 to induce the full levels of ß(1,3)-glucan unmasking observed during *STE11*$^{\Delta N467}$ expression (Figs 2.7 & 2.8).

Studies in *C. albicans* have demonstrated that echinocandin application and certain mutations in genes that impact proper cell wall construction, such as *ENG1* disruption or deletions of the phosphatidylserine synthase gene *CHO1* and the glycosyltransferase gene *KRE5*, induce ß(1,3)-glucan unmasking and attenuate virulence during systemic infection models [5, 6, 18, 51, 52]. Furthermore, it has been shown that even different *C. albicans* strains vary in the baseline level of unmasking [53]. From these findings a clear correlation between *C. albicans* unmasking and immune activation has been established *in vitro* [6, 21, 51]. This relationship is further supported from studies investigating *H.* capsulatum, where unmasking induced by deletion of the endo-1,3-beta-glucanse *ENG1* was shown to attenuate virulence *in vivo* in a dectin-1 dependent manner [17]. Yet, direct interpretation of the impact of unmasking of *C. albicans* cells *in vivo* has largely been confounded by the additional cidal effects of echinocandin application, substantial secondary fitness defects with genetic mutants, such as an ethanolamine auxotrophy in the *cho1ΔΔ* [54], and additional factors that are variable between *C. albicans* strains. Our results indicate that the *STE11/P*$_{tet\text{-}off}$*-STE11*$^{\Delta N467}$ mutant is capable of causing ß(1,3)-glucan unmasking, increasing both total chitin levels and exposure and attenuating virulence in a host immune system dependent manner, without inducing gross secondary fitness defects that impact its ability to colonize the host. This is apparent in the restoration of kidney fungal burden from the observed ~33-fold decrease during systemic infection with the *STE11/P*$_{tet\text{-}off}$*-STE11*$^{\Delta N467}$ strain in immunocompetent mice (Fig 2.1A), to only an ~2-fold difference when compared to the wild-type in cyclophosphamide immunosuppressed mice (Fig 2.2B). Although a significant difference in fungal burden still exists during cyclophosphamide induced immunosuppression, suggesting a modest fitness defect, the ability of immunodepletion to restore fungal burden to the nearly wild-type levels for the *STE11/P*$_{tet\text{-}}$

$_{off}$-*STE11*$^{\Delta N467}$ mutant suggests that the virulence attenuation is primarily host immune system driven. We therefore propose this pathway as an applicable *in vivo* model to analyze how the host immune system recognizes and responds to unmasked *C. albicans* cells to mount an immune response.

In application of this model, we have shown that depletion of neutrophils alone is not sufficient to restore fungal burden of an unmasked hyperactive *STE11*$^{\Delta N467}$ mutant to wild-type levels (Fig 2.2D). Neutrophil depletion was able to change the ~33-fold decrease in fungal burden caused by hyperactive *STE11*$^{\Delta N467}$ expression (Fig 2.1A) to an ~6-fold difference, indicating a major role for these immune cells in clearing the unmasked fungi. However, the inability of neutrophil depletion to restore fungal colonization between these strains to the ~2-fold difference observed during cyclophosphamide treatment suggests that other immune cells are involved in facilitating the enhanced fungal clearance caused by *STE11*$^{\Delta N467}$ expression. Multiple immune cells, aside from neutrophils, harbor receptors capable of recognizing exposed ß(1,3)-glucan and chitin and initiating an immune response. These cell types include important immune modulators such as monocytes, macrophages, dendritic cells and host epithelial cells [7, 14, 34, 38, 55]. Our data have already shown increased immune activation of murine macrophages *in vitro* in response to exposure to unmasked *STE11*$^{\Delta N467}$ cells (Fig 2.3D), and it is likely that tissue resident and infiltrating macrophages play a similar role in recognizing and initiating an immune response against unmasked fungal cells within the kidney. It is possible that unmasked fungi are more readily recognized by tissue resident macrophages, which likely phagocytose to both kill and to establish a more rapid and robust cytokine response that facilitates recruitment of other immune cells, like neutrophils, to the site of infection. However, it is thus far unclear if neutrophils also more readily recognize unmasked fungi to increase their killing efficiency, or whether they are simply recruited more quickly to the site of infection by enhanced recognition of unmasked fungi by tissue resident immune cells. Consequently, more work is needed to understand the interplay within the host immune system in responding to systemic infections with unmasked *C. albicans* cells.

To elucidate how hyperactive *STE11$^{\Delta N467}$* expression increases ß(1,3)-glucan exposure, we have shown that deletion of either the MAPKK *HST7* or the MAPK *CEK1* in a hyperactive *STE11$^{\Delta N467}$* mutant background effectively blocks ß(1,3)-glucan unmasking (Fig 2.4A and S2.7 Fig). This is expected in our current model, as *STE11$^{\Delta N467}$* expression shows a specific hyperactivation of Cek1 itself [26], and downstream regulons under the control of Cek1 have been shown to regulate cell wall architecture and repair [32, 42, 44, 46]. However, our data is in contradiction with results previously published on *CEK1*, where it was shown that a *cek1ΔΔ* mutation on its own results in increased unmasking [38, 39]. We have shown that this does not appear to be the consequence of strain variation between studies analyzing *cek1ΔΔ*-induced unmasking, as we were unable to observe increased ß(1,3)-glucan exposure in CIA4 *CEK1* deletion mutants (S2.6 Fig). However, lab to lab strain variations cannot be ruled out either.

The transcription factor Cph1 has previously been reported to be involved in phenotypic switching that allows mating [42], as well as in filament formation [44]. Here, we have shown that Cph1 causes unmasking downstream of hyperactive *STE11$^{\Delta N467}$* (Fig 2.4B), as well as when overexpressed on its own (Fig 2.4F). Furthermore, *CPH1* is also required for increased chitin exposure induced by hyperactive *STE11$^{\Delta N467}$* expression (Fig 2.4D). This suggests that altered expression of components within the Cph1 regulon are capable of inducing unmasking and impacting the overall architecture of the yeast cell wall. Cph1 has been shown to regulate multiple components involved in cell wall construction. Some of these include chitin synthase genes [56], as well genes involved in hyphal development [41, 56]. Our previous results, based on RNA sequencing and Als3 protein levels, revealed that expression of *STE11$^{\Delta N467}$* did not induce a strong yeast to hyphae transition (Fig 2.3E&F), but did show overexpression of several genes involved in regulating cell wall architecture [25, 26]. Among these genes, chitin synthase 3 (*CHS3*) and 7 (*CHS7*) were both found to be upregulated by *STE11$^{\Delta N467}$* expression [25]. Several studies have shown that areas of increased chitin deposition in hyphal cells co-localize with unmasked ß(1,3)-glucan foci [57, 58]. As we have observed an increase in both total chitin and exposed chitin within the yeast cells of *C. albicans*, it may be possible that Cph1

induces ß(1,3)-glucan unmasking by increased expression of chitin synthase genes that cause a disruption in the normal cell wall architecture of *C. albicans*. Alternatively, there has been a number of recent publications showing the impacts that secreted glucanases have on regulating unmasking. For example, the exo-1,3-beta-glucanase Xog1 has been implicated as the mechanism driving ß(1,3)-glucan masking in *C. albicans* in response to lactate exposure [19], while the endo-1,3-beta-glucanse Eng1 has recently been shown to predominantly regulate unmasking in *C. albicans* yeast cells [18]. With regards to the Cek1 pathway, our previous transcriptomics results have shown that *XOG1* was ~50-fold up-regulated and *ENG1* was ~2-fold down-regulated during hyperactive $STE11^{\Delta N467}$ expression [25]. It is possible that the reduced expression of *ENG1* may play a role in the observed unmasking. However, due to the observed up-regulation of Xog1, it seems unlikely that it is the sole mechanism driving increased ß(1,3)-glucan exposure during hyperactive $STE11^{\Delta N467}$ expression, although it is possible that it still may be contributing to reduce unmasking to the levels reported in this publication.

Previous RNA sequencing results have shown an up-regulation in the transcript levels of several components upstream of Cph1 in the Cek1 MAPK pathway, including *CEK1* and the cell wall sensor genes *DFI1* and *OPY2* [25]. Here, we have shown that in addition to inducing unmasking, Cph1 can regulate the activation of its own upstream MAPK, Cek1 (Fig 2.6). However, the total Cek1 levels were unchanged during *CPH1* deletion, suggesting that looping into the Cek1 MAPK pathway occurs at a different point than Cek1. Although the location in the pathway where the loop is occurring is thus far unknown, we originally hypothesized that this looping may take place at the cell wall sensor *DFI1*, a two transmembrane protein that has previously been implicated in Cek1 activation during invasive filamentation [48, 49, 59]. However, western blot analysis revealed that changes in *DFI1* expression levels did not alter Cek1 activation (Fig 2.8), suggesting that Dfi1 stimulates a parallel signaling pathway capable of regulating ß(1,3)-glucan exposure during $STE11^{\Delta N467}$ expression. We therefore propose a model in which active Cph1 functions in a positive feedback loop within the Cek1 MAPK pathway to mediate Cek1 activation, while simultaneously increasing the expression levels of the cell wall sensor Dfi1 to induce activation of a parallel, unidentified signaling pathway capable

of regulating ß(1,3)-glucan exposure (Fig 2.9). Although the additional pathway has yet to be identified, Dfi1 has been found to have interactions with calmodulin [49], and may influence unmasking via this interaction. Alternatively, the *S. cerevisiae* cell wall sensor Mid2, a protein sharing strong structural similarity to Dfi1, has been shown to interact with the guanine nucleotide exchange factor Rom2, which is a regulator of Rho1 activation and the Mkc1 MAPK pathway [60]. We have previously shown that expression of a hyperactive $RHO1^{Q67L}$ mutant is capable of inducing unmasking [26], and it may be possible that Dfi1 plays a similar role as Mid2 in stimulating this pathway during $STE11^{\Delta N467}$ expression.

Although it is unclear which signal cascade Dfi1 stimulates during hyperactive $STE11^{\Delta N467}$ expression, our data does suggest that the levels of *DFI1* expression are important for regulating the magnitude of the observed unmasking during $STE11^{\Delta N467}$ expression, as overexpression of *DFI1* on a third allele increased both unmasking (Fig 2.7C) and murine macrophage TNFα secretion *in vitro* (Fig 2.7F) for strains already expressing $STE11^{\Delta N467}$. This suggests that Dfi1 contributes to a graded response in signal transduction, where the strength of the response is dependent on the levels of Dfi1 in the cell. This is not uncommon for upstream components within a signal transduction pathway. In *Saccharomyces cerevisiae*, expression of the Gß subunit *STE4*, a component of the G-protein-coupled-receptor involved in α-pheromone sensing and mating, under the control of the inducible *GAL1* promoter showed a graded signaling response that was dependent on *STE4* expression levels to induce a corresponding increase in promoter activation of its downstream MAPK, Fus3 [61]. Thus, further research is warranted to identify how Dfi1 expression levels feed into appropriate signal cascades to mediate ß(1,3)-glucan exposure.

Materials and Methods

Growth media and culture conditions. *C. albicans* strains were grown in YPD media (1% yeast extract, 2% peptone, 2% dextrose) at 30°C while shaking at 225 rpm [62]. To repress expression of the tetracycline repressible promoter, 0.5ug/ml of doxycycline (Sigma-Aldrich) was added to the growth media. Minimal media (0.67% yeast nitrogen base

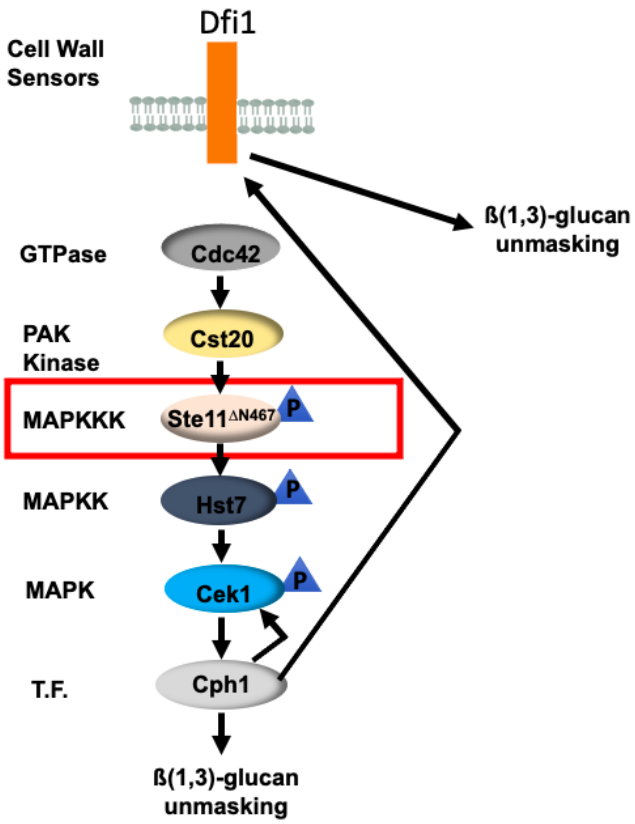


Fig 2.9: Proposed model for hyperactive *STE11*$^{\Delta N467}$ induced unmasking.
In this model, expression of the hyperactive *STE11*$^{\Delta N467}$ allele (red box) induces activation of the canonical Cek1 MAPK pathway (Ste11-Hst7-Cek1) and activates the downstream transcription factor Cph1. Cph1 activation in turn induces increased ß(1,3)-glucan exposure through regulated expression of genes within its regulon, and mediates a positive feedback loop into the pathway to further hyperactivate the upstream MAPK Cek1 and increase its transcriptional output. Simultaneously, Cph1 activation causes an upregulation in the transcript levels of the cell wall sensor Dfi1, which is then stimulated as a result of hyperactivation of the Cek1 MAPK pathway and initiates signaling in a parallel, unidentified, pathway that is also necessary to achieve the full levels of unmasking during *STE11*$^{\Delta N467}$ expression.

without amino acids, 2% dextrose, 2% agar) (Thermo Fisher Scientific) was used to select for loss of the genomically integrated guide RNA, Cas9, and nourseothricin resistance genes after CRISPR-Cas9 gene deletion [63]. YPM media (1% yeast extract, 2% peptone, 2% maltose)(Thermo Fisher Scientific) was used for flipping out the *SAT1*-flipper cassette [64]. DH5-α *Escherichia coli* strains (NEB) were cultured in LB media (0.5% yeast extract, 1% tryptone, 1% NaCl) (Thermo Fisher Scientific) and grown at 37°C on a rotator. RAW264.7 macrophages were cultured in Dulbecco's modified eagle medium with L-glutamine (Gibco) containing 10% fetal bovine serum (Invitrogen) and 1% penicillin-streptomycin (Thermo Fisher Scientific) and grown at 37°C in 5% CO_2 [65].

Plasmid construction. Plasmids constructed during this project are listed in S2.1 Table and primers are listed in S2.2 Table. Unless otherwise stated all *C. albicans* genes and flanking regions were amplified from SC5314 *C. albicans* genomic DNA. The *LEU2* deletion construct was created using the *SAT1* flipper method [64]. The primer set AWO35 and AWO36 were used to amplify a 524bp fragment of the 5' untranslated region (UTR) of *LEU2* that was flanked by *Kpn1* and *Xho1* cut sites introduced by the primers, respectively. The PCR fragment and the pSFS2A *SAT1* flipper cassette were then both digested with *KpnI* and *XhoI* and ligated together using T4 DNA ligase (NEB) to create the pAW006 plasmid. To introduce the 3' UTR of *LEU2* to the 3' end of pAW006, the primer set AWO37 and AWO38 were used to amplify a 520bp fragment of the 3' UTR of *LEU2* that was flanked by *SacII* and *SacI* cut sites introduced by each primer, respectively. Both the PCR product and pAW006 were then digested with *SacII* and *SacI*, and ligated together to create the pAW011 plasmid that harbors the full *LEU2-SAT1* flipper cassette.

The *CPH1-FLAG* reintegrate cassette was created using the *SAT1* flipper cassette pSFS2A [64]. A 484bp fragment of the 3' UTR of *CPH1* was amplified using TC0173 and TCO174 that additionally introduced *NotI* and *SacI* cut sites, respectively, on the flanking ends. Both pSDS2A and the PCR fragment were digested with *NotI* and *SacI* restriction enzymes (NEB) and ligated using T4 DNA ligase (NEB) to create pTCO74. To introduce a tagged *CPH1* gene to the 5' end of the *SAT1* flipper cassette in the pTCO74 plasmid, a 2,361bp fragment containing 326bp of the *CPH1* 5' UTR immediately upstream of the start

codon and the *CPH1* open reading frame (ORF) with an added C-terminal FLAG-tag sequence before the stop codon was amplified using AWO187 and AWO188, which further introduced flanking *ApaI* and *XhoI* cut sites, respectively. The final *CPH1-Flag-SAT1* reintegrate cassette (pAW071) was then created by digesting both pTCO74 and the PCR product with *ApaI* and *XhoI*, and subsequently ligating the digested vector and insert together.

The *CEK1* overexpression cassette was created by placing *CEK1* under the control of the constitutive phosphoenolpyruvate carboxykinase (*PCK1*) promoter in the *SAT1*-flipper-cassette pSFS2A background. To create this, a PCR fragment containing 495bp of the 3' UTR of *PCK1* was amplified with AWO265 and AWO266 primers that introduced *SacII* and *SacI* cut sites, respectively. The PCR product and pSFS2A were then digested using *SacII* and *SacI* and ligated to create pAW085. To introduce the *PCK1* promoter to the 5' end of the *SAT1* flipper cassette in pAW085, a PCR product consisting of the 712bp in the 5' UTR of *PCK1* that sits immediately upstream of the *PCK1* ORF was amplified with the AWO263 and AWO264 primer set that introduced flanking *KpnI* and *ApaI* cut sites, respectively. The plasmid and 5' UTR PCR product were then subsequently digested with *KpnI* and *ApaI* and ligated to create the P_{PCK1}*-SAT1* flipper cassette (pAW087). *CEK1* was then subcloned under the control of the *PCK1* promoter by amplifying the *CEK1* ORF with the AWO267 and AWO268 primer set that introduced flanking *ApaI* and *XhoI* cutsites, respectively. pAW087 and the *CEK1* ORF PCR product were then digested with *ApaI* and *XhoI*, and subsequently ligated to create the P_{PCK1}*-CEK1-SAT1* flipper cassette (pAW091).

The *HST7* overexpression cassette was created by placing the *HST7* gene under the control the phosphoenolpyruvate carboxykinase (*PCK1*) promoter in plasmid pAW087. The *HST7* ORF was amplified with the primer set AWO348 and AWO349 with flanking *ApaI* cut sites flanking the ends. pAWO87 and the *HST7* ORF PCR product were then digested with *ApaI* and ligated together to create the P_{PCK1}*-HST7-SAT1* flipper cassette (pAW105).

The *DFI1* overexpression cassette was created by placing the *DFI1* ORF under the regulatory control of the constitutive enolase *(ENO1*) promoter [66]. To achieve this, a

1,529bp PCR product consisting of the *DFI1* ORF and 441bp of the *DFI1* 3' UTR immediately following the stop codon was amplified with the AWO176 and AWO177 primer set that introduced flanking *NotI* and *SacI* cut sites. The P_{ENO1} overexpression plasmid, pBT1 [66], and the PCR product were then digested using *NotI* and *SacI*, and ligated to create the P_{ENO1}-*DFI1-SAT1* overexpression cassette (pAW066).

Strain construction. *Candida albicans* deletion strains (S2.3 Table) were created with the use of CRISPR-Cas9 as previously described [63]. The *LEU2/leu2Δ* mutant was generated with the use of the *SAT1* flipper method [64]. The *LEU2* deletion construct (pAW011) was digested with *KpnI* and *SacI*, and the fragment containing the *SAT1* gene flanked by homologous regions to the 5' and 3' UTRs of *LEU2* was gel purified with the use of the QIAquick Gel Extraction Kit (Qiagen). The purified fragment was then transformed via electroporation into the SC5314 *C. albicans* strain as previously described [54], and successful transformants were selected on YPD plates containing 200μg/ml nourseothricin.

To generate the *STE11/*$P_{tet\text{-}off}$*-STE11*$^{\Delta N467}$ strain in the SC5314 *C. albicans* background, the primer set AWO156 and AWO157 were used to amplify the tetracycline repressible promotor with an additional ~500bp of homology flanking both sides of the *STE11* locus ($P_{tet\text{-}off}$-*STE11*$^{\Delta N467}$) from purified genomic DNA of the previously constructed *STE11/*$P_{tet\text{-}off}$*-STE11*$^{\Delta N467}$ strain in the Day286 background [25]. The resulting PCR product contained the Hygromycin selectable and the tetracycline repressible promotor 5' to the $P_{tet\text{-}off}$ -regulated N-terminally truncated *STE11*$^{\Delta N467}$ allele. The PCR product was then purified and transformed into the appropriate strains via electroporation and transformants were selected for on YPD+HYG plates containing 2mg/ml of Hygromycin B (Gold Biotechnology).

The *CPH1-FLAG* reintegrate strain was generated with the use of the *SAT1*-flipper method [64]. The *CPH1-FLAG-SAT1* reintegrate cassette (pAW071) was digested using *ApaI* and *SacI*, and subsequently purified using the QIAquick Gel Extraction Kit (Qiagen). The purified fragment was then transformed into the appropriate strains via electroporation and transformants were selected on YPD + nourseothricin plates.

The *CEK1* and *HST7* overexpression mutants were generated by digestion of the P_{PCK1}-*CEK1-SAT1* flipper cassette (pAW091) or the P_{PCK1}-*HST7-SAT1* flipper cassette (pAW105) with *KpnI,* followed by purification of the linear plasmid with the QIAquick PCR Purification Kit (Qiagen). The linear plasmid was then transformed into the appropriate *C. albicans* strains via electroporation and transformants selected for on YPD + nourseothricin media.

DFI1 overexpression strains were created by digesting the P_{ENO1}-*DFI1-SAT1* plasmid (pAW066) with *MscI* (which cuts a single time within the *ENO1* promoter). The linear plasmid was then purified and transformed into the appropriate *C. albicans* strains via electroporation. Successful transformants were selected for on YPD + nourseothricin media.

Mouse Model. Outbred ICR mice (ENVIGO) were used for all experiments in this study. To prepare for inoculation, 50ml cultures of *C. albicans* strains were grown overnight in YPD media containing 0.5μg/ml of doxycycline (Sigma-Aldrich) at 30°C while shaking at 225 rpm. The following morning, cells were transferred to 50ml conical tubes (Thomas Scientific) and spun at 3,500 rpm for 5 minutes. Cells were subsequently washed 2 times with 25ml of PBS and then counted using a hemocytometer. Cells were diluted to either $1x10^7$ cells/ml (for immunocompetent mice) or $1x10^5$ cells/ml (for immunosuppressed mice). Mice were then intravenously injected via the lateral tail vein with 0.1ml of the previously prepared cell suspension. Following injection, cell viability for each strain was assessed by plating on YPD and allowing cells to grow at 30°C for 24 hours. Four days post infection, mice were anesthetized, and peripheral blood was isolated via cardiac puncture in heparin treated tubes (BD Biosciences). Mice were then euthanized, and their kidneys, spleens, brains or livers were harvested to assess fungal burden. Organs were placed in pre-weighed whirl-pack bags (Thermo Fisher Scientific) containing 1ml of water. The bags were weighed once more to determine the weight of the organ and then the tissue were homogenized. Serial dilutions of the tissue homogenates (10^{-1}, 10^{-2}, 10^{-3}) were created, and 1ml of each dilution was added to 15ml of YPD + 75μg/ml chloramphenicol (Thermo Fisher Scientific) precooled to 55°C and plated. Plates were then left to incubate

for 2 days at 30°C to determine fungal colony forming units (CFU) per gram of tissue. Distribution normality of the data collected was then assessed with the use of a Shapiro-Wilk test and statistical significance was determined with the use of either Student's unpaired T-test for data that followed a Gaussian distribution, or a non-parametric Kruskal-Wallis test for data that did not follow a Gaussian distribution (GraphPad Prism, v7.0c software) (The number of mice used for each experiment is listed in the figure legend associated with the data).

For experiments in which the regulation of the hyperactive *STE11*$^{\Delta N467}$ allele was controlled *in vivo*, mice were given either 5% sucrose water or 5% sucrose + 2mg/ml of doxycycline [25]. Three days prior to infection, all mice were given sucrose water to begin acclimation. Two days prior to infection, mice in the appropriate control groups were then switched to sucrose water + doxycycline. All supplied water was then changed every other day to ensure the efficacy of the supplemented doxycycline.

Immune cell depletion in mice. Non-specific immune cell depletion *in vivo* was achieved via recurring injections with cyclophosphamide (Sigma-Aldrich). ICR mice were weighed prior to treatment to determine the average weight of all mice. Mice were then treated with 150mg/kg of cyclophosphamide, based on their average weight, via intraperitoneal (I.P.) injections starting 4 days prior to infection. Immune depletion was then maintained with recurring I.P. injections of 150mg/kg of cyclophosphamide every 3 days until the experiment was terminated.

In vivo neutrophil depletion was achieved through the use of an anti-mouse Ly6G (1A8) monoclonal antibody (BioXCell) [29, 30]. Mice were intraperitoneally injected with 300ug of 1A8 starting 1 day prior to infection. Neutrophil depletion was then maintained via recurring I.P. administration of 300ug of 1A8 every other day until the end of the experiment. Control mice were alternatively injected with a corresponding I.P. injection with a PBS vehicle control.

Ethics statement. All animal work used in this study was done under an approved protocol (0016) that was previously approved by the University of Tennessee, Knoxville Institution

Animal Care and Use Committee (IACUC), and was done in accordance with the National Institute of Health's (NIH) ethical guidelines for animal research.

Staining of cell wall components and flow cytometry or microscopy analysis. For staining of yeast cells, 5ml cultures of *C. albicans* strains in YPD were started the morning prior to staining. Cultures were left to grow shaking at 225 rpm at 30°C for ~8 hours, and then back diluted to an OD_{600} of 0.1 in fresh YPD media. Dilutions were then incubated with shaking at 225 rpm and 30°C overnight (~16 hours) for staining the following morning. After overnight growth, cells were diluted to an OD_{600} of 0.5. Immunofluorescent staining of exposed ß(1,3)-glucan in stationary phase yeast cells was performed as previously described [26]. Total chitin was assessed by staining cells with 500µl of a 10µg/ml calcofluor white solution in PBS for 5 minutes shaking at room temperature. To assess exposed chitin, cells were stained with 500µl of a 10ug/ml fluorescein-labeled wheat germ agglutinin (WGA)(Vector Laboratories) solution in PBS and incubated with shaking at 4°C for 30 minutes. Mannan levels were assessed by staining cells with 500µl of a 50ug/ml solution of Alexa Fluor 647 conjugated concanavalin A (Thermo Fisher Scientific) in PBS and were incubated with shaking at 4°C for 30 minutes. A minimum of 3 biological replicates with 2-3 technical replicates consisting of 100,000 recorded events each was used to assess all strains by flow cytometry and statistical significance was determined with the use of a one-way ANOVA with Tukey's post hoc analysis (GraphPad Prism, v7.0c software).

Immunofluorescent staining of hyphal cells for exposed ß(1,3)-glucan was performed as previously described [51]. Quantification of microscopy images was then achieved with the use of ImageJ (National Institute of Health, Bethesda, MD). A total of 3 biological replicates were stained for each strain and 30 hyphal cells were quantified per biological replicate. Statistical significance was then determined with the use of Student's t-test (GraphPad Prism, v7.0c software).

Immunofluorescent staining of leukocytes was achieved using peripheral blood that was isolated via cardiac puncture in heparin treated tubes (BD Biosciences). Blood was

resuspended in 1x PBS and erythrocytes were lysed using two sequential ACK (Ammonium-Chloride-Potassium) lysis steps. Cells were then counted and stained using myeloid markers (α-Ly6C: HK1.4 clone, APC, BioLegend) (α-Ly6G: 1A8 clone, PerCP-Cy5.5, BioLegend) (α-CD11b: M1/70 clone, BV421, BioLegend) (α-F4/80: BM8 clone, PE, BioLegend) (Fixable NIR Live-Dead: under APC-Cy7 filter, Invitrogen; cat #:L34975).

For all stains, relative abundance and representative plots were generated using an LSRII flow cytometer (BD Biosciences), and analysis was performed using FlowJo v10.7 (Becton, Dickinson and Company). For strains in which microscopy was performed, cells were analyzed using the Leica SP8 confocal microscope and analyzed using the LAS X analysis software (Leica).

Serum Cytokine Quantification. Serum cytokine concentrations were determined using the manufacturer's protocol for the LEGENDplex Mouse Anti-Virus Response Panel 740622 (Biolegend). In brief, peripheral blood from anesthetized mice was collected and allowed to clot for 30 minutes prior to centrifugation at 1,000 x g for 20 minutes for serum separation. Serum was then collected and stored at -80°C until use. Frozen samples were then allowed to thaw completely and diluted 2-fold for kit analysis. All assays were performed using the manufacturer supplied 96-well v-bottom plate. Once samples were thawed and diluted, each well was filled with 25µl of the appropriate sample or standard, 25µl of assay buffer, and 25µl of capture beads. The plate was then covered and left shaking at 800 rpm at room temperature for 2 hours. Following incubation, beads were pelleted by centrifugation at 200 x g for 5 minutes, the supernatant was removed, and beads were washed two times with 200µl of 1X wash buffer. Detection antibody (25µl) was then added to each well, and the plate was left to incubate covered at room temperature for 1 hour while shaking at 800 rpm. Following incubation, 25µl of SA-PE was added to each well and plates were left to incubate shaking in the dark for 30 minutes. Samples were then spun at 200 x g for 5 minutes, washed one time with 200µl of 1X wash buffer and finally resuspended in 150µl of wash buffer. Following resuspension, samples were analyzed via

flow cytometry using an LSRII flow cytometer (BD Biosciences), and data was analyzed using the manufacturer supplied LEGENDplex data analysis software suite (Biolegend). Distribution normality of the data collected was then assessed with the use of a Shapiro-Wilk test and statistical significance was determined by a Mann-Whitney test. (The number of mice used for each experiment is listed in the figure legend associated with the data and all samples were run with technical duplicates).

TNFα Enzyme Linked Immunosorbent Assay (ELISA). One day prior to infection, $5x10^5$ RAW264.7 murine macrophages were seeded in each well of a 24-well plate and left to incubate overnight at 37°C in 5% CO_2. Cultures of *C. albicans* strains in YPD were then started and left to grow shaking at 225 rpm at 30°C overnight. The following morning, *C. albicans* cultures were washed with PBS and diluted to an OD_{600} of 1.25 in 5ml of PBS in a 6-well plate. Diluted cultures were then UV-inactivated by placing the 6-well plate in the Spectrolinker XL-1000 UV Crosslinker (Spectroline Inc.) and adjusting the ENERGY setting to 100,000 $\mu J/cm^2$. UV-irradiation was then repeated for a total of 5 exposures. UV-inactivated *Candida* cells, or a PBS control, were then added to the RAW264.7 macrophages at 1:10 macrophage to *Candida* ratio and left to co-incubate for 4 hours at 37°C in 5% CO_2. For analysis of the impact that dectin-1 binding had on TNFα production, macrophages were co-incubated with 5ug/ml of an anti-dectin-1 neutralizing antibody (InvivoGen) for 1 hour prior to co-incubation with UV-inactivated *C. albicans* cells. After *C. albicans* and macrophage co-incubation, the supernatant was collected and filtered through a 0.22μm filter (Thermo Fisher Scientific). Filtered supernatant was then assessed with the use of a Duoset Mouse TNFa ELISA kit (R&D Systems) per the manufacturer's instructions. Three biological replicates with three technical replicates were used to assess each strain, and statistical significance was determined with the use of a one-way ANOVA with Tukey's post hoc analysis (GraphPad Prism, v7.0c software).

Western blot analysis of total and phosphorylated-Cek1. Total and activated levels of Cek1 were assessed as previously described [25]. After blotting, the total levels of

phosphorylated-Cek1 to total Cek1 was determined via densitometry of images generated on the Odyssey Imager (Li-Cor Biosciences) by using ImageJ (National Institute of Health, Bethesda, MD). Quantification was done for three biological replicates of each sample, and statistical significance was determined with the use of a one-way ANOVA with Tukey's post hoc analysis (GraphPad Prism, v7.0c software).

Statistics. All statistical analyses used are stated in the methods section corresponding to the assay performed. For all figures, statistical significance between two samples is denoted by a horizontal line, where the end points of the line indicate the two samples that were compared to generate significance.

References

1. Brown GD, Denning DW, Gow NA, Levitz SM, Netea MG, White TC. Hidden killers: human fungal infections. Sci Transl Med. 2012;4(165):165rv13. Epub 2012/12/21. doi: 10.1126/scitranslmed.3004404. PubMed PMID: 23253612.

2. Netea MG, Joosten LA, van der Meer JW, Kullberg BJ, van de Veerdonk FL. Immune defence against Candida fungal infections. Nat Rev Immunol. 2015;15(10):630-42. Epub 2015/09/22. doi: 10.1038/nri3897. PubMed PMID: 26388329.

3. Gow NAR, Latge JP, Munro CA. The Fungal Cell Wall: Structure, Biosynthesis, and Function. Microbiol Spectr. 2017;5(3). Epub 2017/05/18. doi: 10.1128/microbiolspec.FUNK-0035-2016. PubMed PMID: 28513415.

4. Hopke A, Brown AJP, Hall RA, Wheeler RT. Dynamic Fungal Cell Wall Architecture in Stress Adaptation and Immune Evasion. Trends Microbiol. 2018;26(4):284-95. Epub 2018/02/18. doi: 10.1016/j.tim.2018.01.007. PubMed PMID: 29452950; PubMed Central PMCID: PMCPMC5869159.

5. Wheeler RT, Kombe D, Agarwala SD, Fink GR. Dynamic, morphotype-specific Candida albicans beta-glucan exposure during infection and drug treatment. PLoS Pathog. 2008;4(12):e1000227. Epub 2008/12/06. doi: 10.1371/journal.ppat.1000227. PubMed PMID: 19057660; PubMed Central PMCID: PMCPMC2587227.

6. Wheeler RT, Fink GR. A drug-sensitive genetic network masks fungi from the immune system. PLoS Pathog. 2006;2(4):e35. Epub 2006/05/03. doi: 10.1371/journal.ppat.0020035. PubMed PMID: 16652171; PubMed Central PMCID: PMCPMC1447670.

7. Gow NA, Netea MG, Munro CA, Ferwerda G, Bates S, Mora-Montes HM, et al. Immune recognition of Candida albicans beta-glucan by dectin-1. J Infect Dis. 2007;196(10):1565-71. Epub 2007/11/17. doi: 10.1086/523110. PubMed PMID: 18008237; PubMed Central PMCID: PMCPMC2655640.

8. Brown GD, Taylor PR, Reid DM, Willment JA, Williams DL, Martinez-Pomares L, et al. Dectin-1 is a major beta-glucan receptor on macrophages. J Exp Med.

2002;196(3):407-12. Epub 2002/08/07. doi: 10.1084/jem.20020470. PubMed PMID: 12163569; PubMed Central PMCID: PMCPMC2193936.

9. Brown GD, Gordon S. Immune recognition. A new receptor for beta-glucans. Nature. 2001;413(6851):36-7. Epub 2001/09/07. doi: 10.1038/35092620. PubMed PMID: 11544516.

10. Taylor PR, Brown GD, Reid DM, Willment JA, Martinez-Pomares L, Gordon S, et al. The beta-glucan receptor, dectin-1, is predominantly expressed on the surface of cells of the monocyte/macrophage and neutrophil lineages. J Immunol. 2002;169(7):3876-82. Epub 2002/09/24. doi: 10.4049/jimmunol.169.7.3876. PubMed PMID: 12244185.

11. Brown GD, Herre J, Williams DL, Willment JA, Marshall AS, Gordon S. Dectin-1 mediates the biological effects of beta-glucans. J Exp Med. 2003;197(9):1119-24. Epub 2003/04/30. doi: 10.1084/jem.20021890. PubMed PMID: 12719478; PubMed Central PMCID: PMCPMC2193964.

12. van Bruggen R, Drewniak A, Jansen M, van Houdt M, Roos D, Chapel H, et al. Complement receptor 3, not Dectin-1, is the major receptor on human neutrophils for beta-glucan-bearing particles. Mol Immunol. 2009;47(2-3):575-81. Epub 2009/10/09. doi: 10.1016/j.molimm.2009.09.018. PubMed PMID: 19811837.

13. Swidergall M, Solis NV, Wang Z, Phan QT, Marshall ME, Lionakis MS, et al. EphA2 Is a Neutrophil Receptor for Candida albicans that Stimulates Antifungal Activity during Oropharyngeal Infection. Cell Rep. 2019;28(2):423-33 e5. Epub 2019/07/11. doi: 10.1016/j.celrep.2019.06.020. PubMed PMID: 31291578; PubMed Central PMCID: PMCPMC6638578.

14. Swidergall M, Solis NV, Lionakis MS, Filler SG. EphA2 is an epithelial cell pattern recognition receptor for fungal beta-glucans. Nat Microbiol. 2018;3(1):53-61. Epub 2017/11/15. doi: 10.1038/s41564-017-0059-5. PubMed PMID: 29133884; PubMed Central PMCID: PMCPMC5736406.

15. Carrion Sde J, Leal SM, Jr., Ghannoum MA, Aimanianda V, Latge JP, Pearlman E. The RodA hydrophobin on Aspergillus fumigatus spores masks dectin-1- and dectin-2-dependent responses and enhances fungal survival in vivo. J Immunol.

2013;191(5):2581-8. Epub 2013/08/09. doi: 10.4049/jimmunol.1300748. PubMed PMID: 23926321; PubMed Central PMCID: PMCPMC4020118.

16. Gravelat FN, Beauvais A, Liu H, Lee MJ, Snarr BD, Chen D, et al. Aspergillus galactosaminogalactan mediates adherence to host constituents and conceals hyphal beta-glucan from the immune system. PLoS Pathog. 2013;9(8):e1003575. Epub 2013/08/31. doi: 10.1371/journal.ppat.1003575. PubMed PMID: 23990787; PubMed Central PMCID: PMCPMC3749958.

17. Garfoot AL, Shen Q, Wuthrich M, Klein BS, Rappleye CA. The Eng1 beta-Glucanase Enhances Histoplasma Virulence by Reducing beta-Glucan Exposure. mBio. 2016;7(2):e01388-15. Epub 2016/04/21. doi: 10.1128/mBio.01388-15. PubMed PMID: 27094334; PubMed Central PMCID: PMCPMC4850272.

18. Yang M, Solis NV, Marshall M, Garleb R, Zhou T, Wang D, et al. Control of β-glucan exposure by the endo-1,3-glucanase Eng1 in Candida albicans modulates virulence. bioRxiv. 2020:2020.09.07.285791. doi: 10.1101/2020.09.07.285791.

19. Childers DS, Avelar GM, Bain JM, Pradhan A, Larcombe DE, Netea MG, et al. Epitope Shaving Promotes Fungal Immune Evasion. mBio. 2020;11(4). Epub 2020/07/09. doi: 10.1128/mBio.00984-20. PubMed PMID: 32636248; PubMed Central PMCID: PMCPMC7343991.

20. Casadevall A, Pirofski LA. Adjunctive immune therapy for fungal infections. Clin Infect Dis. 2001;33(7):1048-56. Epub 2001/08/31. doi: 10.1086/322710. PubMed PMID: 11528579.

21. Hasim S, Allison DP, Retterer ST, Hopke A, Wheeler RT, Doktycz MJ, et al. beta-(1,3)-Glucan Unmasking in Some Candida albicans Mutants Correlates with Increases in Cell Wall Surface Roughness and Decreases in Cell Wall Elasticity. Infect Immun. 2017;85(1). Epub 2016/11/17. doi: 10.1128/IAI.00601-16. PubMed PMID: 27849179; PubMed Central PMCID: PMCPMC5203643.

22. Sherrington SL, Sorsby E, Mahtey N, Kumwenda P, Lenardon MD, Brown I, et al. Adaptation of Candida albicans to environmental pH induces cell wall remodelling and enhances innate immune recognition. PLoS Pathog. 2017;13(5):e1006403. Epub

2017/05/26. doi: 10.1371/journal.ppat.1006403. PubMed PMID: 28542528; PubMed Central PMCID: PMCPMC5456412.

23. Pradhan A, Avelar GM, Bain JM, Childers DS, Larcombe DE, Netea MG, et al. Hypoxia Promotes Immune Evasion by Triggering beta-Glucan Masking on the Candida albicans Cell Surface via Mitochondrial and cAMP-Protein Kinase A Signaling. mBio. 2018;9(6). Epub 2018/11/08. doi: 10.1128/mBio.01318-18. PubMed PMID: 30401773; PubMed Central PMCID: PMCPMC6222127.

24. Ballou ER, Avelar GM, Childers DS, Mackie J, Bain JM, Wagener J, et al. Lactate signalling regulates fungal beta-glucan masking and immune evasion. Nat Microbiol. 2016;2:16238. Epub 2016/12/13. doi: 10.1038/nmicrobiol.2016.238. PubMed PMID: 27941860; PubMed Central PMCID: PMCPMC5704895.

25. Chen T, Wagner AS, Tams RN, Eyer JE, Kauffman SJ, Gann ER, et al. Lrg1 Regulates beta (1,3)-Glucan Masking in Candida albicans through the Cek1 MAP Kinase Pathway. mBio. 2019;10(5). Epub 2019/09/19. doi: 10.1128/mBio.01767-19. PubMed PMID: 31530671; PubMed Central PMCID: PMCPMC6751057.

26. Chen T, Jackson JW, Tams RN, Davis SE, Sparer TE, Reynolds TB. Exposure of Candida albicans beta (1,3)-glucan is promoted by activation of the Cek1 pathway. PLoS Genet. 2019;15(1):e1007892. Epub 2019/02/01. doi: 10.1371/journal.pgen.1007892. PubMed PMID: 30703081; PubMed Central PMCID: PMCPMC6372213.

27. Lai WC, Sun HF, Lin PH, Ho Lin HL, Shieh JC. A new rapid and efficient system with dominant selection developed to inactivate and conditionally express genes in Candida albicans. Curr Genet. 2016;62(1):213-35. Epub 2015/10/27. doi: 10.1007/s00294-015-0526-6. PubMed PMID: 26497136.

28. Fulurija A, Ashman RB, Papadimitriou JM. Neutrophil depletion increases susceptibility to systemic and vaginal candidiasis in mice, and reveals differences between brain and kidney in mechanisms of host resistance. Microbiology (Reading). 1996;142 (Pt 12):3487-96. Epub 1996/12/01. doi: 10.1099/13500872-142-12-3487. PubMed PMID: 9004511.

29. Daley JM, Thomay AA, Connolly MD, Reichner JS, Albina JE. Use of Ly6G-specific monoclonal antibody to deplete neutrophils in mice. J Leukoc Biol.

2008;83(1):64-70. Epub 2007/09/22. doi: 10.1189/jlb.0407247. PubMed PMID: 17884993.

30. Carr KD, Sieve AN, Indramohan M, Break TJ, Lee S, Berg RE. Specific depletion reveals a novel role for neutrophil-mediated protection in the liver during Listeria monocytogenes infection. Eur J Immunol. 2011;41(9):2666-76. Epub 2011/06/11. doi: 10.1002/eji.201041363. PubMed PMID: 21660934; PubMed Central PMCID: PMCPMC3517125.

31. Roman E, Correia I, Salazin A, Fradin C, Jouault T, Poulain D, et al. The Cek1mediated MAP kinase pathway regulates exposure of alpha1,2 and beta1,2mannosides in the cell wall of Candida albicans modulating immune recognition. Virulence. 2016;7(5):558-77. Epub 2016/05/19. doi: 10.1080/21505594.2016.1163458. PubMed PMID: 27191378; PubMed Central PMCID: PMCPMC5038168.

32. van Wijlick L, Swidergall M, Brandt P, Ernst JF. Candida albicans responds to glycostructure damage by Ace2-mediated feedback regulation of Cek1 signaling. Mol Microbiol. 2016;102(5):827-49. Epub 2016/09/03. doi: 10.1111/mmi.13494. PubMed PMID: 27589033.

33. Roman E, Nombela C, Pla J. The Sho1 adaptor protein links oxidative stress to morphogenesis and cell wall biosynthesis in the fungal pathogen Candida albicans. Mol Cell Biol. 2005;25(23):10611-27. Epub 2005/11/17. doi: 10.1128/MCB.25.23.10611-10627.2005. PubMed PMID: 16287872; PubMed Central PMCID: PMCPMC1291223.

34. Wagener J, Malireddi RK, Lenardon MD, Koberle M, Vautier S, MacCallum DM, et al. Fungal chitin dampens inflammation through IL-10 induction mediated by NOD2 and TLR9 activation. PLoS Pathog. 2014;10(4):e1004050. Epub 2014/04/12. doi: 10.1371/journal.ppat.1004050. PubMed PMID: 24722226; PubMed Central PMCID: PMCPMC3983064.

35. Wagener J, MacCallum DM, Brown GD, Gow NA. Candida albicans Chitin Increases Arginase-1 Activity in Human Macrophages, with an Impact on Macrophage Antimicrobial Functions. mBio. 2017;8(1). Epub 2017/01/26. doi: 10.1128/mBio.01820-16. PubMed PMID: 28119468; PubMed Central PMCID: PMCPMC5263244.

36. Seman BG, Moore JL, Scherer AK, Blair BA, Manandhar S, Jones JM, et al. Yeast and Filaments Have Specialized, Independent Activities in a Zebrafish Model of Candida albicans Infection. Infect Immun. 2018;86(10). Epub 2018/07/25. doi: 10.1128/IAI.00415-18. PubMed PMID: 30037799; PubMed Central PMCID: PMCPMC6204735.
37. Saville SP, Lazzell AL, Monteagudo C, Lopez-Ribot JL. Engineered control of cell morphology in vivo reveals distinct roles for yeast and filamentous forms of Candida albicans during infection. Eukaryot Cell. 2003;2(5):1053-60. Epub 2003/10/14. doi: 10.1128/ec.2.5.1053-1060.2003. PubMed PMID: 14555488; PubMed Central PMCID: PMCPMC219382.
38. Galan-Diez M, Arana DM, Serrano-Gomez D, Kremer L, Casasnovas JM, Ortega M, et al. Candida albicans beta-glucan exposure is controlled by the fungal CEK1-mediated mitogen-activated protein kinase pathway that modulates immune responses triggered through dectin-1. Infect Immun. 2010;78(4):1426-36. Epub 2010/01/27. doi: 10.1128/IAI.00989-09. PubMed PMID: 20100861; PubMed Central PMCID: PMCPMC2849429.
39. Correia I, Prieto D, Roman E, Wilson D, Hube B, Alonso-Monge R, et al. Cooperative Role of MAPK Pathways in the Interaction of Candida albicans with the Host Epithelium. Microorganisms. 2019;8(1). Epub 2019/12/29. doi: 10.3390/microorganisms8010048. PubMed PMID: 31881718; PubMed Central PMCID: PMCPMC7023383.
40. Csank C, Schroppel K, Leberer E, Harcus D, Mohamed O, Meloche S, et al. Roles of the Candida albicans mitogen-activated protein kinase homolog, Cek1p, in hyphal development and systemic candidiasis. Infect Immun. 1998;66(6):2713-21. Epub 1998/05/29. doi: 10.1128/IAI.66.6.2713-2721.1998. PubMed PMID: 9596738; PubMed Central PMCID: PMCPMC108260.
41. Huang H, Harcus D, Whiteway M. Transcript profiling of a MAP kinase pathway in C. albicans. Microbiol Res. 2008;163(4):380-93. Epub 2008/05/10. doi: 10.1016/j.micres.2008.03.001. PubMed PMID: 18467082.

42. Ramirez-Zavala B, Weyler M, Gildor T, Schmauch C, Kornitzer D, Arkowitz R, et al. Activation of the Cph1-dependent MAP kinase signaling pathway induces white-opaque switching in Candida albicans. PLoS Pathog. 2013;9(10):e1003696. Epub 2013/10/17. doi: 10.1371/journal.ppat.1003696. PubMed PMID: 24130492; PubMed Central PMCID: PMCPMC3795047.

43. Yi S, Sahni N, Daniels KJ, Pujol C, Srikantha T, Soll DR. The same receptor, G protein, and mitogen-activated protein kinase pathway activate different downstream regulators in the alternative white and opaque pheromone responses of Candida albicans. Mol Biol Cell. 2008;19(3):957-70. Epub 2007/12/29. doi: 10.1091/mbc.e07-07-0688. PubMed PMID: 18162580; PubMed Central PMCID: PMCPMC2262975.

44. Liu H, Kohler J, Fink GR. Suppression of hyphal formation in Candida albicans by mutation of a STE12 homolog. Science. 1994;266(5191):1723-6. Epub 1994/12/09. doi: 10.1126/science.7992058. PubMed PMID: 7992058.

45. Mulhern SM, Logue ME, Butler G. Candida albicans transcription factor Ace2 regulates metabolism and is required for filamentation in hypoxic conditions. Eukaryot Cell. 2006;5(12):2001-13. Epub 2006/09/26. doi: 10.1128/EC.00155-06. PubMed PMID: 16998073; PubMed Central PMCID: PMCPMC1694816.

46. Desai PR, van Wijlick L, Kurtz D, Juchimiuk M, Ernst JF. Hypoxia and Temperature Regulated Morphogenesis in Candida albicans. PLoS Genet. 2015;11(8):e1005447. Epub 2015/08/15. doi: 10.1371/journal.pgen.1005447. PubMed PMID: 26274602; PubMed Central PMCID: PMCPMC4537295.

47. Herrero de Dios C, Roman E, Diez C, Alonso-Monge R, Pla J. The transmembrane protein Opy2 mediates activation of the Cek1 MAP kinase in Candida albicans. Fungal Genet Biol. 2013;50:21-32. Epub 2012/11/15. doi: 10.1016/j.fgb.2012.11.001. PubMed PMID: 23149115.

48. Zucchi PC, Davis TR, Kumamoto CA. A Candida albicans cell wall-linked protein promotes invasive filamentation into semi-solid medium. Mol Microbiol. 2010;76(3):733-48. Epub 2010/04/14. doi: 10.1111/j.1365-2958.2010.07137.x. PubMed PMID: 20384695; PubMed Central PMCID: PMCPMC3163599.

49. Davis TR, Zucchi PC, Kumamoto CA. Calmodulin binding to Dfi1p promotes invasiveness of Candida albicans. PLoS One. 2013;8(10):e76239. Epub 2013/10/25. doi: 10.1371/journal.pone.0076239. PubMed PMID: 24155896; PubMed Central PMCID: PMCPMC3796530.

50. Borneman AR, Gianoulis TA, Zhang ZD, Yu H, Rozowsky J, Seringhaus MR, et al. Divergence of transcription factor binding sites across related yeast species. Science. 2007;317(5839):815-9. Epub 2007/08/11. doi: 10.1126/science.1140748. PubMed PMID: 17690298.

51. Davis SE, Hopke A, Minkin SC, Jr., Montedonico AE, Wheeler RT, Reynolds TB. Masking of beta(1-3)-glucan in the cell wall of Candida albicans from detection by innate immune cells depends on phosphatidylserine. Infect Immun. 2014;82(10):4405-13. Epub 2014/08/13. doi: 10.1128/IAI.01612-14. PubMed PMID: 25114110; PubMed Central PMCID: PMCPMC4187869.

52. Herrero AB, Magnelli P, Mansour MK, Levitz SM, Bussey H, Abeijon C. KRE5 gene null mutant strains of Candida albicans are avirulent and have altered cell wall composition and hypha formation properties. Eukaryot Cell. 2004;3(6):1423-32. Epub 2004/12/14. doi: 10.1128/EC.3.6.1423-1432.2004. PubMed PMID: 15590817; PubMed Central PMCID: PMCPMC539026.

53. Marakalala MJ, Vautier S, Potrykus J, Walker LA, Shepardson KM, Hopke A, et al. Differential adaptation of Candida albicans in vivo modulates immune recognition by dectin-1. PLoS Pathog. 2013;9(4):e1003315. Epub 2013/05/03. doi: 10.1371/journal.ppat.1003315. PubMed PMID: 23637604; PubMed Central PMCID: PMCPMC3630191.

54. Chen YL, Montedonico AE, Kauffman S, Dunlap JR, Menn FM, Reynolds TB. Phosphatidylserine synthase and phosphatidylserine decarboxylase are essential for cell wall integrity and virulence in Candida albicans. Mol Microbiol. 2010;75(5):1112-32. Epub 2010/02/06. doi: 10.1111/j.1365-2958.2009.07018.x. PubMed PMID: 20132453.

55. Halder LD, Jo EAH, Hasan MZ, Ferreira-Gomes M, Kruger T, Westermann M, et al. Immune modulation by complement receptor 3-dependent human monocyte TGF-beta1-transporting vesicles. Nat Commun. 2020;11(1):2331. Epub 2020/05/13. doi:

10.1038/s41467-020-16241-5. PubMed PMID: 32393780; PubMed Central PMCID: PMCPMC7214408.

56. Maiti P, Ghorai P, Ghosh S, Kamthan M, Tyagi RK, Datta A. Mapping of functional domains and characterization of the transcription factor Cph1 that mediate morphogenesis in Candida albicans. Fungal Genet Biol. 2015;83:45-57. Epub 2015/08/21. doi: 10.1016/j.fgb.2015.08.004. PubMed PMID: 26291891.

57. Hopke A, Nicke N, Hidu EE, Degani G, Popolo L, Wheeler RT. Neutrophil Attack Triggers Extracellular Trap-Dependent Candida Cell Wall Remodeling and Altered Immune Recognition. PLoS Pathog. 2016;12(5):e1005644. Epub 2016/05/26. doi: 10.1371/journal.ppat.1005644. PubMed PMID: 27223610; PubMed Central PMCID: PMCPMC4880299.

58. Pericolini E, Perito S, Castagnoli A, Gabrielli E, Mencacci A, Blasi E, et al. Epitope unmasking in vulvovaginal candidiasis is associated with hyphal growth and neutrophilic infiltration. PLoS One. 2018;13(7):e0201436. Epub 2018/08/01. doi: 10.1371/journal.pone.0201436. PubMed PMID: 30063729; PubMed Central PMCID: PMCPMC6067721.

59. Herwald SE, Zucchi PC, Tan S, Kumamoto CA. The two transmembrane regions of Candida albicans Dfi1 contribute to its biogenesis. Biochem Biophys Res Commun. 2017;488(1):153-8. Epub 2017/05/10. doi: 10.1016/j.bbrc.2017.04.158. PubMed PMID: 28483525; PubMed Central PMCID: PMCPMC5521179.

60. Philip B, Levin DE. Wsc1 and Mid2 are cell surface sensors for cell wall integrity signaling that act through Rom2, a guanine nucleotide exchange factor for Rho1. Mol Cell Biol. 2001;21(1):271-80. Epub 2000/12/13. doi: 10.1128/MCB.21.1.271-280.2001. PubMed PMID: 11113201; PubMed Central PMCID: PMCPMC88800.

61. Takahashi S, Pryciak PM. Membrane localization of scaffold proteins promotes graded signaling in the yeast MAP kinase cascade. Curr Biol. 2008;18(16):1184-91. Epub 2008/08/30. doi: 10.1016/j.cub.2008.07.050. PubMed PMID: 18722124; PubMed Central PMCID: PMCPMC2562168.

62. Styles C. How to set up a yeast laboratory. Methods Enzymol. 2002;350:42-71. Epub 2002/06/21. doi: 10.1016/s0076-6879(02)50955-1. PubMed PMID: 12073328.

63. Nguyen N, Quail MMF, Hernday AD. An Efficient, Rapid, and Recyclable System for CRISPR-Mediated Genome Editing in Candida albicans. mSphere. 2017;2(2). Epub 2017/05/13. doi: 10.1128/mSphereDirect.00149-17. PubMed PMID: 28497115; PubMed Central PMCID: PMCPMC5422035.

64. Reuss O, Vik A, Kolter R, Morschhauser J. The SAT1 flipper, an optimized tool for gene disruption in Candida albicans. Gene. 2004;341:119-27. Epub 2004/10/12. doi: 10.1016/j.gene.2004.06.021. PubMed PMID: 15474295.

65. Raschke WC, Baird S, Ralph P, Nakoinz I. Functional macrophage cell lines transformed by Abelson leukemia virus. Cell. 1978;15(1):261-7. Epub 1978/09/01. doi: 10.1016/0092-8674(78)90101-0. PubMed PMID: 212198.

66. Tams RN, Cassilly CD, Anaokar S, Brewer WT, Dinsmore JT, Chen YL, et al. Overproduction of Phospholipids by the Kennedy Pathway Leads to Hypervirulence in Candida albicans. Front Microbiol. 2019;10:86. Epub 2019/02/23. doi: 10.3389/fmicb.2019.00086. PubMed PMID: 30792701; PubMed Central PMCID: PMCPMC6374345.

Appendix

S2.1 Table: Plasmids used in this study.

Strain Name	Description	Markers (Bacterial, Fungal)	Parent/Source
pYLC146	*FLP-CaNAT*	Chloramphenicol, Nourseothricin	[1]
pBT1	*CaNAT-*P_{ENO1}	Ampicillin, Nourseothricin	[2]
pADH110	CRISPR fragment A template	Ampicillin, Nourseothricin*	[3]
pADH119	CRISPR fragment B template	Ampicillin, Nourseothricin*	[3]
pADH137	CRISPR Cas9 expression Plasmid	Ampicillin, Nourseothricin*	[3]
pAW006	*LEU2 5'UTR-FLP-CaNAT*	Chloramphenicol, Nourseothricin	pYLC146
pAW011	*FLP-CaNAT-LEU2* Knockout Plasmid	Chloramphenicol, Nourseothricin	pAW006
pTC074	FLP-CaNAT-*CPH1* 3'UTR	Chloramphenicol, Nourseothricin	pYLC146
pAW054	*CaNAT-Peno1-CPH1*	Ampicillin, Nourseothricin	pBT1
pAW066	*CaNAT-Peno1-DFI1*	Ampicillin, Nourseothricin	pBT1
pAW071	*FLP-CaNAT-CPH1-flag* reintegrate plasmid	Chloramphenicol, Nourseothricin	pTC074
pAW085	*FLP-CaNAT-PCK1* 3'UTR	Chloramphenicol, Nourseothricin	pYLC146
pAW087	*FLP-CaNAT-*P_{PCK1} overexpression cassette	Chloramphenicol, Nourseothricin	pAW085
pAW091	*FLP-CaNAT-*P_{PCK1}*-CEK1*	Chloramphenicol, Nourseothricin	pAW087
pAW105	*FLP-CaNAT-P* $_{PCK1}$*-HST7*	Chloramphenicol, Nourseothricin	pAW087

*These plasmids each function together to make a split nourseothricin gene that comes together to form a functional open reading frame after successful transformation and recombination into the *Candida albicans LEU2* locus.

References:

1. Chen YL, Montedonico AE, Kauffman S, Dunlap JR, Menn FM, Reynolds TB. Phosphatidylserine synthase and phosphatidylserine decarboxylase are essential for cell wall integrity and virulence in Candida albicans. Mol Microbiol. 2010;75(5):1112-32. Epub 2010/02/06. doi: 10.1111/j.1365-2958.2009.07018.x. PubMed PMID: 20132453.

2. Tams RN, Cassilly CD, Anaokar S, Brewer WT, Dinsmore JT, Chen YL, et al. Overproduction of Phospholipids by the Kennedy Pathway Leads to Hypervirulence in Candida albicans. Front Microbiol. 2019;10:86. Epub 2019/02/23. doi: 10.3389/fmicb.2019.00086. PubMed PMID: 30792701; PubMed Central PMCID: PMCPMC6374345.

3. Nguyen N, Quail MMF, Hernday AD. An Efficient, Rapid, and Recyclable System for CRISPR-Mediated Genome Editing in Candida albicans. mSphere. 2017;2(2). Epub 2017/05/13. doi: 10.1128/mSphereDirect.00149-17. PubMed PMID: 28497115; PubMed Central PMCID: PMCPMC5422035.

S2.2 Table: Primers used in this study.

Primer Name	Sequence (5' to 3')	Description	Source
AWO117	GTACACTTCACACCTCAG	*CPH1* sequencing primer (sits at -324).	This Study
AWO150	aacttgcggccgcCATGTCAATTA CTAAAACATAC	Forward primer flanked by NotI cut site to amplify CPH1 ORF and 3' UTR for cloning into pBT1. Also used for sequencing.	This Study
AWO151	TAAAAgagctCGAAATCCTTA AAAGACAAGC	Reverse primer flanked by SacI cut site to amplify CPH1 ORF and 3' UTR for cloning into pBT1 and for checking CPH1 gene deletion.	This Study
AWO156	GGTAATATCATCGATGAACAG	*STE11* forward primer for amplifying $P_{tet\text{-}off}$ promotor from TC147 (sits -512bp from start codon in *STE11* 5' untranslated region).	This Study
AWO157	CAACATCGATTGAACTGAAC	*STE11* reverse primer for amplifying $P_{tet\text{-}off}$ promotor from TC147 (sits at 1906 in open reading frame and 505bp downstream of the homologous region for the *Ptet-off* insert (that's at 1401)).	This Study
AWO158	GAGGTTCCAAAATTGCATC	Reverse primer *Peno1-CPH1* Genomic integration check.	This Study
AWO162	CGTAAACTATTTTTAATT TGtgagttggtacaagtgatgtGTTT TAGAGCTAGAAATAGC	*CPH1* gRNA forward primer for fragment B amplification for CRISPR-mediated gene deletion.	This Study
AWO171	CGTAAACTATTTTTAATTT GctggtcgagtgattatggtgGTTTT AGAGCTAGAAATAGC	*DFI1* gRNA forward primer for fragment B amplification for CRISPR-mediated gene deletion.	This Study
AWO174	CTCTCATCTACCAAGAATG	Forward primer for checking *DFI1* gene deletion.	This Study
AWO176	aacttgcggccgcATGGAGAAA CTTTCAATCAAC	Forward primer flanked by NotI cut site to amplify DFI1 ORF and 3' UTR for cloning into pBT1. Also used for DFI1 sequencing check.	This Study

S2.2 Table Continued

Primer Name	Sequence (5' to 3')	Description	Source
AWO177	TAAAAgagctCCGAACCTT TGATTTCTGTC	Reverse primer flanked by SacI cut site to amplify DFI1 ORF and 3' UTR for cloning into pBT1 and for checking DFI1 gene deletion. Also used for DFI1 sequencing check.	This Study
AWO181	CACCAAGTCAATACAAAGC	*CPH1* sequencing primer (sits at +857 in ORF).	This Study
AWO182	CAACCTATATAAAGGCA ATAC	*CPH1* sequencing primer (sits at +1350 in ORF).	This Study
AWO179	TAAAAgagctCGCGTCCTTA CATCATTATTAG	Reverse primer flanked by SacI cut site for checking OPY2 gene deletion.	This Study
AWO187	AACTTgggcccGAGTACACT TCACACCTCAG	Forward primer flanked by an ApaI cut site that sits at -326 in CPH1 5'UTR for amplifying CPH1 ORF with 326bp of homology to the CPH1 promoter.	This Study
AWO188	aacttctcGAGttagccgctgctCTTG TCGTCATCGTCTTTGTAGT CgcatatgccTGTTTGTGACTGT TTTACTTC	Reverse primer flanked by a XhoI cut site and flag-tag sequence for amplifying the CPH1 ORF with a C-terminal flag-tag.	This Study
AWO199	CGTAAACTATTTTTAATTTGa caacaacaagctcaggctcGTTTTAGA GCTAGAAATAGC	*CEK1* gRNA forward primer for fragment B amplification for CRISPR-mediated gene deletion.	This Study
AWO205	CTCCAATTCCAACTCTAAC	Forward primer for checking *CEK1* gene deletion.	This Study
AWO227	CGTAAACTATTTTTAATTTGct actaaaaagagacgaaaaGTTTTAGAG CTAGAAATAGC	*OPY2* gRNA forward primer for fragment B amplification for CRISPR-mediated gene deletion.	This Study
AWO232	GGAATATAAGGTACATCACC	Reverse primer for checking *OPY2* gene deletion.	This Study

S2.2 Table Continued

Primer Name	Sequence (5' to 3')	Description	Source
AWO250	CACGTGATCAACAAATTG	Reverse primer for checking *CEK1* gene deletion.	This Study
AWO263	AACTTggtacCGAATATTAC GTATTCTCCTCCTTC	Forward primer for amplifying PCK1 promoter (-712 to -1) with flanking KpnI cut site. Also used for CEK1 sequencing check.	This Study
AWO264	AACTTgggcccGATTGATAAT TATTTGAATAAGTTAATG	Reverse primer for amplifying PCK1 promoter (-712 to -1) with flanking ApaI cut site.	This Study
AWO265	TAAAAccgcGGACAAACA AATAAACAAAAAAAAAA AAG	Forward primer for amplifying PCK1 3' UTR (495bp immedietly after stop codon) with flanking SacII cut site.	This Study
AWO266	TAAAAgagctCGGATTATGAG ACCTAATCTTATCAATG	Reverse primer for amplifying PCK1 3' UTR (495bp immedietly after stop codon) with flanking SacI cut site.	This Study
AWO267	AACTTgggcccATGATGAATATA GATCAACATCATC	Forward primer for amplifying CEK1 ORF with flanking ApaI cut site for cloning into pAW087 plasmid. Also used for CEK1 sequencing check.	This Study
AWO268	aacttctcgagCTTTATAATGGTTTC ATAATCTCTTC	Reverse primer for amplifying CEK1 ORF with flanking XhoI cut site for cloning into pAW087 plasmid. Also used for CEK1 sequencing check.	This Study
AWO343	CGTAAACTATTTTTAATTTG gataatggtgaaggcactggGTTTTAG AGCTAGAAATAGC	*HST7* gRNA forward primer for fragment B amplification for CRISPR-mediated gene deletion.	This Study
AWO346	GAATGAGAGACAGAATGA AAAG	Forward primer for checking *HST7* gene deletion.	This Study
AWO347	GAGGAATTTTTGTTGGATTTG	Reverse primer for checking *HST7* gene deletion.	This Study
AWO348	AACTTgggcccATGACAAGAACA ACTCGTATAGA	*HST7* forward primer with flanked by an ApaI Cutsite for cloning into pAW087 plasmid. Also used for *HST7* sequencing check.	This Study

S2.2 Table Continued

Primer Name	Sequence (5' to 3')	Description	Source
AWO349	AACTTgggcccGATTCCTGGTTAT GCAATG	*HST7* reverse primer with ApaI Cutsite for cloning into pAW087 plasmid.	This Study
AWO350	GTGGGTAAATGAAGTATAGGTG	*Ppck1-HST* ligation check primer (reverse). Also used for *HST7* sequencing check.	This Study
AWO351	CTGGGTCAGGTGTAATTGTG	*HST7* sequencing primer forward (Sits +364)	This Study
AWO352	CCACCCAAAAAACAATGG	*HST7* sequencing primer forward (Sits +808)	This Study
AWO353	GACACTTTTGTCGGTACTTC	*HST7* sequencing primer forward (Sits +1218)	This Study
AWO354	CAATCCTGTGACAAAGTTGCC	*HST7* sequencing primer forward (Sits +1571)	This Study
AHIO1096	GACGGCACGGCCACGCGTTTA AACCGCC	Fragment A forward primer for CRISPR-mediated gene deletion.	1
AHO1097	CCCGCCAGGCGCTGGGGTTTA AACACCG	Fragment B reverse primer for CRISPR-mediated gene deletion.	1
AHO1098	caaattaaaaatagtttacgcaag	Fragment A reverse primer for CRISPR-mediated gene deletion.	1
AHO1237	aggtgatgctgaagctattgaag	Fragment C forward primer for CRISPR-mediated gene deletion.	1
AHO1238	TGTATTTTGTTTTAAAATTTTAGTGACTGTTTC	Fragment C reverse primer for CRISPR-mediated gene deletion.	1
BTO33	GACTAACGATTTCTATAAGG	P_{ENO1} colony PCR forward check primer and primer for sequencing P_{ENO1} overexpression constructs	2

S2.2 Table Continued

Primer Name	Sequence (5' to 3')	Description	Source
JCO95	GATTATTAGTTAAACCACTGC	P_{MAL2} reverse primer for checking successful ligation into pYLC146 vectors on the 5' end of the internal nourseothricin marker	2
JCO96	TGAAGGGGGAGATTTTCACT	*URA3* terminator forward primer for checking successful ligation into pYLC146 vectors on the 3' end of the internal nourseothricin marker	3
TCO168	CTGTTCTTTCATGGTATTCT	Forward primer that sits at -117bp of the *STE11* promoter to check if $P_{tet\text{-}off}$-$STE11^{\Delta N467}$ was integrated into the genome in AWY080	4
TCO169	ACTGATTTATTCAATTGATGG	Reverse primer that sits in the P_{TDH3} in the pWTF1 construct to check if $P_{tet\text{-}off}$-$STE11^{\Delta N467}$ was integrated into the genome in AWY080	4
TCO173	AAAAGCGGCCGCGATGAATA GATACAGAGAGAA	Forward primer flanked by a NotI cut site for amplifying the 3'UTR of CPH1	This Study
TCO174	AAAAGAGCTCCCTTAAAAGACA AGCAACATT	Reverse primer flanked by a SacI cut site for amplifying the 3'UTR of CPH1	This Study
AWO222	TACACTCTTTCGCCATGTCAATTA CTAAAACATACAATGGTGATCCT ACAATGAATAGATACAGAGAGAA AGAGAAAGAAAGAAAAAAACTAA GTAAATG	*CPH1* repair template for whole gene deletion (sense oligomer)	This Study
AWO223	CATTTACTTAGTTTTTTTCTTTCTT TCTCTTTCTCTCTGTATCTATTCAT TGTAGGATCACCATTGTATGTTTT AGTAATTGACATGGCGAAAGAGT GTA	*CPH1* repair template for whole gene deletion (antisense oligomer)	This Study
AWO228	CATGCCAATACCCAGATCGTTTAT ATTTGAACCTGAGTTGGAACAGCT ACGTCCCTGGTAATTGAGGCTTTA CAAATGATTTCTATACTTGATATT AGAG	*OPY2* repair template for whole gene deletion (sense oligomer)	This Study

S2.2 Table Continued

Primer Name	Sequence (5' to 3')	Description	Source
AWO229	CTCTAATATCAAGTATAGAAATCA TTTGTAAAGCCTCAATTACCAGGG ACGTAGCTGTTCCAACTCAGGTTC AAATATAAACGATCTGGGTATTGG CATG	*OPY2* repair template for whole gene deletion (antisense oligomer)	This Study
AWO230	CACTGTATCGACGTATTTTGTCAAC AGCTACACATGCAATCAACCACAC CACAAGGCTTATTTTGGATGAGGGT GGTTTTTTTTATAAGTATTTTGTAGT	*DFI1* repair template for whole gene deletion (sense oligomer)	This Study
AWO231	ACTACAAAATACTTATAAAAAAAAC CACCCTCATCCAAAATAAGCCTTGTG GTGTGGTTGATTGCATGTGTAGCTGT TGACAAAATACGTCGATACAGTG	*DFI1* repair template for whole gene deletion (antisense oligomer)	This Study
AWO249	ATAGATCAACATCATCAGCTTCAACA GCAACATCAACAACAAATGTTACATA AAGAGGTCAAGCYAAGTTAAGCTAA ACTAAACTAAACTAAACTAAACT	*CEK1* repair template for whole gene deletion (sense oligomer)	This Study
AWO250	AGTTTAGTTTAGTTTAGTTTAGTTTAG CTTAACTTRGCTTGACCTCTTTATGTAA CATTTGTTGTTGATGTTGCTGTTGAAGC TGATGATGTTGATCTAT	*CEK1* repair template for whole gene deletion (antisense oligomer)	This Study
AWO344	CCTCAACAATGACAAGAACAACTCGT ATAGATACACAAGAAGCTACAAAGTA AACACAACTCATATACATATACAAAA AAAAAACGCATTTATGCATCAT	*HST7* repair template for whole gene deletion (sense oligomer)	This Study
AWO345	ATGATGCATAAATGCGTTTTTTTTTTG TATATGTATATGAGTTGTGTTTACTTTG TAGCTTCTTGTGTATCTATACGAGTTGT TCTTGTCATTGTTGAGG	*HST7* repair template for whole gene deletion (antisense oligomer)	This Study

References:

1) Nguyen N, Quail MMF, Hernday AD. An Efficient, Rapid, and Recyclable System for CRISPR-Mediated Genome Editing in Candida albicans. mSphere. 2017;2(2). Epub 2017/05/13. doi: 10.1128/mSphereDirect.00149-17. PubMed PMID: 28497115; PubMed Central PMCID: PMCPMC5422035.
2) Tams RN, Cassilly CD, Anaokar S, Brewer WT, Dinsmore JT, Chen YL, et al. Overproduction of Phospholipids by the Kennedy Pathway Leads to Hypervirulence in Candida albicans. Front Microbiol. 2019;10:86. Epub 2019/02/23. doi: 10.3389/fmicb.2019.00086. PubMed PMID: 30792701; PubMed Central PMCID: PMCPMC6374345.
3) Chen YL, Montedonico AE, Kauffman S, Dunlap JR, Menn FM, Reynolds TB. Phosphatidylserine synthase and phosphatidylserine decarboxylase are essential for cell wall integrity and virulence in Candida albicans. Mol Microbiol. 2010;75(5):1112-32. Epub 2010/02/06. doi: 10.1111/j.1365-2958.2009.07018.x. PubMed PMID: 20132453.
4) Chen T, Wagner AS, Tams RN, Eyer JE, Kauffman SJ, Gann ER, et al. Lrg1 Regulates beta (1,3)-Glucan Masking in Candida albicans through the Cek1 MAP Kinase Pathway. mBio. 2019;10(5). Epub 2019/09/19. doi: 10.1128/mBio.01767-19. PubMed PMID: 31530671; PubMed Central PMCID: PMCPMC6751057.

S2.3 Table: Strains used in this study.

Strain	Genotype	Parent	Source or Reference
SC5314	Prototrophic Wild Type	Clinical Isolate	[1]
DAY286	*ura3::imm434/ura3::imm434, his1::hisG/his1::hisG, pARG4::URA3::arg4::hisG/arg4::hisG*)	SC5314	[2]
CAI-4	*ura3*::imm434/*ura3*::imm434 *iro1/iro1*::imm434	SC5314	[3]
TC147	*STE11/*$P_{tet\text{-}off}$*-STE11*$^{\Delta N467}$	Day286	[4]
AWY006	*LEU2/leu2*Δ (Wild Type)	SC5314	This Study
AWY080	*STE11/*$P_{tet\text{-}off}$*-STE11*$^{\Delta N467}$ *LEU2/leu2*Δ	AWY006	This Study
AWY109	P_{ENO1}*-CPH1 LEU2/leu2*Δ	AWY006	This Study
AWY112	P_{ENO1}*-DFI1 LEU2/leu2*Δ	AWY006	This Study
AWY144	*STE11/*$P_{tet\text{-}off}$*-STE11*$^{\Delta N467}$*cph1*ΔΔ *LEU2/leu2*Δ	AWY080	This Study
AWY154	*STE11/*$P_{tet\text{-}off}$*-STE11*$^{\Delta N467}$*cph1*ΔΔ*::CPH1-Flag LEU2/leu2*Δ	AWY144	This Study
AWY173	*opy2*ΔΔ *LEU2/leu2*Δ	AWY006	This Study
AWY174	*STE11/*$P_{tet\text{-}off}$*-STE11*$^{\Delta N467}$opy2ΔΔ LEU2/leu2Δ	AWY080	This Study
AWY182	*cph1*ΔΔ *LEU2/leu2*Δ	AWY006	This Study
AWY183	*dfi1*ΔΔ *LEU2/leu2*Δ	AWY006	This Study
AWY184	*opy2*ΔΔ *dfi1*ΔΔ *LEU2/leu2*Δ	AWY173	This Study
AWY187	*STE11/*$P_{tet\text{-}off}$*-STE11*$^{\Delta N467}$ *dfi1*ΔΔ *LEU2/leu2*Δ	AWY080	This Study
AWY188	*STE11/*$P_{tet\text{-}off}$*-STE11*$^{\Delta N467}$ *opy2*ΔΔ *dfi1*ΔΔ *LEU2/leu2*Δ	AWY174	This Study
AWY208	*cek1*ΔΔ *LEU2/leu2*Δ	AWY006	This Study
AWY212	*STE11/*$P_{tet\text{-}off}$*-STE11*$^{\Delta N467}$ *dfi1*ΔΔ P_{ENO1}*-DFI1 LEU2/leu2*Δ	AWY187	This Study
AWY215	*STE11/*$P_{tet\text{-}off}$*-STE11*$^{\Delta N467}$ *opy2*ΔΔ *dfi1*ΔΔ P_{ENO1}*-DFI1 LEU2/leu2*Δ	AWY188	This Study

S2.3 Table Continued

Strain	Genotype	Parent	Source or Reference
AWY220	*STE11/P$_{tet\text{-}off}$-STE11$^{\Delta N467}$ P$_{ENO1}$-DFI1 LEU2/leu2*Δ	AWY080	This Study
AWY236	*STE11/P$_{tet\text{-}off}$-STE11$^{\Delta N467}$ cek1*ΔΔ *LEU2/leu2*Δ	AWY080	This Study
AWY221	*cek1*ΔΔ *leu2*ΔΔ	CAI-4	This Study
AWY240	*P$_{PCK1}$-CEK1 LEU2/leu2*Δ	AWY006	This Study
AWY242	*STE11/P$_{tet\text{-}off}$-STE11$^{\Delta N467}$ cek1*ΔΔ *P$_{PCK1}$-CEK1 LEU2/leu2*Δ	AWY236	This Study
AWY264	*hst7*ΔΔ *LEU2/leu2*Δ	AWY006	This Study
AWY266	*STE11/P$_{tet\text{-}off}$-STE11*Δ*N467 hst7*ΔΔ *LEU2/leu2*Δ	AWY080	This Study
AWY270	*STE11/P$_{tet\text{-}off}$-STE11$^{\Delta N467}$ hst7*ΔΔ *P$_{PCK1}$-CEK1 LEU2/leu2*Δ	AWY266	This Study
AWY272	*Ppck1-HST7 LEU2/leu2*Δ	AWY264	This Study

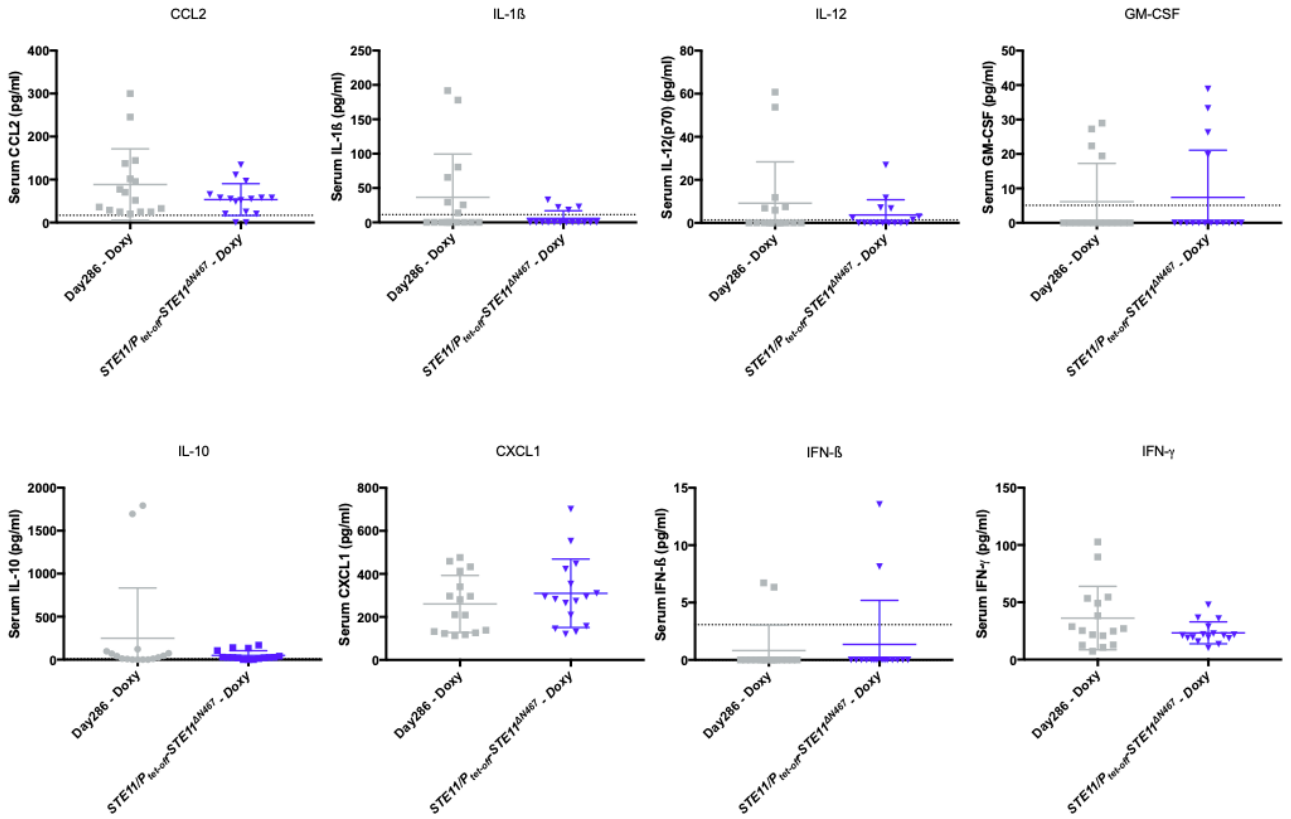
References:

1. Gillum AM, Tsay EY, Kirsch DR. Isolation of the Candida albicans gene for orotidine-5'-phosphate decarboxylase by complementation of S. cerevisiae ura3 and E. coli pyrF mutations. Mol Gen Genet. 1984;198(2):179-82. Epub 1984/01/01. doi: 10.1007/BF00328721. PubMed PMID: 6394964.

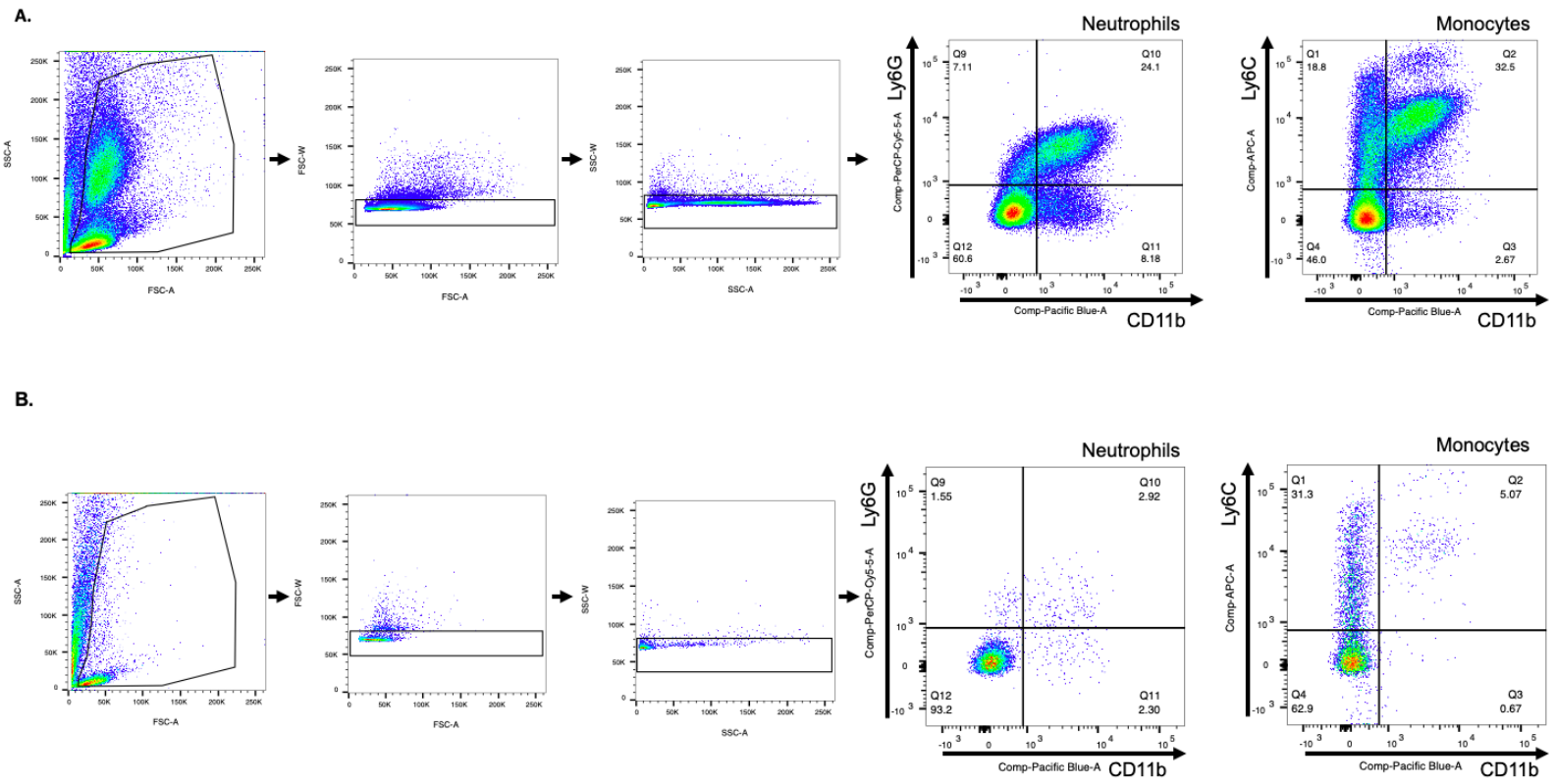
2. Davis DA, Bruno VM, Loza L, Filler SG, Mitchell AP. Candida albicans Mds3p, a conserved regulator of pH responses and virulence identified through insertional mutagenesis. Genetics. 2002;162(4):1573-81. Epub 2003/01/14. PubMed PMID: 12524333; PubMed Central PMCID: PMCPMC1462392.

3. Fonzi WA, Irwin MY. Isogenic strain construction and gene mapping in Candida albicans. Genetics. 1993;134(3):717-28. Epub 1993/07/01. PubMed PMID: 8349105; PubMed Central PMCID: PMCPMC1205510.

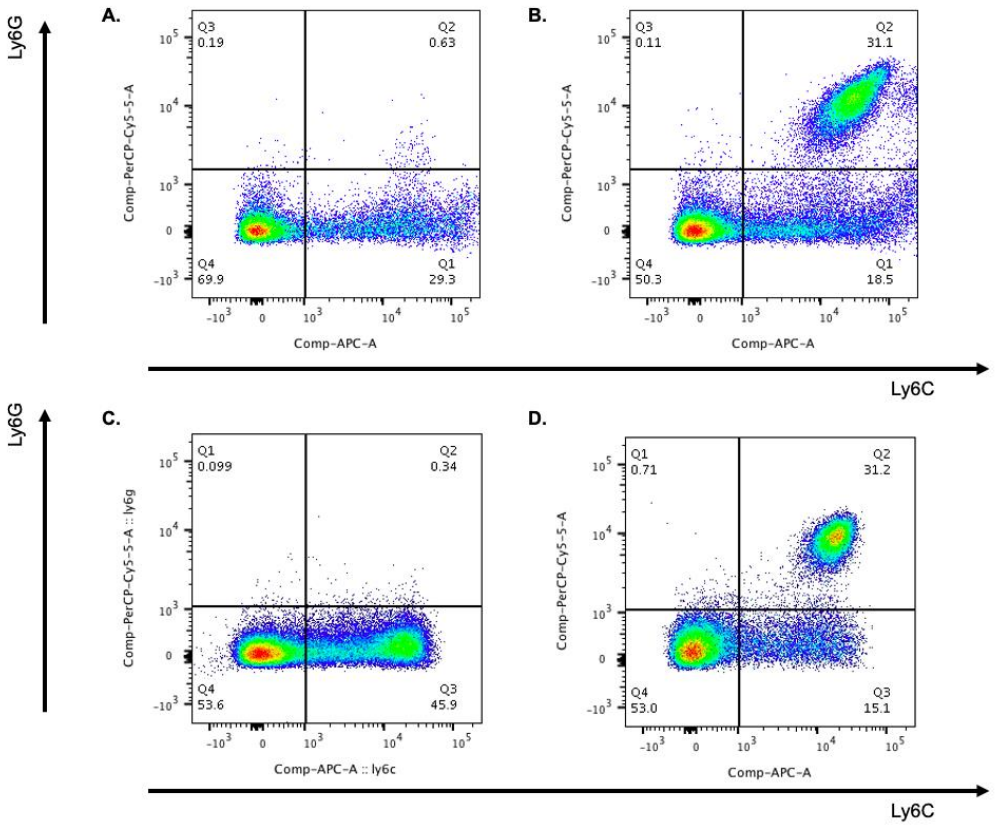
4. Chen T, Wagner AS, Tams RN, Eyer JE, Kauffman SJ, Gann ER, et al. Lrg1 Regulates beta (1,3)-Glucan Masking in Candida albicans through the Cek1 MAP Kinase Pathway. mBio. 2019;10(5). Epub 2019/09/19. doi: 10.1128/mBio.01767-19. PubMed PMID: 31530671; PubMed Central PMCID: PMCPMC6751057.



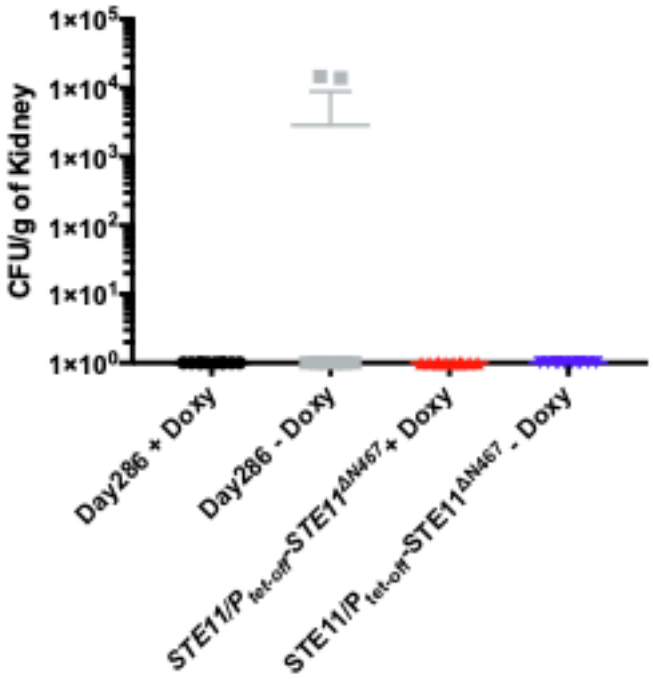
S2.1 Fig: Characterization of serum cytokines during systemic infection with a hyperactive *STE11* mutant.
ICR mice were intravenously infected with $1x10^6$ cells of *C. albicans* wild-type (Day286) or the *STE11/*$P_{tet\text{-}off}$*-STE11*$^{\Delta N467}$ strain. Serum was collected 4 days post infection and the concentrations of CCL2, IL-1ß, IL-12, GM-CSF, CXCL1, IL-10, IFN-ß and IFN-γ were determined via flow cytometry using the LEGENDplex cytokine bead based array kit. (n = 8 mice)(*$p<0.05$, by Mann-Whitney test)(Horizontal dotted lines indicate the kit detection limit for each cytokine).



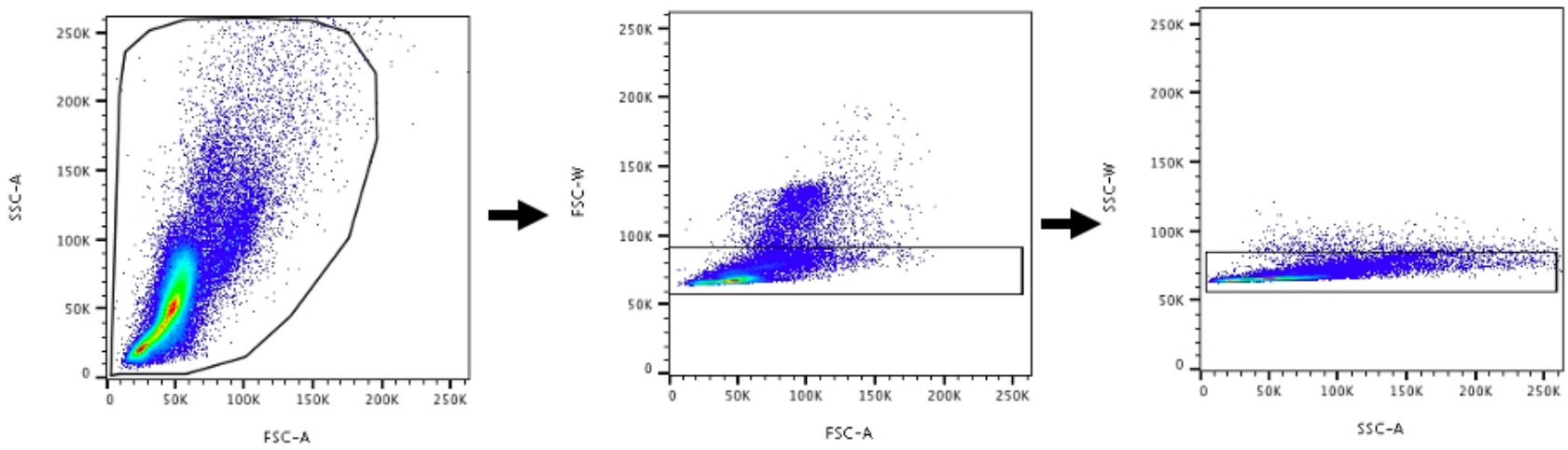
S2.2 Fig: Representative Staining of Peripheral Blood during immunosuppression by cyclophosphamide.
Peripheral blood samples from Cyclophosphamide (Cyclo) and PBS treated mice were analyzed for circulating myeloid cells. Mice were anesthetized, and peripheral blood was isolated via cardiac puncture in heparin treated tubes (BD Biosciences; San Jose, CA). Erythrocytes were lysed using 2 ACK lysis steps (ref), cells were counted and stained using myeloid markers (α-Ly6C: HK1.4, APC, BioLegend) (α-Ly6G: 1A8, PerCP-Cy5.5, BioLegend) (α-CD11b: M1/70 clone, BV421, BioLegend) (α-F4/80: BM8, PE, BioLegend) (Fixable NIR Live-Dead: APC-Cy7, Invitrogen; cat #:L34975). Relative abundance and representative plots were generated using an LSRII flow cytometer (BD Biosciences; San Jose, CA), and analysis was performed using FlowJo (Becton, Dickinson and Company; Ashland, OR). Flow cytometric analysis shows a marked decrease in circulating Monocytes (Lyc6C+/ CD11b+) and Neutrophils (Ly6G+/ CD11b+) after three doses of Cyclo (B) versus PBS (A).



S2.3 Fig: Representative scatter plots of leukocyte populations during 1A8 neutrophil depletion.
Peripheral blood of 1A8 depleted mice and mice receiving the PBS depletion control were analyzed for circulating myeloid cells. Myeloid populations were assessed via staining using myeloid markers (α-Ly6C: HK1.4, APC, BioLegend) (α-Ly6G: 1A8, PerCP-Cy5.5, BioLegend) (α-CD11b: M1/70 clone, BV421, BioLegend) (α-F4/80: BM8, PE, BioLegend) (Fixable NIR Live-Dead: APC-Cy7, Invitrogen; cat #:L34975). Relative abundance and representative plots were generated using an LSRII flow cytometer (BD Biosciences), and analysis was performed using FlowJo (Becton, Dickinson and Company). Flow cytometric analysis revealed that the levels of Ly6C+/Ly6G+ cells were markedly decreased in (A) 1A8 treated mice, when compared to (B) PBS treated mice at day 0 following infection with Day286 wild-type *C. albicans* cells. (C) 1A8 treated mice, when compared to (D) PBS treated mice at day 4 post infection following infection with Day286 wild-type *C. albicans* cells.

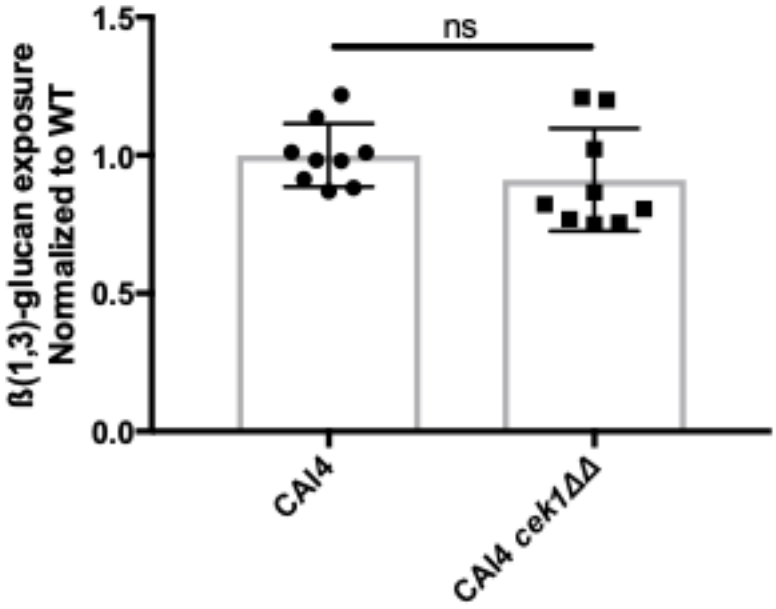


S2.4 Fig: Kidney fungal burden in 1A8 control mice treated with PBS and infected with 1x10^4 cells of the *STE11/P$_{tet\text{-}off}$-STE11$^{\Delta N467}$* or wild-type strains.
Starting one day prior to infection (day -1), ICR mice were treated every 3 days with recurring injections of 200µl of PBS intraperitoneally as a drug vehicle control for 1A8 treatment. At day 0, mice were then intravenously infected with 1x10^4 cells of *C. albicans* wild-type (Day286) or the *STE11/P$_{tet\text{-}off}$-STE11$^{\Delta N467}$* strain and their kidneys were harvested at 4 days post infection (d.p.i.) to assess fungal burden. (n = 5 mice)

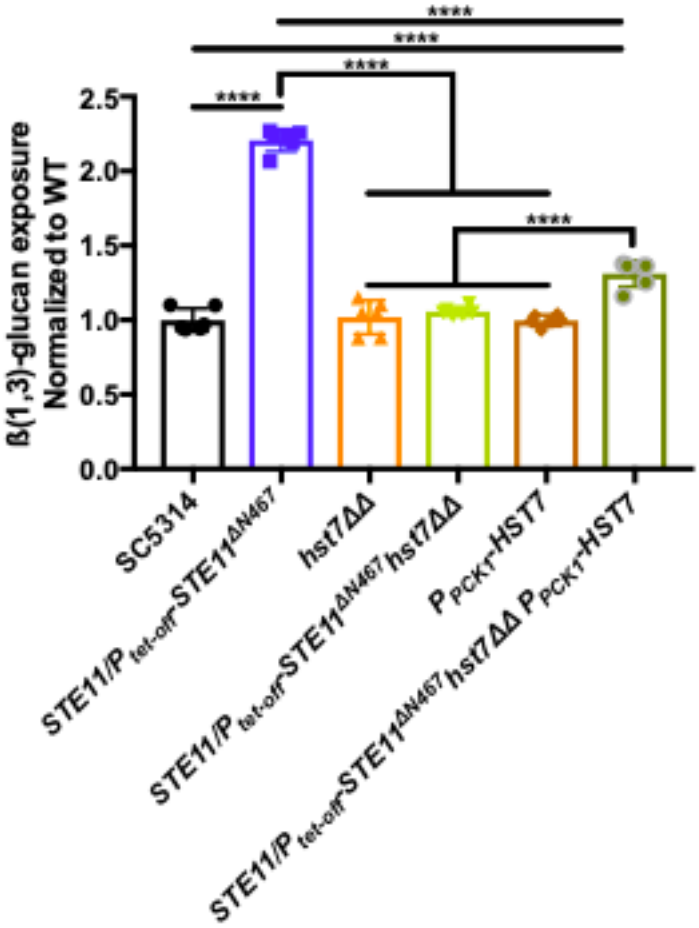


S2.5 Fig

S2.5 Fig: Gating strategy for yeast cell population of *C. albicans.*



S2.6 Fig: *CEK1* deletion in the CAI4 wild-type background does not induce unmasking.
Overnight cultures of wild-type and *cek1*ΔΔ mutant cells in the CAI4 background were stained with anti-ß(1,3)-glucan antibody and a phycoerythrin-conjugated secondary antibody for flow cytometry analysis to assess the levels of ß(1,3)-glucan exposure. Three biological replicates were run for each sample. (p=0.2828, by student's t-test)



S2.7 Fig: The *hst7*ΔΔ mutation blocks ß(1,3)-glucan unmasking by hyperactive *STE11*$^{\Delta N467}$. Overnight cultures of the wild-type and *hst7ΔΔ* mutants were stained with an anti-ß(1,3)-glucan antibody and a phycoerythrin-conjugated secondary antibody followed by flow cytometry analysis to assess the levels of ß(1,3)-glucan exposure (****p<0.0001, by one-way ANOVA with Tukey's post hoc analysis).

CHAPTER 3 - CEK1 REGULATES ß(1,3)-GLUCAN EXPOSURE THROUGH CALCINEURIN EFFECTORS IN *CANDIDA ALBICANS*

This work was performed by: Andrew S. Wagner, Stephen W. Lumsdaine, Mikayla M. Mangrum, Ainsley E. King, Trevor J. Hancock, Timothy E. Sparer and Todd B. Reynolds

Author Contributions: Conceptualization, ASW and TBR.; Methodology, ASW, TJH and AEK; Formal analysis, ASW; Investigation, ASW, SWL (generated *FGR41* and *CRZ1* knockout mutants, and Fig. 3.2D), MMM (Generated PGA13 overexpression mutant and Fig. 3.5E), AEK (Generated *CWP419* overexpression mutants and did hyphal measurement assays in Fig. S3.7) and TJH (Generated panel and helped the analysis for immunosuppression checks in Fig. S3.9); Writing–original draft preparation, ASW; Writing–review and editing, ASW and TBR; Visualization, ASW; Funding Acquisition, TES and TBR.

This chapter has been published in PLoS Genetics:
- Wagner AS, Lumsdaine SW, Mangrum MM, King AE, Hancock TJ, Sparer TE, et al. Cek1 regulates ss(1,3)-glucan exposure through calcineurin effectors in Candida albicans. PLoS Genet. 2022;18(9):e1010405. Epub 2022/09/20. doi: 10.1371/journal.pgen.1010405. PubMed PMID: 36121853; PubMed Central PMCID: PMCPMC9521907.

Abstract

In order to successfully induce disease, the fungal pathogen *Candida albicans* regulates exposure of antigens like the cell wall polysaccharide ß(1,3)-glucan to the host immune system. *C. albicans* covers (masks) ß(1,3)-glucan with a layer of mannosylated glycoproteins, which aids in immune system evasion by acting as a barrier to recognition by host pattern recognition receptors. Consequently, enhanced ß(1,3)-glucan exposure (unmasking) makes fungal cells more visible to host immune cells and facilitates more robust fungal clearance. However, an understanding of how *C. albicans* regulates its exposure levels of ß(1,3)-glucan is needed to leverage this phenotype. Signal transduction pathways and their corresponding effector genes mediating these changes are only beginning to be defined. Here, we report that the phosphatase calcineurin mediates

unmasking of ß(1,3)-glucan in response to inputs from the Cek1 MAPK pathway and in response to caspofungin exposure. In contrast, calcineurin reduces ß-glucan exposure in response to high levels of extracellular calcium. Thus, depending on the input, calcineurin acts as a switchboard to regulate ß(1,3)-glucan exposure levels. By leveraging these differential ß(1,3)-glucan exposure phenotypes, we identified two novel effector genes in the calcineurin regulon, *FGR41* and *C1_11990W_A*, that encode putative cell wall proteins and mediate masking/unmasking. Loss of either effector caused unmasking and attenuated virulence during systemic infection in mice. Furthermore, immunosuppression restored the colonization decrease seen in mice infected with the *fgr41Δ/Δ* mutant to wild-type levels, demonstrating a reliance on the host immune system for virulence attenuation. Thus, calcineurin and its downstream regulon are general regulators of unmasking.

Introduction

In order to successfully disseminate, colonize and induce disease, fungal pathogens must overcome numerous stressors deployed by the host. These include limitations on nutrient availability [1-3], pH changes [4-6], or altered oxygen levels within specific host niches [7-10]. In addition to these barriers, a repertoire of pattern recognition receptors (PRRs) that recognize multiple components of the fungal cell wall are present on both hematopoietic and non-hematopoietic immune cells to effectively recognize and mount an immune response to the invading fungal pathogen. These include receptors that sense mannosylated proteins on the outermost cell wall, as well as PRRs for structural polysaccharides within the cell wall's basal layers [11]. Amongst these basal layer polysaccharides, ß(1,3)-glucan is highly immunogenic, and PRRs that recognize exposed (unmasked) ß(1,3)-glucan moieties include dectin-1 [12-17], complement receptor 3 (CR3)[18, 19] and the ephrin type A receptor 2 (EphA2) [20, 21]. These receptors induce strong pro-inflammatory immune responses and are necessary for efficient fungal clearance. Thus, leveraging the impact that unmasked ß(1,3)-glucan has on host-pathogen interactions is a potential immunotherapeutic strategy for disease control.

In response to host derived environmental and immune-mediated stressors, fungal pathogens employ strategies to sense their surrounding environments and alter their levels

of exposed ß(1,3)-glucan. *Aspergillus fumigatus* uses galactosaminogalactan or hydrophobins to cover (mask) ß(1,3)-glucan in hyphae and conidia, respectively [22, 23]. Similarly, *Histoplasma capsulatum* masks ß(1,3)-glucan under a layer of α-glucan, and further reduces unmasked foci via expression of the glycosylhydrolyase Eng1 [24, 25]. *Candida albicans* covers ß(1,3)-glucan in its cell wall under an outer layer of densely populated mannoproteins, and mutations that prevent proper glycosylphosphatidylinositol (GPI)-anchored protein synthesis or protein mannosylation induce unmasking [26-28]. Similarly, *C. albicans* senses environmental signals and stressors, such as lactate [29, 30], acidic pH [31, 32], hypoxia [33], and iron-replete environments [34] and responds by further altering ß(1,3)-glucan exposure. These stimulus driven events are mediated by activation of appropriate signal transduction pathways, such as the cyclic AMP/Protein Kinase A (cAMP/PKA) pathway [33, 34] and the Cek1 mitogen activated protein kinase (MAPK) pathway [35-37]. These pathways therefore represent targets that can be utilized to better understand how ß-glucan exposure is regulated by *C. albicans*. Yet, our understanding of how these signaling pathways work together to regulate overall ß-glucan exposure is only beginning to be understood, and their downstream effector genes driving these structural changes remain to be fully elucidated.

Hyperactivation of the Cek1 MAPK pathway induces unmasking and attenuates virulence through the Cph1 transcription factor in a manner that is dependent, primarily, on a functional immune response [35-37]. The transcriptional regulon downstream of the Cek1 pathway includes the Dfi1 cell wall sensor, and Dfi1 mediates a significant portion of Cek1-induced ß(1,3)-glucan unmasking through a previously unidentified parallel signaling pathway [37]. Here, we expand on these findings and show that the calmodulin/calcineurin pathway is the parallel signaling pathway working downstream of Dfi1 and in synergy with the Cek1 MAPK pathway to induce the full levels of unmasking observed during Cek1 hyperactivation. Moreover, we show that calcineurin plays a more general role in mediating ß-glucan exposure, and is necessary to induce unmasking in response to the echinocandin caspofungin. In contrast, calcineurin reduces ß(1,3)-glucan exposure in response to extracellular calcium via the transcription factor Crz1. Using this information we identify two novel cell wall proteins, Fgr41 and Cwp419,

that are necessary for maintaining homeostatic levels of ß(1,3)-glucan exposure, and show that loss of Fgr41 leads to reduced fungal burden in mice during systemic infection in a manner that is host immune system dependent.

Results

Ste11$^{\Delta N467}$-induced Dfi1 activation causes unmasking through the calmodulin-calcineurin signal transduction pathway.

We have previously shown that expression of a single hyperactive allele of the MAP3K *STE11* (*STE11*$^{\Delta N467}$) under the control of a tetracycline repressible promoter ($P_{tet\text{-}off}$) induces unmasking through both the Cek1 MAPK pathway [35, 36], and a previously unidentified pathway that is activated by the cell wall sensor Dfi1 [37]. Thus, in order to identify effector proteins driving Ste11$^{\Delta N467}$-induced unmasking, it was necessary to elucidate the parallel signaling pathway that contributes to the ß(1,3)-glucan exposure observed during *STE11*$^{\Delta N467}$ expression. Dfi1 has been shown to interact with calmodulin through a calmodulin binding motif in its C-terminal tail [38]. We hypothesized that, once expression is enhanced by *STE11*$^{\Delta N467}$, Dfi1 interacts with calmodulin to further increase ß(1,3)-glucan unmasking. To test this, we introduced two point mutations, W305Q and W308Q, into the C-terminal calmodulin binding motif of Dfi1. These mutations impair Dfi1-calmodulin interactions *in vitro* [38]. As previously reported [37], immunofluorescent staining with an anti-ß(1,3)-glucan antibody showed a significant increase in ß(1,3)-glucan exposure in the *STE11/*$P_{tet\text{-}off}$*-STE11*$^{\Delta N467}$ mutant when compared to the wild-type (Fig. 3.1A and S3.1 Fig). Moreover, deletion of *DFI1* in the *STE11/*$P_{tet\text{-}off}$*-STE11*$^{\Delta N467}$ strain reduced its unmasking. Introduction of the W305Q and W308Q mutations in Dfi1 at residues critical for Dfi1-calmodulin binding reduced Ste11$^{\Delta N467}$-induced unmasking to the level observed in the *STE11/*$P_{tet\text{-}off}$*-STE11*$^{\Delta N467}$*dfi1*Δ/Δ mutant. Thus, Dfi1 mediates Ste11$^{\Delta N467}$-induced unmasking through an interaction with calmodulin.

One of the functions of calmodulin is to activate calcineurin, which is a phosphatase that can propagate signal transduction that affects the cell wall [39-42]. Therefore, we assessed if signal transduction is mediated through calcineurin to induce the full levels of

unmasking caused by *STE11*$^{\Delta N467}$ expression. Yeast cells were grown overnight in the presence of the calcineurin inhibitor cyclosporinee A [43, 44], and ß(1,3)-glucan unmasking was assessed by flow cytometry. Similarly to *STE11/P*$_{tet\text{-}off}$-*STE11*$^{\Delta N467}$*DFI1*^{W305Q,W308Q}/*DFI1*^{W305Q,W308Q} double mutant cells (Fig. 3.1A), cyclosporine A treated cells exhibited a partial block of Ste11$^{\Delta N467}$-induced unmasking (Fig. 3.1B). These data indicate that once stimulated by Dfi1, calmodulin mediates signal transduction through calcineurin to induce unmasking during *STE11*$^{\Delta N467}$ expression.

The calcineurin pathway plays a role in mediating caspofungin-driven unmasking.

Since unmasking by the Cek1 MAPK pathway is mediated in part by the calmodulin/calcineurin pathway [35-37] (Fig. 3.1), we assessed if these pathways play a more general role in mediating unmasking induced by additional stimuli. Exposure to a sublethal concentration of the echinocandin caspofungin induces unmasking [45, 46], and both the Cek1 and the calcineurin pathways are activated in response to caspofungin treatment [47-49]. Therefore, we hypothesized that these pathways help drive caspofungin-induced unmasking. To assess this, we tested mutants that block Ste11$^{\Delta N467}$-induced unmasking, including a *cph1Δ/Δ* mutant (transcription factor downstream of Cek1) [37] and the *dfi1Δ/Δ* mutant. Wild-type and mutant cells were grown to mid-log phase before being exposed to a sublethal concentration of caspofungin and ß(1,3)-glucan exposure was subsequently measured. Although Cph1 was the major transcription factor driving Ste11$^{\Delta N467}$-induced unmasking [37], deletion of *CPH1* did not significantly impact caspofungin-induced unmasking (Fig. 3.1C). However, deletion of *DFI1* significantly reduced the unmasking caused by caspofungin treatment by ~16% (Fig. 3.1D). This observation suggested that the calmodulin/calcineurin pathway, but not the Cek1 MAPK pathway, plays a role in driving caspofungin-induced unmasking. To directly test this hypothesis, we pharmacologically inhibited calcineurin with cyclosporinee A and assessed the unmasking levels following caspofungin treatment. Inhibition of calcineurin with cyclosporinee A caused a significant, ~41% reduction in the unmasking induced by caspofungin (Fig. 3.1E&F). Therefore, calcineurin plays a role in mediating unmasking

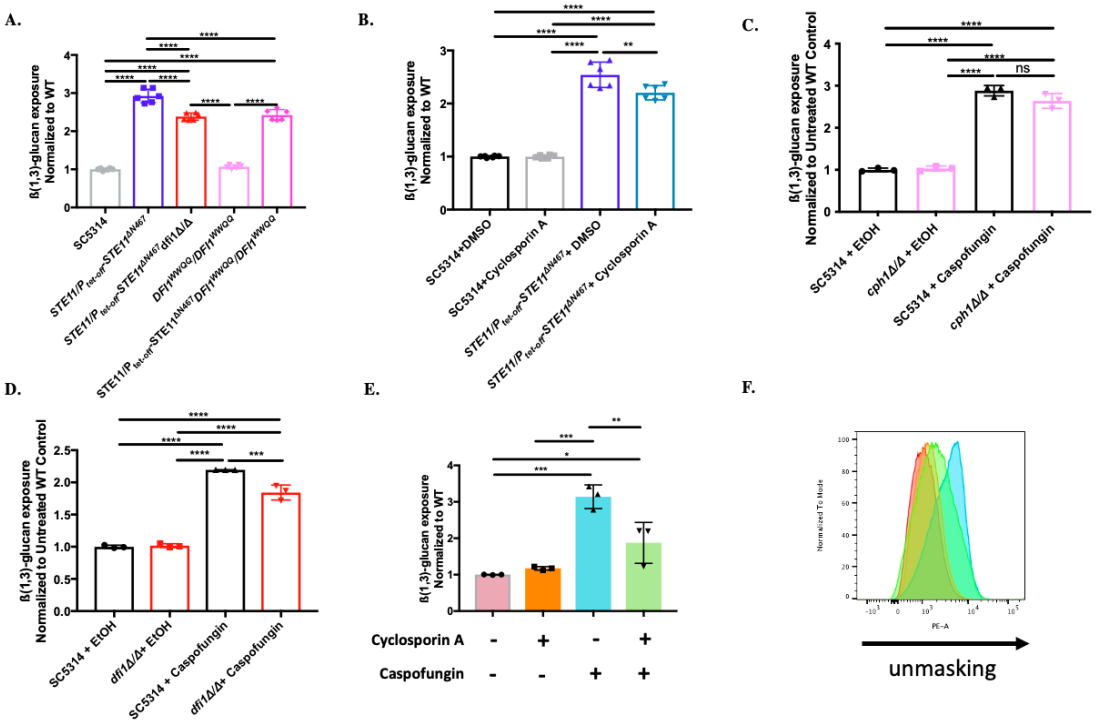


Fig 3.1: Calcineurin mediates hyperactive Ste11$^{\Delta N467}$-induced and caspofungin-induced unmasking in *C. albicans.*

(A) Disruption of the Dfi1-calmodulin interaction reduces Ste11$^{\Delta N467}$-induced unmasking. Cells from overnight cultures were stained with an anti-ß(1,3)-glucan antibody and a phycoerythrin-conjugated secondary antibody, and flow cytometry analysis was used to assess the levels of ß(1,3)-glucan exposure. (n=3 biological replicates with 1 technical replicate for each)(****p<0.0001, by one-way ANOVA). (B) Cyclosporine A inhibition of calcineurin reduces Ste11$^{\Delta N467}$-induced unmasking. The SC5314 wild-type or the *STE11/P$_{tet-off}$-STE11$^{\Delta N467}$* mutant was grown overnight in either the presence of 100µg/ml of cyclosporine A or an appropriate volume of the DMSO solvent control, and ß(1,3)-glucan exposure was assessed via flow cytometry. (n=3 biological replicates with 1 technical replicate for each)(**p<0.005, ****p<0.0001, by one-way ANOVA). (C-D) Genes that are necessary for Ste11$^{\Delta N467}$-induced unmasking were tested for their roles in caspofungin-induced unmasking by treating cells grown to mid-log phase with 46.9ng/ml of caspofungin for 30 minutes followed by flow cytometry. (C) ß(1,3)-glucan unmasking in *cph1Δ/Δ* cells treated with sublethal concentrations of caspofungin. (n=3 biological replicates)(****p<0.0001, by one-way ANOVA). (D) ß(1,3)-glucan unmasking in *dfi1Δ/Δ* cells treated with sublethal concentrations of caspofungin. (n=3 biological replicates)(***p=0.0005, ****p<0.0001, by one-way ANOVA). (E) Calcineurin inhibition attenuates caspofungin-induced unmasking. SC5314 wild-type cells grown to mid-log phase in either the presence of 100µg/ml of cyclosporine A, or an appropriate volume of the DMSO solvent control, were exposed to 46.9ng/ml of caspofungin for 30 minutes, and ß(1,3)-glucan exposure was measured via flow cytometry. (n=3 biological replicates)(*p<0.05, **p<0.01, ***p<0.0005, by one-way ANOVA). (F) Representative histogram of the impact that cyclosporine A-mediated calcinuerin inhibition has on caspofungin induced ß(1,3)-glucan exposure. Colors of each sample match those shown in 1E.

during both hyperactive *STE11*$^{\Delta N467}$ expression and in response to sublethal concentrations of caspofungin.

Growth in exogenous calcium induces masking in *C. albicans*.

The observation that calcineurin induces unmasking during both hyperactive *STE11*$^{\Delta N467}$ expression and in response to caspofungin (Fig 3.1) raised the possibility that the calcineurin pathway may induce unmasking upon direct stimulation. The calmodulin/calcineurin pathway mediates signaling in response to high levels of exogenous calcium [50, 51]. We hypothesized that activation of the calcineurin pathway via calcium addition would also increase ß(1,3)-glucan exposure. Thus, cells were grown in the presence of 50mM $CaCl_2$, but unexpectedly, these cells had significantly less ß(1,3)-glucan exposure (an ~34% reduction) than wild-type cells grown in non-supplemented media (Fig. 3.2A). This trend was even more apparent when the already unmasked *STE11/P*$_{tet\text{-}off}$-*STE11*$^{\Delta N467}$ mutant was grown in media with 50mM calcium. The extracellular calcium significantly reduced Ste11$^{\Delta N467}$-induced unmasking to only ~40% of the levels observed during growth in YPD alone (Fig. 3.2B). Interestingly, calcineurin inhibition via cyclosporine A treatment blocked the masking induced by exogenous calcium in wild-type cells, and actually resulted in increased unmasking (Fig. 3.2C). Therefore, growth in high levels of extracellular calcium can induce masking in *C. albicans* in a calcineurin dependent manner.

Crz1 mediates calcineurin induced masking, but not unmasking.

Our results have shown that calcineurin plays a role in regulating ß(1,3)-glucan exposure in response to specific stimuli. However, calcineurin's impacts on epitope exposure appear to be stimulus-dependent, with caspofungin treatment and *STE11*$^{\Delta N467}$ expression both increasing ß(1,3)-glucan exposure in a calcineurin-dependent manner (Fig. 3.1), and exposure to high levels of exogenous calcium inducing masking via calcineurin (Fig. 3.2). To address these differences, we tested the impact that the downstream transcription factor Crz1 has on regulating these changes. Crz1 is the canonical

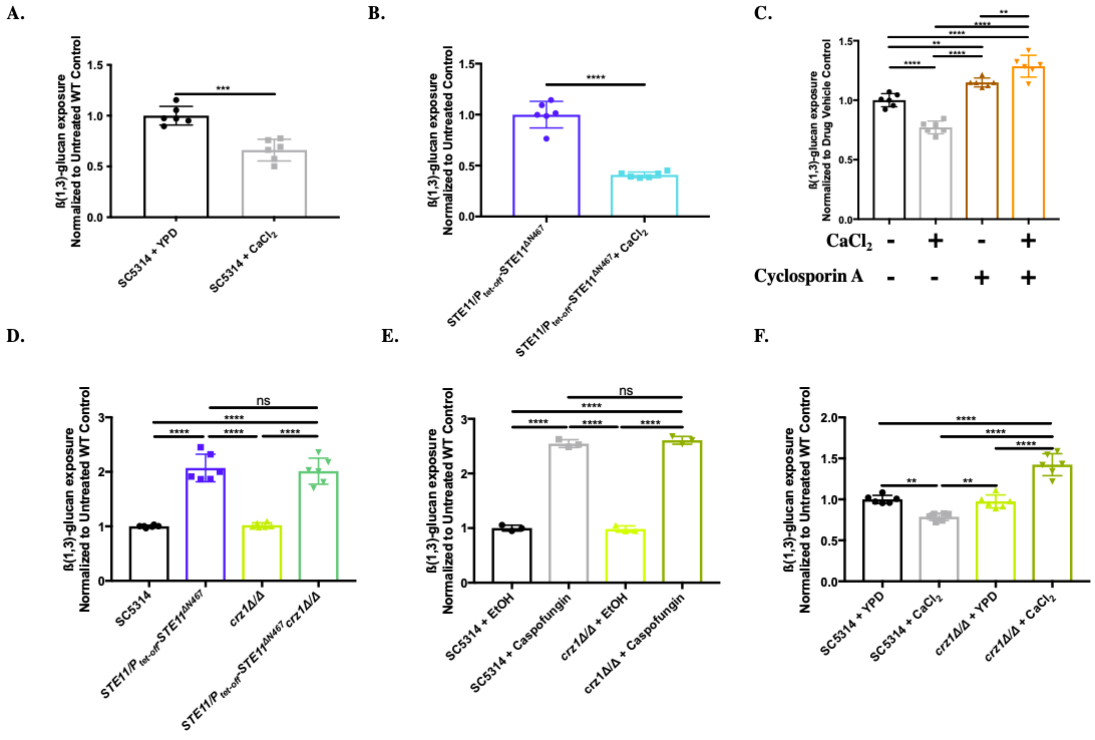


Fig 3.2: Crz1 mediates masking in response to exogenous calcium.
(A-B) Cells were grown overnight in the absence or presence of 50mM $CaCl_2$ in YPD broth. Cells were stained with an anti-ß(1,3)-glucan antibody and a phycoerythrin-conjugated secondary antibody followed by flow cytometry to assess the levels of ß(1,3)-glucan exposure. (A) Calcium-induced masking of SC5314 wild-type cells. (n=3 biological replicates with 1 technical replicate for each) (***p=0.0002, by student's t-test). (B) Calcium induced masking of *STE11/*$P_{tet\text{-}off}$*-STE11*$^{\Delta N467}$ cells. (n=3 biological replicates with 1 technical replicate for each) (****p<0.0001, by student's t-test). (C) Calcineurin inhibition blocks calcium-induced masking. SC5314 cells were grown overnight in the absence or presence of 50mM $CaCl_2$ and either 100µg/ml of cyclosporine A or an appropriate volume of the DMSO solvent control in YPD media. ß(1,3)-glucan exposure was then assessed via flow cytometry. (n=3 biological replicates with 1 technical replicate for each)(**p<0.01, ****p<0.0001, by one-way ANOVA). (D) Loss of *CRZ1* does not impact Ste11$^{\Delta N467}$-induced unmasking. Overnight cultures were stained for ß(1,3)-glucan exposure and flow cytometry was subsequently run to assess unmasking. (n=3 biological replicates with 1 technical replicate for each)(ns = not significant, ****p<0.0001, by one-way ANOVA). (E) Loss of *CRZ1* does not impact caspofungin-induced unmasking. Cells grown to mid-log phase prior to being exposed to 46.9ng/ml of caspofungin for 30 minutes and ß(1,3)-glucan exposure was subsequently assessed via flow cytometry. (n=3 biological replicates)(ns = not significant, ****p<0.0001, by one-way ANOVA). (F) Loss of *CRZ1* blocks calcium-induced masking. Overnight cultures of cells grown in the absence or presence of 50mM $CaCl_2$ were stained for ß(1,3)-glucan exposure and flow cytometry was subsequently run to assess ß(1,3)-glucan exposure levels. (n=3 biological replicates with 1 technical replicate for each)(**p<0.01, ****p<0.0001, by one-way ANOVA).

transcription factor that sits downstream of calcineurin in the calcium response pathway [52-54]. Its activation has also been shown to induce masking in response to exogenous lactate, although this occurs in a manner that is independent of calcineurin [29, 30]. Due to the masking induced by activation of the canonical Ca^{2+}/Calmodulin/Calcineurin pathway, we hypothesized that Crz1 mediates masking during exposure to high levels of extracellular calcium, but is likely not involved in the unmasking induced by non-canonical calcineurin activation in response to *STE11$^{\Delta N467}$* expression or caspofungin treatment. To test this, we generated a *crz1Δ/Δ* mutation in both the wild-type and *STE11/P$_{tet\text{-}off}$-STE11$^{\Delta N467}$* parent strains and tested the impact that loss of this transcription factor had on regulating ß-glucan exposure. Loss of *CRZ1* did not impact unmasking during *STE11$^{\Delta N467}$* expression (Fig. 3.2D), nor did it have an impact on caspofungin-induced unmasking (Fig. 3.2E). However, the *crz1Δ/Δ* mutant failed to induce masking in response to exogenous calcium (Fig. 3.2F), and actually resulted in an increase in unmasking compared to wild-type cells grown in non-supplemented YPD. This is consistent with the impact that chemical inhibition of calcineurin had on calcium-induced masking (Fig. 3.2C) and provides strong support for Crz1's role in specifically mediating epitope masking in response to high extracellular calcium levels.

Loss of key cell wall proteins causes ß(1,3)-glucan unmasking.

Our data have shown a role for calcineurin in regulating ß(1,3)-glucan exposure in response to three distinct stimuli: *STE11$^{\Delta N467}$* expression, caspofungin exposure and growth in high extracellular concentrations of calcium (Figs 3.1 and 3.2). We have also shown that masking in response to exogenous calcium is induced by the transcription factor Crz1, which has been additionally implicated in regulating masking in response to extracellular lactate [29, 30]. This creates a model in which calcineurin serves as a node within multiple signaling pathways to regulate ß(1,3)-glucan exposure in *C. albicans* (Fig. 3.3). However, *STE11$^{\Delta N467}$* expression, caspofungin exposure and exogenous calcium all cause large changes in the cell wall architecture and metabolism of *C. albicans* [36, 37, 54-56]. Calcineurin activation and subsequent ß(1,3)-glucan (un)masking are one set of

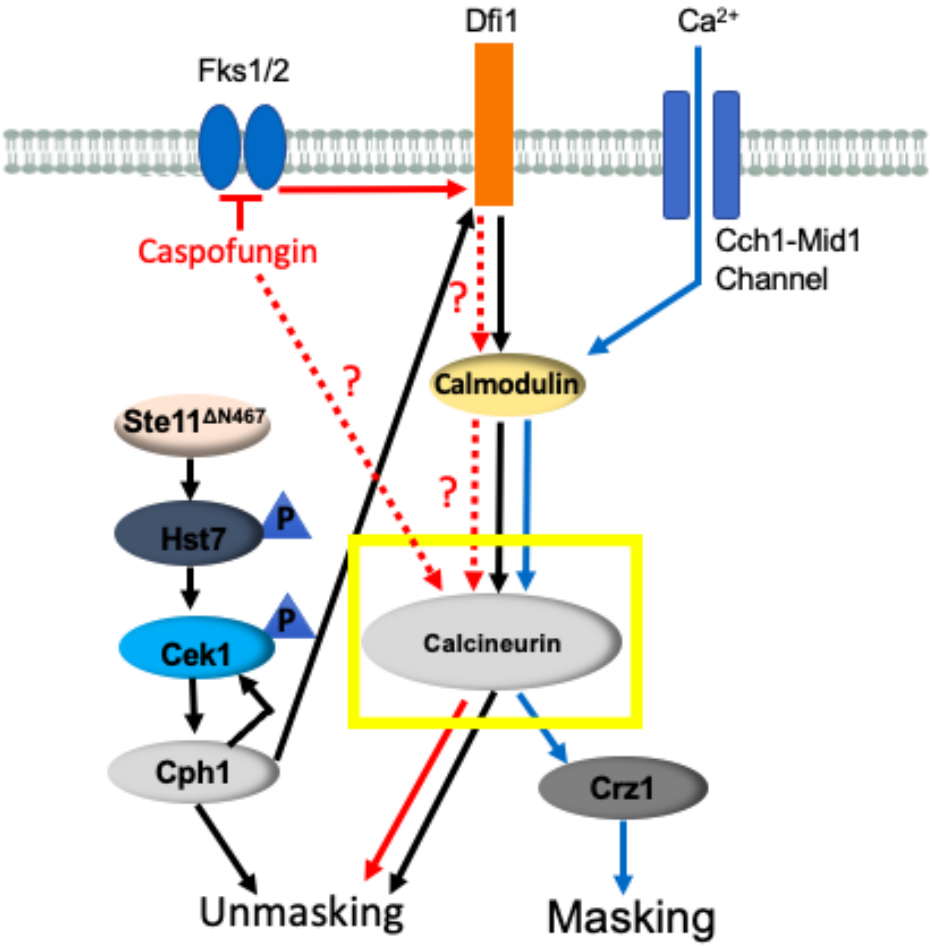


Fig 3.3: Proposed model for calcineurin-regulated ß(1,3)-glucan exposure.
Our data suggest that calcineurin serves as a switchboard in mediating ß(1,3)-glucan exposure in response to different stimuli: hyperactive *STE11*$^{\Delta N467}$ expression (black lines), caspofungin exposure (red lines), and high levels of exogenous calcium (blue lines). With regards to hyperactive *STE11*$^{\Delta N467}$ expression, we propose that activation of the downstream transcription factor Cph1 leads to increased expression of the cell wall sensor Dfi1 as well as architectural cell wall changes that are then sensed by these same Dfi1 proteins. This sensor in turn interacts with calmodulin to initiate signal transduction down a Dfi1/calmodulin/calcineurin signal transduction pathway and further increases ß(1,3)-glucan unmasking. In response to caspofungin exposure, calcineurin is also necessary to induce the full levels of unmasking observed in wild-type cells. Based on our data, calcineurin may act in a partially Dfi1 dependent manner, but an alternative regulator also mediates calcineurin activity in response to caspofungin treatment. Lastly, we propose that calcineurin is also capable of decreasing ß(1,3)-glucan exposure levels in response to growth in high levels of exogenous calcium, and is likely mediated via the canonical calmodulin/calcineurin/Crz1 signal transduction pathway. Dotted arrows indicate putative pathways that have not yet been experimentally confirmed.

multiple changes induced by these stimuli, and effector genes that impact ß(1,3)-glucan exposure are likely a small subset of the total genes differentially regulated in the *C. albicans* transcriptional response to each stimulus. Identifying shared genes that are induced in response to all of these stimuli may be an efficient way to highlight conserved effector genes within the calcineurin regulon that drive changes in ß(1,3)-glucan exposure in response to multiple stimuli. Consequently, we utilized public data sets to identify genes that are differently regulated during both *STE11$^{\Delta N467}$* expression [36] and caspofungin treatment [55], and overlaid them with a Cytoscape predicted Crz1 regulon [29]. Overlapping these datasets revealed that only 3 genes were conserved amongst them (Fig. 3.4A); *PGA13, FGR41* and a gene of unknown function *C1_11990W_A* (which we have termed cell wall protein 419, *CWP419)*. Interestingly, all three genes are predicted to encode outer cell wall proteins based on the presence of putative secretion signals and glycosylphosphatidylinositol anchors in their sequences. This observation fits the model that alterations in outer cell wall components are capable of affecting ß(1,3)-glucan exposure [26-28] and encouraged further exploration of these targets.

Within the datasets used to identify the effector genes, *FGR41* and *CWP419* were both down-regulated during *STE11$^{\Delta N467}$* expression and caspofungin exposure, while *PGA13* was up-regulated in each condition [36, 55]. In contrast, *FGR41* and *CWP419* are predicted to be positively regulated by Crz1, while *PGA13* is predicted to be down-regulated [29]. Thus, the differential expression profiles of these genes in conditions that either increase or decrease ß(1,3)-glucan exposure provides a basis to assess their contributions to unmasking. To recapitulate the role that these genes may have in mediating unmasking in response to these stimuli, we created knockout mutants of *FGR41* and *CWP419,* and an overexpression mutant of *PGA13* under the control of the enolase promoter (*P_{ENO1}-PGA13*). Interestingly, both *fgr41Δ/Δ* (Fig. 3.4B) and *cwp419Δ/Δ* (Fig. 3.4C) mutants showed a significant increase in unmasking compared to their respective wild-type and reintegrant controls, while overexpression of *PGA13* appeared to have no impact on ß-glucan exposure (Fig. 3.4D). Microscopy further revealed that unmasking in the *fgr41Δ/Δ* mutant occurs primarily at the bud neck and bud scars, while the *cwp419Δ/Δ* mutant showed a more scattered pattern of unmasking throughout the periphery of the cell

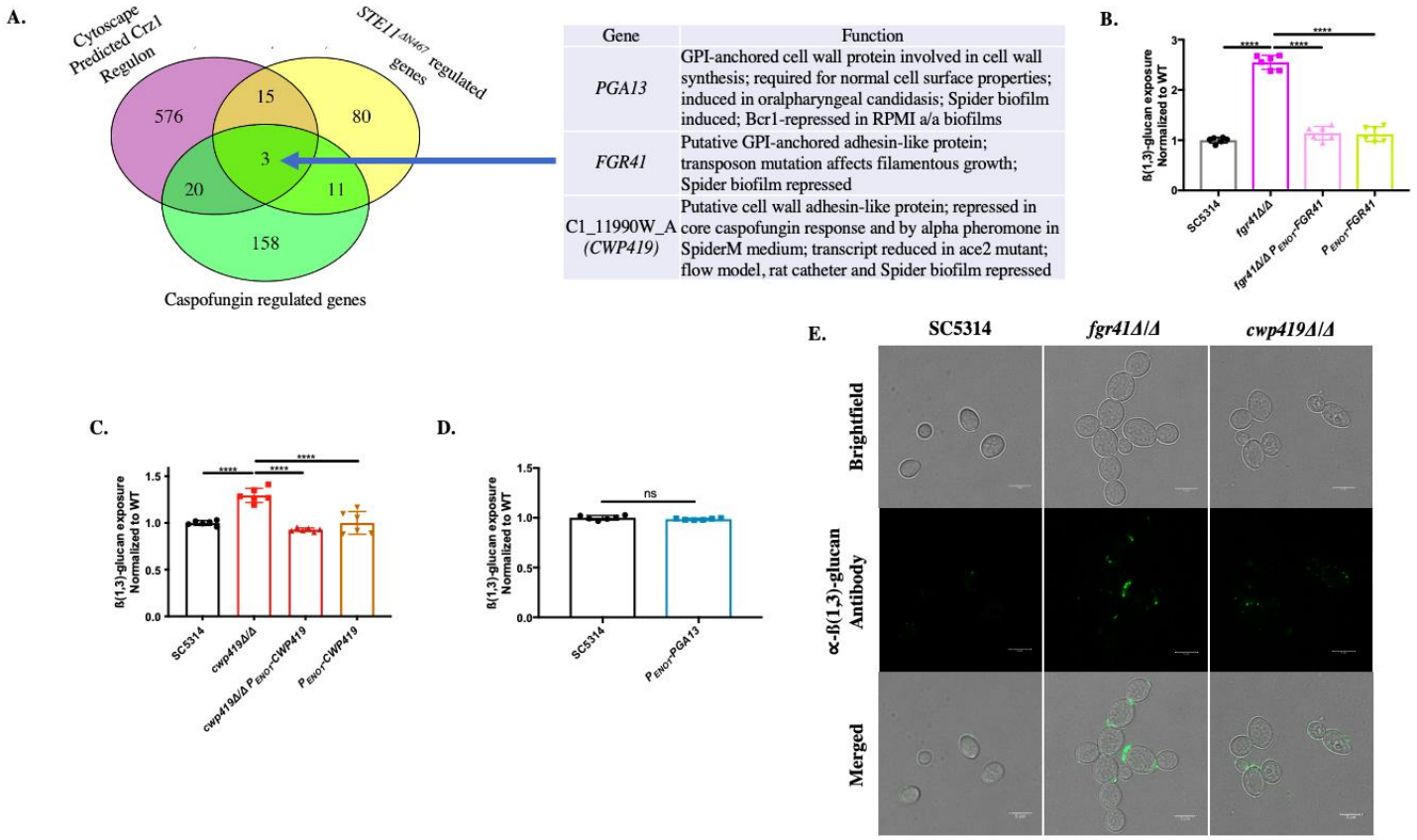


Fig 3.4: Key cell wall proteins mediate ß(1,3)-glucan exposure in *C. albicans*.
(A) Comparative analysis of public data sets to identify conserved genes that are differentially regulated in conditions that involve calcineurin-mediated ß(1,3)-glucan exposure (*STE11*$^{\Delta N467}$ expression [36] and caspofungin exposure [55]) and fall within a predicted Crz1 regulon [29]. Gene ontology descriptions were taken from the Candida Genome Database. (B-D) Genetic analysis of conserved target genes identified during comparative analysis. Overnight cultures of cells were stained with anti-ß(1,3)-glucan antibody and a phycoerythrin-conjugated secondary antibody followed by flow cytometry analysis to assess the levels of ß(1,3)-glucan exposure. (B) ß(1,3)-glucan unmasking of *fgr41Δ/Δ* mutants. (C) ß(1,3)-glucan unmasking of *cwp419Δ/Δ* mutants. (D) ß(1,3)-glucan unmasking of *PGA13* overexpression mutants. (n=3 biological replicates with 1 technical replicate for each mutant analyzed)(****p<0.0001, by one-way ANOVA). (E) Representative microscopy images of ß(1,3)-glucan exposure of the *fgr41Δ/Δ* and *cwp419Δ/Δ* mutants. (The scale bar indicates 5μm).

wall (Fig. 3.4E). Thus, it appears that down-regulation of *FGR41* and *CWP419* may be responsible, in part, for the unmasking observed during *STE11*$^{\Delta N467}$ expression and caspofungin exposure.

As loss of either *FGR41* or *CWP419* increased unmasking, we were curious if changes in other structural components of the cell wall were also present in either of these mutants. To assess this, the wild-type, *fgr41Δ/Δ* and *cwp419Δ/Δ* strains were stained with calcofluor white, wheat germ agglutinin and concanavalin A to assess the levels of total chitin, exposed chitin and mannan within their cell walls, respectively. Staining revealed that the *fgr41Δ/Δ* mutant displayed significant increases in both total chitin and mannan within its cell wall, while the *cwp419Δ/Δ* mutant displayed wild-type levels of staining for these cell wall components (S3.2 Fig.). Furthermore, both mutants displayed a very modest, but significant increase in exposed chitin levels as well, accounting for only a ~1.10 to 1.20-fold increase in wheat germ agglutinin staining. Although we suspect that the increase in exposed chitin is not biologically significant within the samples, our data does suggest that loss of *FGR41,* but not *CWP419,* induces robust changes in the cell wall architecture of *C. albicans*.

We next wished to see if differential gene regulation of any of these constructs could impact the unmasking induced by *STE11*$^{\Delta N467}$ expression or caspofungin exposure. Overexpression of *FGR41* was able to reduce the unmasking observed during *STE11*$^{\Delta N467}$ expression (Fig. 3.5A). In addition, deletion of *FGR41* in a *STE11/P*$_{tet\text{-}off}$*-STE11*$^{\Delta N467}$ background led to a further increase in ß-glucan exposure (Fig. 3.5B). However, neither overexpression nor deletion of *CWP419,* nor overexpression of *PGA13* impacted Ste11$^{\Delta N467}$-induced unmasking (Fig. 3.5C-E). In contrast, none of the overexpression mutants were able to affect caspofungin-induced unmasking (Fig. 3.5F-H), which represents a much more pleiotropic impact on the cell wall.

Both *FGR41* and *CWP419* are predicted to be positively regulated by Crz1 [29], and the inability for the *crz1Δ/Δ* mutant to show calcium-induced masking may be the consequence of misregulation of these downstream targets. We were therefore curious if overexpression of each of these components alone could restore the ability of the *crz1Δ/Δ*

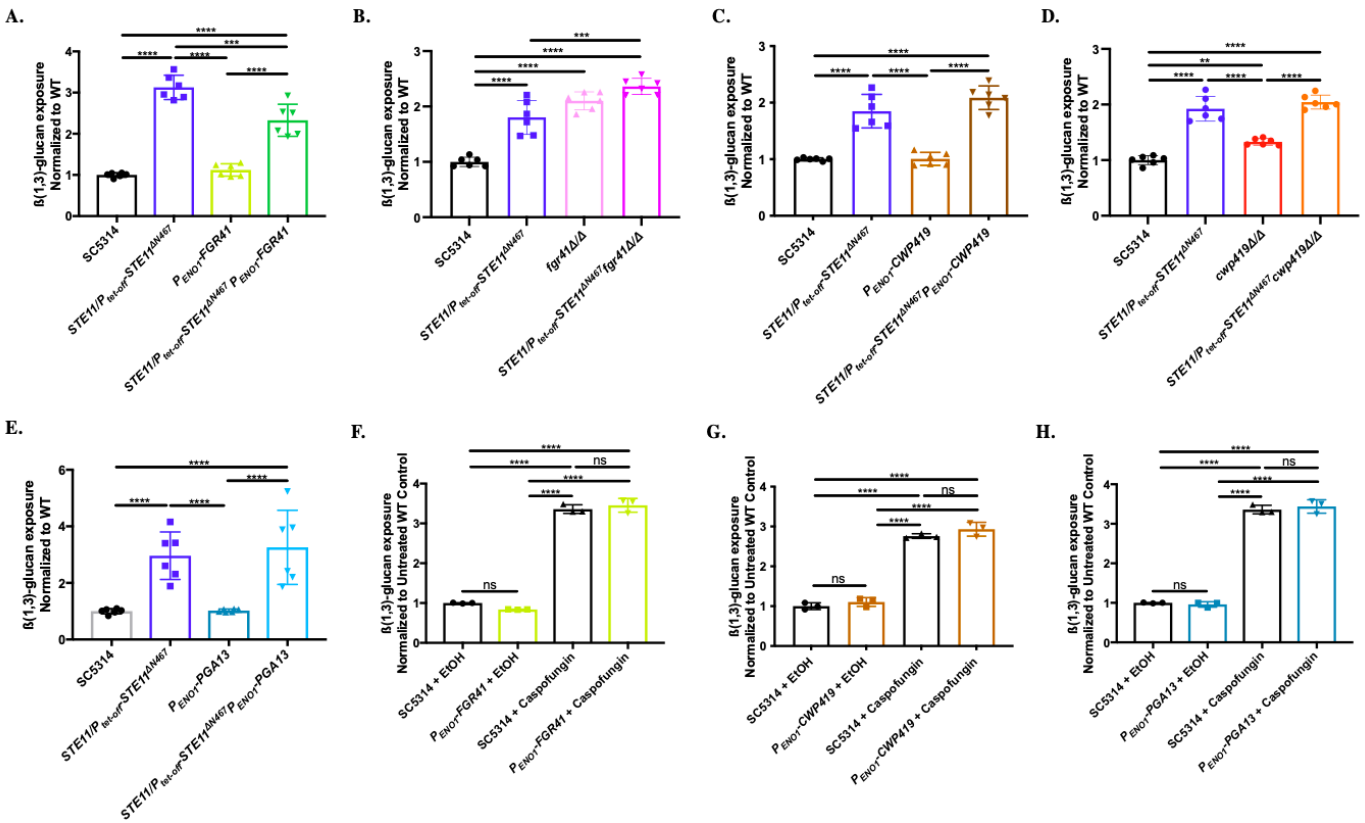


Fig 3.5: *FGR41* overexpression and deletion modulates Ste11$^{\Delta N467}$-induced, but not caspofungin-induced, ß(1,3)-glucan unmasking.
(A-E) Overnight cultures of cells were stained with anti-ß(1,3)-glucan antibody and a phycoerythrin-conjugated secondary antibody to assess the levels of ß(1,3)-glucan exposure by flow cytometry. (A) ß(1,3)-glucan exposure during *FGR41* overexpression. (B) ß(1,3)-glucan exposure in *FGR41* deletion mutants. (C) ß(1,3)-glucan exposure during *CWP419* overexpression. (D) ß(1,3)-glucan exposure in *CWP419* deletion mutants (E) ß(1,3)-glucan exposure during *PGA13* overexpression. (n=3 biological replicates with 1 technical replicate for each mutant analyzed)(**p<0.005, ***p<0.0005, ****p<0.0001, by one-way ANOVA). (F-H) Cells grown to mid-log phase were exposed to 46.9ng/ml of caspofungin for 30 minutes and ß(1,3)-glucan exposure was subsequently assessed via flow cytometry. (F) ß(1,3)-glucan exposure of *FGR41* overexpression cells treated with sublethal concentrations of caspofungin. (G) ß(1,3)-glucan exposure of *CWP419* overexpression cells treated with sublethal concentrations of caspofungin. (H) ß(1,3)-glucan exposure of *PGA13* overexpression cells treated with sublethal concentrations of caspofungin. (n=3 biological replicates)(ns = not significant, ****p<0.0001, by one-way ANOVA).

mutant to induce masking in response to growth in exogenous calcium. However, in the presence of exogenous calcium, neither the *crz1Δ/ΔP$_{ENO1}$-FGR41* nor the *crz1Δ/ΔP$_{ENO1}$-CWP419* double mutant had altered ß(1,3)-glucan exposure when compared to the *crz1Δ/Δ* parent strain (S3.3 Fig.). Therefore, it appears that overexpression of each of these targets alone is insufficient to restore calcium-induced masking in the *crz1Δ/Δ* mutant.

Loss of *FGR41* attenuates virulence during systemic infection in mice.

As both *fgr41Δ/Δ* and *cwp419Δ/Δ* display increased unmasking, and neither displays an aberrant growth rate *in vitro* (S3.4 Fig.), we measured the impact that these mutations had on systemic infection in mice. We intravenously infected mice with $1x10^6$ cells of wild-type, *fgr41Δ/Δ, P$_{ENO1}$-FGR41, cwp419Δ/Δ*, or their respective reintegrants and determined fungal burden and serum cytokine levels 4 days post infection (d.p.i). Mice infected with the *fgr41Δ/Δ* mutant displayed a significant (~3-fold) reduction in kidney fungal burden at 4 d.p.i. (Fig. 3.6A), with an accompanying decrease in core pro-inflammatory cytokines, like TNFα, CCL2, CCL5, IL-1ß and IFNα (Fig. 3.6B and S3.5 Fig.). However, the *P$_{ENO1}$-FGR41* mutant displayed wild-type levels of kidney fungal burden (S3.6 Fig.). The *cwp419Δ/Δ* mutant displayed a modest and insignificant decrease in fungal burden compared to the wild-type, but was significantly different than the reintegrant (Fig. 3.6C), and this is likely reflective of the modest increase in unmasking induced by loss of this gene (Fig. 3.4C).

FGR41 is a putative GPI-anchored protein, and transposon library screening has implicated it as a regulator for filamentous growth [57]. Since hyphal formation is an important virulence factor, we tested the impact of *fgr41*Δ/Δ on the yeast-to-hyphae transition *in vitro*. The *fgr41Δ/Δ* showed a significant reduction in the percentage of cells that formed germ tubes in the first 2 hours post-induction in serum, but by 3 hours there was no significant difference (S3.7A Fig.). Additionally, of hyphae that were generated at 1 or 2 hours, there was a significant increase in *fgr41Δ/Δ* hyphal length, but by 3 hours there was no significant difference (S3.7B Fig). Thus, there was only a modest impact on early hyphal formation in *the fgr41*Δ/Δ mutant.

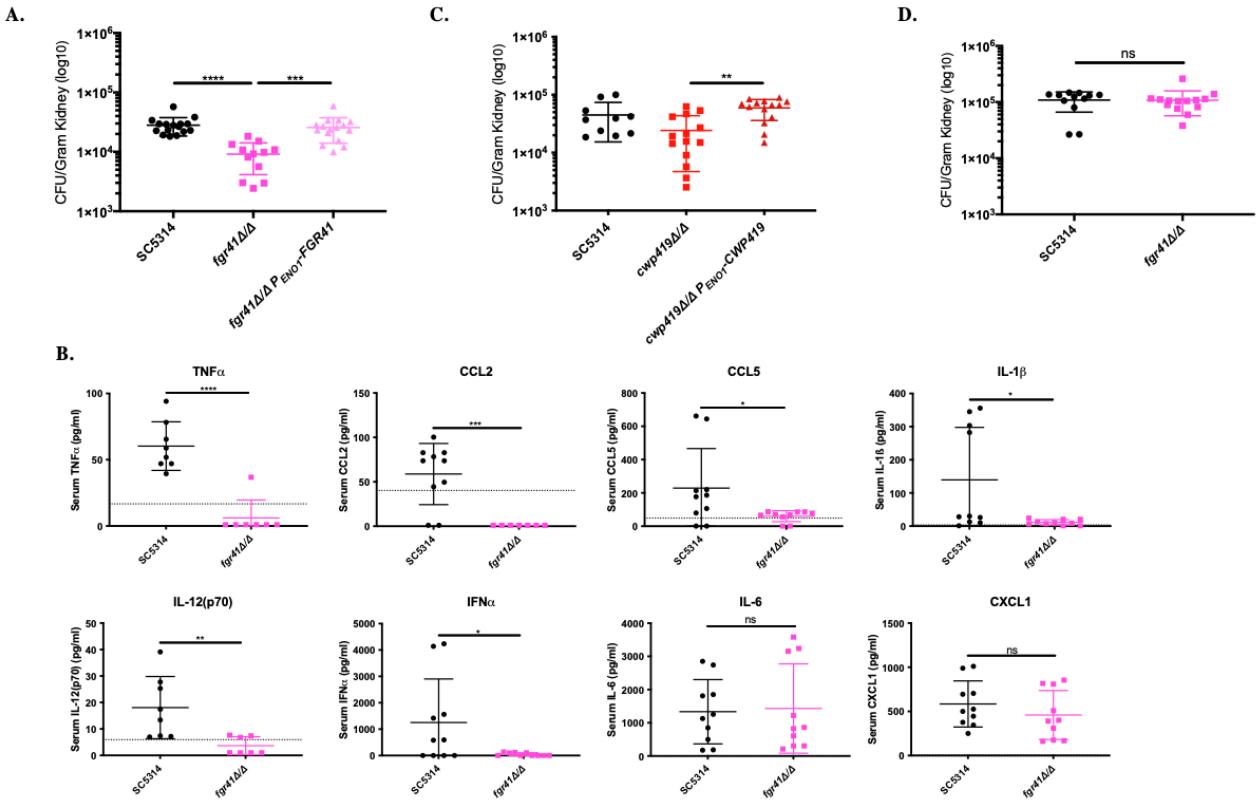


Fig 3.6: Loss of *FGR41* attenuates virulence in a host immune system dependent manner.
(A) ICR mice were intravenously infected with 1x10^6 cells of *C. albicans* wild-type (SC5314), the *fgr41Δ/Δ* mutant, or the *fgr41Δ/ΔP$_{ENO1}$-FGR41* reintegrant strain, and kidneys were subsequently harvested 4 days post infection (d.p.i.) to assess fungal burden. (n=7-8 mice per strain)(***p<0.0005, ****p<0.0001, by Kruskal-Wallis test with Dunn's multiple comparisons post-hoc analysis). (B) Serum collected 4 d.p.i. was assessed via flow cytometry using the LEGENDplex cytokine bead-based array kit to measure circulatory cytokine levels following infection with either the *C. albicans* wild-type (SC5314) or the *fgr41Δ/Δ* mutant. (n=5 mice)(The dashed line across the x-axis represents the limit of detection.)(ns = not significant, *p<0.05, **p<0.01, ***p=0.0005, ****p<0.0001, by either student's t-test or Mann-Whitney test). (C) ICR mice were intravenously infected with 1x10^6 cells of *C. albicans* wild-type (SC5314), the *cwp419Δ/Δ* mutant, or the *cwp419Δ/ΔP$_{ENO1}$-CWP419* reintegrant strain, and kidneys were subsequently harvested 4 d.p.i. to assess fungal burden. (n=6-8 mice per strain)(**p<0.01, by one-way ANOVA). (D) ICR mice were immunosuppressed with recurring intraperitoneal injections of 150mg/kg of cyclophosphamide every 3 days starting 4 days prior to infection. At day 0, mice were intravenously injected with 1x10^4 cells of *C. albicans* wild-type (SC5314) or the *fgr41Δ/Δ* mutant and kidneys were harvested 3 days post infection (d.p.i.) to assess fungal burden. (n=6-7 mice)(ns = not significant, by Mann-Whitney test).

The ability to adapt to exogenous stressors that impact the integrity of the cellular envelope is an additional variable that may contribute to observed virulence defects seen *in vivo*. However, neither the *fgr41Δ/Δ* mutant nor the *cwp419Δ/Δ* mutant displayed altered sensitivities to calcofluor white, caspofungin or sodium dodecyl sulfate (SDS) during spot dilution assays (S3.8 Fig.). Therefore, no apparent fitness defects appear to exist to these common cell wall stressors that may be indicative of reduced cell wall integrity in these mutants.

To more clearly assess if the unmasking phenotype of the *fgr41Δ/Δ* mutant was responsible for the reduced fungal burden, we determined if the virulence defect was dependent on the host immune response. We tested this by repeating the infection with $1x10^4$ cells in cyclophosphamide immunosuppressed mice and analyzing kidney fungal burden at 3 d.p.i. (to prevent mice from pre-maturely succumbing to the infection). Cyclophosphamide treatment depleted cell types from both the adaptive and innate immune response (S3.9 Fig.) and completely restored *fgr41Δ/Δ* fungal burden to wild-type levels (Fig. 3.6D). Thus, the reduced fungal burden during *fgr41Δ/Δ* infection is dependent on an intact host immune system. This suggests that unmasking of ß(1,3)-glucan plays the driving role in virulence attenuation, rather than an overall fitness defect or filamentation delay.

Discussion

We have previously shown that hyperactivation of the Cek1 MAPK pathway of *C. albicans* is capable of inducing ß(1,3)-glucan unmasking [35, 36]. We have also shown that this is mediated by the transcription factor Cph1, and that its activation stimulates a parallel signaling pathway to further increase ß-glucan exposure [37]. Here we have expanded on this work to show that the calmodulin/calcineurin signaling pathway is this parallel pathway and is required to fully induce unmasking caused by $STE11^{\Delta N467}$ expression (Fig 3.1). Furthermore, we have shown that calcineurin plays a more general role in mediating ß(1,3)-glucan exposure, as it is necessary for caspofungin-induced unmasking (Fig 3.1). In contrast, we also show that calcineurin reduces ß(1,3)-glucan exposure during growth in media containing high levels of extracellular calcium (Fig 3.2). Thus, for caspofungin and

Ste11$^{\Delta N467}$-induced unmasking, as well as calcium-induced masking, changes in ß-glucan exposure are mediated via the same calcineurin signal transduction module, but the mechanism of calcineurin activation differs between them (Fig 3.3).

The manner by which calcineurin is activated in response to sublethal concentrations of caspofungin is unknown. We have shown that deletion of *DFI1* impacts caspofungin-induced unmasking (Fig 3.1D), and it is possible that calcineurin is activated by caspofungin in part through the same Dfi1/calmodulin/calcineurin signal cascade stimulated by *STE11$^{\Delta N467}$* expression. However, loss of calcineurin has a greater impact on caspofungin-driven unmasking than loss of Dfi1, so calcineurin may be induced by other inputs in addition to Dfi1. Sublethal concentrations of caspofungin can induce an apoptotic response in *C. albicans* [58, 59], and are regulated by the interaction between the molecular chaperone Hsp90 and calcineurin [60, 61]. Moreover, the calcium response pathway plays a role in mediating *C. albicans* echinocandin resistance [62], and Hsp90-mediated activation of calcineurin is essential for this process [49]. Therefore, Hsp90 may play a role in mediating calcineurin-dependent ß(1,3)-glucan unmasking in response to caspofungin. In any case, the observation that calcineurin is needed to induce the full levels of unmasking observed during caspofungin treatment is interesting, as the mechanism driving caspofungin-induced unmasking has not been previously described.

Caspofungin-driven unmasking may also play an important role in enchinocandin mechanism of action *in vivo*, as there is evidence to suggest that a functional immune response is necessary for proper fungal clearance during echinocandin treatment in mice. Marakalala *et al.* reported that caspofungin efficacy is severely impaired during infection in dectin1$^{-/-}$ mice, suggesting an essential role for this ß(1,3)-glucan receptor in mediating caspofungin-induced fungal clearance [63]. Similarly, the ability of anidulafungin to enhance host survival during systemic infection is impaired in neutropenic mice [64]. Thus, the impact that calcineurin has in regulating ß(1,3)-glucan exposure in response to caspofungin treatment may have additional implications on disease management via echinocandin application.

The role for calcineurin in regulating ß-glucan exposure levels in response to multiple stimuli is not surprising, as this protein complex is capable of regulating multiple

phenotypic outcomes in response to pH [65, 66], ion stress [42, 65, 67], antifungal tolerance [49, 67] and serum growth [50, 65, 68]. Each of these processes requires tailored responses for *C. albicans* to adequately adapt. With respect to altering ß(1,3)-glucan exposure, we have found that this is in part mediated via directed activation of appropriate downstream transcription factors. In this report, Crz1 was found to specifically mediate calcium-induced masking but had no impact in unmasking conditions (Fig 3.2D-F). The transcription factor acting downstream of calcineurin to control unmasking is currently unknown. The observation that Crz1 is capable of inducing masking is consistent with previous literature, as Crz1 has also been implicated in lactate-induced masking [29, 30], although the manner in which it was activated in response to lactate exposure was non-canonical. Although the cAMP/PKA pathway is also capable of responding to multiple host signals to induce masking (lactate and hypoxia exposure, and iron-replete environments)[33, 34], calcineurin is the first signal transduction pathway to our knowledge that can both increase and decrease ß-glucan exposure in response to different stimuli. As such, the role that the calmodulin/calcineurin pathway has on mediating ß-glucan exposure levels may serve as a model to better understand the checks and balances in place to maintain appropriate ß-glucan exposure in *C.* albicans, and to also begin addressing larger questions in eukaryotic cell biology. Namely, how signal transduction is regulated to activate alternative downstream transcription factors.

In an attempt to elucidate the mechanism driving calcineurin-induced changes in ß(1,3)-glucan exposure, we have identified two putative cell wall proteins, Fgr41 and Cwp419, that are down-regulated during *STE11*$^{\Delta N467}$ expression [36] and caspofungin exposure [55], and that cause unmasking when individually deleted (Fig 3.4). In agreement with this, these proteins are also predicted to be positively regulated by Crz1, which induces masking, and their differential expression may therefore contribute to the different calcineurin-mediated changes on ß(1,3)-glucan exposure. The observation that overexpression of *FGR41* can partially restore the unmasking induced by hyperactive *STE11*$^{\Delta N467}$ expression supports this model (Fig 3.5A). However, neither *FGR41* nor *CWP419* overexpression had an impact on caspofungin-induced unmasking (Fig 3.5F-H). Additionally, overexpression of these genes was not able to overcome the loss of *CRZ1* to

restore the masking phenotype observed during growth in exogenous calcium (S3.3 Fig). Yet, the transcriptional responses to both caspofungin and calcium exposure are profound, and we suspect that multiple variables contribute to induce the changes in ß(1,3)-glucan exposure observed. Indeed, in addition to differential regulation of outer cell wall proteins, caspofungin treatment also induces a significant increase in chitin content within the cell wall [69, 70]. Calcineurin has been found to play a role in regulating chitin levels in response to caspofungin [69], and correlations with increased chitin content and increased unmasking have been repeatedly observed in the literature [37, 45, 71-73]. It is therefore possible that increased chitin levels may work in synergy with down-regulation of outer cell wall proteins, such as *FGR41* and *CWP419*, to induce unmasking.

Both Fgr41 and Cwp419 are largely uncharacterized proteins, and the direct role that they may play in cell wall homeostasis and ß(1,3)-glucan exposure are unknown. Loss of *FGR41* was previously shown to impair filamentation in *C. albicans* [57], and in our hands *fgr41*Δ/Δ only causes a delay in filamentous growth in a small percentage of cells (S3.7 Fig). Similarly, *CWP419* was implicated as a putative adhesin-like protein in the Ace2 regulon [74], but its biological role in *C. albicans* is thus far unreported. Knockout mutants of either gene did not show altered susceptibility to common cell envelope stressors (S3.8 Fig), and bioinformatic analysis using BLAST [75] and PROSITE [76] did not reveal any conserved protein domains to hint at their biological function. However, ß(1,3)-glucan staining did reveal that the *fgr41Δ/Δ* mutant had increased unmasking at bud scars and bud necks, and these cells appeared to have impaired septum resolution in microscopy (Fig 3.4E). Therefore, it may be that Fgr41 plays a role in cell division. The *cwp419Δ/Δ* mutant showed scattered foci of unmasking, and this may suggest a broader distribution of this protein throughout the cell wall. It is important to note that although other cell wall proteins have been found to induce unmasking when deleted, such the yeast wall protein *YWP1* [77], this phenotype is not conserved amongst all cell wall proteins. For example, we have shown that deletions of the cell wall sensors *DFI1* and *OPY2*, which intercalate into the outer cell wall, do not induce unmasking, even when both are simultaneously deleted [37]. Therefore, the uncharacterized nature of these proteins

warrants further investigation to elucidate how they regulate cell wall homeostasis and ß-glucan exposure.

In the case of *FGR41,* we found that loss of this cell wall protein leads to virulence attenuation during systemic infection in mice in a manner that is dependent on the host immune system (Fig 3.6). This suggests that the virulence defect is dependent on unmasking rather than the modest filamentation delay. Although the mechanism by which Fgr41 impacts masking is unknown, this mutant should serve as a useful model to understand how unmasking is mediated by cell wall proteins. Furthermore, its application can also be used to assess the impact that unmasking has on immune-driven fungal clearance, without complications from strong *in vivo* fitness defects.

Materials and Methods

Growth media and culture conditions. *C. albicans* strains were grown in YPD media (1% yeast extract, 2% peptone, 2% dextrose)(Thermo Fisher Scientific) while shaking at 225rpm at 30°C [78]. In conditions where exogenous calcium was added, YPD broth was supplemented with $CaCl_2$ to 50mM media [67]. Minimal media (0.67% yeast nitrogen base without amino acids, 2% dextrose, 2% agar)[78] (Thermo Fisher Scientific) was used to remove the genomically integrated CRISPR/Cas9 cassette and nourseothricin selectable marker following successful gene deletion [79]. LB media (0.5% yeast extract, 1% tryptone, 1% NaCl) (Thermo Fisher Scientific) was used for the growth of DH5-α *Escherichia coli* strains (NEB) and cells were grown at 37°C on a rotator drum.

Plasmid Construction. Plasmids constructed during this project can be seen in S3.1 Table and the primers used to create them in S3.2 Table. Overexpression cassettes were created by placing the open reading frame (ORF) for the gene of interest under the regulatory control of the constitutive enolase *(ENO1*) promoter [80]. To create the *FGR41* overexpression cassette, a 1,023bp fragment containing the *FGR41* open reading frame (ORF) and 270bp of its 3' untranslated region (UTR) following the stop codon was amplified with the AWO361 and AWO362 primer set that introduced flanking *NotI* cut sites onto both ends of the PCR product. The P_{ENO1} overexpression plasmid, pBT1 [80] and

the PCR product were then digested using *NotI*, and ligated to create the P_{ENO1}-*FGR41-SAT1* overexpression cassette (pSL003).

The *CWP419* overexpression cassette was created by amplifying a 976bp fragment containing the whole *CWP419* (C1_11990W_A) ORF and 477bp of the 3'UTR immediately following the stop codon with the primer set AKO21 and AKO22, that introduced flanking *NotI* and *SacI* cut sites, respectively. The P_{ENO1} overexpression plasmid, pBT1 [80], and the PCR product were then digested using *NotI* and *SacI*, and ligated to create the P_{ENO1}-*CWP419-SAT1* overexpression cassette (pAEK001).

The *PGA13* overexpression cassette was created by amplifying a 1,663bp PCR fragment containing the *PGA13* ORF and 291bp of the 3'UTR immediately following the stop codon with the primer set AWO336 and AWO337, that introduced flanking *NotI* and *SacI* cut sites, respectively. The P_{ENO1} overexpression plasmid, pBT1 [80], and the PCR product were then digested using *NotI* and *SacI*, and ligated to create the P_{ENO1}-*PGA13-SAT1* overexpression cassette (pMM001).

Strain Construction. All *C. albicans* deletion strains and missense mutants (S3.3 Table) were created with the use of CRISPR-Cas9 as previously described [79]. *FGR41* overexpression mutants were generated by digesting the P_{ENO1}-*FGR41-SAT1* plasmid (pSL003) with *MscI* (which cuts a single time within the *ENO1* promoter). The linear plasmid was then purified and transformed into the SC5314 wild-type or *STE11/*$P_{tet\text{-}off}$-*STE11*$^{\Delta N467}$ strains via electroporation. Successful transformants were selected for on YPD + 200μg/ml nourseothricin. The same method was then used to create *CWP419* and *PGA13* overexpression mutants in their appropriate strain backgrounds using pAEK001 and pMM001, respectively.

Immunofluorescent staining, flow cytometry, and microscopy analysis. To stain cell wall components of stationary phase cells, 5ml cultures of *C. albicans* strains in YPD were started the morning prior to staining. Cultures were grown shaking at 225 rpm at 30°C for ~8 hours before being back diluted to an OD_{600} of 0.1 in fresh YPD and incubated with shaking at 225rpm at 30°C overnight (~16 hours). To inhibit calcineurin, cells were grown

overnight in the presence of either 100μg/ml of cyclosporine A (Torcis) or an appropriate volume of the DMSO solvent control in YPD media. The following morning, cells were diluted to an OD_{600} of 0.5 in PBS and stained to assess ß(1,3)-glucan exposure, total chitin, exposed chitin and mannan as previously described [35, 37]. For flow cytometry, a goat-anti-mouse secondary antibody conjugated to R-Phycoerythrin (Jackson Immuno Research) at a 1:300 dilution was used, while a rabbit-anti-mouse IgG secondary antibody conjugated to Alexa Fluor 488 (Jackson Immuno Research) was used at a 1:300 dilution for microscopy.

To assess caspofungin-induced ß(1,3)-glucan exposure, overnight cultures were started as described above and strains were back diluted the following morning to an OD_{600} of 0.1. Cells were then left to grow for 3 hours while shaking at 225 rpm at 30°C. To assess the impact that pharmacological inhibition of calcineurin has on caspofungin-induced unmasking, 100ug/ml of cyclosporine A or an appropriate volume of the DMSO solvent control was added to the media prior to back dilution in the morning. In either control or cyclosporine-treated samples, after 3 hours of incubation, 46.9ng/ml of caspofungin, or an appropriate volume of an ethanol solvent control, was added to each tube and strains were left to incubate while shaking at 225 rpm at 30°C for an additional 30 minutes. Following incubation, 1ml of each culture was removed to assess ß(1,3)-glucan exposure as previously described [35, 37].

For all yeast cell staining, ≥3 biological replicates consisting of 100,000 recorded events each, were used to assess all strains analyzed by flow cytometry. Visualization and data analyses were performed in FlowJo (Becton, Dickinson and Company). Statistical significance was determined with the use of a student's t-test or a one-way ANOVA with Tukey's post hoc analysis (GraphPad Prism, v7.0c software).

To perform immunofluorescent staining of leukocytes, mouse peripheral blood was collected *via* cardiac puncture into lithium heparin treated collection tubes. 250μL of whole blood were added to 10mL PBS and cells were pelleted at 400x G for 5 minutes. Pelleted cells were depleted of red blood cells (RBCs) by 2 rounds of ACK-lysis. Remaining leukocytes were stained with an antibody cocktail consisting of antibodies against: CD11b (BV421, clone M1/70, BioLegend), CD317 (BV605, clone 927, BioLegend), CD11c

(BV785, clone N418, BioLegend), Ly6G (FITC, clone 1A8, BioLegend), Ly6C (PerCP-Cy5.5, clone HK1.4, BioLegend), CD49b (PE, clone DX5, BioLegend), CD45 (AlexaFluor 532, clone 30-F11, ThermoFisher), CD3 (BV510, clone 17A2, BioLegend), CD45R/B220 (BV570, RA3-6B2, BioLegend). Stained cells were fixed and run on a Cytek Northern Lights flow cytometer (Cytek Biosciences) equipped with 405nm and 488nm lasers (Blue, Violet). Visualization and analysis were performed in FlowJo (Becton, Dickinson and Company).

Comparative analysis of public datasets. Differentially expressed genes identified by Chen *et al.* [36] (genes differentially regulated during hyperactive *STE11*$^{\Delta N467}$ expression) and Bruno *et al.* [55] (genes differentially regulated during caspofungin exposure), as well as genes identified in a Cytoscape predicted Crz1 regulon created by Ballou *et al.* [29], were pulled and manually collated into a single excel file to identify conserved genes within these datasets. This file was then subsequently used as input for the gdata and VennDiagram packages in RStudio (R Version 1.1.456) for the identification of genes common to all datasets.

Ethics statement. All animal work used in this study was done under an approved protocol by the University of Tennessee, Knoxville Institution Animal Care and Use Committee (IACUC), and in accordance with the National Institute of Health's (NIH) ethical guidelines for animal research.

Mouse Model. Outbred ICR mice (ENVIGO) were used for all experiments in this study. To prepare for infection, 50ml cultures of the desired strains were grown overnight in YPD one day prior to injection. Cells were then prepared as previously described [37] and diluted to either $1x10^7$ cells/ml (for immunocompetent mice) or $1x10^5$ cells/ml (for immunosuppressed mice) in PBS. Mice were then intravenously inoculated via the lateral tail vein with 0.1ml of the appropriate cell suspension. To ensure accurate cell counts, cell viability for each strain was assessed by plating on YPD and allowing cells to grow at 30°C for 24 hours following injection. To assess peripheral leukocyte counts and serum cytokine

levels, mice were anesthetized, and peripheral blood was isolated via cardiac puncture in heparin treated tubes (BD Biosciences) prior to being euthanized. To assess kidney fungal burden, mice were euthanized, and their kidneys were harvested and placed into pre-weighed whirl-pack bags (Thermo Fisher Scientific) containing 1ml of water. Each bag was then weighed once more to determine kidney weight and then the kidneys were homogenized. Serial dilutions of the kidney homogenates (10^{-1}, 10^{-2}, 10^{-3}) were created, and 1ml of each dilution was added to 15ml of YPD + 75μg/ml chloramphenicol (Thermo Fisher Scientific) precooled to 55°C for plating. Plates were then left to grow at 30°C for 2 days to determine viable fungal colony forming units per gram of kidney. Once counts were obtained, outliers were determined via an outlier test and distribution normality was assessed with the use of a D'Agostino-Pearson omnibus normality test (GraphPad Prism, v7.0c software). Statistical significance was then determined with the use of either a Mann-Whitney test, a one-way ANOVA with Tukey's post hoc analysis or a non-parametric Kruskal-Wallis test for data that did not follow a Gaussian distribution (GraphPad Prism, v7.0c software). The number of mice used for each experiment is listed in the figure legend associated with the data, and samples were plated with technical duplicates.

Immune Cell Depletion. Non-specific immunosuppression was achieved via recurring injections with cyclophosphamide (Sigma-Aldrich) as previously described [37]. Starting 4 days prior to infection, all mice were weighed and then injected intraperitoneally (I.P.) with 150mg/kg of cyclophosphamide based on their average weights. Immune cell depletion was then maintained by recurring I.P. injections with 150mg/kg of cyclophosphamide every 3 days until the end of the experiment.

Serum Cytokine Quantification. Serum cytokine concentrations were determined as previously described [37] using the manufacturer's protocol for the LEGENDplex Mouse Anti-Virus Response Panel 740622 (Biolegend).

Hyphal Assays. Wild-type, *fgr41Δ/Δ*, and *fgr41Δ/Δ* P_{ENO1}-FGR41 strains were grown overnight in 5 mL of YPD while shaking at 225rpm in a 30°C incubator. For hyphal assays

in liquid media, overnight cultures were spun down at 3,500x g for 5 minutes and washed twice with 25mL of 1X PBS. Washed cells were diluted to an OD_{600} of 0.1 in 1mL EBSS + 2% FBS + 1% Pen/Strep and further serially diluted 1:10 twice. 100 microliters of the 1 x 10^{-2} dilution was placed into each of three wells of a flat-bottomed 96-well plate and incubated at 37°C + 5% CO_2. Replicate plates were incubated for one, two, and three hours and after incubation each plate was analyzed using an inverted microscope. Image analysis was performed using ImageJ software (Version 2.0.0). For germination assays, 3 biological replicates were measured for each strain used. At each time point sampled, 6 separate images were taken per sample and all cells (~25-50) within the field of focus were categorized as undifferentiated or a germinated yeast cell. To determine hyphal length, 3 biological replicates with 3 technical replicates for each strain were used. At all time points, 3 separate images were taken per a sample and 10 hyphal cells per an image were measured via pixel length on ImageJ software (Version 2.0.0). Once data were obtained, distribution normality was assessed with the use of a D'Agostino-Pearson omnibus normality test (GraphPad Prism, v7.0c software). Statistical significance was then determined with the use of either a one-way ANOVA with a Tukey's multiple comparison post-hoc analysis for data that followed a Gaussian distribution or a Kruskal-Wallis test with Dunn's multiple comparisons post-hoc analysis for data that did not.

Spot Dilution Assays and Growth Curves. To assess the sensitivity of mutants to various cell wall stressors, strains were grown overnight in 5ml cultures in YPD one night prior to the experiment. The following morning, the cultures were harvested and washed 3 times with 5ml of PBS, diluted to an OD_{600} of 0.1 in PBS, and four subsequent 1:10 dilutions were further performed. To assess cell wall sensitivity to cell envelope stressors, 3µl of each dilution was spotted onto a plate consisting of YPD (control), YPD + 10µg/ml calcofluor white (Fisher Scientific), YPD + 50ng/ml or 125ng/ml caspofungin (Gold Biotechnology) or YPD + 0.05% sodium dodecyl sulfate (SDS) (Fisher Scientific). Plates were then incubated for 24 hours at 30°C, and images were taken the following day.

For growth curves, strains were grown overnight in 5ml cultures in YPD one night prior to infection. The following morning, the cultures were diluted to an OD_{600} of 0.1 in

5mls of fresh YPD, and left to grow shaking at 225rpm at 30°C. The OD_{600} was then taken at 2, 4, 6, 8, 10, 24 and 48 hours and growth kinetics were analyzed using GraphPad Prism (v7.0c software). Three biological replicates were tested for each strain.

References

1. Hood MI, Skaar EP. Nutritional immunity: transition metals at the pathogen-host interface. Nat Rev Microbiol. 2012;10(8):525-37. Epub 2012/07/17. doi: 10.1038/nrmicro2836. PubMed PMID: 22796883; PubMed Central PMCID: PMCPMC3875331.

2. Crawford A, Wilson D. Essential metals at the host-pathogen interface: nutritional immunity and micronutrient assimilation by human fungal pathogens. FEMS Yeast Res. 2015;15(7). Epub 2015/08/06. doi: 10.1093/femsyr/fov071. PubMed PMID: 26242402; PubMed Central PMCID: PMCPMC4629794.

3. Miramon P, Lorenz MC. A feast for Candida: Metabolic plasticity confers an edge for virulence. PLoS Pathog. 2017;13(2):e1006144. Epub 2017/02/10. doi: 10.1371/journal.ppat.1006144. PubMed PMID: 28182769; PubMed Central PMCID: PMCPMC5300112.

4. Vylkova S, Carman AJ, Danhof HA, Collette JR, Zhou H, Lorenz MC. The fungal pathogen Candida albicans autoinduces hyphal morphogenesis by raising extracellular pH. mBio. 2011;2(3):e00055-11. Epub 2011/05/19. doi: 10.1128/mBio.00055-11. PubMed PMID: 21586647; PubMed Central PMCID: PMCPMC3101780.

5. Gunther LS, Martins HP, Gimenes F, Abreu AL, Consolaro ME, Svidzinski TI. Prevalence of Candida albicans and non-albicans isolates from vaginal secretions: comparative evaluation of colonization, vaginal candidiasis and recurrent vaginal candidiasis in diabetic and non-diabetic women. Sao Paulo Med J. 2014;132(2):116-20. Epub 2014/04/10. doi: 10.1590/1516-3180.2014.1322640. PubMed PMID: 24714993.

6. Fallingborg J. Intraluminal pH of the human gastrointestinal tract. Dan Med Bull. 1999;46(3):183-96. Epub 1999/07/28. PubMed PMID: 10421978.

7. He G, Shankar RA, Chzhan M, Samouilov A, Kuppusamy P, Zweier JL. Noninvasive measurement of anatomic structure and intraluminal oxygenation in the gastrointestinal tract of living mice with spatial and spectral EPR imaging. Proc Natl Acad Sci U S A. 1999;96(8):4586-91. Epub 1999/04/14. doi: 10.1073/pnas.96.8.4586. PubMed PMID: 10200306; PubMed Central PMCID: PMCPMC16376.

8. Rosenbach A, Dignard D, Pierce JV, Whiteway M, Kumamoto CA. Adaptations of Candida albicans for growth in the mammalian intestinal tract. Eukaryot Cell. 2010;9(7):1075-86. Epub 2010/05/04. doi: 10.1128/EC.00034-10. PubMed PMID: 20435697; PubMed Central PMCID: PMCPMC2901676.

9. Eltzschig HK, Carmeliet P. Hypoxia and inflammation. N Engl J Med. 2011;364(7):656-65. Epub 2011/02/18. doi: 10.1056/NEJMra0910283. PubMed PMID: 21323543; PubMed Central PMCID: PMCPMC3930928.

10. Grahl N, Shepardson KM, Chung D, Cramer RA. Hypoxia and fungal pathogenesis: to air or not to air? Eukaryot Cell. 2012;11(5):560-70. Epub 2012/03/27. doi: 10.1128/EC.00031-12. PubMed PMID: 22447924; PubMed Central PMCID: PMCPMC3346435.

11. Netea MG, Joosten LA, van der Meer JW, Kullberg BJ, van de Veerdonk FL. Immune defence against Candida fungal infections. Nat Rev Immunol. 2015;15(10):630-42. Epub 2015/09/22. doi: 10.1038/nri3897. PubMed PMID: 26388329.

12. Taylor PR, Brown GD, Reid DM, Willment JA, Martinez-Pomares L, Gordon S, et al. The beta-glucan receptor, dectin-1, is predominantly expressed on the surface of cells of the monocyte/macrophage and neutrophil lineages. J Immunol. 2002;169(7):3876-82. Epub 2002/09/24. doi: 10.4049/jimmunol.169.7.3876. PubMed PMID: 12244185.

13. Brown GD, Taylor PR, Reid DM, Willment JA, Williams DL, Martinez-Pomares L, et al. Dectin-1 is a major beta-glucan receptor on macrophages. J Exp Med. 2002;196(3):407-12. Epub 2002/08/07. doi: 10.1084/jem.20020470. PubMed PMID: 12163569; PubMed Central PMCID: PMCPMC2193936.

14. Brown GD, Gordon S. Immune recognition. A new receptor for beta-glucans. Nature. 2001;413(6851):36-7. Epub 2001/09/07. doi: 10.1038/35092620. PubMed PMID: 11544516.

15. Kennedy AD, Willment JA, Dorward DW, Williams DL, Brown GD, DeLeo FR. Dectin-1 promotes fungicidal activity of human neutrophils. Eur J Immunol. 2007;37(2):467-78. Epub 2007/01/19. doi: 10.1002/eji.200636653. PubMed PMID: 17230442.

16. Cohen-Kedar S, Baram L, Elad H, Brazowski E, Guzner-Gur H, Dotan I. Human intestinal epithelial cells respond to beta-glucans via Dectin-1 and Syk. Eur J Immunol. 2014;44(12):3729-40. Epub 2014/09/25. doi: 10.1002/eji.201444876. PubMed PMID: 25251945.

17. Gow NA, Netea MG, Munro CA, Ferwerda G, Bates S, Mora-Montes HM, et al. Immune recognition of Candida albicans beta-glucan by dectin-1. J Infect Dis. 2007;196(10):1565-71. Epub 2007/11/17. doi: 10.1086/523110. PubMed PMID: 18008237; PubMed Central PMCID: PMCPMC2655640.

18. van Bruggen R, Drewniak A, Jansen M, van Houdt M, Roos D, Chapel H, et al. Complement receptor 3, not Dectin-1, is the major receptor on human neutrophils for beta-glucan-bearing particles. Mol Immunol. 2009;47(2-3):575-81. Epub 2009/10/09. doi: 10.1016/j.molimm.2009.09.018. PubMed PMID: 19811837.

19. Li X, Utomo A, Cullere X, Choi MM, Milner DA, Jr., Venkatesh D, et al. The beta-glucan receptor Dectin-1 activates the integrin Mac-1 in neutrophils via Vav protein signaling to promote Candida albicans clearance. Cell Host Microbe. 2011;10(6):603-15. Epub 2011/12/20. doi: 10.1016/j.chom.2011.10.009. PubMed PMID: 22177564; PubMed Central PMCID: PMCPMC3244687.

20. Swidergall M, Solis NV, Wang Z, Phan QT, Marshall ME, Lionakis MS, et al. EphA2 Is a Neutrophil Receptor for Candida albicans that Stimulates Antifungal Activity during Oropharyngeal Infection. Cell Rep. 2019;28(2):423-33 e5. Epub 2019/07/11. doi: 10.1016/j.celrep.2019.06.020. PubMed PMID: 31291578; PubMed Central PMCID: PMCPMC6638578.

21. Swidergall M, Solis NV, Lionakis MS, Filler SG. EphA2 is an epithelial cell pattern recognition receptor for fungal beta-glucans. Nat Microbiol. 2018;3(1):53-61. Epub 2017/11/15. doi: 10.1038/s41564-017-0059-5. PubMed PMID: 29133884; PubMed Central PMCID: PMCPMC5736406.

22. Gravelat FN, Beauvais A, Liu H, Lee MJ, Snarr BD, Chen D, et al. Aspergillus galactosaminogalactan mediates adherence to host constituents and conceals hyphal beta-glucan from the immune system. PLoS Pathog. 2013;9(8):e1003575. Epub 2013/08/31.

doi: 10.1371/journal.ppat.1003575. PubMed PMID: 23990787; PubMed Central PMCID: PMCPMC3749958.

23. Carrion Sde J, Leal SM, Jr., Ghannoum MA, Aimanianda V, Latge JP, Pearlman E. The RodA hydrophobin on Aspergillus fumigatus spores masks dectin-1- and dectin-2-dependent responses and enhances fungal survival in vivo. J Immunol. 2013;191(5):2581-8. Epub 2013/08/09. doi: 10.4049/jimmunol.1300748. PubMed PMID: 23926321; PubMed Central PMCID: PMCPMC4020118.

24. Rappleye CA, Eissenberg LG, Goldman WE. Histoplasma capsulatum alpha-(1,3)-glucan blocks innate immune recognition by the beta-glucan receptor. Proceedings of the National Academy of Sciences of the United States of America. 2007;104(4):1366-70. doi: 10.1073/pnas.0609848104. PubMed PMID: 17227865; PubMed Central PMCID: PMCPMC1783108.

25. Garfoot AL, Shen Q, Wuthrich M, Klein BS, Rappleye CA. The Eng1 beta-Glucanase Enhances Histoplasma Virulence by Reducing beta-Glucan Exposure. mBio. 2016;7(2):e01388-15. Epub 2016/04/21. doi: 10.1128/mBio.01388-15. PubMed PMID: 27094334; PubMed Central PMCID: PMCPMC4850272.

26. Graus MS, Wester MJ, Lowman DW, Williams DL, Kruppa MD, Martinez CM, et al. Mannan Molecular Substructures Control Nanoscale Glucan Exposure in Candida. Cell Rep. 2018;24(9):2432-42 e5. Epub 2018/08/30. doi: 10.1016/j.celrep.2018.07.088. PubMed PMID: 30157435; PubMed Central PMCID: PMCPMC6204226.

27. Shen H, Chen SM, Liu W, Zhu F, He LJ, Zhang JD, et al. Abolishing Cell Wall Glycosylphosphatidylinositol-Anchored Proteins in Candida albicans Enhances Recognition by Host Dectin-1. Infect Immun. 2015;83(7):2694-704. Epub 2015/04/22. doi: 10.1128/IAI.00097-15. PubMed PMID: 25895969; PubMed Central PMCID: PMCPMC4468527.

28. Huang X, Liu Y, Ni T, Li L, Yan L, An M, et al. 11g, a Potent Antifungal Candidate, Enhances Candida albicans Immunogenicity by Unmasking beta-Glucan in Fungal Cell Wall. Front Microbiol. 2020;11:1324. Epub 2020/07/23. doi: 10.3389/fmicb.2020.01324. PubMed PMID: 32695076; PubMed Central PMCID: PMCPMC7338940.

29. Ballou ER, Avelar GM, Childers DS, Mackie J, Bain JM, Wagener J, et al. Lactate signalling regulates fungal beta-glucan masking and immune evasion. Nat Microbiol. 2016;2:16238. Epub 2016/12/13. doi: 10.1038/nmicrobiol.2016.238. PubMed PMID: 27941860; PubMed Central PMCID: PMCPMC5704895.

30. Childers DS, Avelar GM, Bain JM, Pradhan A, Larcombe DE, Netea MG, et al. Epitope Shaving Promotes Fungal Immune Evasion. mBio. 2020;11(4). Epub 2020/07/09. doi: 10.1128/mBio.00984-20. PubMed PMID: 32636248; PubMed Central PMCID: PMCPMC7343991.

31. Sherrington SL, Sorsby E, Mahtey N, Kumwenda P, Lenardon MD, Brown I, et al. Adaptation of Candida albicans to environmental pH induces cell wall remodelling and enhances innate immune recognition. PLoS Pathog. 2017;13(5):e1006403. Epub 2017/05/26. doi: 10.1371/journal.ppat.1006403. PubMed PMID: 28542528; PubMed Central PMCID: PMCPMC5456412.

32. Cottier F, Sherrington S, Cockerill S, Del Olmo Toledo V, Kissane S, Tournu H, et al. Remasking of Candida albicans beta-Glucan in Response to Environmental pH Is Regulated by Quorum Sensing. mBio. 2019;10(5). Epub 2019/10/17. doi: 10.1128/mBio.02347-19. PubMed PMID: 31615961; PubMed Central PMCID: PMCPMC6794483.

33. Pradhan A, Avelar GM, Bain JM, Childers DS, Larcombe DE, Netea MG, et al. Hypoxia Promotes Immune Evasion by Triggering beta-Glucan Masking on the Candida albicans Cell Surface via Mitochondrial and cAMP-Protein Kinase A Signaling. mBio. 2018;9(6). Epub 2018/11/08. doi: 10.1128/mBio.01318-18. PubMed PMID: 30401773; PubMed Central PMCID: PMCPMC6222127.

34. Pradhan A, Avelar GM, Bain JM, Childers D, Pelletier C, Larcombe DE, et al. Non-canonical signalling mediates changes in fungal cell wall PAMPs that drive immune evasion. Nat Commun. 2019;10(1):5315. Epub 2019/11/24. doi: 10.1038/s41467-019-13298-9. PubMed PMID: 31757950; PubMed Central PMCID: PMCPMC6876565.

35. Chen T, Jackson JW, Tams RN, Davis SE, Sparer TE, Reynolds TB. Exposure of Candida albicans beta (1,3)-glucan is promoted by activation of the Cek1 pathway. PLoS

Genet. 2019;15(1):e1007892. Epub 2019/02/01. doi: 10.1371/journal.pgen.1007892. PubMed PMID: 30703081; PubMed Central PMCID: PMCPMC6372213.

36. Chen T, Wagner AS, Tams RN, Eyer JE, Kauffman SJ, Gann ER, et al. Lrg1 Regulates beta (1,3)-Glucan Masking in Candida albicans through the Cek1 MAP Kinase Pathway. mBio. 2019;10(5). Epub 2019/09/19. doi: 10.1128/mBio.01767-19. PubMed PMID: 31530671; PubMed Central PMCID: PMCPMC6751057.

37. Wagner AS, Hancock TJ, Lumsdaine SW, Kauffman SJ, Mangrum MM, Phillips EK, et al. Activation of Cph1 causes ss(1,3)-glucan unmasking in Candida albicans and attenuates virulence in mice in a neutrophil-dependent manner. PLoS Pathog. 2021;17(8):e1009839. Epub 2021/08/26. doi: 10.1371/journal.ppat.1009839. PubMed PMID: 34432857.

38. Davis TR, Zucchi PC, Kumamoto CA. Calmodulin binding to Dfi1p promotes invasiveness of Candida albicans. PLoS One. 2013;8(10):e76239. Epub 2013/10/25. doi: 10.1371/journal.pone.0076239. PubMed PMID: 24155896; PubMed Central PMCID: PMCPMC3796530.

39. Cyert MS, Kunisawa R, Kaim D, Thorner J. Yeast has homologs (CNA1 and CNA2 gene products) of mammalian calcineurin, a calmodulin-regulated phosphoprotein phosphatase. Proc Natl Acad Sci U S A. 1991;88(16):7376-80. Epub 1991/08/15. doi: 10.1073/pnas.88.16.7376. PubMed PMID: 1651503; PubMed Central PMCID: PMCPMC52298.

40. Klee CB, Crouch TH, Krinks MH. Calcineurin: a calcium- and calmodulin-binding protein of the nervous system. Proc Natl Acad Sci U S A. 1979;76(12):6270-3. Epub 1979/12/01. doi: 10.1073/pnas.76.12.6270. PubMed PMID: 293720; PubMed Central PMCID: PMCPMC411845.

41. Moser MJ, Geiser JR, Davis TN. Ca2+-calmodulin promotes survival of pheromone-induced growth arrest by activation of calcineurin and Ca2+-calmodulin-dependent protein kinase. Mol Cell Biol. 1996;16(9):4824-31. Epub 1996/09/01. doi: 10.1128/MCB.16.9.4824. PubMed PMID: 8756641; PubMed Central PMCID: PMCPMC231484.

42. Bader T, Bodendorfer B, Schroppel K, Morschhauser J. Calcineurin is essential for virulence in Candida albicans. Infect Immun. 2003;71(9):5344-54. Epub 2003/08/23. doi: 10.1128/IAI.71.9.5344-5354.2003. PubMed PMID: 12933882; PubMed Central PMCID: PMCPMC187310.

43. Liu J, Farmer JD, Jr., Lane WS, Friedman J, Weissman I, Schreiber SL. Calcineurin is a common target of cyclophilin-cyclosporine A and FKBP-FK506 complexes. Cell. 1991;66(4):807-15. Epub 1991/09/02. doi: 10.1016/0092-8674(91)90124-h. PubMed PMID: 1715244.

44. Breuder T, Hemenway CS, Movva NR, Cardenas ME, Heitman J. Calcineurin is essential in cyclosporine A- and FK506-sensitive yeast strains. Proc Natl Acad Sci U S A. 1994;91(12):5372-6. Epub 1994/06/07. doi: 10.1073/pnas.91.12.5372. PubMed PMID: 7515500; PubMed Central PMCID: PMCPMC43997.

45. Wheeler RT, Kombe D, Agarwala SD, Fink GR. Dynamic, morphotype-specific Candida albicans beta-glucan exposure during infection and drug treatment. PLoS Pathog. 2008;4(12):e1000227. Epub 2008/12/06. doi: 10.1371/journal.ppat.1000227. PubMed PMID: 19057660; PubMed Central PMCID: PMCPMC2587227.

46. Wheeler RT, Fink GR. A drug-sensitive genetic network masks fungi from the immune system. PLoS Pathog. 2006;2(4):e35. Epub 2006/05/03. doi: 10.1371/journal.ppat.0020035. PubMed PMID: 16652171; PubMed Central PMCID: PMCPMC1447670.

47. Roman E, Cottier F, Ernst JF, Pla J. Msb2 signaling mucin controls activation of Cek1 mitogen-activated protein kinase in Candida albicans. Eukaryot Cell. 2009;8(8):1235-49. Epub 2009/06/23. doi: 10.1128/EC.00081-09. PubMed PMID: 19542310; PubMed Central PMCID: PMCPMC2725568.

48. Swidergall M, van Wijlick L, Ernst JF. Signaling domains of mucin Msb2 in Candida albicans. Eukaryot Cell. 2015;14(4):359-70. Epub 2015/02/01. doi: 10.1128/EC.00264-14. PubMed PMID: 25636320; PubMed Central PMCID: PMCPMC4385809.

49. Singh SD, Robbins N, Zaas AK, Schell WA, Perfect JR, Cowen LE. Hsp90 governs echinocandin resistance in the pathogenic yeast Candida albicans via calcineurin.

PLoS Pathog. 2009;5(7):e1000532. Epub 2009/08/04. doi: 10.1371/journal.ppat.1000532. PubMed PMID: 19649312; PubMed Central PMCID: PMCPMC2712069.

50. Blankenship JR, Heitman J. Calcineurin is required for Candida albicans to survive calcium stress in serum. Infect Immun. 2005;73(9):5767-74. Epub 2005/08/23. doi: 10.1128/IAI.73.9.5767-5774.2005. PubMed PMID: 16113294; PubMed Central PMCID: PMCPMC1231066.

51. Li W, Shrivastava M, Lu H, Jiang Y. Calcium-calcineurin signaling pathway in Candida albicans: A potential drug target. Microbiol Res. 2021;249:126786. Epub 2021/05/15. doi: 10.1016/j.micres.2021.126786. PubMed PMID: 33989979.

52. Stathopoulos AM, Cyert MS. Calcineurin acts through the CRZ1/TCN1-encoded transcription factor to regulate gene expression in yeast. Genes Dev. 1997;11(24):3432-44. Epub 1998/02/07. doi: 10.1101/gad.11.24.3432. PubMed PMID: 9407035; PubMed Central PMCID: PMCPMC316814.

53. Santos M, de Larrinoa IF. Functional characterization of the Candida albicans CRZ1 gene encoding a calcineurin-regulated transcription factor. Curr Genet. 2005;48(2):88-100. Epub 2005/07/27. doi: 10.1007/s00294-005-0003-8. PubMed PMID: 16044281.

54. Karababa M, Valentino E, Pardini G, Coste AT, Bille J, Sanglard D. CRZ1, a target of the calcineurin pathway in Candida albicans. Mol Microbiol. 2006;59(5):1429-51. Epub 2006/02/14. doi: 10.1111/j.1365-2958.2005.05037.x. PubMed PMID: 16468987.

55. Bruno VM, Kalachikov S, Subaran R, Nobile CJ, Kyratsous C, Mitchell AP. Control of the C. albicans cell wall damage response by transcriptional regulator Cas5. PLoS Pathog. 2006;2(3):e21. Epub 2006/03/23. doi: 10.1371/journal.ppat.0020021. PubMed PMID: 16552442; PubMed Central PMCID: PMCPMC1401495.

56. Xu H, Fang T, Omran RP, Whiteway M, Jiang L. RNA sequencing reveals an additional Crz1-binding motif in promoters of its target genes in the human fungal pathogen Candida albicans. Cell Commun Signal. 2020;18(1):1. Epub 2020/01/05. doi: 10.1186/s12964-019-0473-9. PubMed PMID: 31900175; PubMed Central PMCID: PMCPMC6942403.

57. Uhl MA, Biery M, Craig N, Johnson AD. Haploinsufficiency-based large-scale forward genetic analysis of filamentous growth in the diploid human fungal pathogen C.albicans. EMBO J. 2003;22(11):2668-78. Epub 2003/05/30. doi: 10.1093/emboj/cdg256. PubMed PMID: 12773383; PubMed Central PMCID: PMCPMC156753.

58. Hao B, Cheng S, Clancy CJ, Nguyen MH. Caspofungin kills Candida albicans by causing both cellular apoptosis and necrosis. Antimicrob Agents Chemother. 2013;57(1):326-32. Epub 2012/11/02. doi: 10.1128/AAC.01366-12. PubMed PMID: 23114781; PubMed Central PMCID: PMCPMC3535936.

59. Chin C, Donaghey F, Helming K, McCarthy M, Rogers S, Austriaco N. Deletion of AIF1 but not of YCA1/MCA1 protects Saccharomyces cerevisiae and Candida albicans cells from caspofungin-induced programmed cell death. Microb Cell. 2014;1(2):58-63. Epub 2014/01/15. doi: 10.15698/mic2014.01.119. PubMed PMID: 28357223; PubMed Central PMCID: PMCPMC5348969.

60. Lu H, Zhu Z, Dong L, Jia X, Sun X, Yan L, et al. Lack of trehalose accelerates H2O2-induced Candida albicans apoptosis through regulating Ca2+ signaling pathway and caspase activity. PLoS One. 2011;6(1):e15808. Epub 2011/01/20. doi: 10.1371/journal.pone.0015808. PubMed PMID: 21246042; PubMed Central PMCID: PMCPMC3016397.

61. Dai B, Wang Y, Li D, Xu Y, Liang R, Zhao L, et al. Hsp90 is involved in apoptosis of Candida albicans by regulating the calcineurin-caspase apoptotic pathway. PLoS One. 2012;7(9):e45109. Epub 2012/10/03. doi: 10.1371/journal.pone.0045109. PubMed PMID: 23028789; PubMed Central PMCID: PMCPMC3445616.

62. Wiederhold NP, Kontoyiannis DP, Prince RA, Lewis RE. Attenuation of the activity of caspofungin at high concentrations against candida albicans: possible role of cell wall integrity and calcineurin pathways. Antimicrob Agents Chemother. 2005;49(12):5146-8. Epub 2005/11/24. doi: 10.1128/AAC.49.12.5146-5148.2005. PubMed PMID: 16304189; PubMed Central PMCID: PMCPMC1315970.

63. Marakalala MJ, Vautier S, Potrykus J, Walker LA, Shepardson KM, Hopke A, et al. Differential adaptation of Candida albicans in vivo modulates immune recognition by

dectin-1. PLoS Pathog. 2013;9(4):e1003315. Epub 2013/05/03. doi: 10.1371/journal.ppat.1003315. PubMed PMID: 23637604; PubMed Central PMCID: PMCPMC3630191.

64. Wiederhold NP, Najvar LK, Bocanegra R, Kirkpatrick WR, Patterson TF. Comparison of anidulafungin's and fluconazole's in vivo activity in neutropenic and non-neutropenic models of invasive candidiasis. Clin Microbiol Infect. 2012;18(2):E20-3. Epub 2011/12/02. doi: 10.1111/j.1469-0691.2011.03712.x. PubMed PMID: 22128831.

65. Bader T, Schroppel K, Bentink S, Agabian N, Kohler G, Morschhauser J. Role of calcineurin in stress resistance, morphogenesis, and virulence of a Candida albicans wild-type strain. Infect Immun. 2006;74(7):4366-9. Epub 2006/06/23. doi: 10.1128/IAI.00142-06. PubMed PMID: 16790813; PubMed Central PMCID: PMCPMC1489686.

66. Kullas AL, Martin SJ, Davis D. Adaptation to environmental pH: integrating the Rim101 and calcineurin signal transduction pathways. Mol Microbiol. 2007;66(4):858-71. Epub 2007/10/12. doi: 10.1111/j.1365-2958.2007.05929.x. PubMed PMID: 17927701.

67. Sanglard D, Ischer F, Marchetti O, Entenza J, Bille J. Calcineurin A of Candida albicans: involvement in antifungal tolerance, cell morphogenesis and virulence. Mol Microbiol. 2003;48(4):959-76. Epub 2003/05/20. doi: 10.1046/j.1365-2958.2003.03495.x. PubMed PMID: 12753189.

68. Blankenship JR, Wormley FL, Boyce MK, Schell WA, Filler SG, Perfect JR, et al. Calcineurin is essential for Candida albicans survival in serum and virulence. Eukaryot Cell. 2003;2(3):422-30. Epub 2003/06/11. doi: 10.1128/EC.2.3.422-430.2003. PubMed PMID: 12796287; PubMed Central PMCID: PMCPMC161442.

69. Walker LA, Munro CA, de Bruijn I, Lenardon MD, McKinnon A, Gow NA. Stimulation of chitin synthesis rescues Candida albicans from echinocandins. PLoS Pathog. 2008;4(4):e1000040. Epub 2008/04/05. doi: 10.1371/journal.ppat.1000040. PubMed PMID: 18389063; PubMed Central PMCID: PMCPMC2271054.

70. Yang F, Zhang L, Wakabayashi H, Myers J, Jiang Y, Cao Y, et al. Tolerance to Caspofungin in Candida albicans Is Associated with at Least Three Distinctive Mechanisms That Govern Expression of FKS Genes and Cell Wall Remodeling.

Antimicrob Agents Chemother. 2017;61(5). Epub 2017/02/23. doi: 10.1128/AAC.00071-17. PubMed PMID: 28223384; PubMed Central PMCID: PMCPMC5404545.

71. Hopke A, Nicke N, Hidu EE, Degani G, Popolo L, Wheeler RT. Neutrophil Attack Triggers Extracellular Trap-Dependent Candida Cell Wall Remodeling and Altered Immune Recognition. PLoS pathogens. 2016;12(5):e1005644. doi: 10.1371/journal.ppat.1005644. PubMed PMID: 27223610; PubMed Central PMCID: PMC4880299.

72. Davis SE, Hopke A, Minkin SC, Jr., Montedonico AE, Wheeler RT, Reynolds TB. Masking of beta(1-3)-glucan in the cell wall of Candida albicans from detection by innate immune cells depends on phosphatidylserine. Infection and immunity. 2014. doi: 10.1128/IAI.01612-14. PubMed PMID: 25114110.

73. Pericolini E, Perito S, Castagnoli A, Gabrielli E, Mencacci A, Blasi E, et al. Epitope unmasking in vulvovaginal candidiasis is associated with hyphal growth and neutrophilic infiltration. PLoS One. 2018;13(7):e0201436. Epub 2018/08/01. doi: 10.1371/journal.pone.0201436. PubMed PMID: 30063729; PubMed Central PMCID: PMCPMC6067721.

74. Mulhern SM, Logue ME, Butler G. Candida albicans transcription factor Ace2 regulates metabolism and is required for filamentation in hypoxic conditions. Eukaryot Cell. 2006;5(12):2001-13. Epub 2006/09/26. doi: 10.1128/EC.00155-06. PubMed PMID: 16998073; PubMed Central PMCID: PMCPMC1694816.

75. Sayers EW, Bolton EE, Brister JR, Canese K, Chan J, Comeau DC, et al. Database resources of the national center for biotechnology information. Nucleic Acids Res. 2022;50(D1):D20-D6. Epub 2021/12/02. doi: 10.1093/nar/gkab1112. PubMed PMID: 34850941; PubMed Central PMCID: PMCPMC8728269.

76. Sigrist CJ, de Castro E, Cerutti L, Cuche BA, Hulo N, Bridge A, et al. New and continuing developments at PROSITE. Nucleic Acids Res. 2013;41(Database issue):D344-7. Epub 2012/11/20. doi: 10.1093/nar/gks1067. PubMed PMID: 23161676; PubMed Central PMCID: PMCPMC3531220.

77. Yang M, Solis NV, Marshall M, Garleb R, Zhou T, Wang D, et al. Control of beta-glucan exposure by the endo-1,3-glucanase Eng1 in Candida albicans modulates

virulence. PLoS Pathog. 2022;18(1):e1010192. Epub 2022/01/08. doi: 10.1371/journal.ppat.1010192. PubMed PMID: 34995333; PubMed Central PMCID: PMCPMC8775328.

78. Styles C. How to set up a yeast laboratory. Methods Enzymol. 2002;350:42-71. Epub 2002/06/21. doi: 10.1016/s0076-6879(02)50955-1. PubMed PMID: 12073328.

79. Nguyen N, Quail MMF, Hernday AD. An Efficient, Rapid, and Recyclable System for CRISPR-Mediated Genome Editing in Candida albicans. mSphere. 2017;2(2). Epub 2017/05/13. doi: 10.1128/mSphereDirect.00149-17. PubMed PMID: 28497115; PubMed Central PMCID: PMCPMC5422035.

80. Tams RN, Cassilly CD, Anaokar S, Brewer WT, Dinsmore JT, Chen YL, et al. Overproduction of Phospholipids by the Kennedy Pathway Leads to Hypervirulence in Candida albicans. Front Microbiol. 2019;10:86. Epub 2019/02/23. doi: 10.3389/fmicb.2019.00086. PubMed PMID: 30792701; PubMed Central PMCID: PMCPMC6374345.

Appendix

S3.1 Table: Plasmids used in this study.

Strain Name	Description	Marker	Parent /Source
pBT1	*CaNAT-P_{ENO1}*	Ampicillin, Nourseothricin	1
pSL003	*CaNAT-P_{ENO}1-FGR41*	Ampicillin, Nourseothricin	pBT1
pAEK001	*CaNAT- P_{ENO}1-CWP419*	Ampicillin, Nourseothricin	pBT1
pMM001	*CaNAT- P_{ENO}1-PGA13*	Ampicillin, Nourseothricin	pBT1

References

1 Tams RN, Cassilly CD, Anaokar S, Brewer WT, Dinsmore JT, Chen YL, et al. Overproduction of Phospholipids by the Kennedy Pathway Leads to Hypervirulence in Candida albicans. Front Microbiol. 2019;10:86. Epub 2019/02/23. doi: 10.3389/fmicb.2019.00086. PubMed PMID: 30792701; PubMed Central PMCID: PMCPMC6374345

S3.2 Table: Primers used in this study.

Primer Name	Sequence (5' to 3')	Description	Source
AHO1096	GACGGCACGGCCACGCGTTTAAACCGCC	Fragment A forward primer for CRISPR-mediated gene deletion.	1
AHO1097	CCCGCCAGGCGCTGGGGTTTAAACACCG	Fragment B reverse primer for CRISPR-mediated gene deletion.	1
AHO1098	caaattaaaaatagtttacgcaag	Fragment A reverse primer for CRISPR-mediated gene deletion.	1
AHO1237	aggtgatgctgaagctattgaag	Fragment C forward primer for CRISPR-mediated gene deletion.	1
AHO1238	TGTATTTTGTTTTAAAATTTTAGTGACTGTTTC	Fragment C reverse primer for CRISPR-mediated gene deletion.	1
BTO33	GACTAACGATTTCTATAAGG	P_{ENO1} colony PCR forward check primer and primer for sequencing P_{ENO1} overexpression constructs	2
AWO320	CGTAAACTATTTTTAATTTGATGAAGGTGGA TGGACTTTCGTTTTAGAGCTAGAAATAGC	*DFI1* gRNA forward primer for fragment B amplification for CRISPR-mediated gene clevage.	This Study
AWO335	GTTGTTGGTGTAGTTGTTGG	DFI1^WWQQ Sequencing Primer Forward (Sits at +810 and is 101bp upstream of the first missense mutation)	This Study
AWO355	CGTAAACTATTTTTAATTTGcaaataagct ggaattaagtGTTTTAGAGCTAGAAATAGC	*FGR41* gRNA forward primer for fragment B amplification for CRISPR-mediated gene deletion.	This Study
AWO359	GAGACAAGAAGTATTATTTCATCTC	*FGR41* whole gene deletion check primer forward (Sits -502bp upstream from start codon in 5'UTR)	This Study
AWO360	CAATTGAAAATTGTGCATG	*FGR41* whole gene deletion check primer reverse (Sits +455bp from stop codon in 3'UTR)	This Study
AWO361	aacttgcggccgcATGAAGATTTCCAACTTAATTCC	*FGR41* forward primer with NotI cutsite (For cloning into pBT1) (Amplifies ORF + 3'UTR with AWO362)	This Study
AWO362	aacttgcggccgcCAAGAAATTCCAAAAGTCTCC	*FGR41* reverse primer with NotI cutsite reverse (For cloning into pBT1) (Sits +270 from stop codon)	This Study

S3.2 Table Continued

Primer Name	Sequence (5' to 3')	Description	Source
AWO363	GAGAGTGACAGTTGTAGTGATTG	*FGR41* Cloning check primer into pBT1 and sequencing reverse (Use with BTO33). Also used to confirm loss of ORF in deletion mutant.	This Study
AWO378	CGTAAACTATTTTTAATTTGaaataatgat aataaaacgaGTTTTAGAGCTAGAAATAGC	*CWP419 (C1_11990W_A)* gRNA forward primer for fragment B amplification for CRISPR-mediated gene deletion.	This Study
AWO382	CTTTGAAAACTGAATTATTGTAAAC	*CWP419 (C1_11990W_A)* whole gene deletion check primer forward (sits -439 from start)	This Study
AWO383	GATGGTGCTAACAATAATATTCC	*CWP419 (C1_11990W_A)* whole gene deletion check primer reverse (sits +318 from stop in 3'UTR)	This Study
AKO021	AAAAGCGGCCGCCCACTCCTACATAATGCTTAG	*CWP419 (C1_11990W_A)* forward primer with NotI cutsite (For cloning into pBT1) (Amplifies ORF + 3'UTR with AKO22)	This Study
AKO022	AAAAGAGCTCTGCCACTAATTTCAAGAAAC	*CWP419 (C1_11990W_A)* reverse primer with SacI cutsite (For cloning into pBT1) (Amplifies ORF + 3'UTR with AKO21)	This Study
AKO023	CCTTCTGGAACTTCAACTTT	*CWP419* Cloning check primer into pBT1 and sequencing reverse (Use with BTO33)	This Study
AWO384	GCTGTTATCATCACTACTTGAGG	*CWP419 (C1_11990W_A)* whole gene deletion check primer reverse (sits +288 from start in ORF)	This Study
SLO015	CGTAAACTATTTTTAATTTGatagctgtg acccatcatccGTTTTAGAGCTAGAAATAGC	*CRZ1* gRNA forward primer for fragment B amplification for CRISPR-mediated gene deletion.	This Study
SLO021	TAATCAAGCTTACCAAGCTATTTTTATTG	*CRZ1* whole gene deletion check primer forward (sits -166bp from start codon in 5'UTR)	This Study
SLO022	TGGCTACTTCTTTTTCTGCGTGTGTGT	*CRZ1* whole gene deletion check primer reverse (sits +305bp from stop codon in 3'UTR)	This Study
SLO023	GAGTACTGCAGCTACGAACAATTCT	*CRZ1* whole gene deletion check primer forward (sits +1205bp from start codon in ORF)	This Study

S3.2 Table Continued

Primer Name	Sequence (5' to 3')	Description	Source
AWO336	aacttgcggccgcATGAGATCTCCATCACTCG	*PGA13* forward primer with NotI cutsite (For cloning into pBT1) (Amplifies ORF + 3'UTR with AWO337)(Also used for sequencing)	This Study
AWO337	TAAAAgagctCCTTTATAGAAACCAGATCCACC	*PGA13* reverse primer with SacI cutsite (For cloning into pBT1) (Amplifies ORF + 3'UTR with AWO336)	This Study
AWO338	CACATTTGGTGATGGTTAATG	*PGA13* ligation/transformation check primer reverse (Use with BTO33) (Sits +371bp from start codon in ORF)	This Study
AWO339	CCAACCACATTAACCATCAC	*PGA13* sequencing primer forward (sits +363bp in ORF from start)	This Study
AWO340	GGTTGTCACTACTGGTGTCAC	*PGA13* sequencing primer forward (sits +746bp in ORF from start)	This Study
AWO341	CAAGCAGCCATACTACTCAAG	*PGA13* sequencing primer forward (sits +1138bp in ORF from start)	This Study
AWO321	TATTTTACTTGAGAAAGAGAAACAAC CGTGATTATGAAGGTGGccaGACT TTCc aGAGAAAGAATGAGAAATTGGGAAGT GATGAGTTCTTCAATGGTGA	Repair template (sense oligomer) for making *DFI1^WWQQ* (Dfi1-calmodulin interaction deficient) mutants. (introduces pt mutations to change W305Q and W308Q, these changes also correspond to the PAM sequences as well to delete create a silent mutation within it in the repair template.) (Check for integration by screening for unique MscI cut site in mutant -> silent mutations for all point mutations introduced).	This Study
AWO337	TAAAAgagctCCTTTATAGAAACCAGATCCACC	*PGA13* reverse primer with SacI cutsite (For cloning into pBT1) (Amplifies ORF + 3'UTR with AWO336)	This Study

S3.2 Table Continued

Primer Name	Sequence (5' to 3')	Description	Source
AWO322	TCACCATTGAAGAACTCATCACTTC CCAATTTCTCATTCTTTCTCtgGAAAG TCtggCCACCTTCATAATCACGGTTGT TTCTCTTTCTCAAGTAAAATA	Repair template (antisense oligomer) for making *DFI1^WWQQ* (Dfi1-calmodulin interaction deficient) mutants. (introduces pt mutations to change W305Q and W308Q, these changes also correspond to the PAM sequences as well to delete create a silent mutation within it in the repair template.) (Check for integration by screening for unique MscI cut site in mutant -> silent mutations for all point mutations introduced).	This Study
AWO357	TCAACTCAAGTCGTTCCTTTAACA ATATCAACATGAAGATTTCCAACT TATGATATGGTGAGTAATGATTGA AAAAAAAAACAACACCCCTTTTAGTTTC	*FGR41* repair template for whole gene deletion (sense oligomer)	This Study
AWO358	GAAACTAAAAGGGGTGTTGTTTTT TTTTTCAATCATTACTCACCATATCAT AAGTTGGAAATCTTCATGTTGATATT GTTAAAGGAACGACTTGAGTTGA	*FGR41* repair template for whole gene deletion (antisense oligomer)	This Study
AWO380	TCTACAACTACCACTCCTACATAAT GCTTAGTTCTAAAATTTATTCCCTCTA AAGCAAAAAAAAAAAAGAATACCTAA GGTTTTGAATTAAACATCAATTT	*CWP419 (C1_11990W_A)* repair template for whole gene deletion (sense oligomer)	This Study
AWO381	AAATTGATGTTTAATTCAAAACCTTA GGTATTCTTTTTTTTTTTGCTTTAGA GGGAATAAATTTTAGAACTAAGCAT TATGTAGGAGTGGTAGTTGTAGA	*CWP419 (C1_11990W_A)* repair template for whole gene deletion (antisense oligomer)	This Study
SLO019	TTTATATCTAAATTTCATAAATCCCA ATCATGTCTAACAATCCTCATCCCTG ATTTGTTTTTTATTTTTGACATTTATA CTTTTTTTTTTTTCATATCTT	*CRZ1* repair template for whole gene deletion (sense oligomer)	This Study

S3.2 Table Continued

Primer Name	Sequence (5' to 3')	Description	Source
SLO020	AAGATATGAAAAAAAAAAAAGTATA AATGTCAAAAATAAAAAACAAATC AGGGATGAGGATTGTTAGACATGATT GGGATTTATGAAATTTAGATATAAA	*CRZ1* repair template for whole gene deletion (antisense oligomer)	This Study

References

1 Nguyen N, Quail MMF, Hernday AD. An Efficient, Rapid, and Recyclable System for CRISPR-Mediated Genome Editing in Candida albicans. mSphere. 2017;2(2). Epub 2017/05/13. doi: 10.1128/mSphereDirect.00149-17. PubMed PMID: 28497115; PubMed Central PMCID: PMCPMC5422035.

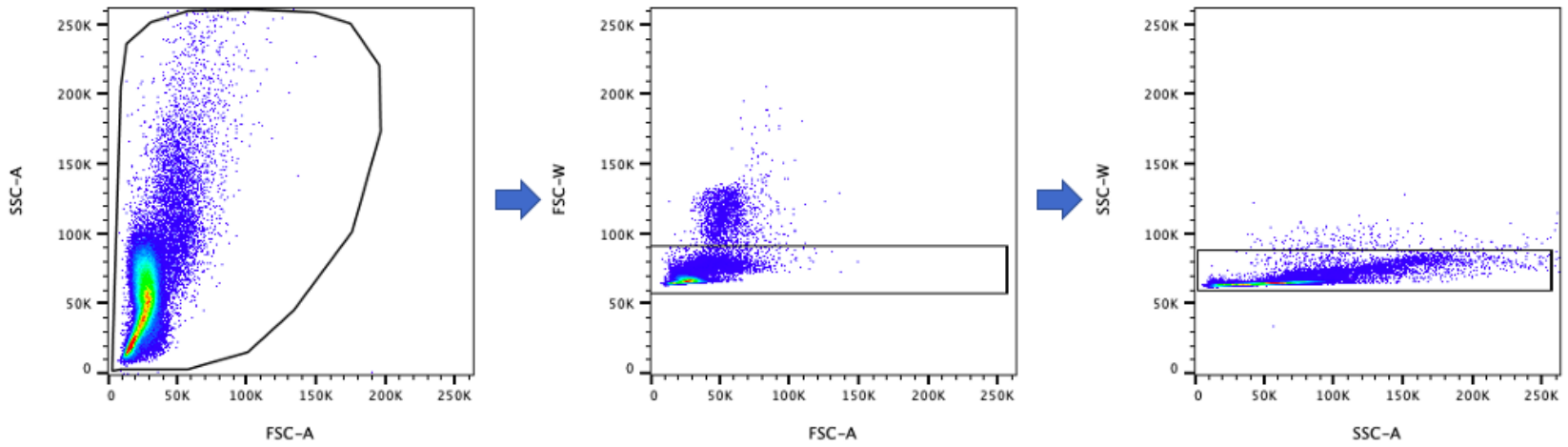
2 Tams RN, Cassilly CD, Anaokar S, Brewer WT, Dinsmore JT, Chen YL, et al. Overproduction of Phospholipids by the Kennedy Pathway Leads to Hypervirulence in Candida albicans. Front Microbiol. 2019;10:86. Epub 2019/02/23. doi: 10.3389/fmicb.2019.00086. PubMed PMID: 30792701; PubMed Central PMCID: PMCPMC6374345.

S3.3 Table: Strains used in this study.

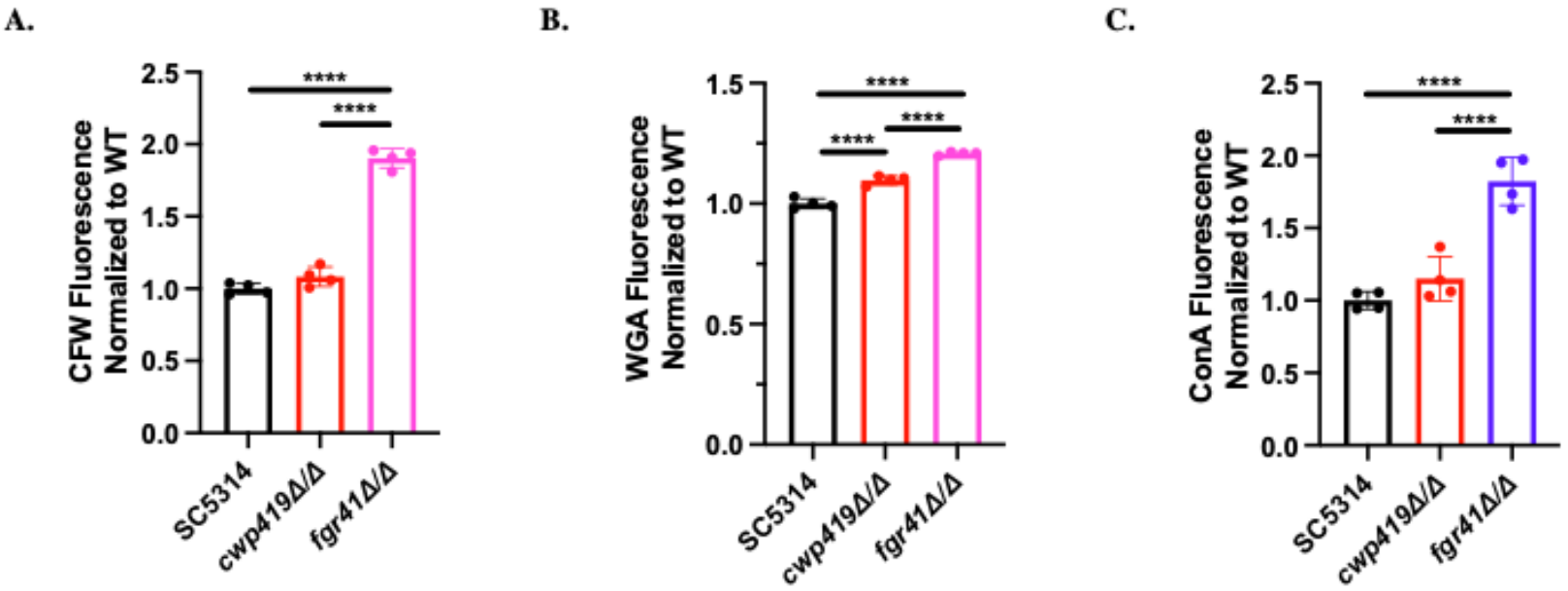
Strain	Genotype	Parent	Source or Reference
AWY006	*LEU2/leu2*Δ (Wild Type)	SC5314	1
AWY080	*STE11/P*$_{tet\text{-}off}$*-STE11*$^{\Delta N467}$ *LEU2/leu2*Δ	AWY006	1
AWY187	*STE11/P*$_{tet\text{-}off}$*-STE11*$^{\Delta N467}$ *dfi1*Δ/Δ *LEU2/leu2*Δ	AWY080	1
AWY182	*cph1*Δ/Δ *LEU2/leu2*Δ	AWY006	1
AWY254	*DFI1*^{W305Q,W308Q}*/ DFI1*^{W305Q,W308Q}	AWY006	This study
AWY255	*STE11/P*$_{tet\text{-}off}$*-STE11*$^{\Delta N467}$ *Dfi1*^{W305Q,W308Q}*/ Dfi1*^{W305Q,W308Q} *LEU2/leu2*Δ	AWY080	This study
SLY020	*crz1*Δ/Δ *LEU2/leu2*Δ	AWY006	This study
SLY023	*STE11/P*$_{tet\text{-}off}$*-STE11*$^{\Delta N467}$ crz1Δ/Δ *LEU2/leu2*Δ	AWY080	This study
SLY005	*fgr41*Δ/Δ *LEU2/leu2*Δ	AWY006	This study
SLY007	*STE11/P*$_{tet\text{-}off}$*-STE11*$^{\Delta N467}$ *fgr41*Δ/Δ *LEU2/leu2*Δ	AWY080	This study
SLY015	*P*$_{ENO1}$*-FGR41 LEU2/leu2*Δ	AWY006	This study
SLY013	*fgr41*Δ/Δ *P*$_{ENO1}$*-FGR41 LEU2/leu2*Δ	SLY005	This study
SLY017	*STE11/P*$_{tet\text{-}off}$*-STE11*$^{\Delta N467}$ *P*$_{ENO1}$*-FGR41 LEU2/leu2*Δ	AWY080	This study
AWY290	*cwp419*Δ/Δ *LEU2/leu2*Δ	AWY006	This study
AWY292	*STE11/P*$_{tet\text{-}off}$*-STE11*$^{\Delta N467}$ *cwp419*Δ/Δ *LEU2/leu2*Δ	AWY080	This study
AKY001	*P*$_{ENO1}$*-CWP419 LEU2/leu2*Δ	AWY006	This study
AKY004	*STE11/P*$_{tet\text{-}off}$*-STE11*$^{\Delta N467}$ *P*$_{ENO1}$*-CWP419 LEU2/leu2*Δ	AWY080	This study
AWY295	*cwp419*Δ/Δ *P*$_{ENO1}$*-CWP419 LEU2/leu2*Δ	AWY290	This study
MMY002	*P*$_{ENO1}$*-PGA13 LEU2/leu2*Δ	AWY006	This study
MMY003	*STE11/P*$_{tet\text{-}off}$*-STE11*$^{\Delta N467}$ *P*$_{ENO1}$*-PGA13 LEU2/leu2*Δ	AWY080	This study
AWY298	*crz1*Δ/Δ *P*$_{ENO1}$*-CWP419 LEU2/leu2*Δ	SLY020	This study
AWY302	*crz1*Δ/Δ *P*$_{ENO1}$*-FGR41 LEU2/leu2*Δ	SLY020	This study

References:

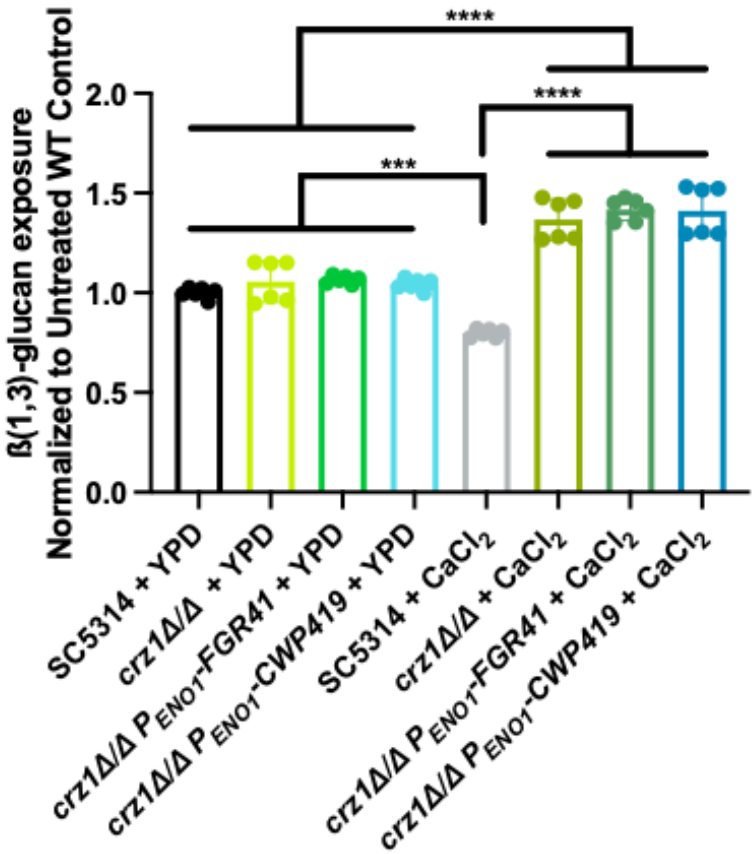
1 Wagner, A. S. *et al.* Activation of Cph1 causes ss(1,3)-glucan unmasking in Candida albicans and attenuates virulence in mice in a neutrophil-dependent manner. *PLoS Pathog* **17**, e1009839, doi:10.1371/journal.ppat.1009839 (2021).



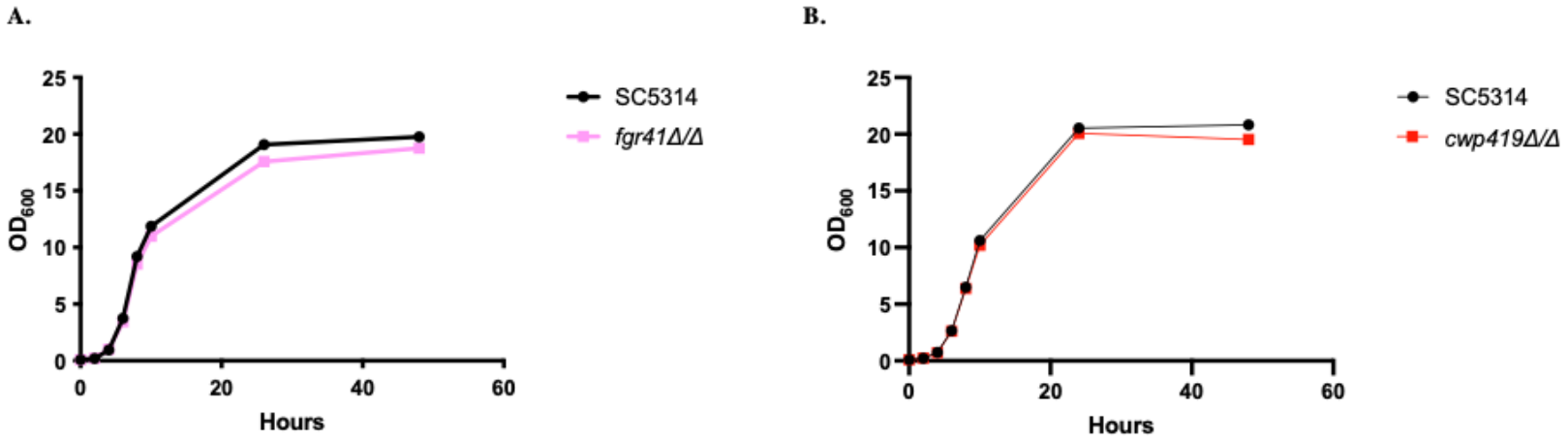
S3.1 Fig: Gating strategy for yeast cell population of *C. albicans*.



S3.2 Fig: Loss of FGR41 induces changes in total chitin and mannan levels in C. albicans.
(A-C) Overnight cultures of cells were stained with calcofluor white (CFW), fluorescein conjugated wheat germ agglutinin (WGA) and concanavalin A (ConA) to measure total chitin, exposed chitin and mannan levels in the cell wall, respectively. 4 biological replicates were stained for each sample. (A) CFW staining, (B) WGA staining and (C) ConA staining. (****p<0.0001, by one-way ANOVA).



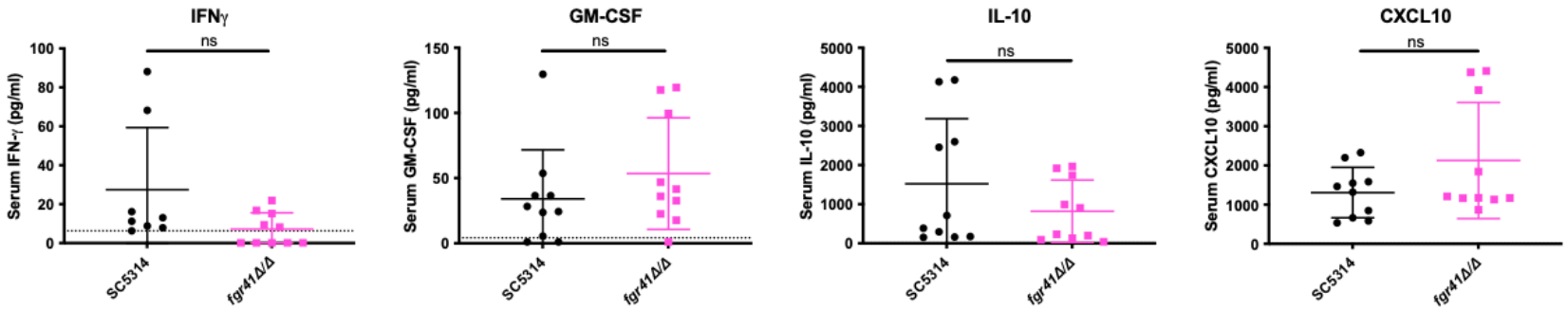
S3.3 Fig: Overexpression of calcineurin effector genes does not restore calcium-induced masking in a *crz1Δ/Δ* mutant.
Cells were grown overnight in the absence or presence of 50mM $CaCl_2$ in YPD broth. Cells were stained with an anti-ß(1,3)-glucan antibody and a phycoerythrin-conjugated secondary antibody followed by flow cytometry to assess the levels of ß(1,3)-glucan exposure. 3 biological replicates with 1 technical replicate for each were assessed for each strain. (***p<0.001, ****p<0.0001, by one-way ANOVA).



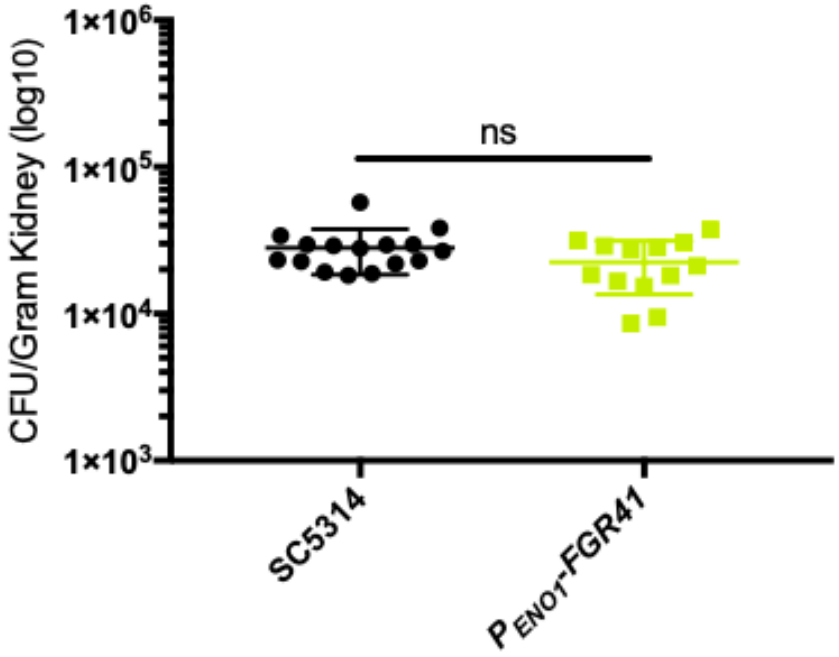
C.

	Generation Time
SC5314	85.65 ± 2.51
fgr41Δ/Δ	84.65 ± 1.51
cwp419Δ/Δ	87.45 ± 1.17

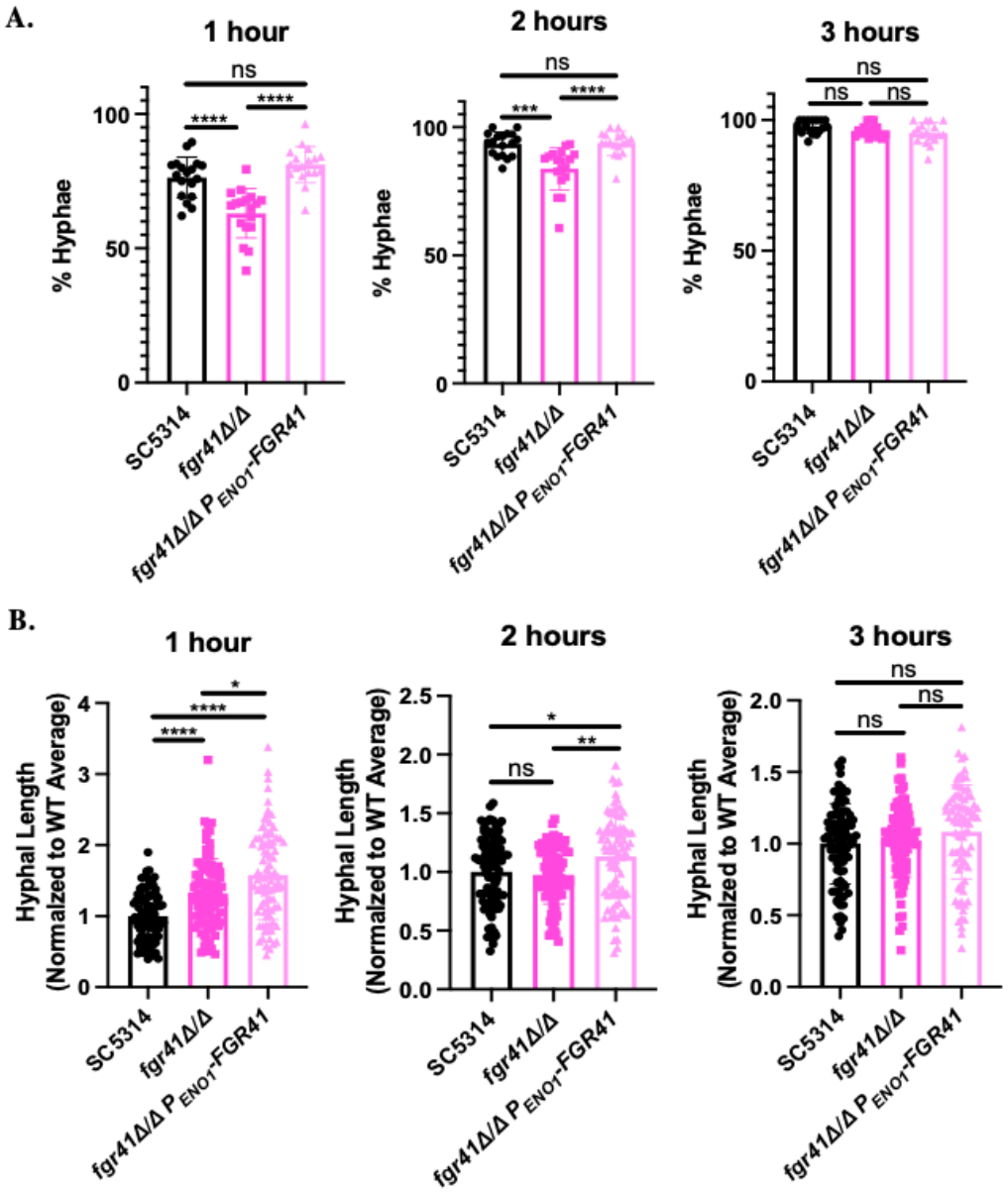
S3.4 Fig: Loss of *FGR41* or *CWP419* does not attenuate fungal growth *in vitro*.
Overnight cultures of cells were diluted to an OD_{600} of 0.1 into 5ml of fresh YPD media and left to grow with shaking at 225rpm at 30°C for 48 hours. Cell density was measured every 2 hours for the first 10 hours by measuring OD_{600} and at 24 and 48 hours as well. All samples were run using 3 biological replicates for each strain. (A) *fgr41Δ/Δ* mutant growth curve in YPD. (B) *cwp419Δ/Δ* mutant growth curve in YPD. (C) Generations time for each strain during exponential growth phase.



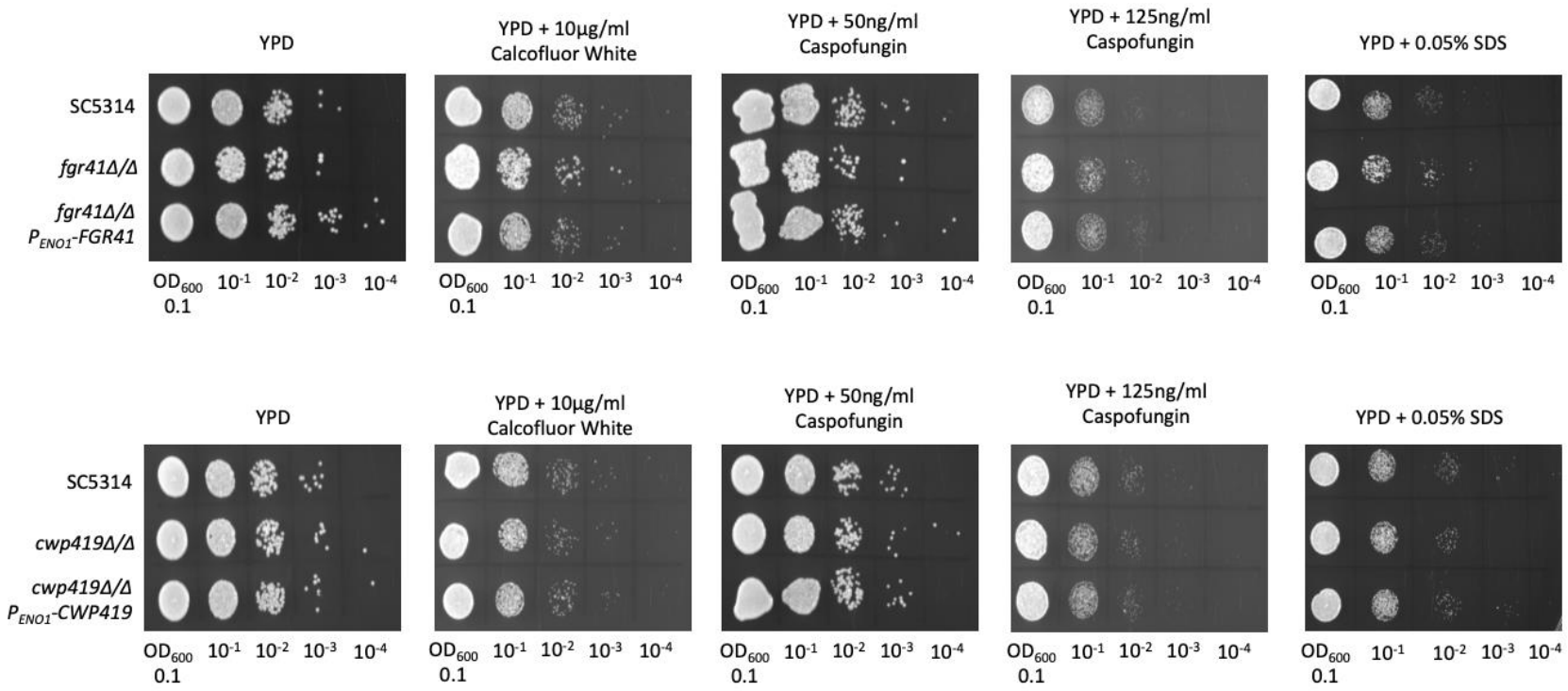
S3.5 Fig: Characterization of serum cytokines during systemic infection with an *fgr41Δ/Δ* mutant.
ICR mice were intravenously infected with $1x10^6$ cells of *C. albicans* wild-type (SC5314) or the *fgr41Δ/Δ* mutant. Serum was then collected 4 d.p.i. and cytokines were measured via flow cytometry using the LEGENDplex cytokine bead-based array kit to measure circulatory cytokine levels. (n=5 mice) (ns = not significant, by Mann-Whitney test).



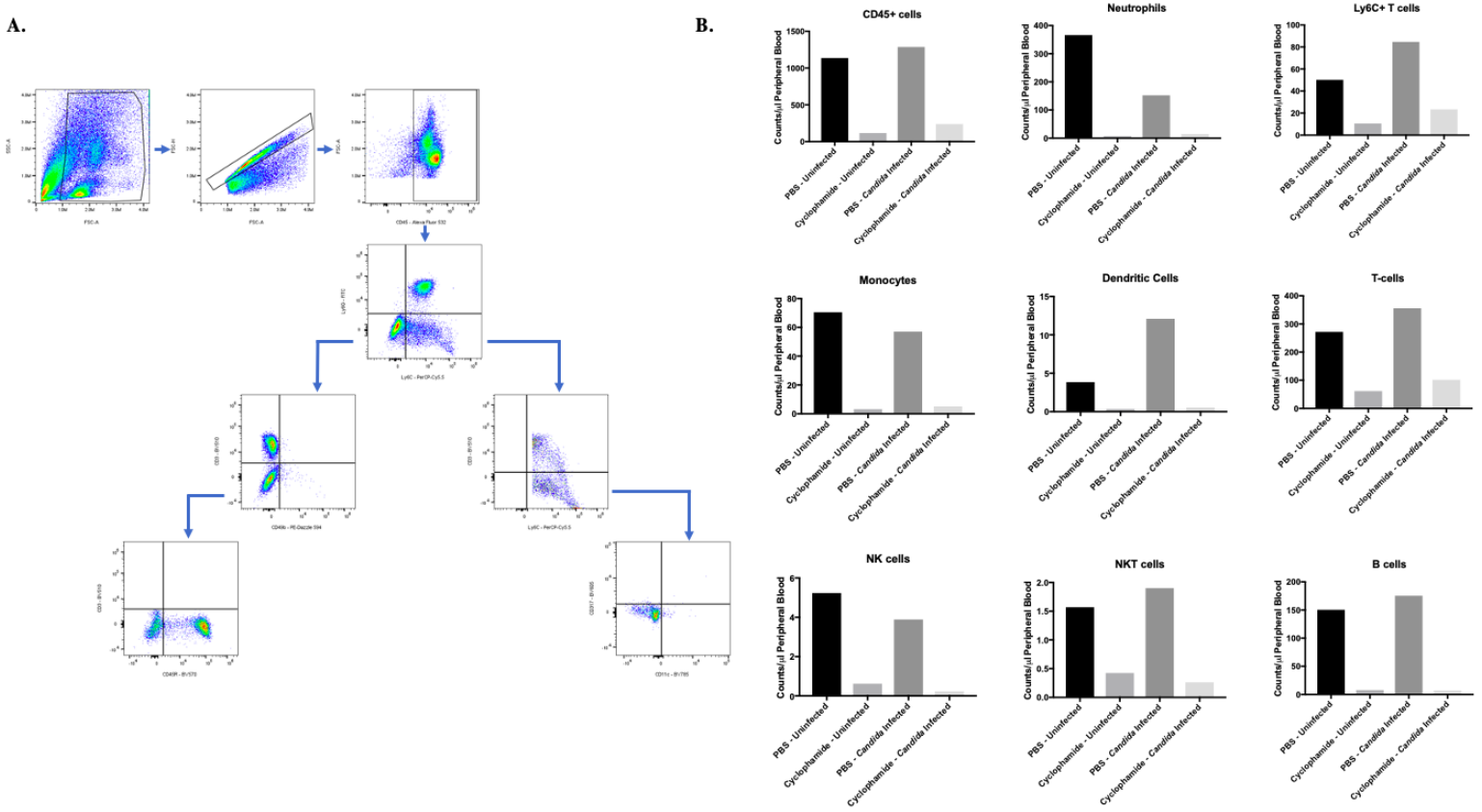
S3.6 Fig: *FGR41* overexpression does not impact fungal burden 4 days post infection.
ICR mice were intravenously infected with $1x10^6$ cells of *C. albicans* wild-type (SC5314) or the P_{ENO1}-*FGR41* overexpression strain, and kidneys were subsequently harvested 4 days post infection (d.p.i.) to assess fungal burden. (n=7-8 mice per strain)(ns = not significant, by Mann-Whitney test).



S3.7 Fig: Loss of *FGR41* modestly delays hyphal development *in vitro*.
(A & B) To assess germination frequency and hyphal length, overnight cultures were diluted to an OD_{600} of 0.1 in EBSS + 2% fetal bovine serum and allowed to grow for three hours at 37°C at 5% CO_2. (A) Samples were measured at each hour to assess germination frequency (n=3 biological replicates for each strain, with all cells (25-50) counted within 6 separate fields of view for each replicate at all time points sampled). (B) Germinated hyphae were then measured to assess hyphal length. (n=3 biological replicates with 3 technical replicates for each strain. For each strain, three separate images were taken and 10 hyphal cells for each image were measured using Image J, making an n=90 for each time point measured). (*p<0.05, **p<0.01, ***p<0.0005, ****p<0.0001 and ns = not significant, via either a one-way ANOVA with Tukey's multiple comparisons post-hoc analysis or a Kruskal-Wallis test with Dunn's multiple comparisons post-hoc analysis).



S3.8 Fig: Loss of *FGR41* or *CWP419* does not impact susceptibility to cell wall stressors.
Sensitivity phenotypes of the wild-type, *fgr41Δ/Δ* , *cwp419Δ/Δ* and their respective reintegrant controls to 10µg/ml calcofluor white, 50ng/ml and 125ng/ml caspofungin and 0.05% SDS were assessed via a spot dilution assay. (A) Representative images of the growth of the *FGR41* mutants. (B) Representative images of the growth of the *CWP419* mutants.



S3.9 Fig: Cyclophosphamide treatment globally diminishes immune cells at early timepoints.
(A) Representative gating strategy used to identify immune cell populations. Leukocytes were stained with antibodies against CD45, Ly6G, Ly6C, CD11b, CD3, CD49b, B220/CD45R, CD317/mPDCA-1, and CD11c. (B) Quantification of respective immune cells in peripheral blood. Mice were treated with either PBS (control) or two recurring injections of 150mg/kg of Cyclophosphamide (Cyclo) (at 4 days prior to infection and 1 day prior to infection). Mice were then further separated into infected (intravenously injected with $1x10^4$ of SC5314 *C. albicans* cells) or PBS mock infected control groups and serum was collected 5 hours post infection to assess circulatory leukocyte levels. Immune cells were stratified based on marker expression and cells/µL are shown for each type. CD45+ represents total leukocyte levels. Other cell types examined include neutrophils (Ly6G+/Ly6C+), monocytes (Ly6C+/Ly6G-/CD3-/CD11c-), Dendritic cells (Ly6C+/Ly6G-/CD11c+), NK cells (Ly6G-/Ly6C-/CD3-/CD49b+), NK T cells (Ly6c-/Ly6G-/CD3+/CD49b+), T cells (Ly6G-/Ly6C-/CD3+/CD49b-), Ly6C+ T cells (Ly6G-/Ly6C+/CD3+), and B cells (Ly6G-/Ly6C-/CD45R+). (n=1 mouse per treatment).

CHAPTER 4 - CHITIN LEVELS IMPACT CASPOFUNGIN-INDUCED ß(1,3)-GLUCAN UNMASKING IN *CANDIDA ALBICANS*

This work was performed by: Andrew S. Wagner, Stephen W. Lumsdaine, and Todd B. Reynolds

Author Contributions: Conceptualization, ASW and TBR.; Methodology, ASW and SWL; Formal analysis, ASW; Investigation, ASW and SWL (*CHS3-GFP* mutant construction and Chs3-GFP microscopy); Writing–original draft preparation, ASW; Writing–review and editing, ASW and TBR; Visualization, ASW; Funding Acquisition, TBR

Abstract

Immune system evasion is an important virulence factor utilized by fungal pathogens to induce disease. One way that the fungal pathogen *Candida albicans* achieves this is by masking immunogenic ß(1,3)-glucan epitopes within its cell wall under an outer layer of mannosylated proteins. Consequently, inducing ß(1,3)-glucan exposure (in a process termed unmasking) via genetic and chemical manipulation has been shown to increase fungal recognition by host immune cells *in vitro* and attenuate disease progression during systemic infection in mice. Treatment with the echinocandin caspofungin is one of the most potent drivers for ß(1,3)-glucan exposure, and several reports using murine infection models suggest a role for an intact immune system, and specifically host ß(1,3)-glucan receptors, in mediating the efficacy of echinocandin treatment *in vivo*. Thus, an understanding for how caspofungin induces unmasking within the fungal cell wall is needed. We have previously shown that pharmacological inhibition of calcineurin partially blocks caspofungin-induced unmasking in *C. albicans*. In this report, we show that both the calcineurin and Mkc1 MAPK pathways work synergistically to regulate ß(1,3)-glucan exposure and chitin synthesis in response to caspofungin. We also show that foci of unmasking co-localize with areas of increased chitin within the cell wall in response to caspofungin, and that bimodal populations of cells expressing low and high levels of chitin are present when either of these pathways are interrupted. Importantly, we show a strong and persistent correlation between chitin levels and unmasking, where cells containing higher chitin content consistently display increased ß(1,3)-glucan exposure. Collectively,

our work presents a model in which chitin synthesis induces unmasking within the cell wall in response to caspofungin.

Introduction

The fungal cell wall is a dynamic structure that sits at the interface between pathogen and host. In *Candida albicans*, the cell wall consists of three major layers; a basal chitin layer, followed by a central layer of ß(1,3) and ß(1,6)-glucan moieties and an outer layer of mannosylated glycoproteins [1, 2]. Given the direct exposure of these outer epitopes to the surrounding host environment, multiple pattern recognition receptors (PRRs) are expressed within various host cell types to detect and appropriately respond to invading fungal pathogens. For example, mannoproteins in the outer cell wall can be recognized by at least six different host PRRs, including the c-type lectin receptor dectin-2 [3, 4], galectin-3 [5-7], mannose receptor [8, 9], dendritic cell-specific intracellular adhesion molecule-3-grabbing non-integrin (DC-SIGN) [9], and the toll-like receptors TLR2 [10] and TLR4 [8]. Exposed ß(1,3)-glucan is capable of being recognized by three different receptors expressed on both hematopoietic and non-hematopoietic cell lines, including dectin-1[11-16], complement receptor 3 (CR3) [17, 18] and the ephrin type A receptor 2 (EphA2) [19, 20]. Chitin recognition is thus far poorly understood, but evidence suggests that the intracellular receptors TLR2 and NOD2 can recognize this cell wall epitope as well, and the extracellular epithelial cell receptor LYSMD3 was recently reported to recognize chitin [21, 22].

Amongst the cell wall components, ß(1,3)-glucan is highly pro-inflammatory, and its exposure has been found to attenuate disease progression. Given this observation, inappropriately exposing ß(1,3)-glucan moieties (in a process termed unmasking) has begun to gain attention as a potential immunotherapeutic strategy [23-25]. Accordingly, multiple exogenous stimuli and genetic mutations have been identified that impact the unmasking state of the cell. For example, exposure to exogenous lactate, calcium, hypoxia or iron-limitation all reduce ß(1,3)-glucan exposure (masking) [24, 26-29], while growth in acidic pH or in the presence of the short chain fatty acids acetate and butyrate all induce unmasking [28, 30, 31]. Deletion of the phosphatidylserine synthase *CHO1* [32, 33], the

glycosyltransferase *KRE5* [34], the endoglucanase *ENG1* [35] or the outer cell wall protein *FGR41* [29] all induce unmasking as well and attenuate systemic disease progression. Similarly, hyperactivation of the Cek1 mitogen activated protein kinase (MAPK) pathway also increases ß-glucan exposure and attenuates virulence in a host immune system dependent manner [36-38]. Yet, amongst all stimuli, exposure to the echinocandin caspofungin has been found to be one of the most potent drivers of unmasking [39-41]. However, little is known about how ß-glucan exposure occurs during caspofungin treatment, or of the impact that this may have on drug efficacy.

Echinocandins function by inhibiting the ß(1,3)-glucan synthase enzymes Fks1 and Fks2, and are largely thought to function in a fungicidal manner against *C. albicans* [42]. However, evidence in mice suggests that the full mechanism of action for these drugs during treatment is also dependent on a functional host immune response. For example, when comparing anidulafungin efficacy in immunocompetent and neutropenic mice systemically infected with *C. albicans,* the survival rate was found to be much lower in the immunosuppressed mice, regardless of the dosage of anidulafungin treatment [43]. Furthermore, the ability of caspofungin to reduce kidney fungal burden following systemic *C. albicans* infection in immunocompetent and dectin-$1^{-/-}$ mice also showed a reliance on this ß(1,3)-glucan receptor for proper drug-mediated clearance [44]. These host-dependent mechanisms of action during *in vivo* drug treatment are presumably the consequence of increased unmasking induced by these drugs. Therefore, understanding how caspofungin induces unmasking is not only clinically relevant, but also allows for a better understanding of how ß-glucan exposure is regulated by *C. albicans* in response to exogenous stimuli.

Treatment with caspofungin activates at least four signal transduction pathways; the Cek1, Mkc1 and Hog1 MAPK pathways, as well the calcineurin pathway [45-48]. In addition to unmasking, increased chitin synthesis is induced as a compensatory mechanism to counteract inhibition of the ß(1,3)-glucan synthases and provide structural support to the cell [48-50]. Higher basal chitin content has even been shown to reduce caspofungin sensitivity [51-53]. Presumably, both of these cell wall changes are mediated by one or more of these signaling pathways. However, delineation of signal transduction pathways that mediate unmasking specifically and the relationship that increased ß-glucan exposure

has with chitin content remains unknown. We have previously shown that calcineurin, but not the Cek1 MAPK pathway, is needed to induce the full levels of unmasking observed during caspofungin treatment [29]. In this report, we show that foci of exposed ß(1,3)-glucan frequently co-localize with areas of increased chitin deposition during capsofungin exposure, and that the calcineurin and Mkc1 signal transduction pathways play an important role in regulating both unmasking and chitin synthesis. Furthermore, we show that a bimodal population of high and low chitin containing cells is observed during caspofungin treatment in calcineurin-inhibited and *mkc1Δ/Δ* cells, and that the chitin content in the cell wall directly correlates with the levels of ß-glucan exposure following drug treatment. Finally, we find that this strongly correlates with chitin synthase 3 (Chs3) levels within the cell and suggest that chitin serves as a basal driver to induce unmasking in response to caspofungin.

Results

Foci of increased chitin deposition co-localize with unmasked ß(1,3)-glucan during caspofungin exposure.

The mechanism by which caspofungin-induced unmasking occurs is currently unknown. However, in addition to the observation that exposure of yeast cells to sublethal concentrations of caspofungin induces unmasking [39-41], increases in total chitin have also been observed in response to drug treatment [48-50]. In agreement with this, flow cytometry revealed that there is an increase in total chitin content during caspofungin addition at the same sublethal concentration (46.9 ng/ml) that induces unmasking (Fig. 4.1A-B and S4.1 Fig.). We hypothesized that foci of unmasked ß(1,3)-glucan would co-localize with areas of increased chitin deposition within the cell wall. To address this, yeast cells were grown to mid-log phase, treated with 46.9 ng/ml of caspofungin ($3/8^{th}$ of the minimum inhibitory concentration (MIC) of our strain) for 30 minutes and ß(1,3)-glucan exposure and total chitin content were assessed via simultaneous staining with an anti-ß(1,3)-glucan antibody and calcofluor white, respectively. Microscopy analysis revealed a scattered distribution of unmasked ß(1,3)-glucan foci throughout the cell wall of yeast

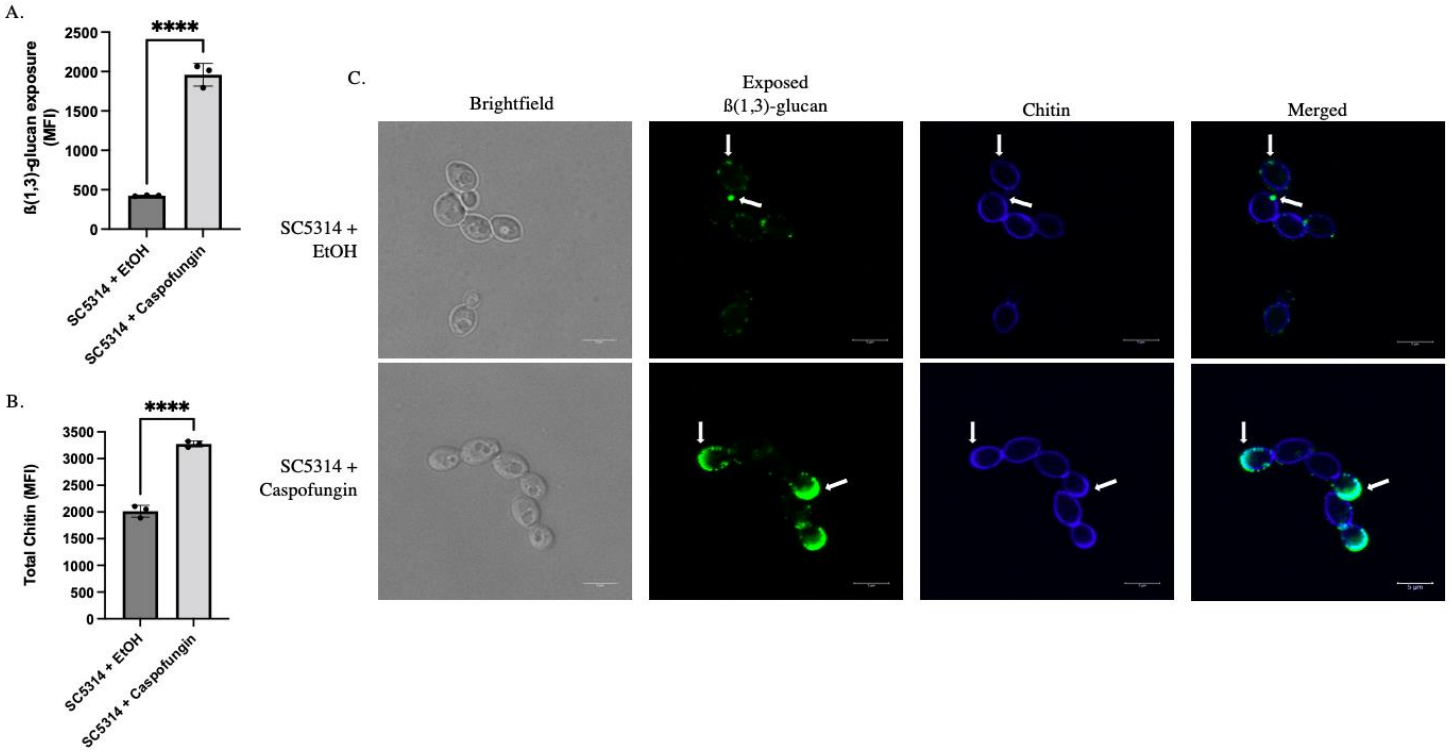


Fig 4.1: Areas of increased chitin co-localize with unmasked foci in response to caspofungin.
(A-B) SC5314 wild-type cells grown to mid-log phase were exposed to 46.9ng/ml of caspofungin for 30 minutes and then stained with anti-ß(1,3)-glucan antibody and a phycoerythrin-conjugated secondary antibody, or calcofluor white (CFW) to assess the levels of ß(1,3)-glucan exposure and total chitin by flow cytometry, respectively. (A) ß(1,3)-glucan unmasking in SC5314 wild-type cells treated with sublethal concentrations of caspofungin. (B) CFW staining of SC5314 wild-type cells treated with sublethal concentrations of caspofungin. (****$p<0.0001$, by student's t-test)($n = 3$ biological replicates). (C) Representative confocal microscopy of mid-log phase grown cells treated with an ethanol solvent control or caspofungin. White arrows highlight example areas of unmasking across images. (Scale bar indicates 5μm).

treated with an ethanol solvent control, that had minimal overlap with areas of dense chitin content (Fig. 4.1C). However, yeast cells that were exposed to caspofungin showed a robust increase in unmasking at the tip of budding daughter cells. Correspondingly, this co-localized with areas of increased chitin deposition at these poles. Thus, it appears that areas of increased unmasking strongly co-localize with increased chitin deposition within the cell wall during caspofungin treatment, and may therefore represent a mechanism by which the cell wall is perturbed to increase ß-glucan exposure.

Calcineurin mediates chitin synthesis and unmasking in response to caspofungin treatment.

We have previously shown that calcineurin is responsible, in part, for the unmasking observed during caspofungin treatment [29]. Additionally, calcineurin has also been implicated as a major regulator of chitin synthesis in response to caspofungin addition [48]. Given the observation that areas of unmasking co-localize with pockets of increased chitin deposition in response to caspofungin (Fig. 4.1), we hypothesized that calcineurin induces unmasking during caspofungin exposure by altering the chitin content within the yeast cell wall. To test this, we pharmacologically inhibited calcineurin via cyclosporine A [54, 55] prior to exposure to caspofungin, and subsequently assessed ß(1,3)-glucan unmasking and chitin levels via flow cytometry. In accordance with our previous observations [29], calcineurin inhibition prior to caspofungin exposure significantly reduced the observed unmasking (Fig. 4.2A-B). Similarly, total chitin content was reduced during calcineurin inhibition (Fig. 4.2C) and followed a trend that strongly resembled that seen when assessing unmasking in these same conditions (Fig. 4.2A). However, population assessment of cells treated with cyclosporine A and caspofungin showed an interesting bimodal distribution during assessment of total chitin levels (Fig. 4.2D). This trend was absent when assessing population dynamics for unmasking (Fig. 4.2B), and thus warranted further assessment.

Calcineurin inhibition during caspofungin exposure generates a bimodal distribution in the population, where one population appears to have caspofungin-like levels of chitin, while the other appears to have wild-type levels of chitin (Fig. 4.2D).

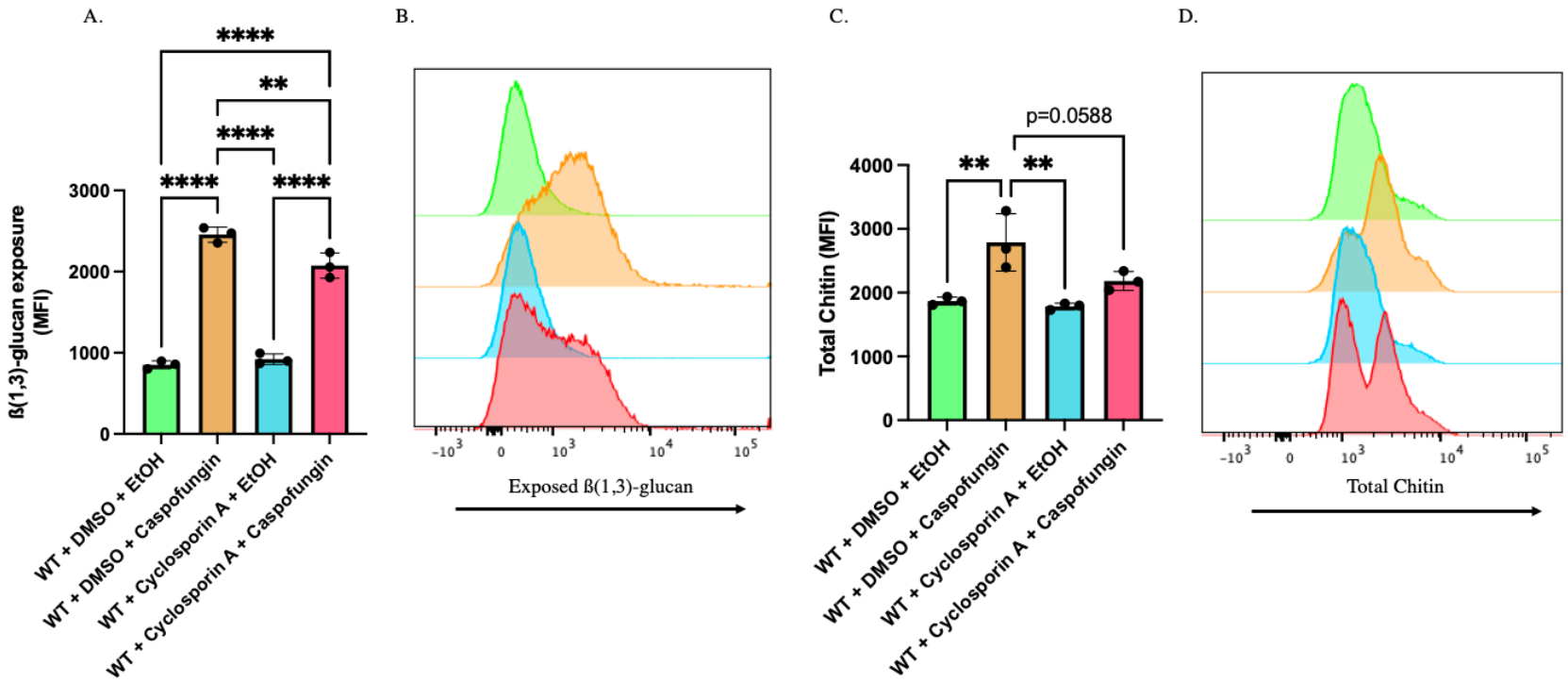


Fig 4.2: Calcineurin inhibition attenuates both unmasking and chitin synthesis in response to caspofungin exposure.
SC5314 wild-type cells grown to mid-log phase in the presence of 100µg/ml of cyclosporine A, or an appropriate volume of the DMSO solvent control, were exposed to 46.9ng/ml of caspofungin for 30 minutes. ß(1,3)-glucan exposure and total chitin levels were then assessed by flow cytometry. (A) ß(1,3)-glucan exposure of cyclosporine A (calcineurin-inhibited) and caspofungin treated cells. (**p<0.01, ****p<0.0001)(n = 3 biological replicates). (B) Representative histogram of the impact that calcineurin inhibition has on caspofungin-induced unmasking. Colors of each sample match those shown in 2A. (C) CFW staining of cyclosporine A (calcineurin-inhibited) and caspofungin treated cells. (**p<0.01)(n = 3 biological replicates). (D) Representative histogram of the impact that calcinuerin inhibition has on caspofungin-induced chitin synthesis. Colors of each sample match those shown in 2C.

Further gating (Fig. 4.3A) revealed an approximate 50/50 split in cells expressing either high (caspofungin-like) or low (wild-type-like) chitin content during simultaneous cyclosporine A and caspofungin treatment (Fig. 4.3B). Interestingly, when assessing the unmasking levels in cells within the high and low chitin populations, we observed a strong correlation in unmasking in cells that have higher chitin content when compared to the low chitin population (Fig. 4.3C). Quantification of unmasking within these two populations revealed a significant increase in ß(1,3)-glucan exposure in the high chitin population, which corresponded to a 3.85-fold increase in unmasking (Fig. 4.3D). Thus, it appears that calcineurin mediates both unmasking and chitin deposition in response to caspofungin exposure, and that ß(1,3)-glucan unmasking strongly correlates with total chitin content within the cell.

Altered viability does not correlate with chitin levels in calcineurin-inhibited cells treated with caspofungin.

The observation that cells simultaneously treated with cyclosporine A and caspofungin have altered chitin content that correlates with ß-glucan exposure strongly implicates chitin as a potential driver of caspofungin-induced unmasking. However, calcineurin is a very pleiotropic signal transduction hub [56], and it is possible that the low-chitin population may simply represent dead cells that are unable to respond to caspofungin and appropriately alter their cell wall. Loss of viability would therefore make it difficult to discern if chitin levels truly impact unmasking. To assess this, cells were grown to mid-log phase in the presence or absence of cyclosporine A prior to treatment with caspofungin or an ethanol solvent control and were assessed for viability via a spot dilution assay onto YPD. Subsequent analysis did not show any difference in growth following drug treatment (S4.2 Fig.), and therefore suggests that all cells are viable within the experimental groups. However, we wished to further confirm this by staining cells simultaneously with calcofluor white and propidium iodide (P.I.) to assess if there are changes in P.I. staining between the high and low chitin groups seen in cyclosporine A and caspofungin treated cells. Propidium iodide is a marker for cell stress [57], and cells that were treated with both cyclosporine A and caspofungin had significantly higher levels of P.I. staining than cells

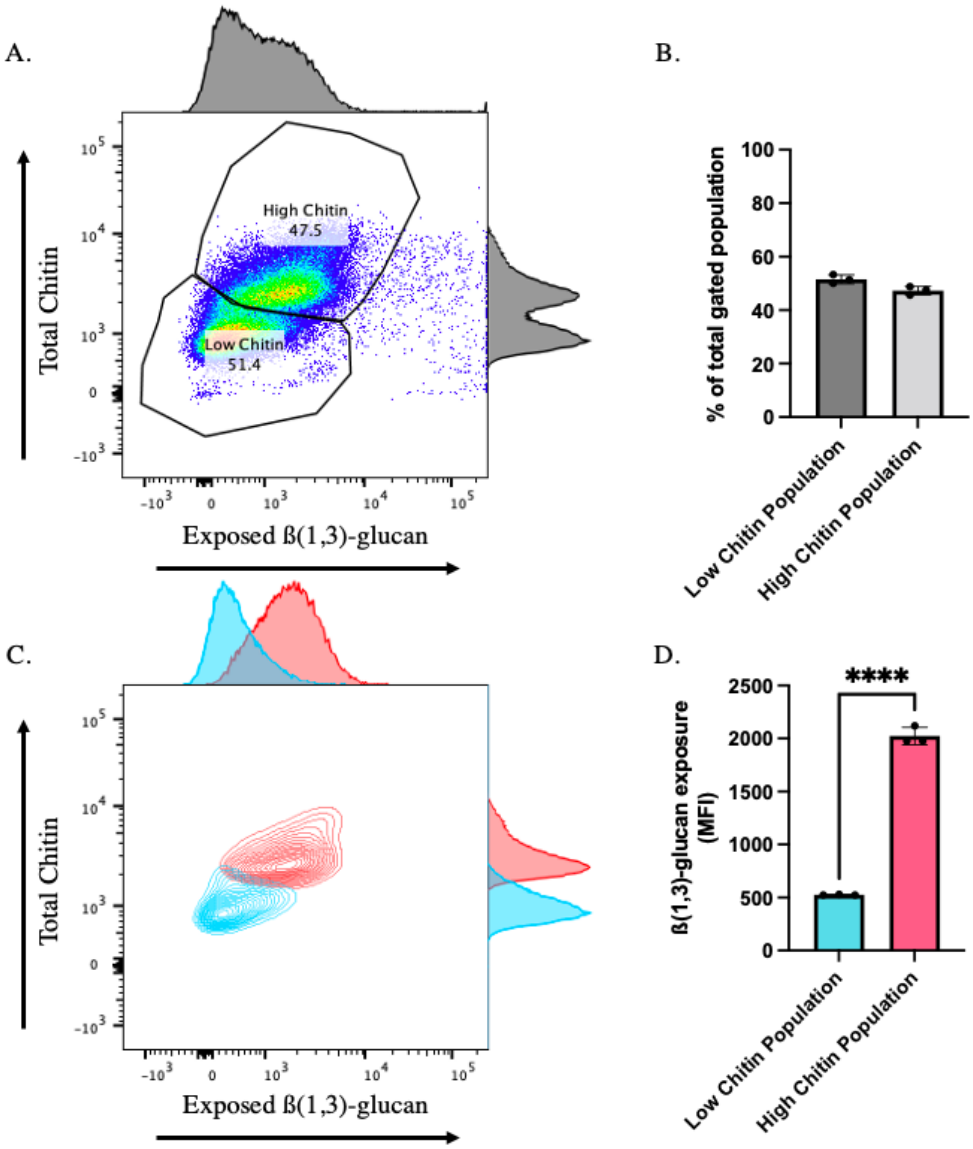


Fig 4.3: Chitin levels correlate with ß(1,3)-glucan exposure following caspofungin treatment in calcineurin-inhibited cells.

SC5314 wild-type cells grown to mid-log phase in the presence of 100µg/ml of cyclosporine A, or an appropriate volume of the DMSO solvent control, were exposed to 46.9ng/ml of caspofungin for 30 minutes, and ß(1,3)-glucan exposure and total chitin levels were assessed by flow cytometry. (A) Representative scatter plot and adjunct histograms of cyclosporine A and caspofungin-treated cells when assessing unmasking and total chitin. Gates represent populations of high and low chitin within the sample. (B) Percent of the total population within low and high chitin gates for cyclosporine A and caspofungin-treated samples. (n = 3 biological replicates). (C) Representative scatter plot with adjunct histograms for CFW staining and exposed ß(1,3)-glucan when plotting low (blue) and high (red) chitin populations independently. (D) ß(1,3)-glucan unmasking of cells within the low and high chitin populations following caspofungin addition to cyclosporine A-treated cells. (****p<0.0001, by student's t-test)(n = 3 biological replicates).

treated with caspofungin alone (S4.3A-B Fig.). However, when gating for high and low chitin content within the population of cyclosporine A and caspofungin treated cells, no clear separation between the two populations was observed when assessing P.I. staining (S4.3C-D Fig.). Therefore, it does not appear that changes in cell stress or viability account for the altered chitin content in cyclosporine A and caspofungin treated cells.

Loss of Mkc1 attenuates caspofungin-induced unmasking and chitin synthesis within the yeast cell wall.

We have thus far shown a role for calcineurin in mediating caspofungin-induced unmasking and chitin deposition within yeast cells (Figs. 4.1&4.2). However, loss of calcineurin only diminishes the unmasking by ~20%, suggesting that additional mechanisms for driving this process remain unknown. In addition to calcineurin, the MAPK Mkc1 has also been implicated as a major regulator of chitin synthesis in response to caspofungin exposure [48]. Furthermore, caspofungin-mediated crosstalk between both calcineurin and Mkc1 has recently been observed [49]. We were therefore curious if calcineurin is interacting with Mkc1 to regulate changes in chitin levels in response to drug treatment, or if it perhaps works independently of calcineurin to also mediate this phenotype. To assess this, we generated a *mkc1Δ/Δ* mutant and assessed the impact that loss of this MAPK had on caspofungin-induced unmasking and chitin synthesis. Similar to what was observed during calcineurin inhibition (Fig. 4.1), *mkc1Δ/Δ* cells showed significant reductions in both unmasking (Fig. 4.4A-B) and chitin levels (Fig. 4.4C-D) after caspofungin exposure. Similarly, assessment of *mkc1Δ/Δ* cells treated with caspofungin showed the same bimodal distribution in chitin staining (Fig. 4.4D) that was observed in cyclosporine A and caspofungin treated cells (Fig. 4.1D). Gating on the two chitin populations in *mkc1Δ/Δ*-caspofungin treated cells (Fig. 4.4E) revealed a similar ~50/50 split in the population between these two groups (Fig. 4F), and further assessment again revealed a strong and significant trend in unmasking levels between high and low chitin populations within these samples (Fig. 4.4G-H). The observed difference between the high and low chitin populations corresponded to a 3.10-fold difference in unmasking between them (Fig. 4.4H). Collectively, this implicates Mkc1 as a regulator of chitin synthesis and

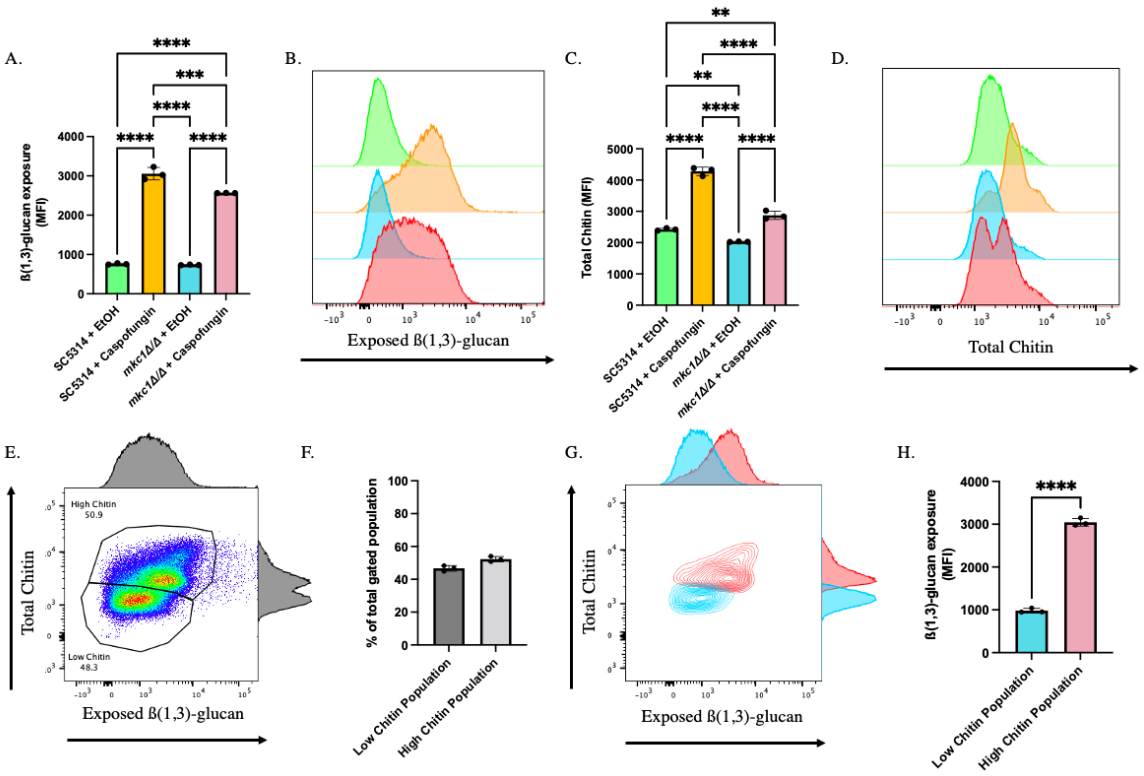


Fig 4.4: Loss of *MKC1* attenuates caspofungin-driven unmasking and chitin synthesis.
(A-D) *mkc1Δ/Δ* cells grown to mid-log phase were exposed to 46.9ng/ml of caspofungin for 30 minutes, and ß(1,3)-glucan exposure and total chitin levels were assessed by flow cytometry. (A) ß(1,3)-glucan unmasking of *mkc1Δ/Δ* cells treated with sublethal concentrations of caspofungin. (***p<0.0005, ****p<0.0001, by one-way ANOVA)(n = 3 biological replicates). (B) Representative histogram of the impact that loss of *MKC1* has on caspofungin-induced unmasking. Colors of each sample match those shown in 4A. (C) CFW staining of SC5314 wild-type cells treated with sublethal concentrations of caspofungin. (**p<0.01, ****p<0.0001, by one-way ANOVA)(n = 3 biological replicates). (D) Representative histogram of the impact that loss of *MKC1* has on caspofungin-induced chitin synthesis. Colors of each sample match those shown in 4C. (E) Representative scatter plot and adjunct histograms for CFW staining and exposed ß(1,3)-glucan of *mkc1Δ/Δ* cells treated with caspofungin. Gates represent populations of high and low chitin within the sample. (F) Percent of the total population within low and high chitin gates for *mkc1Δ/Δ* cells treated with caspofungin. (n = 3 biological replicates). (G) Representative scatter plot with adjunct histograms for CFW staining and exposed ß(1,3)-glucan when plotting low (blue) and high (red) chitin populations independently. (H) ß(1,3)-glucan unmasking of cells within the low and high chitin populations following caspofungin addition to *mkc1Δ/Δ* cells. (****p<0.0001, by student's t-test)(n = 3 biological replicates).

unmasking during caspofungin addition, and the strong and persistent correlation between chitin levels and unmasking further connects chitin as a driver of ß(1,3)-glucan exposure.

Calcineurin and Mkc1 each contribute to caspofungin-induced chitin synthesis and unmasking.

Given the similarities in unmasking and chitin trends between calcineurin-inhibited and *mkc1Δ/Δ* cells treated with caspofungin (Figs. 4.1&4.4), we hypothesized that calcineurin induces changes in unmasking and chitin via Mkc1 activation. To assess the linearity of this pathway, we treated *mkc1Δ/Δ* cells with cyclosporine A prior to caspofungin addition and measured the levels of ß(1,3)-glucan exposure and chitin within the cell wall via flow cytometry. If calcineurin was inducing unmasking via Mkc1, inhibition of calcineurin in a *mkc1Δ/Δ* mutant should not further impact the changes observed in unmasking and chitin content following caspofungin exposure. However, if they make independent contributions, then we would expect to see an additive impact on cell wall changes following calcineurin inhibition in an *mkc1Δ/Δ* mutant. Indeed, inhibition of calcineurin in an *mkc1Δ/Δ* mutant further reduced both unmasking and chitin levels in response to caspofungin when compared to the *mkc1Δ/Δ* mutant treated with caspofungin alone (Fig. 4.5A-D). The additive impact that calcineurin inhibition had on a *mkc1Δ/Δ* mutant treated with caspofungin was apparent when assessing the population dynamics for chitin, in which ~66% of the population now showed low (wild-type-like) levels of chitin within their cell wall (Fig. 4.5E-F). However, when assessing unmasking within the high and low chitin populations of *mkc1Δ/Δ* cells treated with both cyclosporine A and caspofungin, the high chitin populations continued to show higher levels of unmasking (Fig. 4.5G-H). In further support that calcineurin does not act via Mkc1 activation, western blot analysis did not show a difference in active (phosphorylated) Mck1 levels in wild-type cells treated with caspofungin alone when compared to cells treated with both cyclosporine A and caspofungin (Fig. 4.6). Thus, although Mkc1 and calcineurin both impact chitin synthesis and unmasking in response to caspofungin exposure, they appear to work in parallel with each other to induce these changes. Yet, the persistent observation that

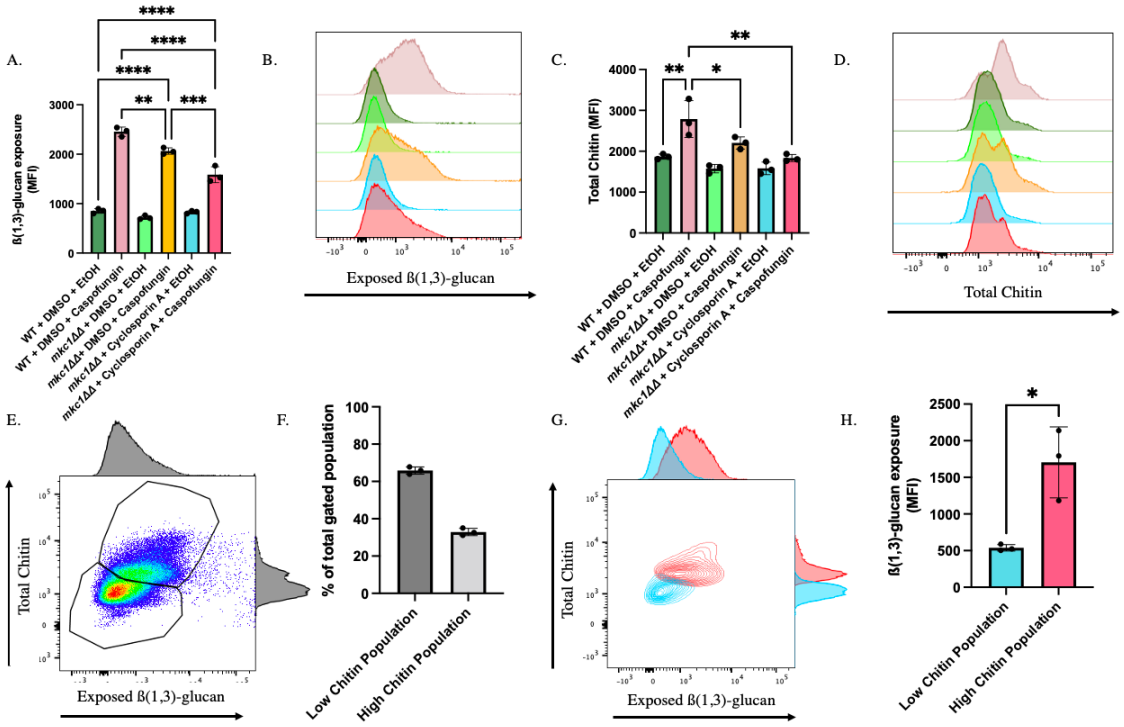


Fig 4.5: Calcineurin and Mkc1 work in parallel to mediate caspofungin-induced chitin synthesis and unmasking.

(A-D) *mkc1Δ/Δ* cells grown to mid-log phase in either the presence of 100µg/ml of cyclosporine A, or the appropriate solvent controls, were exposed to 46.9ng/ml of caspofungin for 30 minutes. ß(1,3)-glucan exposure and total chitin levels were then assessed by flow cytometry. (A) ß(1,3)-glucan exposure of *mkc1Δ/Δ* cells treated with cyclosporine A (calcineurin-inhibited) and caspofungin. (**p<0.01, ***p<0.0005, ****p<0.0001)(n = 3 biological replicates). (B) Representative histogram of the impact that calcinuerin inhibition has on caspofungin-induced unmasking in an *mkc1Δ/Δ* background. Colors of each sample match those shown in 5A. (C) CFW staining of *mkc1Δ/Δ* cells treated with cyclosporine A (calcineurin-inhibited) and caspofungin. (*p<0.05, **p<0.005, by one-way ANOVA)(n = 3 biological replicates). (D) Representative histogram of the impact that calcinuerin inhibition has on caspofungin-induced chitin synthesis in an *mkc1Δ/Δ* background. Colors of each sample match those shown in 5C. (E) Representative scatter plot and adjunct histograms for CFW staining and exposed ß(1,3)-glucan of *mkc1Δ/Δ* cells treated with cyclosporine A and caspofungin. Gates represent populations of high and low chitin within the sample. (F) Percent of the total population within low and high chitin gates for *mkc1Δ/Δ* cells treated with cyclosporine A and caspofungin. (n = 3 biological replicates). (G) Representative scatter plot with adjunct histograms for CFW staining and exposed ß(1,3)-glucan when plotting low (blue) and high (red) chitin populations independently. (H) ß(1,3)-glucan unmasking of cells within the low and high chitin populations following caspofungin exposure and cyclosporine A treatment to *mkc1Δ/Δ* cells. (*p<0.05, by student's t-test)(n = 3 biological replicates).

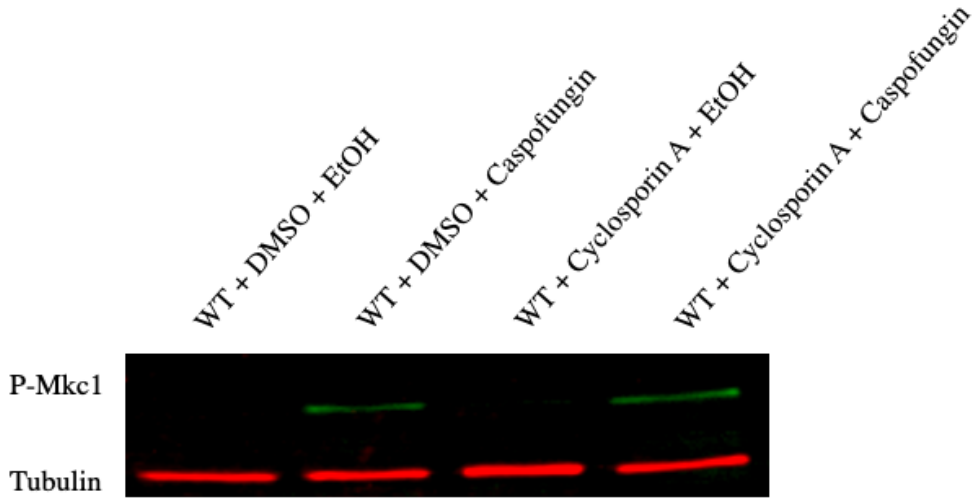


Fig 4.6: Calcineurin inhibition does not impact caspofungin-induced activation of Mkc1.
Cells were grown to mid-log phase in the presence of 100μg/ml of cyclosporine A, or an appropriate volume of the DMSO solvent control, were exposed to 46.9ng/ml of caspofungin for 30 minutes, and proteins were harvested for western blot analysis. Membranes were blotted using an anti-P44/42 antibody for phosphorylated (active) Mkc1 detection. An anti-tubulin antibody was used as a loading control.

increased chitin levels correlate with increased ß(1,3)-glucan exposure further implicates chitin as a driver for caspofungin-induced unmasking.

Chitin synthase 3 levels correlate with changes in chitin content during caspofungin exposure.

Given the observation that changes in chitin content repeatedly correlate with changes in ß(1,3)-glucan exposure, we next wanted to assess how these alterations may be occurring upon caspofungin treatment. *C. albicans* has four major chitin synthase enzymes [58] and altered expression of these genes are capable of dictating the levels of chitin within the cell wall at various stages of growth or in response to exogenous stimuli [59]. Chitin synthase 3 (Chs3) is the major chitin synthase enzyme responsible for chitin deposition within the cell wall [60, 61] and has been identified as the major chitin synthase enzyme responsible for increasing chitin content during caspofungin exposure [48]. Therefore, we hypothesized that calcineurin regulates chitin synthesis during caspofungin treatment via regulation of Chs3. To test this, we created a Chs3 mutant with a C-terminal green fluorescent protein tag (*CHS3-GFP*), and first assessed how caspofungin exposure impacts Chs3-GFP protein levels and localization. We found that wild-type cells treated with an ethanol solvent control show low levels of Chs3-GFP, but that Chs3-GFP fluorescence significantly increases upon caspofungin exposure (Fig. 4.7A). Quantification of the fluorescent intensity of the cells in these microscopy images revealed a 1.42-fold increase in fluorescence following caspofungin treatment (Fig. 4.7B). This fits well with the observation that, although Chs3 is the major chitin synthase enzyme responsible for chitin deposition, only a modest increase in its transcript and protein levels is observed following caspofungin addition [48].

To assess if calcineurin regulates Chs3 levels in response to caspofungin, we pretreated the *CHS3-GFP* mutant with cyclosporine A before caspofungin exposure. Overall, flow cytometry did not reveal a change in green fluorescence between the cyclosporine A and caspofungin treated samples when compared to caspofungin only treated cells (Fig. 4.8A&B). However, gating on the high and low chitin populations revealed a similar trend as was seen for unmasking in these same conditions (Fig. 4.8C-E).

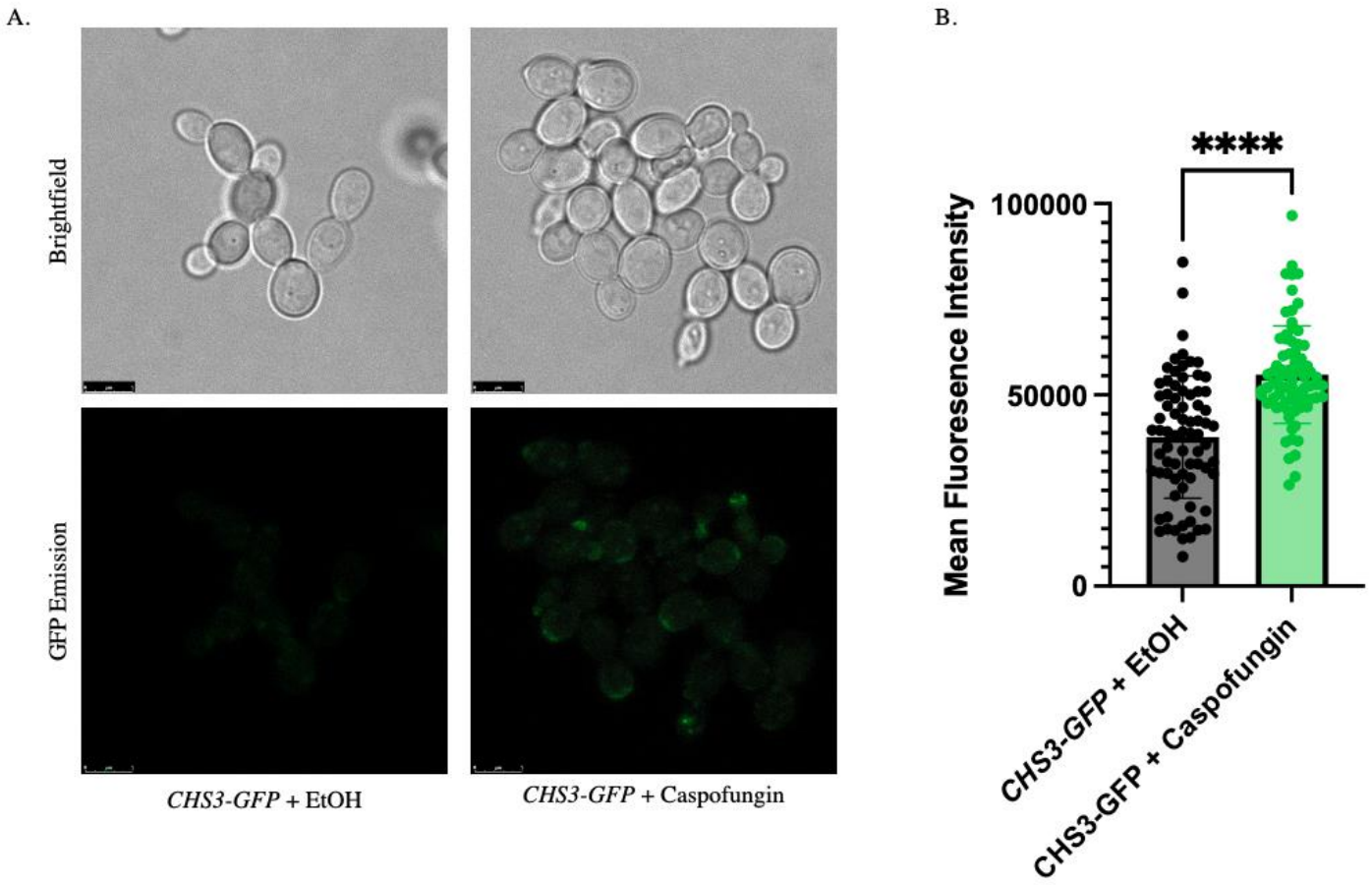


Fig 4.7: Caspfungin exposure increases Chs3 levels.
CHS3-GFP cells grown to mid-log phase were exposed to 46.9ng/ml of caspofungin for 30 minutes, and the corresponding GFP emission was assessed via microscopy. (A) Representative image of *CHS3-GFP* cells exposed to caspofungin or an ethanol solvent control. (B) Quantification of GFP emission in ethanol-treated and caspofungin-treated cells. (n=75 cells per treatment)(****$p<0.0001$, by Mann-Whitney test).

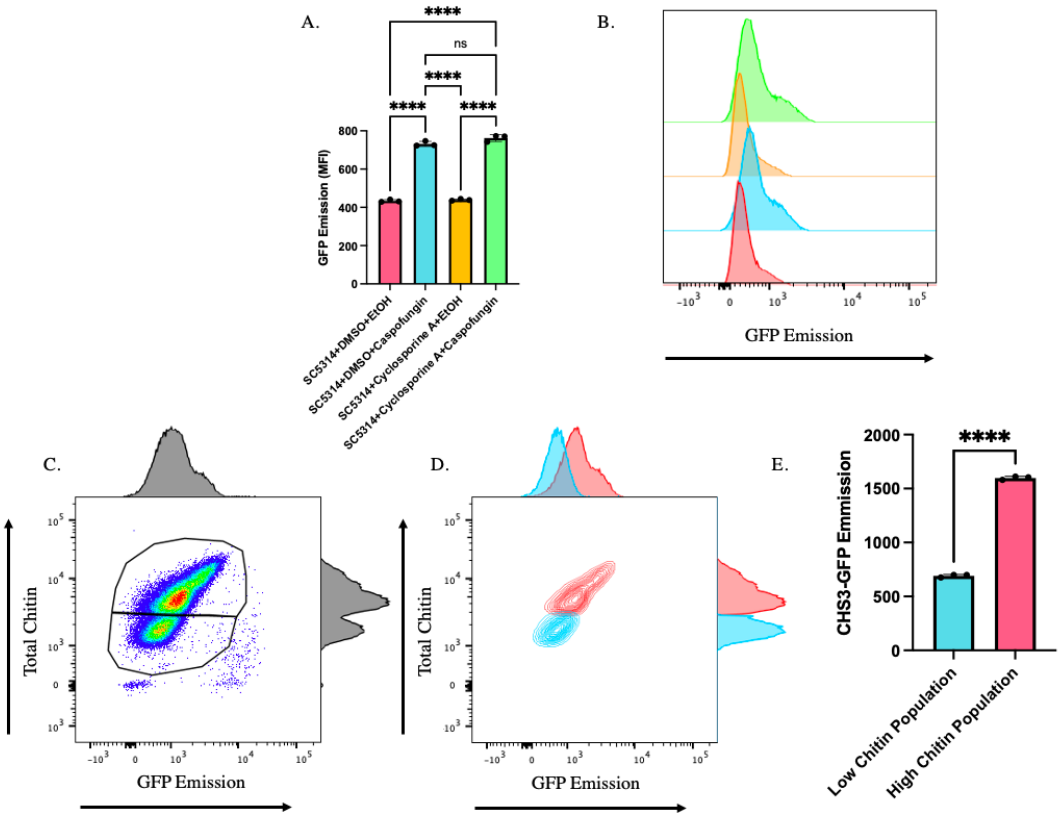


Fig 4.8: Chs3 levels correlate with total chitin content during caspofungin addition to calcineurin-inhibited cells.
(A-B) *CHS3-GFP* cells grown to mid-log phase in either the presence of 100µg/ml of cyclosporine A, or an appropriate volume of the DMSO solvent control, were exposed to 46.9ng/ml of caspofungin for 30 minutes, and GFP emission and CFW staining were assessed via flow cytometry. (A) GFP emission of *CHS3-GFP* cells treated with cyclosporine-A and caspofungin. (****p<0.0001, by one-way ANOVA)(n = 3 biological replicates). (B) Representative histogram for GFP emission of *CHS3-GFP* cells treated with cyclosporine-A and caspofungin. Colors of each sample match those shown in 8A. (C) Representative scatter plot and adjunct histograms for CFW staining and GFP emission of *CHS3-GFP* cells treated with cyclosporine A and caspofungin. Gates represent populations of high and low chitin within the sample. (D) Representative scatter plot with adjunct histograms for CFW staining and GFP emission when plotting low (blue) and high (red) chitin populations independently. (E) GFP emission of cells within the low and high chitin populations following caspofungin exposure and cyclosporine A treatment to *CHS3-GFP* cells. (****p<0.05, by student's t-test)(n = 3 biological replicates).

Specifically, high chitin populations displayed higher levels of GFP intensity, while low chitin populations had reduced GFP emission. Thus, although it does not appear that calcineurin directly regulates *CHS3-GFP* expression, our data does suggest a relationship between total chitin content, Chs3 levels and unmasking. We suspect Chs3 levels may also be mediated by Mkc1, and a compensatory role for this MAPK may be mediating Chs3 activity following calcineurin inhibition.

Caspofungin-induced unmasking relies on chemical inhibition of *FKS1*.

Our data highlight a tight relationship between total chitin content and unmasking during caspofungin exposure. However, it is unknown if unmasking is induced by direct inhibition of the ß(1,3)-glucan synthase Fks1, or if it is a secondary consequence to drug exposure. To test this, we utilized two caspofungin-resistant isolates that harbor a S645P mutation in the Fks1 protein that impairs caspofungin inhibiton of this enzyme [42]. Staining for ß(1,3)-glucan exposure and chitin revealed a baseline increase in both unmasking and total chitin within these isolates when compared to the SC5314 wild-type control (Fig. S4.4A-B). This is in agreement with studies assessing other caspofungin resistant isolates, where increased chitin is commonly observed [51-53]. However, treatment with caspofungin did not increase the unmasking in either of the resistant isolates (Fig. S4.4C), suggesting that chemical inhibition of the Fks1 protein is necessary to induce unmasking following caspofungin addition. Interestingly, although both isolates showed increased chitin content that corresponded to increases in unmasking, one of the isolates (Ca199) showed the same bimodal distribution in chitin content seen during caspofungin addition to calcineurin-inhibited or *mkc1Δ/Δ* cells (Fig. S4.4B). Further gating on these two populations again revealed a correlation between chitin content and unmasking, as the high chitin population showed a robust increase in ß(1,3)-glucan exposure when compared to the low chitin population (Fig. S4.4D-E). Collectively, this observation further supports the role that changes in basal chitin content are capable of altering ß-glucan exposure.

Discussion

We have previously shown that calcineurin inhibition attenuates caspofungin-induced unmasking in *C. albicans*. However, the mechanism by which inhibition of calcineurin impacts ß(1,3)-glucan exposure has thus far been elusive. In this report, we show that pockets of ß-glucan unmasking strongly co-localize with areas of increased chitin deposition in response to caspofungin (Fig. 4.1C). Accordingly, we find that inhibition of calcineurin via cyclosporine A also reduces calcofluor white staining following caspofungin addition (Fig. 4.2C-D). Interestingly, calcineurin-inhibited cells that were exposed to caspofungin displayed a bimodal distribution in the population when assessing total chitin content. When further gating was applied to these two populations, a clear correlation between increased chitin content and increased unmasking was observed (Fig. 4.3). Crosstalk between calcineurin and Mkc1 has recently been reported [49], and we found that deletion of *MKC1* induced similar reductions in both unmasking and total chitin content following caspofungin treatment (Fig. 4.4). Furthermore, the same bimodal distribution in chitin content that corresponded with altered ß-glucan exposure was observed. However, simultaneous inhibition of calcineurin in a *mkc1Δ/Δ* mutant further attenuated both unmasking and chitin deposition in response to caspofungin (Fig. 4.5), suggesting an additive and independent role for these pathways in inducing these changes. Finally, we find that Chs3 levels strongly correlate with chitin content in these cells (Fig. 4.8) and suggest that this likely plays a mechanistic role in mediating these cell wall changes in response to caspofungin. Our data also indicate that there may be chitin-independent contributions to unmasking. The loss of both calcineurin and Mkc1 activity results in basal levels of chitin in response to caspofungin, but unmasking of ß(1,3)-glucan is reduced by only about 50% (Figure 4.5).

Our data highlights a strong correlation between foci of exposed ß(1,3)-glucan and increased chitin deposition during caspofungin exposure. Although this is the first time that this has been empirically shown in response to caspofungin, altered chitin content and unmasking have been repeatedly observed within the fungal cell wall in response to both genetic manipulation and exogenous stressors. For example, increased chitin content in hyphae strongly corresponds to areas of unmasking induced by NETosis [62] and

unmasking in hyphal cells of clinical vaginal isolates has been found to repeatedly co-localize with areas of increased chitin [63]. Furthermore, genetic deletion of the phosphatidylserine synthase *CHO1* and expression of a hyperactive allele of the MAP3K *STE11* both display increases in basal chitin content and unmasking in standard laboratory growth conditions [32, 33, 38]. Collectively, our data and these observations support a model in which increased chitin deposition disrupts the normal fungal cell wall architecture and consequently increases ß(1,3)-glucan exposure.

This report has implicated both calcineurin and Mkc1 as drivers for inducing increased chitin synthesis and unmasking in response to caspofungin. This observation supports previous studies showing a major regulatory role for these pathways in inducing changes in chitin content during caspofungin treatment [48]. However, we have found that these pathways work independently of each other in an additive fashion (Fig. 4.5), which differs from previously published results that show crosstalk between calcineurin and Mkc1 in response to caspofungin. This previous work reported a regulatory role for calcineurin in reducing Mkc1-mediated chitin synthesis during exposure to high concentrations of caspofungin [49]. However, the drug concentrations used in those studies were ~40-times greater than the concentrations used in this study and dealt with cells experiencing the "paradoxical growth effect", in which *C. albicans* cells can grow and persist at drug treatments well above the MIC [64]. We believe that these discrepancies in assay conditions account for the differences observed in calcineurin and Mkc1 crosstalk. However, it is still entirely possible that each of these pathways play a redundant and compensatory role when one of them is perturbed, which still highlights the interconnected nature of signal transduction pathways during caspofungin treatment.

Although Mkc1 and calcineurin have both been implicated in driving chitin synthesis and unmasking in response to caspofungin, the exact mechanism through which drug-induced cell wall changes are made remains poorly understood. Microscopy revealed increased areas of chitin deposition at the poles of daughter cells that strongly co-localized with pockets of unmasking (Fig. 4.1C). Chitin is the last polymer deposited within the cell wall of budding daughter cells in *S. cerevisiae* [65, 66], and an increase in compensatory chitin deposition at these areas makes sense, as these are likely the most structurally

unstable points within budding cells. However, how these weak areas are sensed, and how chitin is directed to these foci is still unknown. Our data suggests a role for Chs3 in mediating these changes, as calcineurin-inhibited cells that displayed low levels of chitin content following caspofungin exposure showed reduced levels of Chs3 (Fig. 4.8). Yet, the transcription factors mediating the observed changes in Chs3 expression and the signals that direct precise post-translational localization of this enzyme to the membrane following caspofungin exposure remain elusive. A link between altered phosphatidylinositol 4,5 biphosphate ($PI(4,5)P_2$), an important precursor of secondary messengers, and septin localization have been observed during caspofungin treatment [67, 68]. Interestingly, these altered foci also co-localize with areas of increased chitin. In *Saccharomyces cerevisiae*, $PI(4,5)P_2$ is a regulator of Rho1 activation [69], the upstream GTPase of Mkc1 and a regulator of the Fks enzymes [70-73]. It may be possible that caspofungin exposure stimulates Mkc1 via this $PI(4,5)P_2$-Rho1 interaction in *C. albicans*, and may help direct the appropriate enzymes to mediate chitin synthesis at specific foci within the cell wall. However, further analysis on these processes is needed.

Materials and Methods

Growth media and culture conditions. *C. albicans* strains were grown in YPD media (1% yeast extract, 2% peptone, 2% dextrose)(Thermo Fisher Scientific) while shaking at 225rpm at 30°C [74]. Minimal media (0.67% yeast nitrogen base without amino acids, 2% dextrose, 2% agar)[74] (Thermo Fisher Scientific) was used to remove the genomically integrated CRISPR/Cas9 cassette and nourseothricin selectable marker following successful gene deletion [75].

Strain Construction. All *C. albicans* deletion strains (S1 Table) were generated with the use of CRISPR-Cas9 as previously described [75]. All plasmids and primers used to create each mutant can be found in S2 Table and S3 Table, respectively.

The *CHS3-GFP* mutant was generated by amplifying ~5500bp fragment of GFP-NAT from pTR198 using primers AWO146 and AWO147, which introduce 80bp of

homology to the regions immediately upstream and downstream of the *CHS3* stop codon in the genome to each side of the PCR fragment. The PCR product was gel purified with the use of the QIAquick Gel Extraction Kit (Qiagen) and the purified fragment was then transformed via electroporation into the SC5314 *C. albicans* strain as previously described [33]. Successful transformants were selected on YPD plates containing 200μg/ml nourseothricin.

Immunofluorescent staining, flow cytometry, and microscopy analysis. To quantify caspofungin-induced ß(1,3)-glucan exposure and chitin synthesis, 5ml overnight cultures of *C. albicans* strains in YPD were started the day prior to staining, and were left to grow shaking overnight at 225rpm at 30°C. The following morning, strains were back diluted to an OD_{600} of 0.1. Cells were then left to grow for 3 hours while shaking at 225rpm at 30°C. To assess the impact that pharmacological inhibition of calcineurin has on caspofungin-induced unmasking and chitin deposition, 100ug/ml of cyclosporine A or an appropriate volume of the DMSO solvent control was added to the media prior to back dilution in the morning. In either control or cyclosporine-treated samples, after 3 hours of incubation, 46.9ng/ml of caspofungin, or an appropriate volume of an ethanol solvent control, was added to each tube and strains were left to incubate while shaking at 225rpm at 30°C for an additional 30 minutes.

Following incubation, 1ml of each culture was removed to assess ß(1,3)-glucan exposure as previously described [36, 38]. For flow cytometry, a goat-anti-mouse secondary antibody conjugated to R-Phycoerythrin (Jackson Immuno Research) at a 1:300 dilution was used, while a rabbit-anti-mouse IgG secondary antibody conjugated to Alexa Fluor 488 (Jackson Immuno Research) was used at a 1:300 dilution for microscopy. To simultaneously assess total chitin levels, samples were washed one time with 500μl of PBS following incubation with the secondary antibody used for ß-glucan staining, and then were incubated with 500μl of a 10μg/ml calcofluor white solution (Fisher Scientific) in water for 5 minutes while rocking at room temperature. Samples were subsequently washed three more times. For flow cytometry, samples were then fixed for 30 minutes in 4%

formaldehyde and resuspended in 500µl of FACS buffer (1x PBS + 0.01% Sodium azide) for analysis. Samples prepared for microscopy were not fixed but were resuspended in 300µl of water prior to visualization on the confocal microscope.

To assess correlations between chitin content and membrane stress, cells were grown as described above. Following drug treatment, cells were washed once with 500µl of PBS and were then incubated in a solution consisting of 10µg/ml calcofluor white and 5µl of eBioscience propidium iodide dye (Thermo Fisher) for 5 minutes while rocking at room temperature. Following staining, cells were washed three additional times, fixed, and resuspended in 500µl of FACS buffer for flow cytometry analysis.

For all yeast cell staining, 3 biological replicates consisting of 100,000 recorded events each were used to assess all strains analyzed by flow cytometry. Visualization and data analyses were performed in FlowJo (Becton, Dickinson and Company). Statistical significance was determined with the use of a student's t-test, Mann-Whitney test (for samples with a non-gaussian distribution, as determined by a D'Agostino-Pearson omnibus normality test) or a one-way ANOVA with Tukey's post hoc analysis (GraphPad Prism, v7.0c software).

Spot Dilution Assays. To assess the viability of cells following drug exposure, strains were grown overnight in 5ml cultures in YPD one night prior to the experiment. The following morning, strains were back diluted to an OD_{600} of 0.1 into fresh YPD media that either contained 100µg/ml of cyclosporine A or an appropriate volume of the DMSO solvent control. Samples were then left to grow for 3 hours while shaking at 225rpm at 30°C. After incubation, 46.9ng/ml of caspofungin, or an appropriate volume of an ethanol solvent control, was added to each tube and strains were left to incubate for an additional 30 minutes. Following drug treatment, all samples were washed three times with 500µl of PBS, back diluted to an OD_{600} of 0.1 in PBS, and four subsequent 1:10 dilutions were further performed. To assess viability, 3µl of each dilution was spotted onto a fresh YPD plate. Plates were then incubated for 24 hours at 30°C, and images were taken the following day.

Western blot analysis of phosphorylated-Mkc1. Activated (phosphorylated) levels of Mkc1 were assessed as previously described [37].

References

1. Chaffin WL. Candida albicans cell wall proteins. Microbiol Mol Biol Rev. 2008;72(3):495-544. Epub 2008/09/06. doi: 10.1128/MMBR.00032-07. PubMed PMID: 18772287; PubMed Central PMCID: PMCPMC2546859.

2. Hopke A, Brown AJP, Hall RA, Wheeler RT. Dynamic Fungal Cell Wall Architecture in Stress Adaptation and Immune Evasion. Trends Microbiol. 2018;26(4):284-95. Epub 2018/02/18. doi: 10.1016/j.tim.2018.01.007. PubMed PMID: 29452950; PubMed Central PMCID: PMCPMC5869159.

3. McGreal EP, Rosas M, Brown GD, Zamze S, Wong SY, Gordon S, et al. The carbohydrate-recognition domain of Dectin-2 is a C-type lectin with specificity for high mannose. Glycobiology. 2006;16(5):422-30. Epub 2006/01/21. doi: 10.1093/glycob/cwj077. PubMed PMID: 16423983.

4. Saijo S, Ikeda S, Yamabe K, Kakuta S, Ishigame H, Akitsu A, et al. Dectin-2 recognition of alpha-mannans and induction of Th17 cell differentiation is essential for host defense against Candida albicans. Immunity. 2010;32(5):681-91. Epub 2010/05/25. doi: 10.1016/j.immuni.2010.05.001. PubMed PMID: 20493731.

5. Fradin C, Poulain D, Jouault T. beta-1,2-linked oligomannosides from Candida albicans bind to a 32-kilodalton macrophage membrane protein homologous to the mammalian lectin galectin-3. Infect Immun. 2000;68(8):4391-8. Epub 2000/07/19. doi: 10.1128/IAI.68.8.4391-4398.2000. PubMed PMID: 10899835; PubMed Central PMCID: PMCPMC98331.

6. Kohatsu L, Hsu DK, Jegalian AG, Liu FT, Baum LG. Galectin-3 induces death of Candida species expressing specific beta-1,2-linked mannans. J Immunol. 2006;177(7):4718-26. Epub 2006/09/20. doi: 10.4049/jimmunol.177.7.4718. PubMed PMID: 16982911.

7. Jouault T, El Abed-El Behi M, Martinez-Esparza M, Breuilh L, Trinel PA, Chamaillard M, et al. Specific recognition of Candida albicans by macrophages requires galectin-3 to discriminate Saccharomyces cerevisiae and needs association with TLR2 for signaling. J Immunol. 2006;177(7):4679-87. Epub 2006/09/20. doi: 10.4049/jimmunol.177.7.4679. PubMed PMID: 16982907.

8. Netea MG, Gow NA, Munro CA, Bates S, Collins C, Ferwerda G, et al. Immune sensing of Candida albicans requires cooperative recognition of mannans and glucans by lectin and Toll-like receptors. J Clin Invest. 2006;116(6):1642-50. Epub 2006/05/20. doi: 10.1172/JCI27114. PubMed PMID: 16710478; PubMed Central PMCID: PMCPMC1462942.

9. Cambi A, Netea MG, Mora-Montes HM, Gow NA, Hato SV, Lowman DW, et al. Dendritic cell interaction with Candida albicans critically depends on N-linked mannan. J Biol Chem. 2008;283(29):20590-9. Epub 2008/05/17. doi: 10.1074/jbc.M709334200. PubMed PMID: 18482990; PubMed Central PMCID: PMCPMC2459306.

10. Jouault T, Ibata-Ombetta S, Takeuchi O, Trinel PA, Sacchetti P, Lefebvre P, et al. Candida albicans phospholipomannan is sensed through toll-like receptors. J Infect Dis. 2003;188(1):165-72. Epub 2003/06/26. doi: 10.1086/375784. PubMed PMID: 12825186.

11. Taylor PR, Brown GD, Reid DM, Willment JA, Martinez-Pomares L, Gordon S, et al. The beta-glucan receptor, dectin-1, is predominantly expressed on the surface of cells of the monocyte/macrophage and neutrophil lineages. J Immunol. 2002;169(7):3876-82. Epub 2002/09/24. doi: 10.4049/jimmunol.169.7.3876. PubMed PMID: 12244185.

12. Brown GD, Taylor PR, Reid DM, Willment JA, Williams DL, Martinez-Pomares L, et al. Dectin-1 is a major beta-glucan receptor on macrophages. J Exp Med. 2002;196(3):407-12. Epub 2002/08/07. doi: 10.1084/jem.20020470. PubMed PMID: 12163569; PubMed Central PMCID: PMCPMC2193936.

13. Brown GD, Gordon S. Immune recognition. A new receptor for beta-glucans. Nature. 2001;413(6851):36-7. Epub 2001/09/07. doi: 10.1038/35092620. PubMed PMID: 11544516.

14. Kennedy AD, Willment JA, Dorward DW, Williams DL, Brown GD, DeLeo FR. Dectin-1 promotes fungicidal activity of human neutrophils. Eur J Immunol. 2007;37(2):467-78. Epub 2007/01/19. doi: 10.1002/eji.200636653. PubMed PMID: 17230442.

15. Cohen-Kedar S, Baram L, Elad H, Brazowski E, Guzner-Gur H, Dotan I. Human intestinal epithelial cells respond to beta-glucans via Dectin-1 and Syk. Eur J Immunol.

2014;44(12):3729-40. Epub 2014/09/25. doi: 10.1002/eji.201444876. PubMed PMID: 25251945.

16. Gow NA, Netea MG, Munro CA, Ferwerda G, Bates S, Mora-Montes HM, et al. Immune recognition of Candida albicans beta-glucan by dectin-1. J Infect Dis. 2007;196(10):1565-71. Epub 2007/11/17. doi: 10.1086/523110. PubMed PMID: 18008237; PubMed Central PMCID: PMCPMC2655640.

17. van Bruggen R, Drewniak A, Jansen M, van Houdt M, Roos D, Chapel H, et al. Complement receptor 3, not Dectin-1, is the major receptor on human neutrophils for beta-glucan-bearing particles. Mol Immunol. 2009;47(2-3):575-81. Epub 2009/10/09. doi: 10.1016/j.molimm.2009.09.018. PubMed PMID: 19811837.

18. Li X, Utomo A, Cullere X, Choi MM, Milner DA, Jr., Venkatesh D, et al. The beta-glucan receptor Dectin-1 activates the integrin Mac-1 in neutrophils via Vav protein signaling to promote Candida albicans clearance. Cell Host Microbe. 2011;10(6):603-15. Epub 2011/12/20. doi: 10.1016/j.chom.2011.10.009. PubMed PMID: 22177564; PubMed Central PMCID: PMCPMC3244687.

19. Swidergall M, Solis NV, Wang Z, Phan QT, Marshall ME, Lionakis MS, et al. EphA2 Is a Neutrophil Receptor for Candida albicans that Stimulates Antifungal Activity during Oropharyngeal Infection. Cell Rep. 2019;28(2):423-33 e5. Epub 2019/07/11. doi: 10.1016/j.celrep.2019.06.020. PubMed PMID: 31291578; PubMed Central PMCID: PMCPMC6638578.

20. Swidergall M, Solis NV, Lionakis MS, Filler SG. EphA2 is an epithelial cell pattern recognition receptor for fungal beta-glucans. Nat Microbiol. 2018;3(1):53-61. Epub 2017/11/15. doi: 10.1038/s41564-017-0059-5. PubMed PMID: 29133884; PubMed Central PMCID: PMCPMC5736406.

21. Wagener J, Malireddi RK, Lenardon MD, Koberle M, Vautier S, MacCallum DM, et al. Fungal chitin dampens inflammation through IL-10 induction mediated by NOD2 and TLR9 activation. PLoS Pathog. 2014;10(4):e1004050. Epub 2014/04/12. doi: 10.1371/journal.ppat.1004050. PubMed PMID: 24722226; PubMed Central PMCID: PMCPMC3983064.

22. He X, Howard BA, Liu Y, Neumann AK, Li L, Menon N, et al. LYSMD3: A mammalian pattern recognition receptor for chitin. Cell Rep. 2021;36(3):109392. Epub 2021/07/22. doi: 10.1016/j.celrep.2021.109392. PubMed PMID: 34289364; PubMed Central PMCID: PMCPMC8344708.

23. Hasim S, Allison DP, Retterer ST, Hopke A, Wheeler RT, Doktycz MJ, et al. beta-(1,3)-Glucan Unmasking in Some Candida albicans Mutants Correlates with Increases in Cell Wall Surface Roughness and Decreases in Cell Wall Elasticity. Infect Immun. 2017;85(1). Epub 2016/11/17. doi: 10.1128/IAI.00601-16. PubMed PMID: 27849179; PubMed Central PMCID: PMCPMC5203643.

24. Childers DS, Avelar GM, Bain JM, Pradhan A, Larcombe DE, Netea MG, et al. Epitope Shaving Promotes Fungal Immune Evasion. mBio. 2020;11(4). Epub 2020/07/09. doi: 10.1128/mBio.00984-20. PubMed PMID: 32636248; PubMed Central PMCID: PMCPMC7343991.

25. Chen T, Wagner AS, Reynolds TB. When Is It Appropriate to Take Off the Mask? Signaling Pathways That Regulate ß(1,3)-Glucan Exposure in Candida albicans. Frontiers in Fungal Biology. 2022;3. doi: 10.3389/ffunb.2022.842501.

26. Ballou ER, Avelar GM, Childers DS, Mackie J, Bain JM, Wagener J, et al. Lactate signalling regulates fungal beta-glucan masking and immune evasion. Nat Microbiol. 2016;2:16238. Epub 2016/12/13. doi: 10.1038/nmicrobiol.2016.238. PubMed PMID: 27941860; PubMed Central PMCID: PMCPMC5704895.

27. Pradhan A, Avelar GM, Bain JM, Childers DS, Larcombe DE, Netea MG, et al. Hypoxia Promotes Immune Evasion by Triggering beta-Glucan Masking on the Candida albicans Cell Surface via Mitochondrial and cAMP-Protein Kinase A Signaling. mBio. 2018;9(6). Epub 2018/11/08. doi: 10.1128/mBio.01318-18. PubMed PMID: 30401773; PubMed Central PMCID: PMCPMC6222127.

28. Pradhan A, Avelar GM, Bain JM, Childers D, Pelletier C, Larcombe DE, et al. Non-canonical signalling mediates changes in fungal cell wall PAMPs that drive immune evasion. Nat Commun. 2019;10(1):5315. Epub 2019/11/24. doi: 10.1038/s41467-019-13298-9. PubMed PMID: 31757950; PubMed Central PMCID: PMCPMC6876565.

29. Wagner AS, Lumsdaine SW, Mangrum MM, King AE, Hancock TJ, Sparer TE, et al. Cek1 regulates ss(1,3)-glucan exposure through calcineurin effectors in Candida albicans. PLoS Genet. 2022;18(9):e1010405. Epub 2022/09/20. doi: 10.1371/journal.pgen.1010405. PubMed PMID: 36121853; PubMed Central PMCID: PMCPMC9521907.
30. Sherrington SL, Sorsby E, Mahtey N, Kumwenda P, Lenardon MD, Brown I, et al. Adaptation of Candida albicans to environmental pH induces cell wall remodelling and enhances innate immune recognition. PLoS Pathog. 2017;13(5):e1006403. Epub 2017/05/26. doi: 10.1371/journal.ppat.1006403. PubMed PMID: 28542528; PubMed Central PMCID: PMCPMC5456412.
31. Cottier F, Sherrington S, Cockerill S, Del Olmo Toledo V, Kissane S, Tournu H, et al. Remasking of Candida albicans beta-Glucan in Response to Environmental pH Is Regulated by Quorum Sensing. mBio. 2019;10(5). Epub 2019/10/17. doi: 10.1128/mBio.02347-19. PubMed PMID: 31615961; PubMed Central PMCID: PMCPMC6794483.
32. Davis SE, Hopke A, Minkin SC, Jr., Montedonico AE, Wheeler RT, Reynolds TB. Masking of beta(1-3)-glucan in the cell wall of Candida albicans from detection by innate immune cells depends on phosphatidylserine. Infect Immun. 2014;82(10):4405-13. Epub 2014/08/13. doi: 10.1128/IAI.01612-14. PubMed PMID: 25114110; PubMed Central PMCID: PMCPMC4187869.
33. Chen YL, Montedonico AE, Kauffman S, Dunlap JR, Menn FM, Reynolds TB. Phosphatidylserine synthase and phosphatidylserine decarboxylase are essential for cell wall integrity and virulence in Candida albicans. Mol Microbiol. 2010;75(5):1112-32. Epub 2010/02/06. doi: 10.1111/j.1365-2958.2009.07018.x. PubMed PMID: 20132453.
34. Herrero AB, Magnelli P, Mansour MK, Levitz SM, Bussey H, Abeijon C. KRE5 gene null mutant strains of Candida albicans are avirulent and have altered cell wall composition and hypha formation properties. Eukaryot Cell. 2004;3(6):1423-32. Epub 2004/12/14. doi: 10.1128/EC.3.6.1423-1432.2004. PubMed PMID: 15590817; PubMed Central PMCID: PMCPMC539026.

35. Yang M, Solis NV, Marshall M, Garleb R, Zhou T, Wang D, et al. Control of beta-glucan exposure by the endo-1,3-glucanase Eng1 in Candida albicans modulates virulence. PLoS Pathog. 2022;18(1):e1010192. Epub 2022/01/08. doi: 10.1371/journal.ppat.1010192. PubMed PMID: 34995333; PubMed Central PMCID: PMCPMC8775328.
36. Chen T, Jackson JW, Tams RN, Davis SE, Sparer TE, Reynolds TB. Exposure of Candida albicans beta (1,3)-glucan is promoted by activation of the Cek1 pathway. PLoS Genet. 2019;15(1):e1007892. Epub 2019/02/01. doi: 10.1371/journal.pgen.1007892. PubMed PMID: 30703081; PubMed Central PMCID: PMCPMC6372213.
37. Chen T, Wagner AS, Tams RN, Eyer JE, Kauffman SJ, Gann ER, et al. Lrg1 Regulates beta (1,3)-Glucan Masking in Candida albicans through the Cek1 MAP Kinase Pathway. mBio. 2019;10(5). Epub 2019/09/19. doi: 10.1128/mBio.01767-19. PubMed PMID: 31530671; PubMed Central PMCID: PMCPMC6751057.
38. Wagner AS, Hancock TJ, Lumsdaine SW, Kauffman SJ, Mangrum MM, Phillips EK, et al. Activation of Cph1 causes ss(1,3)-glucan unmasking in Candida albicans and attenuates virulence in mice in a neutrophil-dependent manner. PLoS Pathog. 2021;17(8):e1009839. Epub 2021/08/26. doi: 10.1371/journal.ppat.1009839. PubMed PMID: 34432857.
39. Wheeler RT, Fink GR. A drug-sensitive genetic network masks fungi from the immune system. PLoS Pathog. 2006;2(4):e35. Epub 2006/05/03. doi: 10.1371/journal.ppat.0020035. PubMed PMID: 16652171; PubMed Central PMCID: PMCPMC1447670.
40. Wheeler RT, Kombe D, Agarwala SD, Fink GR. Dynamic, morphotype-specific Candida albicans beta-glucan exposure during infection and drug treatment. PLoS Pathog. 2008;4(12):e1000227. Epub 2008/12/06. doi: 10.1371/journal.ppat.1000227. PubMed PMID: 19057660; PubMed Central PMCID: PMCPMC2587227.
41. Tams RN, Wagner AS, Jackson JW, Gann ER, Sparer TE, Reynolds TB. Pathways That Synthesize Phosphatidylethanolamine Impact Candida albicans Hyphal Length and Cell Wall Composition through Transcriptional and Posttranscriptional

Mechanisms. Infect Immun. 2020;88(3). Epub 2019/12/04. doi: 10.1128/IAI.00480-19. PubMed PMID: 31792076; PubMed Central PMCID: PMCPMC7035933.

42. Perlin DS. Current perspectives on echinocandin class drugs. Future Microbiol. 2011;6(4):441-57. Epub 2011/04/30. doi: 10.2217/fmb.11.19. PubMed PMID: 21526945; PubMed Central PMCID: PMCPMC3913534.

43. Wiederhold NP, Najvar LK, Bocanegra R, Kirkpatrick WR, Patterson TF. Comparison of anidulafungin's and fluconazole's in vivo activity in neutropenic and non-neutropenic models of invasive candidiasis. Clin Microbiol Infect. 2012;18(2):E20-3. Epub 2011/12/02. doi: 10.1111/j.1469-0691.2011.03712.x. PubMed PMID: 22128831.

44. Marakalala MJ, Vautier S, Potrykus J, Walker LA, Shepardson KM, Hopke A, et al. Differential adaptation of Candida albicans in vivo modulates immune recognition by dectin-1. PLoS Pathog. 2013;9(4):e1003315. Epub 2013/05/03. doi: 10.1371/journal.ppat.1003315. PubMed PMID: 23637604; PubMed Central PMCID: PMCPMC3630191.

45. Roman E, Cottier F, Ernst JF, Pla J. Msb2 signaling mucin controls activation of Cek1 mitogen-activated protein kinase in Candida albicans. Eukaryot Cell. 2009;8(8):1235-49. Epub 2009/06/23. doi: 10.1128/EC.00081-09. PubMed PMID: 19542310; PubMed Central PMCID: PMCPMC2725568.

46. Swidergall M, van Wijlick L, Ernst JF. Signaling domains of mucin Msb2 in Candida albicans. Eukaryot Cell. 2015;14(4):359-70. Epub 2015/02/01. doi: 10.1128/EC.00264-14. PubMed PMID: 25636320; PubMed Central PMCID: PMCPMC4385809.

47. Singh SD, Robbins N, Zaas AK, Schell WA, Perfect JR, Cowen LE. Hsp90 governs echinocandin resistance in the pathogenic yeast Candida albicans via calcineurin. PLoS Pathog. 2009;5(7):e1000532. Epub 2009/08/04. doi: 10.1371/journal.ppat.1000532. PubMed PMID: 19649312; PubMed Central PMCID: PMCPMC2712069.

48. Walker LA, Munro CA, de Bruijn I, Lenardon MD, McKinnon A, Gow NA. Stimulation of chitin synthesis rescues Candida albicans from echinocandins. PLoS Pathog. 2008;4(4):e1000040. Epub 2008/04/05. doi: 10.1371/journal.ppat.1000040. PubMed PMID: 18389063; PubMed Central PMCID: PMCPMC2271054.

49. da Silva Dantas A, Nogueira F, Lee KK, Walker LA, Edmondson M, Brand AC, et al. Crosstalk between the calcineurin and cell wall integrity pathways prevents chitin overexpression in Candida albicans. J Cell Sci. 2021;134(24). Epub 2021/11/19. doi: 10.1242/jcs.258889. PubMed PMID: 34792152; PubMed Central PMCID: PMCPMC8729787.

50. Walker LA, Munro CA. Caspofungin Induced Cell Wall Changes of Candida Species Influences Macrophage Interactions. Front Cell Infect Microbiol. 2020;10:164. Epub 2020/06/13. doi: 10.3389/fcimb.2020.00164. PubMed PMID: 32528900; PubMed Central PMCID: PMCPMC7247809.

51. Lee KK, Maccallum DM, Jacobsen MD, Walker LA, Odds FC, Gow NA, et al. Elevated cell wall chitin in Candida albicans confers echinocandin resistance in vivo. Antimicrob Agents Chemother. 2012;56(1):208-17. Epub 2011/10/12. doi: 10.1128/AAC.00683-11. PubMed PMID: 21986821; PubMed Central PMCID: PMCPMC3256049.

52. Plaine A, Walker L, Da Costa G, Mora-Montes HM, McKinnon A, Gow NA, et al. Functional analysis of Candida albicans GPI-anchored proteins: roles in cell wall integrity and caspofungin sensitivity. Fungal Genet Biol. 2008;45(10):1404-14. Epub 2008/09/04. doi: 10.1016/j.fgb.2008.08.003. PubMed PMID: 18765290; PubMed Central PMCID: PMCPMC2649418.

53. Yang F, Zhang L, Wakabayashi H, Myers J, Jiang Y, Cao Y, et al. Tolerance to Caspofungin in Candida albicans Is Associated with at Least Three Distinctive Mechanisms That Govern Expression of FKS Genes and Cell Wall Remodeling. Antimicrob Agents Chemother. 2017;61(5). Epub 2017/02/23. doi: 10.1128/AAC.00071-17. PubMed PMID: 28223384; PubMed Central PMCID: PMCPMC5404545.

54. Liu J, Farmer JD, Jr., Lane WS, Friedman J, Weissman I, Schreiber SL. Calcineurin is a common target of cyclophilin-cyclosporin A and FKBP-FK506 complexes. Cell. 1991;66(4):807-15. Epub 1991/09/02. doi: 10.1016/0092-8674(91)90124-h. PubMed PMID: 1715244.

55. Breuder T, Hemenway CS, Movva NR, Cardenas ME, Heitman J. Calcineurin is essential in cyclosporin A- and FK506-sensitive yeast strains. Proc Natl Acad Sci U S A.

1994;91(12):5372-6. Epub 1994/06/07. doi: 10.1073/pnas.91.12.5372. PubMed PMID: 7515500; PubMed Central PMCID: PMCPMC43997.

56. Juvvadi PR, Lamoth F, Steinbach WJ. Calcineurin as a Multifunctional Regulator: Unraveling Novel Functions in Fungal Stress Responses, Hyphal Growth, Drug Resistance, and Pathogenesis. Fungal Biol Rev. 2014;28(2-3):56-69. Epub 2014/11/11. doi: 10.1016/j.fbr.2014.02.004. PubMed PMID: 25383089; PubMed Central PMCID: PMCPMC4219591.

57. Davey HM, Hexley P. Red but not dead? Membranes of stressed Saccharomyces cerevisiae are permeable to propidium iodide. Environ Microbiol. 2011;13(1):163-71. Epub 2011/01/05. doi: 10.1111/j.1462-2920.2010.02317.x. PubMed PMID: 21199254.

58. Lenardon MD, Munro CA, Gow NA. Chitin synthesis and fungal pathogenesis. Curr Opin Microbiol. 2010;13(4):416-23. Epub 2010/06/22. doi: 10.1016/j.mib.2010.05.002. PubMed PMID: 20561815; PubMed Central PMCID: PMCPMC2923753.

59. Munro CA, Selvaggini S, de Bruijn I, Walker L, Lenardon MD, Gerssen B, et al. The PKC, HOG and Ca2+ signalling pathways co-ordinately regulate chitin synthesis in Candida albicans. Mol Microbiol. 2007;63(5):1399-413. Epub 2007/02/17. doi: 10.1111/j.1365-2958.2007.05588.x. PubMed PMID: 17302816; PubMed Central PMCID: PMCPMC2649417.

60. Bulawa CE, Miller DW, Henry LK, Becker JM. Attenuated virulence of chitin-deficient mutants of Candida albicans. Proc Natl Acad Sci U S A. 1995;92(23):10570-4. Epub 1995/11/07. doi: 10.1073/pnas.92.23.10570. PubMed PMID: 7479842; PubMed Central PMCID: PMCPMC40653.

61. Mio T, Yabe T, Sudoh M, Satoh Y, Nakajima T, Arisawa M, et al. Role of three chitin synthase genes in the growth of Candida albicans. J Bacteriol. 1996;178(8):2416-9. Epub 1996/04/01. doi: 10.1128/jb.178.8.2416-2419.1996. PubMed PMID: 8636047; PubMed Central PMCID: PMCPMC177954.

62. Hopke A, Nicke N, Hidu EE, Degani G, Popolo L, Wheeler RT. Neutrophil Attack Triggers Extracellular Trap-Dependent Candida Cell Wall Remodeling and Altered Immune Recognition. PLoS Pathog. 2016;12(5):e1005644. Epub 2016/05/26.

doi: 10.1371/journal.ppat.1005644. PubMed PMID: 27223610; PubMed Central PMCID: PMCPMC4880299.

63. Pericolini E, Perito S, Castagnoli A, Gabrielli E, Mencacci A, Blasi E, et al. Epitope unmasking in vulvovaginal candidiasis is associated with hyphal growth and neutrophilic infiltration. PLoS One. 2018;13(7):e0201436. Epub 2018/08/01. doi: 10.1371/journal.pone.0201436. PubMed PMID: 30063729; PubMed Central PMCID: PMCPMC6067721.

64. Stevens DA, Espiritu M, Parmar R. Paradoxical effect of caspofungin: reduced activity against Candida albicans at high drug concentrations. Antimicrob Agents Chemother. 2004;48(9):3407-11. Epub 2004/08/26. doi: 10.1128/AAC.48.9.3407-3411.2004. PubMed PMID: 15328104; PubMed Central PMCID: PMCPMC514730.

65. Shaw JA, Mol PC, Bowers B, Silverman SJ, Valdivieso MH, Duran A, et al. The function of chitin synthases 2 and 3 in the Saccharomyces cerevisiae cell cycle. J Cell Biol. 1991;114(1):111-23. Epub 1991/07/01. doi: 10.1083/jcb.114.1.111. PubMed PMID: 2050738; PubMed Central PMCID: PMCPMC2289062.

66. Cabib E, Arroyo J. How carbohydrates sculpt cells: chemical control of morphogenesis in the yeast cell wall. Nat Rev Microbiol. 2013;11(9):648-55. Epub 2013/08/21. doi: 10.1038/nrmicro3090. PubMed PMID: 23949603.

67. Badrane H, Nguyen MH, Blankenship JR, Cheng S, Hao B, Mitchell AP, et al. Rapid redistribution of phosphatidylinositol-(4,5)-bisphosphate and septins during the Candida albicans response to caspofungin. Antimicrob Agents Chemother. 2012;56(9):4614-24. Epub 2012/06/13. doi: 10.1128/AAC.00112-12. PubMed PMID: 22687514; PubMed Central PMCID: PMCPMC3421880.

68. Badrane H, Nguyen MH, Clancy CJ. Highly Dynamic and Specific Phosphatidylinositol 4,5-Bisphosphate, Septin, and Cell Wall Integrity Pathway Responses Correlate with Caspofungin Activity against Candida albicans. Antimicrob Agents Chemother. 2016;60(6):3591-600. Epub 2016/03/30. doi: 10.1128/AAC.02711-15. PubMed PMID: 27021331; PubMed Central PMCID: PMCPMC4879351.

69. Audhya A, Emr SD. Stt4 PI 4-kinase localizes to the plasma membrane and functions in the Pkc1-mediated MAP kinase cascade. Dev Cell. 2002;2(5):593-605. Epub 2002/05/23. doi: 10.1016/s1534-5807(02)00168-5. PubMed PMID: 12015967.

70. Drgonova J, Drgon T, Tanaka K, Kollar R, Chen GC, Ford RA, et al. Rho1p, a yeast protein at the interface between cell polarization and morphogenesis. Science. 1996;272(5259):277-9. Epub 1996/04/12. doi: 10.1126/science.272.5259.277. PubMed PMID: 8602514.

71. Qadota H, Python CP, Inoue SB, Arisawa M, Anraku Y, Zheng Y, et al. Identification of yeast Rho1p GTPase as a regulatory subunit of 1,3-beta-glucan synthase. Science. 1996;272(5259):279-81. Epub 1996/04/12. doi: 10.1126/science.272.5259.279. PubMed PMID: 8602515.

72. Levin DE. Regulation of cell wall biogenesis in Saccharomyces cerevisiae: the cell wall integrity signaling pathway. Genetics. 2011;189(4):1145-75. Epub 2011/12/17. doi: 10.1534/genetics.111.128264. PubMed PMID: 22174182; PubMed Central PMCID: PMCPMC3241422.

73. Xie JL, Grahl N, Sless T, Leach MD, Kim SH, Hogan DA, et al. Signaling through Lrg1, Rho1 and Pkc1 Governs Candida albicans Morphogenesis in Response to Diverse Cues. PLoS Genet. 2016;12(10):e1006405. Epub 2016/10/28. doi: 10.1371/journal.pgen.1006405. PubMed PMID: 27788136; PubMed Central PMCID: PMCPMC5082861.

74. Styles C. How to set up a yeast laboratory. Methods Enzymol. 2002;350:42-71. Epub 2002/06/21. doi: 10.1016/s0076-6879(02)50955-1. PubMed PMID: 12073328.

75. Nguyen N, Quail MMF, Hernday AD. An Efficient, Rapid, and Recyclable System for CRISPR-Mediated Genome Editing in Candida albicans. mSphere. 2017;2(2). Epub 2017/05/13. doi: 10.1128/mSphereDirect.00149-17. PubMed PMID: 28497115; PubMed Central PMCID: PMCPMC5422035.

Appendix

S4.1 Table: Plasmids used in this study.

Strain Name	Description	Marker	Parent /Source
pTB198	*GFP-CaNAT*	Ampicillin, Nourseothricin	This Study
pADH110	CRISPR fragment A template	Ampicillin, Nourseothricin*	[1]
pADH119	CRISPR fragment B template	Ampicillin, Nourseothricin*	[1]
pADH137	CRISPR Cas9 expression Plasmid	Ampicillin, Nourseothricin*	[1]

References

1. Nguyen N, Quail MMF, Hernday AD. An Efficient, Rapid, and Recyclable System for CRISPR-Mediated Genome Editing in Candida albicans. mSphere. 2017;2(2). Epub 2017/05/13. doi: 10.1128/mSphereDirect.00149-17. PubMed PMID: 28497115; PubMed Central PMCID: PMCPMC5422035.

S4.2 Table: Primers used in this study.

Primer Name	Sequence (5' to 3')	Description	Source
AHO1096	GACGGCACGGCCACGCGTTTAAACCGCC	Fragment A forward primer for CRISPR-mediated gene deletion.	1
AHO1097	CCCGCCAGGCGCTGGGGTTTAAACACCG	Fragment B reverse primer for CRISPR-mediated gene deletion.	1
AHO1098	caaattaaaaatagtttacgcaag	Fragment A reverse primer for CRISPR-mediated gene deletion.	1
AHO1237	aggtgatgctgaagctattgaag	Fragment C forward primer for CRISPR-mediated gene deletion.	1
AHO1238	TGTATTTTGTTTTAAAATTTTAGTGACTGTTTC	Fragment C reverse primer for CRISPR-mediated gene deletion.	1
AWO242	CGTAAACTATTTTTAATTTGAGAACCCCGACG AAAATGCTGTTTTAGAGCTAGAAATAGC	*MKC1* gRNA forward primer for fragment B amplification for CRISPR-mediated gene cleavage	This Study
AWO244	ATTTCCATAATGGATCAACAAGAAGCACCCA TATATTATGGCAGATCCGTTAGTTGAAACAC ACAACCACGTTATCCCGGGGTATGTTACTCTC GAATTA	*MKC1* repair template for whole gene deletion (sense oligomer)	This Study
AWO245	TAATTCGAGAGTAACATACCCCGGGATAACG TGGTTGTGTGTTTCAACTAACGGATCTGCCAT AATATATGGGTGCTTCTTGTTGATCCATTATG GAAAT	*MKC1* repair template for whole gene deletion (antisense oligomer)	This Study
AWO246	GATGTCACATCAACTTCAC	*MKC1* whole gene deletion check primer forward (Sits -560bp upstream from start codon in 5'UTR)	This Study
AWO247	GAGACAAGAAGTATTATTTCATCTC	*MKC1* whole gene deletion check primer reverse (Sits +513bp from stop codon in 3'UTR)	This Study
AWO146	CTTGGGATCCATCTAATACTGGGGGAAATT TGATTGATGATTTAAGTCAAGGATCTTCTTC AGGGTCCAGTggtggtggttctaaaggtgaagaattatt	GFP forward primer with 80bp overhang of *CHS3* (80bp upstream stop codon)	This Study

S4.2 Table Continued

Primer Name	Sequence (5' to 3')	Description	Source
AWO147	TTTTTATATTGTTAATAATTTTATATAACCATATACATAAATAAAAGTCCTTTCTCTCTCTCTTTTTTAAGCTTTAACCCAAagaactagtggatccccc	GFP reverse primer with 80bp overhang of *CHS3* (80bp downstream stop codon)	This Study
AWO270	CTATTTGTACAATTCATCCATAC	*CHS3-GFP* reverse primer for screening insertion at C-terminal end of *CHS3* (Sits at end of *GFP* ORF)	This Study
SLO12	GCAGTTATTTTCGGGTTACCTGGTTGTT	*CHS3-GFP* forward check primer. (Sits in *CHS3* ORF -3247 bp downstream of start codon)	This Study

References

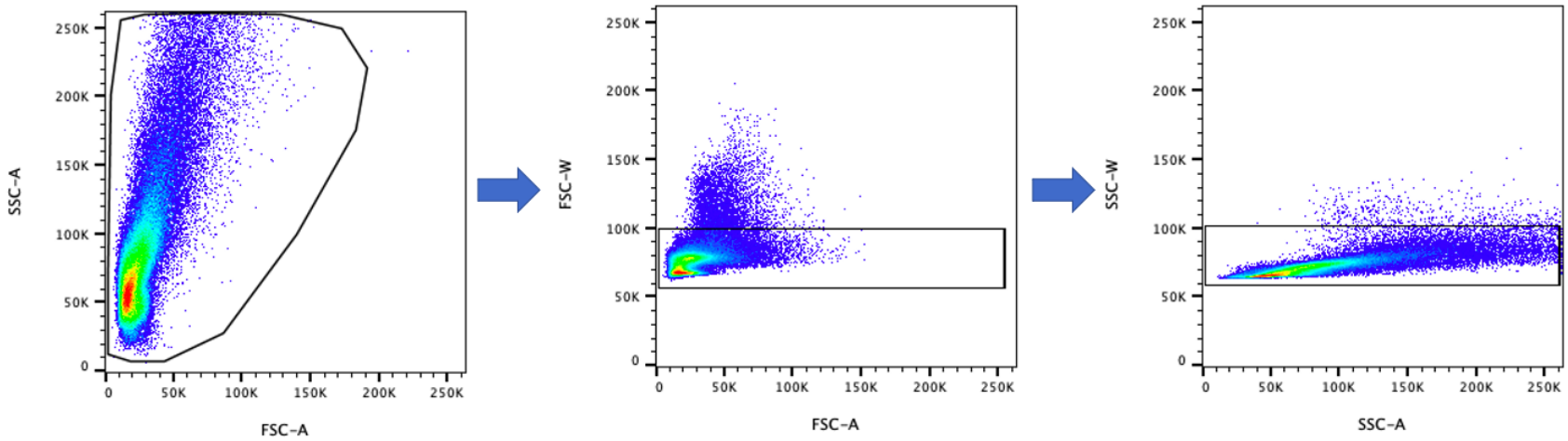
1. Nguyen N, Quail MMF, Hernday AD. An Efficient, Rapid, and Recyclable System for CRISPR-Mediated Genome Editing in Candida albicans. mSphere. 2017;2(2). Epub 2017/05/13. doi: 10.1128/mSphereDirect.00149-17. PubMed PMID: 28497115; PubMed Central PMCID: PMCPMC5422035.

S4.3 Table: Strains used in this study.

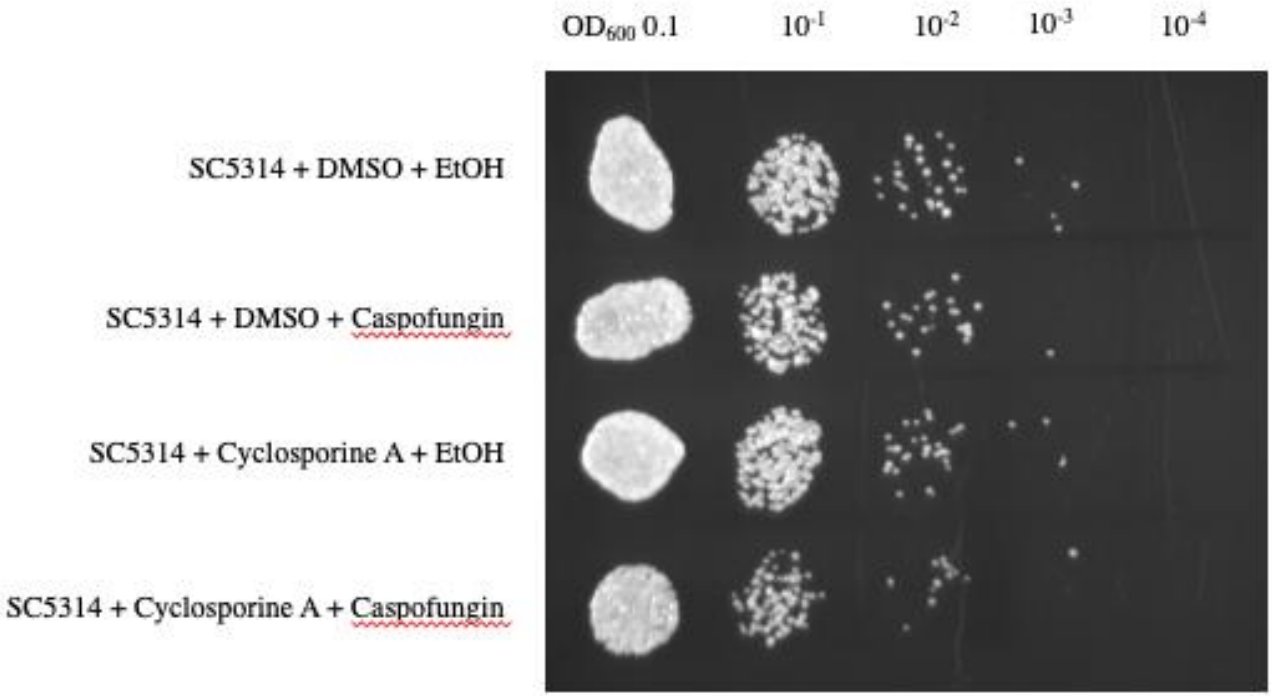
Strain	Genotype	Parent	Source or Reference
AWY006	*LEU2/leu2*Δ (Wild Type)	SC5314	1
AWY203	*mkc1Δ/Δ LEU2/leu2*Δ	AWY006	This Study
AWY245	*CHS3/CHS3-GFP LEU2/leu2*Δ	AWY006	This Study

References:

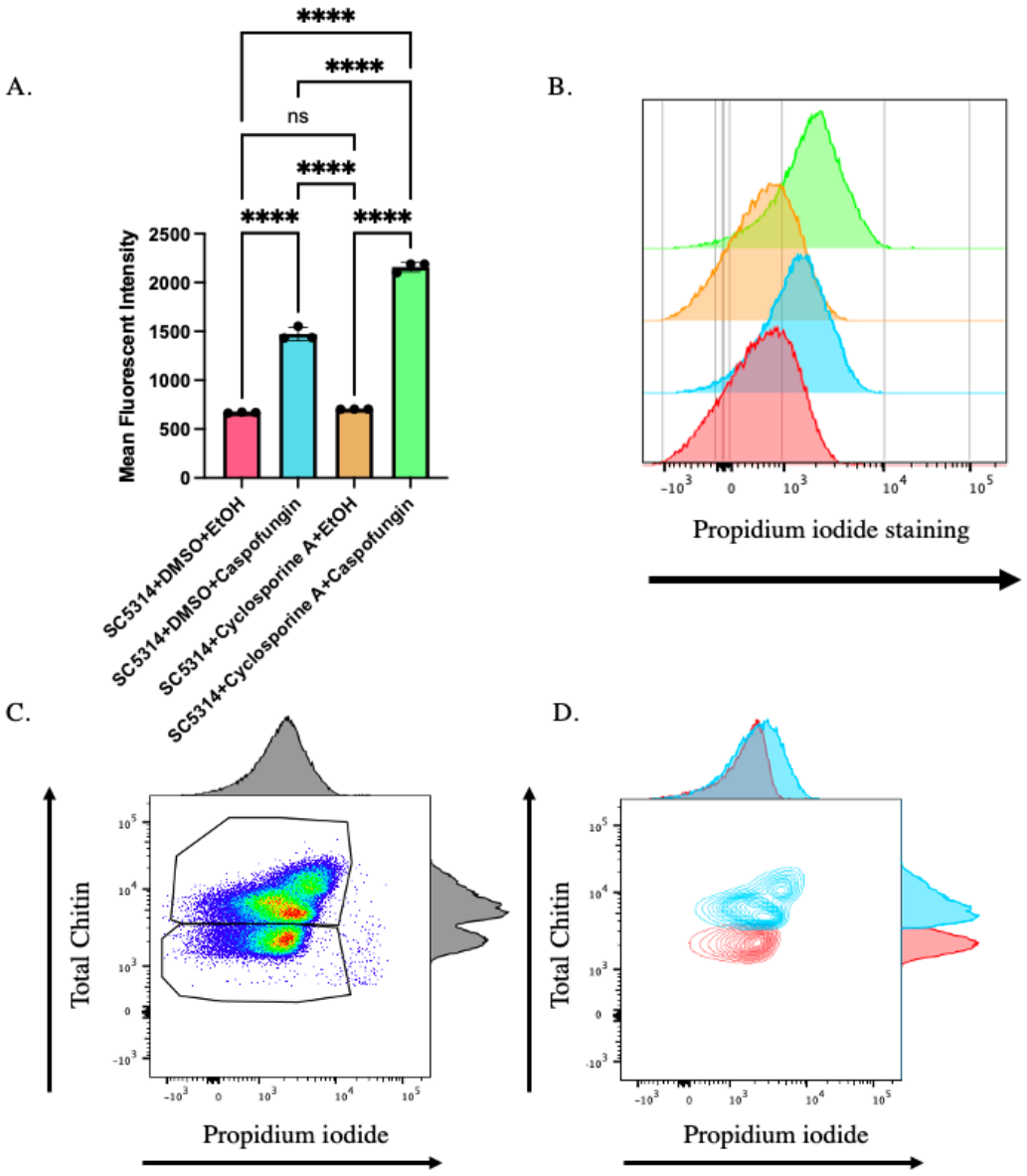
1. Wagner, A. S. et al. Activation of Cph1 causes ß(1,3)-glucan unmasking in Candida albicans and attenuates virulence in mice in a neutrophil-dependent manner. PLoS Pathog 17, e1009839, doi:10.1371/journal.ppat.1009839 (2021).



S4.1 Fig: Gating strategy for single yeast cells.

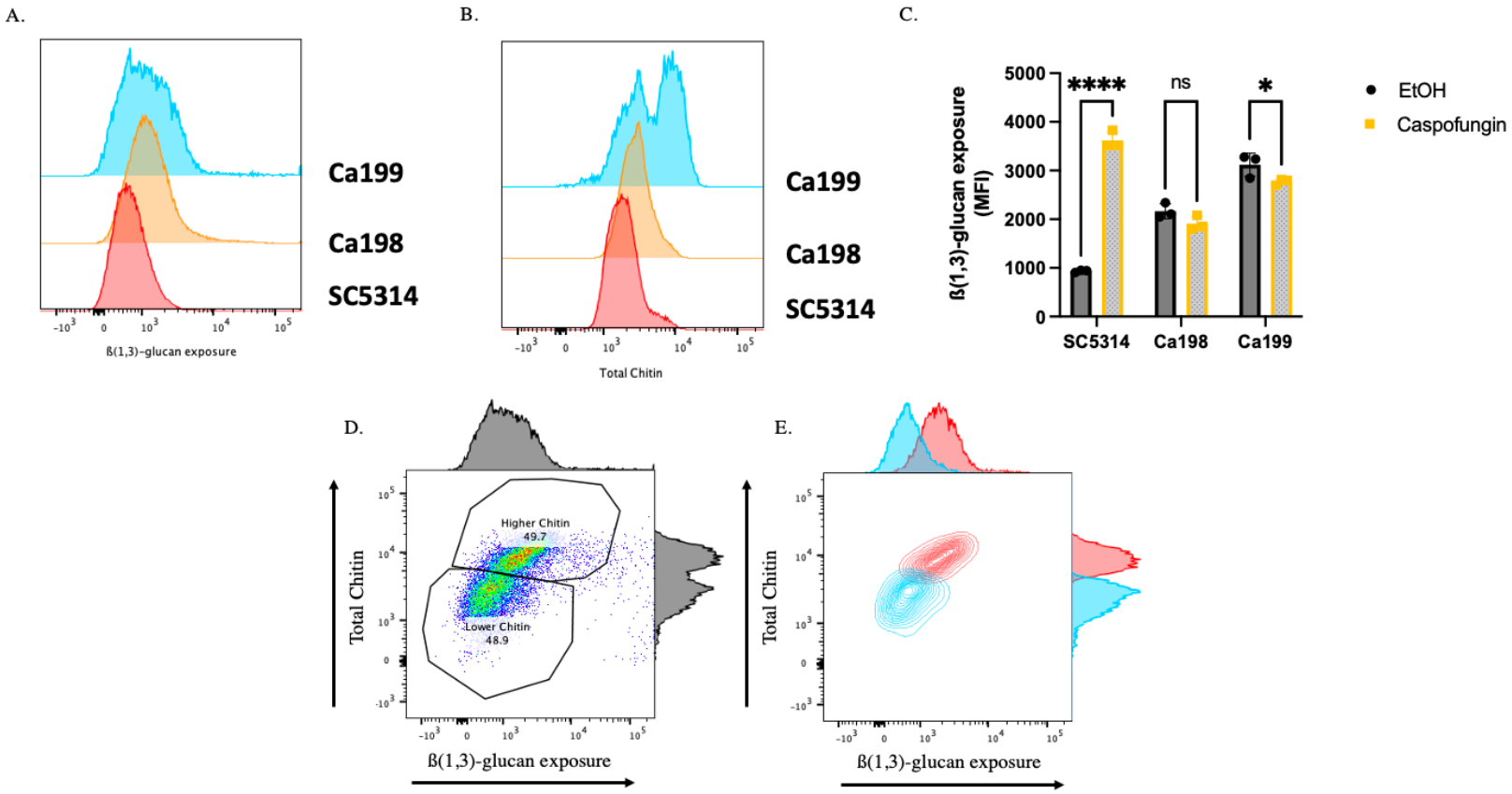


S4.2 Fig: Calcineurin inhibition does not impact cell survival following caspofungin exposure.
SC5314 wild-type cells grown to mid-log phase in either the presence of 100μg/ml of cyclosporine A, or an appropriate volume of the DMSO solvent control, were exposed to 46.9ng/ml of caspofungin for 30 minutes. Cells were then washed, back diluted to OD_{600} of 0.1, and serially diluted to assess viability via a spot dilution assay onto YPD.



S4.3 Fig: Propidium iodide staining does not correlate with chitin content following caspofungin exposure to calcineurin-inhibited cells.

SC5314 wild-type cells grown to mid-log phase in either the presence of 100μg/ml of cyclosporine A, or an appropriate volume of the DMSO solvent control, were exposed to 46.9ng/ml of caspofungin for 30 minutes. CFW and propidium iodide (P.I.) staining were then assessed by flow cytometry. (A) P.I. staining of cyclosporine A (calcineurin-inhibited) and caspofungin treated cells. (****p<0.0001, by one-way ANOVA)(n = 3 biological replicates). (B) Representative histogram of the impact that calcineurin-inhibition has on caspofungin-induced P.I. staining. Colors of each sample match those shown in 2A. (C) Representative scatter plot and adjunct histograms for CFW and P.I. staining of cells treated with cyclosporine A and caspofungin. Gates represent populations of high and low chitin within the sample. (D) Representative scatter plot with adjunct histograms for CFW and PI staining when plotting low (blue) and high (red) chitin populations independently.



S4.4 Fig: Caspofungin-induced unmasking requires drug-mediated inhibition of Fks1.
(A-C) The SC5314 wild-type strain and two caspofugin resistant *C. albicans* isolates (Ca198 and Ca199) were grown to mid-log phase and exposed to 46.9ng/ml of caspofungin for 30 minutes. ß(1,3)-glucan exposure and total chitin levels were then assessed by flow cytometry. (A) Representative histogram for basal ß(1,3)-glucan exposure of mid-log phase cells treated with an ethanol solvent control. (B) Representative histogram for basal chitin levels of mid-log phase cells treated with an ethanol solvent control. (C) ß(1,3)-glucan unmasking of strains treated with an ethanol solvent control or caspofungin. (*p<0.05, ****p<0.0001, by students t-test). (D) Representative scatter plot and adjunct histograms for CFW staining and unmasking of Ca199 cells. Gates represent populations of low and high chitin within the sample. (E) Representative scatter plot with adjunct histograms for CFW staining and unmasking when plotting low (blue) and high (red) chitin populations independently.

CHAPTER 5 - MUCOSAL INFECTION WITH UNMASKED *CANDIDA ALBICANS* CELLS IMPACTS DISEASE PROGRESSION IN A HOST NICHE SPECIFIC MANNER

This work was performed by: Andrew S. Wagner, Amanda K. Vogel, Stephen W. Lumsdaine, Elise K. Phillips, Hubertine M. E. Willems, Brian M. Peters and Todd B. Reynolds

Author Contributions: Conceptualization, ASW and TBR.; Methodology, ASW, AKV, EKV (established QRT-PCR method) and HMEW; Formal analysis, ASW; Investigation, ASW, AKV (VVC infection), SWL (Helped in OPC infections) and HMEW (VVC infections); Writing–original draft preparation, ASW; Writing–review and editing, ASW and TBR; Visualization, ASW; Funding Acquisition, BMP and TBR.

This work is *in revision* at Infection and Immunity.

Abstract

Shielding the immunogenic cell wall epitope ß(1,3)-glucan under an outer layer of mannosylated glycoproteins is an essential virulence factor deployed by *Candida albicans* during systemic infection. Accordingly, mutants with increased ß(1,3)-glucan exposure (unmasking) display increased immunostimulatory capabilities *in vitro* and attenuated virulence during systemic infection in mice. However, little work has been done to assess the impact of increased unmasking during the two most common manifestations of candidiasis: oropharyngeal (OPC) and vulvovaginal (VVC) candidiasis. We have previously shown that expression of a single hyperactive allele of the MAP3K $STE11^{\Delta N467}$ induces unmasking via the Cek1 MAPK pathway, attenuates fungal burden, and prolongs survival during systemic infection in mice. Here we expand on these findings and show that infection with an unmasked $STE11^{\Delta N467}$ mutant also impacts disease progression during OPC and VVC murine infection models. Male mice sublingually infected with the $STE11^{\Delta N467}$ mutant showed a significant reduction in tongue fungal burden at 2 days post infection, and a modest reduction at 5 days post infection. However, we find that selection for $STE11^{\Delta N467}$ suppressor mutants that no longer display increased unmasking occurs within the oral cavity, and is likely responsible for the restoration of fungal burden trends to wild-type levels later into infection. In the VVC infection model, no attenuation in fungal

burden was observed. However, polymorphonuclear cell recruitment and IL-1ß levels within the vaginal lumen, markers of immunopathogenesis, were increased in mice infected with unmasked *STE11*$^{\Delta N467}$ cells. Thus, our data suggests a niche specific impact for unmasking on disease progression.

Introduction

Candida albicans is an opportunistic fungal pathogen that resides as a commensal organism of mucosal surfaces throughout the human body. However, under specific conditions a transition to its pathogenic state can quickly ensue [1, 2]. Once induced, disease most typically manifests as non-lethal, superficial, mucosal infections, such as oropharyngeal (OPC) and vulvovaginal (VVC) candidiasis [3]. These diseases are associated with high morbidity and prevalence, as reports have estimated that nearly 90% of individuals with acquired autoimmune deficiency syndrome (AIDS) will acquire OPC at some point throughout disease progression and nearly 75% of women will experience an episode of VVC throughout their lifetime [4, 5]. Moreover, in patients with conditions that compromise their innate immunity, *Candida spp.* can cause life-threatening systemic infection as well, with an attributed mortality rate as high as 42% [6]. Due to the high frequency of mucosal infections and the extensive medical care required for systemic disease treatment, both invasive and non-invasive candidiasis infections are projected to impose an economic burden exceeding 4 billion dollars within the United States alone [7]. Thus, there is a need for effective antifungals capable of controlling disease progression.

The current antifungal armamentarium consists of three main classes of drugs: the echinocandins, the azoles and the polyenes. However, increasing resistance, poor oral availability and secondary cytotoxic side effects have limited their use [8-10]. Alternatively, leveraging exposure of immunogenic cell wall epitopes has begun to gain attention as a potential immunotherapeutic approach to control disease progression [11-14]. For *C. albicans*, emphasis has been placed on how altered exposure levels of the highly immunogenic cell wall epitope ß(1,3)-glucan impact disease progression. ß(1,3)-glucan is normally covered (masked) by an outer layer of mannosylated glycoproteins that act as a barrier to host pattern recognition receptors (PRRs) that bind exposed epitopes of this

polysaccharide and initiate an immune response [15, 16]. Therefore, ß(1,3)-glucan masking is a mechanism of immune system evasion deployed by *C. albicans* during infection. Both hematopoietic and non-hematopoietic cells express receptors capable of binding exposed ß(1,3)-glucan foci, such as the C-type lectin receptor Dectin-1 [17-22], the Ephrin type A receptor 2 (EphA2) [23-25] and Complement Receptor 3 (Mac-1) [26, 27]. Given the pro-inflammatory nature of ß(1,3)-glucan and the high prevalence of host PRRs capable of binding this epitope, increased ß(1,3)-glucan exposure (in a process termed unmasking) should render *C. albicans* more visible to host immune cells and facilitate more rapid and robust fungal clearance.

In accordance with this model, multiple mutations have been identified that inappropriately increase ß(1,3)-glucan unmasking and attenuate virulence. For example, homozygous deletion of the phosphatidylserine synthase gene *CHO1*, the glycosyltransferase gene *KRE5*, or the endoglucanase *ENG1* all induce unmasking and attenuate virulence during systemic infection in mice [28-31]. Furthermore, we have found that hyperactivation of the Cek1 mitogen activated protein kinase (MAPK) pathway, via expression of a hyperactive allele of the upstream MAP3K *STE11* (*STE11*$^{\Delta N467}$), also increases ß(1,3)-glucan exposure [32]. Mice infected with an unmasked *STE11*$^{\Delta N467}$ mutant display reduced fungal burden in the kidneys, brain and spleen, as well as prolonged survival during systemic infection [33, 34]. Importantly, immunosuppression restores fungal colonization and survival trends to near wild-type levels, demonstrating that the virulence attenuation observed during systemic infection with this mutant is host immune system dependent. Although strong evidence exists that unmasking impacts virulence during systemic infection, less work has been done to study the impact that increased ß(1,3)-glucan exposure has during mucosal infections.

In this report, we expand on our findings during systemic infections and address how the *STE11*$^{\Delta N467}$ mutant behaves in the two most common manifestations of mucosal candidiasis: OPC and VVC. We find that infection with an unmasked *STE11*$^{\Delta N467}$ mutant attenuates fungal burden within the oral cavity, and leads to a positive selection *in vivo* for suppressor mutants that no longer display increased ß(1,3)-glucan exposure. Furthermore, we find that during VVC, fungal burden trends are unaltered between

unmasked and wild-type cells, but immunopathogenesis biomarkers are increased in mice infected with the unmasked *STE11*$^{\Delta N467}$ mutant. Therefore, mucosal infection with unmasked fungal cells impacts disease progression, but the outcome for the host varies depending on the anatomical location where fungal colonization is occurring.

Results

Hyperactivation of the Cek1 MAPK pathway modestly attenuates tongue fungal burden late into oropharyngeal infection.

An unmasked hyperactive *STE11* mutant (*STE11/P*$_{tet\text{-}off}$*STE11*$^{\Delta N467}$) increases immune system recognition by macrophages in a Dectin-1 dependent manner *in vitro*, and attenuates fungal burden during mouse systemic infections in a neutrophil-dependent manner [34]. Given the importance of both oral epithelial ß(1,3)-glucan receptors and neutrophils in controlling oropharyngeal candidiasis [23, 24, 35, 36], we hypothesized that mice infected sublingually with the hyperactive *STE11/P*$_{tet\text{-}off}$*STE11*$^{\Delta N467}$ mutant would also display attenuated virulence during an oropharyngeal candidiasis infection model. To assess this, male and female C57BL/6 mice were immunocompromised via recurring cortisone injections, sublingually infected with $1x10^6$ cells of either the Day286 wild-type control or the *STE11/P*$_{tet\text{-}off}$*STE11*$^{\Delta N467}$ mutant, and tongue fungal burden was assessed 5 days post-infection (d.p.i.). Interestingly, female mice infected with either strain did not show a difference in fungal burden at 5 d.p.i. (Fig. 5.1A). This was also reflected in weight trends over the infection period, as all mice lost weight at similar rates, regardless of strain (Fig. 5.1B). However, male mice infected with the unmasked *STE11/P*$_{tet\text{-}off}$*STE11*$^{\Delta N467}$ mutant did show a modest, but significant decrease in tongue fungal burden (~4-fold reduction) at 5 d.p.i. when compared to wild-type infected male mice (Fig. 5.1C). This decrease was also mirrored in weight loss trends over the infection period, as wild-type infected mice generally lost more weight than *STE11/P*$_{tet\text{-}off}$*STE11*$^{\Delta N467}$ infected mice (Fig. 5.1D). Together, this suggests that oral infection with unmasked fungal cells may attenuate virulence in a sex dependent manner.

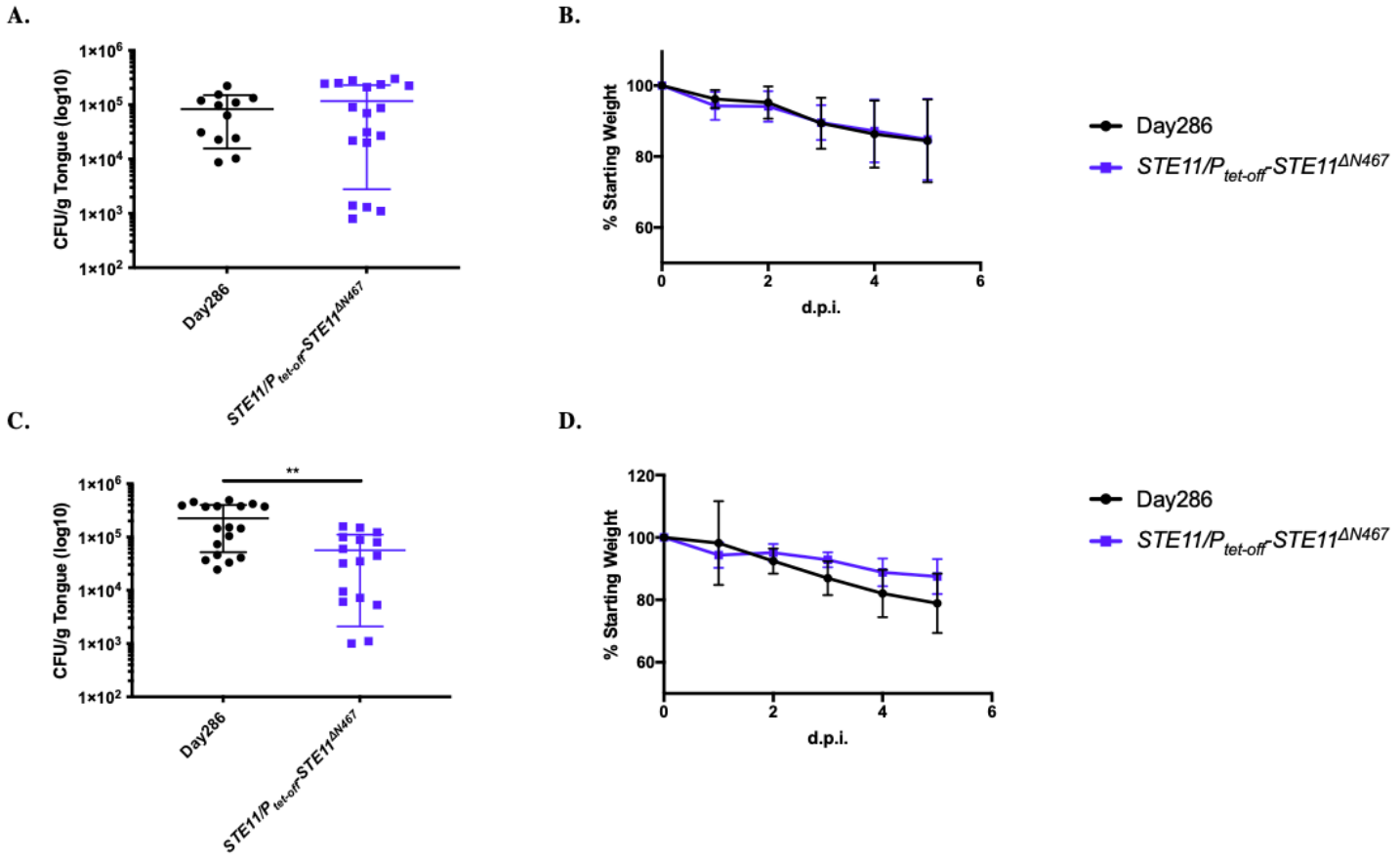


Fig 5.1: Oropharyngeal infection with an unmasked *STE11$^{\Delta N467}$* mutant attenuates tongue fungal burden at 5 days post infection.
Male and female C57BL/6 mice were sublingually infected with 1x10^6 cells of *C. albicans* wild-type (Day286) or the unmasked *STE11/P$_{tet-off}$-STE11$^{\Delta N467}$* mutant. The weights of all mice were then monitored over a five-day period and tongues harvested at 5 d.p.i. to assess disease progression. (A) Tongue fungal burden in female mice at 5 d.p.i. (p=0.8187, by Mann-Whitney Test). (B) Weight trends (as shown as percent of starting weight at day 0) of female mice over the infection period. (B) Tongue fungal burden in male mice at 5 d.p.i. (**p=0.0018, by Mann-Whitney Test). (B) Weight trends (as shown as percent of starting weight at day 0) of male mice over the infection period. (n=7-9 mice per strain).

Oral isolates at 5 days post-infection show suppressor mutations against hyperactive *STE11$^{\Delta N467}$*-induced unmasking.

We have shown that oral infection with an unmasked *STE11/P$_{tet\text{-}off}$STE11$^{\Delta N467}$* mutant leads to a modest virulence attenuation in male mice at 5 days post infection (Fig. 5.1). However, the fitness pressure exerted on this mutant is quite large, as unmasking induces a robust pro-inflammatory immune response upon recognition by both host epithelia and hematopoietic immune cells [16, 24, 34, 37]. With this in mind, we were curious about the possibility of suppressor mutations arising that block the downstream signaling events caused by *STE11$^{\Delta N467}$* expression. As this mutant is heterozygous at the *STE11* allele, mutations that block hyperactive *STE11$^{\Delta N467}$* activity should effectively cause these isolates to behave like wild-type cells through the remaining native *STE11* locus and may alleviate pressure imposed by the surrounding host environment. To assess the presence of suppressor mutants, oral isolates were collected at 5 d.p.i. from both male and female mice that had been infected with the *STE11/P$_{tet\text{-}off}$STE11$^{\Delta N467}$* mutant. Isolates were then immunofluorescently stained with an anti-ß(1,3)-glucan antibody that specifically binds to exposed ß(1,3)-glucan foci and their unmasking was assessed. Surprisingly, all 30 isolates randomly collected from 6 different mice had significant reductions in ß(1,3)-glucan exposure when compared to the *STE11/P$_{tet\text{-}off}$STE11$^{\Delta N467}$* parent strain (Fig. 5.2). Thus, it does indeed appear that suppressor mutations against hyperactive Ste11$^{\Delta N467}$ activity are being positively selected for *in vivo* in the oral cavity.

To further characterize how hyperactive Ste11$^{\Delta N467}$ activity is being suppressed, we next looked at RNA and protein markers for possible clues. One representative isolate from each mouse was used for further analysis. PCR amplification of part of the *P$_{tet\text{-}off}$STE11$^{\Delta N467}$* overexpression gene revealed that all isolates tested retained genetic markers for this cassette (Fig. 5.3A), indicating that all isolates still had the same primary mutation as the *STE11/P$_{tet\text{-}off}$STE11$^{\Delta N467}$* parent strain. We next hypothesized that suppression may be occurring as a consequence of reduced *STE11* transcript levels within the oral isolates. However, while quantitative-reverse transcription (qRT) PCR revealed that some of the isolates screened did indeed have a modest reduction in *STE11* transcript levels when

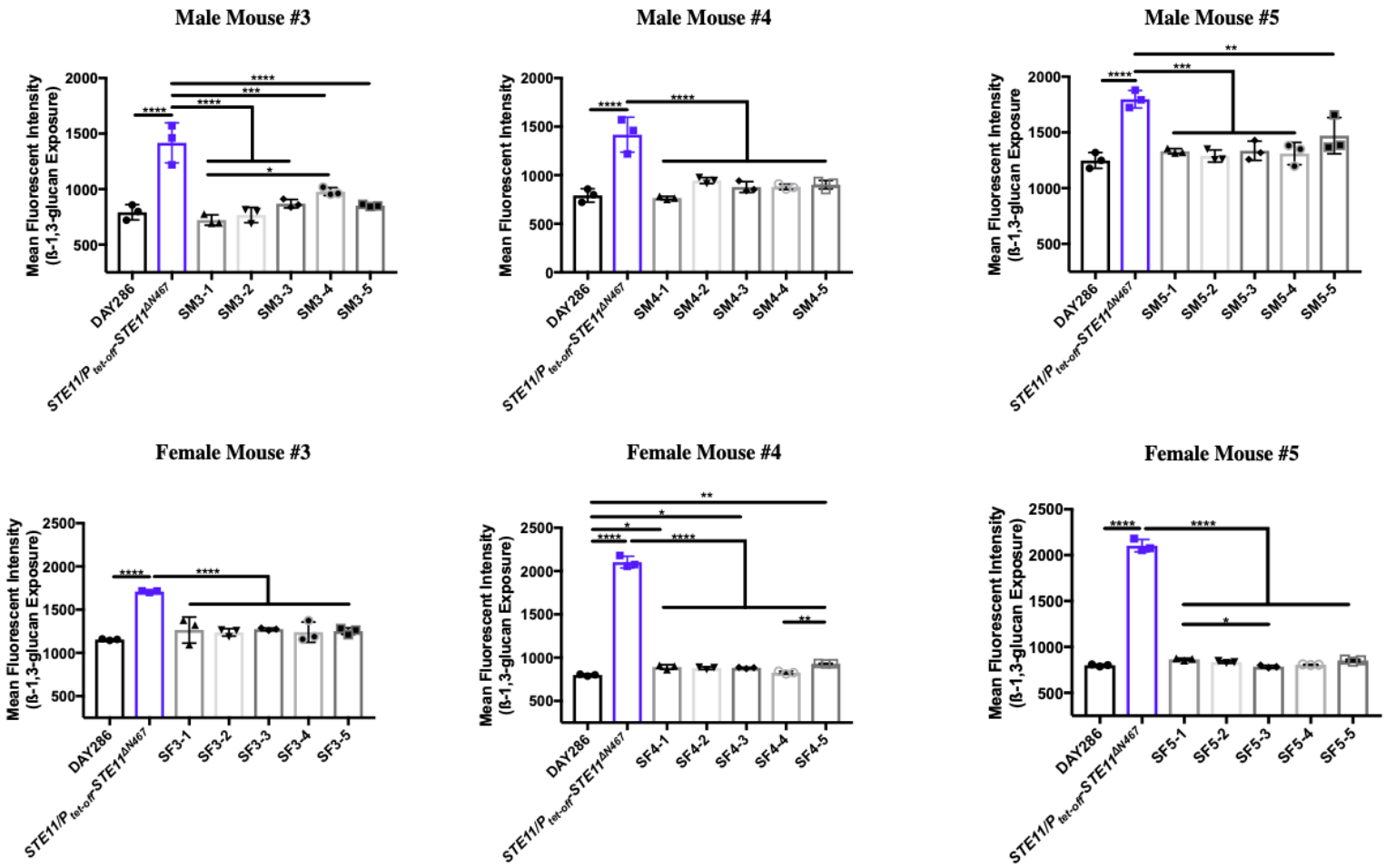


Fig 5.2: *STE11$^{\Delta N467}$* oral isolates collected at 5 days post infection show wild-type levels of ß(1,3)-glucan exposure.
Overnight cultures of *STE11/P$_{tet\text{-}off}$-STE11$^{\Delta N467}$* oral isolates, the *STE11/P$_{tet\text{-}off}$-STE11$^{\Delta N467}$* parental strain and the Day286 wild-type control were stained with anti-ß(1,3)-glucan antibody and a phycoerythrin-conjugated secondary antibody to assess the levels of ß(1,3)-glucan exposure by flow cytometry. (n=3 biological replicates)(*p<0.05, **p<0.01 ***p<0.0005 and ****p<0.0001, by one-way ANOVA).

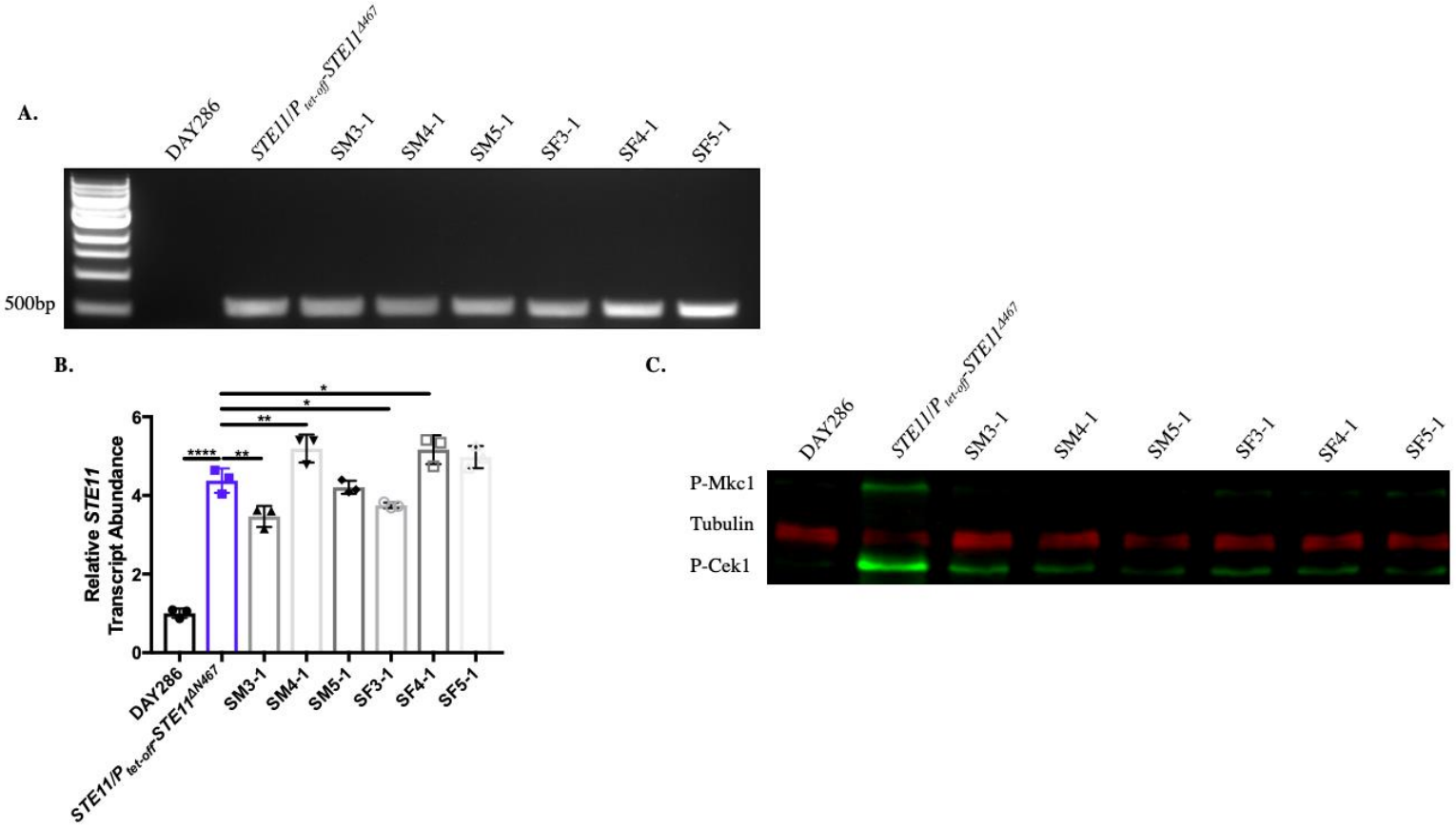


Fig 5.3: *STE11$^{\Delta N467}$* oral isolates collected at 5 days post infection show reduced levels of Cek1 activation.
(A) PCR was used to confirm that all oral isolates retain the parental *$P_{tet\text{-}off}$-STE11$^{\Delta N467}$* mutation that is responsible for hyperactivation of the Cek1 MAPK pathway and subsequent unmasking. (B) *STE11* transcript levels were assessed via qRT-PCR using primers specific to *STE11* mRNA. Cells were grown to mid-log phase (OD_{600} = 0.8) before their RNA was harvested for analysis. (n=3 replicates, shown as the relative transcript abundance compared to the Day286 wild-type control)(*p<0.05, **p<0.01 and ****p<0.0001, by one-way ANOVA). (C) Activation of the Cek1 MAPK in *STE11$^{\Delta N467}$* oral isolates was assessed by collecting proteins from cells grown to mid-log phase for western blot analysis. Activated Cek1 levels were then determined using an anti-P44/42 antibody for phosphorylated Cek1. An anti-tubulin antibody was used as a loading control.

compared to the *STE11/P$_{tet\text{-}off}$STE11$^{\Delta N467}$* parent strain (Fig. 5.3B), no clear correlation across all isolates was observed between altered transcript levels and suppression. With this in mind, we next hypothesized that suppression may be occurring within the signal transduction cascade itself. To test this, we analyzed the activation levels of the MAPK Cek1, which sits downstream of *STE11* in the signal cascade [32-34, 38]. All oral isolates showed reduced levels of phosphorylated (active) Cek1 when compared to the *STE11/P$_{tet\text{-}off}$STE11$^{\Delta N467}$* parent strain (Fig. 5.3C). Thus, although the exact mechanism for suppression is still unknown, it appears that attenuated activation of the downstream MAPK Cek1 is a conserved knockdown strategy amongst suppressed oral isolates.

Virulence attenuation of an unmasked *STE11$^{\Delta N467}$* mutant is more pronounced during early stages of oropharyngeal candidiasis.

Given the observation that *in vivo* selection is occurring for suppressor mutants that attenuate hyperactive Ste11$^{\Delta N467}$ activity, we hypothesized that virulence attenuation during infection with an unmasked *STE11/P$_{tet\text{-}off}$STE11$^{\Delta N467}$* mutant will be greater at earlier time points of infection, before the population has shifted to suppressor mutants with wild-type levels of unmasking. To test this, we repeated the oropharyngeal infection in male C57BL/6 mice and assessed tongue fungal burden at 2 days post infection. Indeed, mice infected with the *STE11/P$_{tet\text{-}off}$STE11$^{\Delta N467}$* mutant had a significant reduction in tongue fungal burden at 2 d.p.i., which corresponded to an ~26-fold reduction in colonization (Fig. 5.4A). This is approximately 6.5-times greater of a difference then was observed at 5 days post infection (Fig. 5.1C). Furthermore, 20% of oral isolates taken at 2 d.p.i. still displayed comparable levels of unmasking to the *STE11/P$_{tet\text{-}off}$STE11$^{\Delta N467}$* parent strain (Fig. 5.4B), whereas 100% of 5 d.p.i. isolates were suppressed and showed wild-type levels of unmasking (Fig. 2). This suggests that a robust immune response and selection for more masked suppressor mutants is occurring early into the infection, and supports the claim that unmasking is detrimental to fungal colonization during OPC.

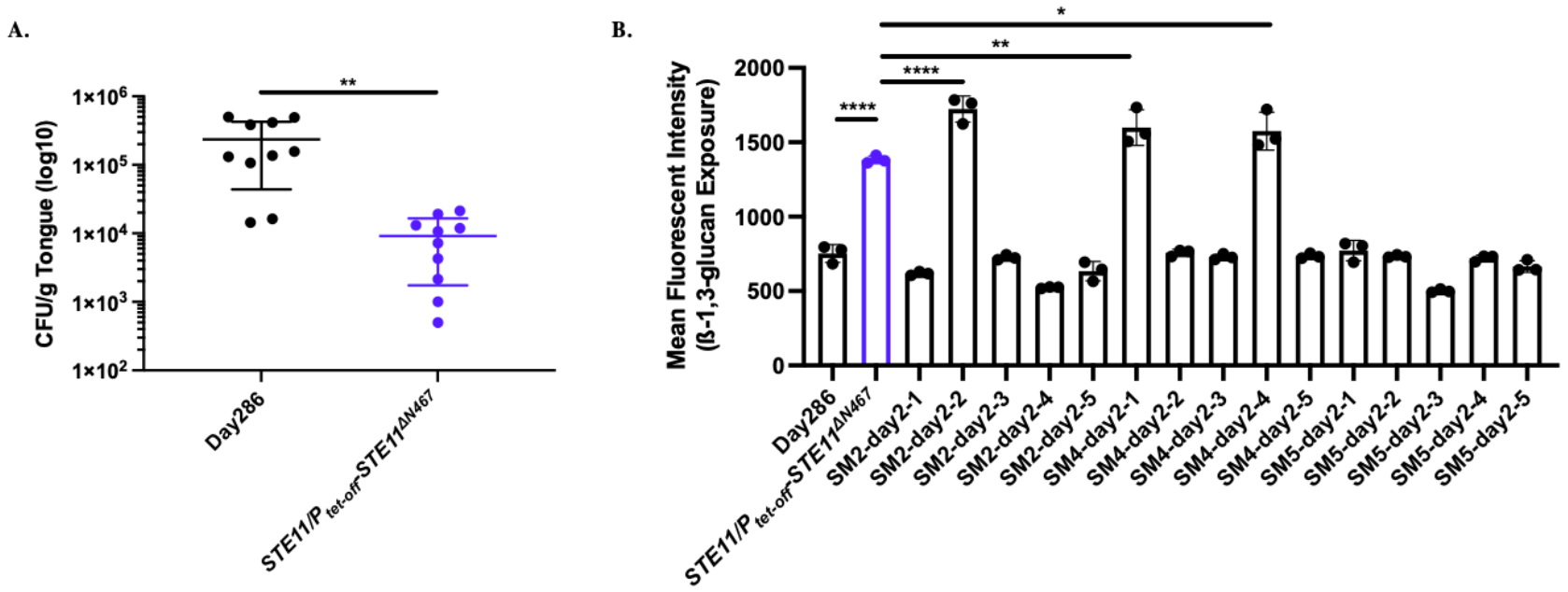


Fig 5.4: Virulence attenuation of the unmasked *STE11$^{\Delta N467}$* mutant is more pronounced early into oropharyngeal infection.
(A) Male C57BL/6 mice were sublingually infected with 1x10^6 cells of *C. albicans* wild-type (Day286) or the unmasked *STE11/P$_{tet-off}$-STE11$^{\Delta N467}$* mutant and their tongues harvested at 2 d.p.i. to assess fungal burden. (n=5-6 mice)(**p=0.0015 by student's t-test). (B) Overnight cultures of *STE11/P$_{tet-off}$-STE11$^{\Delta N467}$* oral isolates collected at 2 d.p.i. were stained with an anti-ß(1,3)-glucan antibody and a phycoerythrin-conjugated secondary antibody to assess the levels of ß(1,3)-glucan exposure by flow cytometry. (n=3 biological replicates)(*p<0.05, **p<0.01 and ****p<0.0001, by one-way ANOVA).

Hyperactivation of the Cek1 MAPK pathway increases immunopathogenesis markers during vulvovaginal candidiasis in mice.

We have thus far shown that infection with an unmasked *STE11/P$_{tet\text{-}off}$STE11$^{\Delta N467}$* mutant attenuates virulence during both systemic infection [33, 34] and oropharyngeal candidiasis in mice (Figs. 5.1&5.4). Given the robust virulence attenuation in both models, we next wished to assess the impact that unmasking may have during a mouse model of vulvovaginal candidiasis (VVC). However, with the strong pro-inflammatory nature of the unmasked *STE11/P$_{tet\text{-}off}$STE11$^{\Delta N467}$* mutant [33, 34] and the observation that neutrophils are not able to effectively clear fungal cells from the vaginal lumen once recruited [39-41], we hypothesized that vulvovaginal infection with an unmasked *STE11/P$_{tet\text{-}off}$STE11$^{\Delta N467}$* mutant will cause increases in immunopathogenesis markers but will not enhance fungal clearance. To test this, C57BL/6 mice were intravaginally inoculated with 5x10^6 cells of either the wild-type or *STE11/P$_{tet\text{-}off}$STE11$^{\Delta N467}$* mutant, and lavage fluids were collected at 3 and 7 d.p.i. to assess fungal burden, neutrophil recruitment, and pro-inflammatory cytokine production within the vaginal lumen. Hyperactivation of the Cek1 pathway in the *STE11/P$_{tet\text{-}off}$-STE11$^{\Delta N467}$* strain was prevented in control conditions *in vivo* by giving mice 2mg/ml doxycycline in their drinking water, which also contains 5% sucrose to encourage consumption. In this condition, the *STE11/P$_{tet\text{-}off}$-STE11$^{\Delta N467}$* strain will behave like the wild-type due to the native *STE11* allele in the genome [33]. The Cek1 pathway was then activated in the *STE11/P$_{tet\text{-}off}$-STE11$^{\Delta N467}$* strain by giving the mice 5% sucrose without doxycycline, leading to *STE11$^{\Delta N467}$* overexpression and unmasking. Fungal burden at both 3 and 7 d.p.i. showed no difference in colonization trends between control and experimental groups (Fig 5.5A), demonstrating that unmasking does not enhance fungal clearance during vaginal infection. However, although there were no differences observed in PMN recruitment at 3 d.p.i., mice infected with the *STE11/P$_{tet\text{-}off}$-STE11$^{\Delta N467}$* strain that did not receive doxycycline in their drinking water (the unmasked condition) showed a significant increase in neutrophils within the vaginal lumen at 7 d.p.i. (Fig. 5.5B). Furthermore, the observed increase in neutrophil recruitment was mirrored by increased levels of IL-1ß at 7 d.p.i., which was not observed at 3 d.p.i. when neutrophil levels were

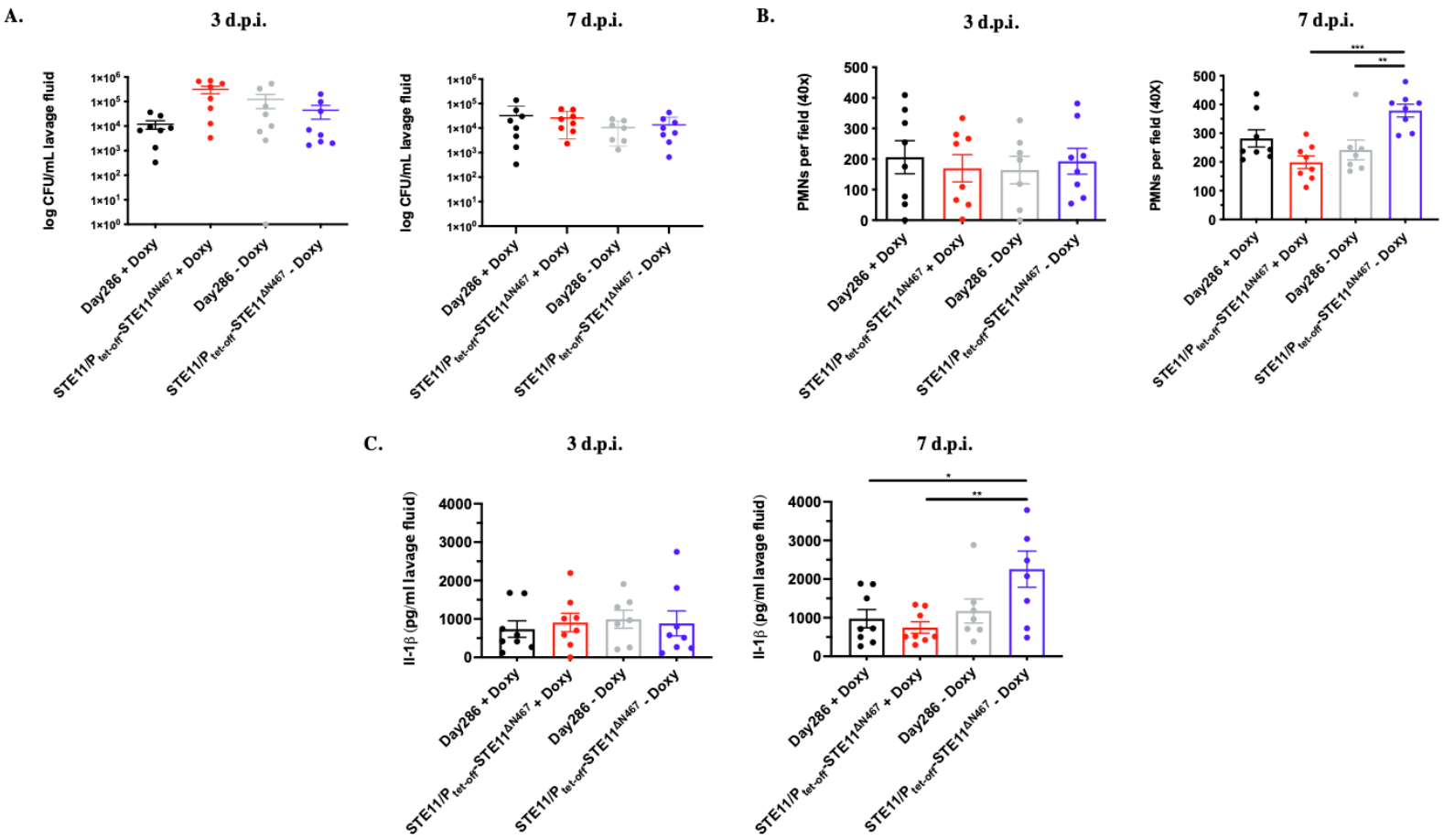


Fig 5.5: Infection with an unmasked *STE11$^{\Delta N467}$* mutant increases immunopathogenesis markers during a murine model of vulvovaginal candidiasis. Estrogen-treated female C57BL/6 mice were intravaginally inoculated with 5x10^6 cells of either the wild-type (Day286) or the unmasked *STE11/P$_{tet\text{-}off}$-STE11$^{\Delta N467}$* mutant. Vaginal lavage fluid was collected at 3 and 7 days post inoculation to assess fungal burden, PMN recruitment and IL-1ß levels within the vaginal lumen. (A) Fungal burden of intravaginally infected mice (n=7-8 mice)($p>0.05$ for all comparisons, by Kruskal-Wallis test). (B) PMN levels within vaginal lavage fluid (**$p<0.01$ and ***$p<0.005$, by one-way ANOVA). (C) IL-1ß levels within vaginal lavage fluid (*$p<0.05$ and **$p<0.01$, by one-way ANOVA).

comparable amongst all infection groups (Fig. 5.5C). Thus, it appears that vulvovaginal infection with an unmasked *STE11/P$_{tet\text{-}off}$-STE11$^{\Delta N467}$* mutant promotes an immunopathogenic environment within the vaginal lumen at 7 d.p.i. but does not promote fungal clearance within this host niche.

Discussion

We have previously shown that hyperactivation of the Cek1 MAPK pathway via expression of a single hyperactive allele of the MAP3K *STE11* induces ß(1,3)-glucan unmasking and attenuates virulence during systemic infection in mice [32-34]. Furthermore, attenuation was found to be dependent on a functional host immune response, and largely depended on the presence of neutrophils to enhance the clearance of unmasked fungal cells [34]. Here, we have expanded this work and assessed the impact that infection with unmasked fungi has in mouse models of the two most common manifestations of candidiasis: OPC and VVC. In doing so, we found that male mice inoculated with the unmasked *STE11/P$_{tet\text{-}off}$-STE11$^{\Delta N467}$* mutant showed attenuated fungal burden in an OPC infection model, and that attenuation is more pronounced earlier in the infection (Figs. 5.1 & 5.4A). Furthermore, we find that during OPC, *in vivo* selection for mutants that have suppressed hyperactive Ste11$^{\Delta N467}$ activity, and thus behave like wild-type cells, occurs early into the infection period (Fig. 5.2 & 5.4B). During VVC, mice infected with the unmasked *STE11/P$_{tet\text{-}off}$-STE11$^{\Delta N467}$* mutant showed comparable levels of fungal burden at 3 and 7 d.p.i. (Fig. 5.5A). However, at 7 d.p.i., mice infected with the unmasked *STE11/P$_{tet\text{-}off}$-STE11$^{\Delta N467}$* mutant displayed higher levels of neutrophil recruitment to the vaginal lumen (Fig. 5.5B) and IL-1ß levels within lavage fluid (Fig. 5.5C). Thus, it appears that mucosal infection with unmasked fungal cells does indeed impact fungal virulence during mucosal infection. However, this impact appears to be niche specific, and does not always promote a favorable outcome for the infected host.

Similar to what we have observed during systemic infection in mice, inoculation with unmasked fungal cells during a murine model of OPC appears to facilitate enhance fungal clearance within the oral cavity in male mice (Fig. 5.1 & 5.4A). Oral epithelial cells display several receptors that are capable of recognizing exposed ß(1,3)-glucan and

initiating an immune response, such as EphA2 and Dectin-1 [23, 24]. Although Dectin-1 has largely been found to be dispensable during OPC [42], loss of EphA2 in either oral epithelia or neutrophils results in increased fungal burden during an OPC infection model [23, 24] and highlights the biological significance that host recognition of ß(1,3)-glucan has on disease progression within the oral cavity. Therefore, it is unsurprising that infection with an unmasked *STE11/P$_{tet\text{-}off}$-STE11$^{\Delta N467}$* mutant attenuates fungal burden during OPC. However, it is important to note that fungal mutants with abnormally high levels of ß(1,3)-glucan exposure have never been assessed in an OPC infection model using either Dectin-1$^{-/-}$ nor EphA2$^{-/-}$ mice, and it may be possible that both Dectin-1 and EphA2 contribute to the immune response to unmasked fungal cells.

Our data has highlighted a sex-based difference in fungal clearance between male and female mice at 5 days post infection (Fig. 5.1). Although evidence suggests that sex plays a role in the disease outcome during systemic infection with an unmasked *ENG1* mutant [31], this is the first study to our knowledge that assesses sex as variable during OPC infection with unmasked fungal cells. It is well established that male and female immune responses vary [43]. Although we do not know the exact mechanism driving the observed sex difference in tongue fungal burden, bone marrow derived macrophages from male mice have been found to more readily differentiate into M1 macrophages and produce more pro-inflammatory cytokines, such as tumor necrosis factor alpha (TNFα), at both basal levels and upon lipopolysaccharide (LPS) stimulation *in vitro* [44, 45]. Macrophages are presumed to be critical drivers in the immune response to unmasked fungal cells, and increased ß(1,3)-glucan exposure has been repeatedly shown to induce TNFα production by macrophages *in vitro* [16, 22, 29, 33, 34]. Therefore, it may be possible that differences in macrophage stimulation may contribute to the observed differences in unmasked fungal cell clearance between the sexes.

The observation that suppressor mutants that block Ste11$^{\Delta N467}$-induced unmasking are positively selected for *in vivo* underscores the biological significance that ß(1,3)-glucan unmasking has during OPC. By 2 d.p.i., 80% of all oral isolates screened displayed wild-type levels of unmasking (Fig. 5.4B), and by 5 d.p.i. this number increased to 100% of the screened isolates (Fig. 5.2). Importantly, as the number of suppressor mutants arose, the

fungal burden trend shifted back toward wild-type levels (Fig. 5.1 & 5.4A). Thus, we propose a model in which unmasked oral isolates are more readily recognized and cleared early into the infection process. This in turn provides a fitness advantage for suppressor mutants with reduced levels of ß(1,3)-glucan exposure, until the population is predominately suppressor isolates that display wild-type-like cell wall architecture and can more effectively colonize the oral cavity. Indeed, suppressor mutants using tetracycline-dependent regulatory systems have been frequently observed in trypanosomes [46-48], highlighting the mutability of this regulatory system. With this in mind, it is likely that unmasking has a more detrimental impact on disease progression within the oral cavity than this data suggests. Yet, reports on the impacts that infection with unmasked *C. albicans* cells have on virulence during OPC have been contradictory. Oral infection with a homozygous knockout of the phosphatidylserine synthase *CHO1*, which displays unmasking, has attenuated tongue colonization as well, but this is confounded by additional auxotrophies that this mutant possesses [49]. Deletion of the phosphatidylinositol-4-kinase *STT4* also displays increased unmasking but did not impact fungal colonization during an OPC infection model in mice [50]. Thus, more work is needed to fully understand the impact that increased ß(1,3)-glucan exposure has during OPC progression.

Unlike the effect that increased ß(1,3)-glucan exposure has during OPC, vulvovaginal infection with unmasked fungal cells appears to stimulate an immunopathogenic environment within the vaginal lumen, and does not enhance fungal clearance. This is evident by the comparable levels of fungal burden between all experimental groups throughout the infection (Fig. 5.5A), and the increase in pro-inflammatory markers such as neutrophils (Fig. 5.5B) and IL-1ß levels (Fig 5.5C) within the vaginal lumen of mice infected with unmasked *STE11/*$P_{tet\text{-}off}$*-STE11*$^{\Delta N467}$ cells. A non-protective role for neutrophils during VVC has been previously observed [39, 40], and it is therefore unsurprising that fungal burden trends are unaltered, even though unmasked *STE11/*$P_{tet\text{-}off}$*-STE11*$^{\Delta N467}$ cells elicit increased neutrophil recruitment. In C57BL/6 mice, heparan sulfate within the vaginal lumen competes with the neutrophil receptor Mac-1 to impair neutrophil recognition of fungal cells [41]. This interaction was reported to function via a competitive inhibition of Mac-1 by heparan sulfate to prevent binding to the pH

regulated antigen 1 protein Pra1. However, Mac-1 has also been shown to directly bind ß(1,3)-glucan [26, 27, 51, 52], and it is possible that heparan sulfate may also impair recognition and effective clearance of unmasked fungal cells within the vaginal lumen. Regardless, the immunopathogenic environment induced by vaginal infection with unmasked fungal cells is consistent with observations previously seen in the literature. A large amount of variability in ß(1,3)-glucan exposure has been observed in clinical vaginal isolates, and increased unmasking has correlated with enhanced immune recognition, neutrophil recruitment and symptom development in individuals [53, 54].

Collectively, our data suggests that infection with an unmasked *STE11/P$_{tet\text{-}off}$-STE11$^{\Delta N467}$* mutant impacts disease progression in a niche specific manner. During candidemia and OPC, unmasking attenuates fungal colonization and provides a beneficial outcome for the host. However, during VVC, fungal cells are not more effectively cleared and increased immunopathogenesis markers are observed. This is significant because leveraging fungal immunogenic epitope exposure is gaining attention as a potential immunotherapeutic strategy to control disease progression [11-14]. However, our findings highlight the importance that niche specificity has on proposed therapeutic approaches, and we suggest that similar studies should be performed for other disease control strategies currently being explored.

Materials and Methods

Ethics statement. All animal work used in this study was done under approved protocols at the University of Tennessee, Knoxville (protocol #0016) or University of Tennessee Health Science Center (UTHSC) (protocol #21-0265) Institutional Animal Care and Use Committees (IACUCs). All work was done in accordance with the National Institute of Health's (NIH) ethical guidelines for animal research.

Growth media and culture conditions. *C. albicans* strains (listed in S5.1 Table) were grown in YPD media (1% yeast extract, 2% peptone, 2% dextrose) at 30°C while shaking at 225 rpm [55]. To repress expression of the tetracycline repressible promoter, 0.5μg/ml of doxycycline (Sigma-Aldrich) was added to the growth media [33].

Mouse model of oropharyngeal candidiasis. The mouse model of oropharyngeal candidiasis was performed as previously described [49, 56]. Briefly, starting 1 day prior to infection, male and female C57BL/6 mice were immunosuppressed via subcutaneous injection with 225mg/kg of cortisone acetate (Sigma-Aldrich) based on their average weights. Immunosuppression was then maintained by recurring injections every 2 days until the experiments' end. One day prior to infection, *C. albicans* strains were grown overnight at 30°C with shaking at 225rpm in 5mL of YPD + 0.5μg/mL doxycycline (to repress premature expression of the hyperactive $P_{tet\text{-}off}$-$STE11^{\Delta N467}$ allele). The following day, the overnight cultures were washed 2 times with 25ml of PBS, counted on a hemocytometer, and then diluted to a concentration of $1x10^6$ cells in sterile Hank's balanced salt solution (HBSS) for inoculation (Invitrogen). Mice were then anesthetized with ketamine and xylazine, and calcium alginate swabs saturated with *C. albicans* were placed sublingually and left to inoculate the oral cavity for 75 minutes. Following inoculation, mice were monitored daily, and their weights were tracked. At 2 or 5 days post infection (d.p.i.), mice were euthanized and their tongues were harvested to assess fungal burden. Once counts were obtained, outliers were determined via an outlier test and distribution normality was assessed with the use of a D'Agostino-Pearson omnibus normality test (GraphPad Prism, v7.0c software). Statistical significance was then determined with the use of either a student's t-test or a Mann-Whitney test (GraphPad Prism, v7.0c software). The number of mice used for each experiment is listed in the figure legend associated with the data and samples were plated with technical duplicates.

Immunofluorescent staining and flow cytometry analysis. ß(1,3)-glucan unmasking was assessed by starting 5ml cultures of yeast cells in YPD the morning prior to staining. Cultures were grown shaking at 225 rpm at 30°C for ~8 hours before being back diluted to an OD_{600} of 0.1 in fresh YPD and incubated with shaking at 225rpm at 30°C overnight. The following morning, cells were diluted to an OD_{600} of 0.5 in PBS and staining to assess ß(1,3)-glucan exposure was performed as previously described [32, 34]. All samples were assessed in biological triplicate and statistical significance was then determined with the

use of a one-way ANOVA with Tukey's post hoc analysis (GraphPad Prism, v7.0c software).

PCR analysis of $P_{tet\text{-}off}STE11^{\Delta N467}$ genomic insert. Oral isolates were assessed for the presence of the hyperactive $P_{tet\text{-}off}STE11^{\Delta N467}$ allele via standard polymerase chain reaction methods with primers TCO168 (5' CTGTTCTTTCATGGTATTCT 3') and TCO169 (5' ACTGATTTATTCAATTGATGG 3') [33]. Successful amplification was assessed by the presence of a 500bp band on a 0.8% agarose gel.

Quantitative-Reverse Transcription (qRT) PCR. To assess *STE11* transcript levels, RNA was extracted as previously described [33]. Following purification, RNA was quantified and diluted to 200ng/μL. Purified RNA was then DNA depleted with the use of a TURBO DNA-free kit (Invitrogen Ambion) following the two step 'rigorous protocol' supplied by the manufacturer. DNA free RNA was then converted to cDNA with a High Capacity cDNA Reverse Transcription kit (Thermofisher) according to the manufacturer's instructions. An additional reaction without reverse transcriptase was performed with each sample to confirm DNA removal. For the reaction, 1μL of cDNA was combined with PowerUp SYBR green master mix. To amplify *STE11* cDNA, primers qEPO65 (5' GGAAGCAGTGGGAGGGAG 3') and qEPO66 (5' GGGAGTGGGAAGAGGAACA 3') were used. *ACT1* cDNA was also quantified as an internal reference control using primers qEPO5 (5' GTGACGACGCTCCAAGAG 3') and qEPO6 (5' GATTGGGCTTCATCACCAAC 3'). qPCR was performed using a QuantStudio3 PCR machine (Applied Biosystems) with the following cycles: 50°C for 2 minutes, 95°C for 2 minutes, 40 cycles of 95°C for 15 seconds and 60°C for 1 minute, followed by a melt curve of 95°C for 15 seconds, 45°C for 1 minute, 95°C for 15 seconds. Changes in transcript levels were then assessed using the Livak ($2^{-\Delta\Delta C_T}$) method.

Western blot analysis of phosphorylated-Cek1. Activated (phosphorylated) levels of Cek1 were assessed as previously described [33].

Murine model of vulvovaginal candidiasis. The murine model of vulvovaginal candidiasis was performed as previously described [40, 57]. Female 6- to 8-week-old C57BL/6 mice (Charles River Laboratories) were administered 0.1mg of estrogen (β-estradiol 17-valerate; Sigma-Aldrich) dissolved in 0.1mL sesame oil subcutaneously 72 hours prior to inoculation with *C. albicans* and weekly thereafter. Expression of the hyperactive *STE11*$^{\Delta N467}$ allele was controlled *in vivo* by giving mice either 5% sucrose water or 5% sucrose + 2mg/ml of doxycycline [33]. Three days prior to infection, all mice were given sucrose water to begin acclimation, and two days prior to infection mice in the appropriate control groups were switched to sucrose water + doxycycline. Bottles containing doxycycline were covered to protect the drug from light and changed every other day. For inoculation, *C. albicans* strains were grown overnight at 30°C with shaking in 5 mL YPD + 0.5μg/mL doxycycline. The following day, stationary phase cultures were washed 3x with sterile PBS and resuspended in 0.4x volume of PBS. Cell suspensions were counted using a hemocytometer and adjusted to $5x10^8$ cells/mL. Mice were intravaginally inoculated with 10μL ($5x10^6$ cells) of this suspension. Mice were then vaginally lavaged at day 3 and day 7 post-inoculation with 100μL PBS. Recovered vaginal lavage fluid was immediately supplemented with 1μL 100X EDTA-free protease inhibitor cocktail (cOmplete; Roche) and kept on ice throughout processing. After aliquots for neutrophil quantification and assessment of fungal burden were removed, remaining vaginal lavage fluid was centrifuged at 3,000rpm for 3 minutes at 4°C. Supernatant was removed and used immediately or stored at -80°C.

To assess fungal burden, vaginal lavage fluid was briefly vortexed to ensure a uniform suspension, and then 10μL of each sample was serially diluted 10-fold in sterile PBS. Using the drop plate method, each dilution was plated in triplicate onto YPD + 50μg/mL chloramphenicol + 0.5μg/mL doxycycline. Plates were incubated for 24 hours at 37°C, and colonies were counted and averaged. Once counts were obtained, distribution normality was assessed with the use of a D'Agostino-Pearson omnibus normality test (GraphPad Prism, v7.0c software) and statistical significance was then determined with the use of a non-parametric Kruskal-Wallis test (GraphPad Prism, v7.0c software). The number of mice used is listed in the figure legend.

PMN quantification

Vaginal lavage fluid was briefly vortexed to ensure a uniform suspension, and 10μL was smeared onto Tissue Path Superfrost Plus Gold slides (Fisher Scientific). Smears were allowed to dry at room temperature, fixed with CytoPrep Cytology Fixative (Fisher Scientific), and stained following the Papanicolaou technique. Using standard light microscopy and a 40X objective, PMNs were manually counted in five nonadjacent fields of view per smear and averaged. Statistical significance was then determined with the use of a one-way ANOVA with Tukey's post hoc analysis (GraphPad Prism, v7.0c software). The number of mice used is listed in the figure legend.

Enzyme-linked immunosorbent assay

Vaginal lavage fluid was assessed for murine IL-1β using the commercially available enzyme-linked immunosorbent assay (ELISA) kit (Invitrogen) according to the manufacturer's protocol. Samples were diluted 1:20 in sample diluent, measured in duplicate, and then averaged. Statistical significance was determined with the use of a one-way ANOVA with Tukey's post hoc analysis (GraphPad Prism, v7.0c software). The number of mice used is listed in the figure legend.

References

1. Patil S, Majumdar B, Sarode SC, Sarode GS, Awan KH. Oropharyngeal Candidosis in HIV-Infected Patients-An Update. Front Microbiol. 2018;9:980. Epub 2018/06/06. doi: 10.3389/fmicb.2018.00980. PubMed PMID: 29867882; PubMed Central PMCID: PMCPMC5962761.

2. Simon D, Page B, Vogel M, Bussmann C, Blanchard C, Straumann A, et al. Evidence of an abnormal epithelial barrier in active, untreated and corticosteroid-treated eosinophilic esophagitis. Allergy. 2018;73(1):239-47. Epub 2017/07/18. doi: 10.1111/all.13244. PubMed PMID: 28712126.

3. Moyes DL, Naglik JR. Mucosal immunity and Candida albicans infection. Clin Dev Immunol. 2011;2011:346307. Epub 2011/07/22. doi: 10.1155/2011/346307. PubMed PMID: 21776285; PubMed Central PMCID: PMCPMC3137974.

4. Vazquez JA. Optimal management of oropharyngeal and esophageal candidiasis in patients living with HIV infection. HIV AIDS (Auckl). 2010;2:89-101. Epub 2010/01/01. doi: 10.2147/hiv.s6660. PubMed PMID: 22096388; PubMed Central PMCID: PMCPMC3218701.

5. Sobel JD. Vaginitis. N Engl J Med. 1997;337(26):1896-903. Epub 1997/12/20. doi: 10.1056/NEJM199712253372607. PubMed PMID: 9407158.

6. Pfaller MA, Diekema DJ. Epidemiology of invasive mycoses in North America. Crit Rev Microbiol. 2010;36(1):1-53. Epub 2010/01/22. doi: 10.3109/10408410903241444. PubMed PMID: 20088682.

7. Benedict K, Whitham HK, Jackson BR. Economic Burden of Fungal Diseases in the United States. Open Forum Infect Dis. 2022;9(4):ofac097. Epub 2022/03/31. doi: 10.1093/ofid/ofac097. PubMed PMID: 35350173; PubMed Central PMCID: PMCPMC8946773.

8. Eggimann P, Garbino J, Pittet D. Management of Candida species infections in critically ill patients. The Lancet Infectious Diseases. 2003;3(12):772-85. doi: 10.1016/s1473-3099(03)00831-4.

9. Perlin DS. Echinocandin Resistance in Candida. Clin Infect Dis. 2015;61 Suppl 6:S612-7. Epub 2015/11/15. doi: 10.1093/cid/civ791. PubMed PMID: 26567278; PubMed Central PMCID: PMCPMC4643482.
10. Whaley SG, Berkow EL, Rybak JM, Nishimoto AT, Barker KS, Rogers PD. Azole Antifungal Resistance in Candida albicans and Emerging Non-albicans Candida Species. Front Microbiol. 2016;7:2173. Epub 2017/01/28. doi: 10.3389/fmicb.2016.02173. PubMed PMID: 28127295; PubMed Central PMCID: PMCPMC5226953.
11. Casadevall A, Pirofski LA. Adjunctive immune therapy for fungal infections. Clin Infect Dis. 2001;33(7):1048-56. Epub 2001/08/31. doi: 10.1086/322710. PubMed PMID: 11528579.
12. Hasim S, Allison DP, Retterer ST, Hopke A, Wheeler RT, Doktycz MJ, et al. beta-(1,3)-Glucan Unmasking in Some Candida albicans Mutants Correlates with Increases in Cell Wall Surface Roughness and Decreases in Cell Wall Elasticity. Infect Immun. 2017;85(1). Epub 2016/11/17. doi: 10.1128/IAI.00601-16. PubMed PMID: 27849179; PubMed Central PMCID: PMCPMC5203643.
13. Childers DS, Avelar GM, Bain JM, Pradhan A, Larcombe DE, Netea MG, et al. Epitope Shaving Promotes Fungal Immune Evasion. mBio. 2020;11(4). Epub 2020/07/09. doi: 10.1128/mBio.00984-20. PubMed PMID: 32636248; PubMed Central PMCID: PMCPMC7343991.
14. Chen T, Wagner AS, Reynolds TB. When Is It Appropriate to Take Off the Mask? Signaling Pathways That Regulate ß(1,3)-Glucan Exposure in Candida albicans. Frontiers in Fungal Biology. 2022;3. doi: 10.3389/ffunb.2022.842501.
15. Wheeler RT, Kombe D, Agarwala SD, Fink GR. Dynamic, morphotype-specific Candida albicans beta-glucan exposure during infection and drug treatment. PLoS Pathog. 2008;4(12):e1000227. Epub 2008/12/06. doi: 10.1371/journal.ppat.1000227. PubMed PMID: 19057660; PubMed Central PMCID: PMCPMC2587227.
16. Wheeler RT, Fink GR. A drug-sensitive genetic network masks fungi from the immune system. PLoS Pathog. 2006;2(4):e35. Epub 2006/05/03. doi:

10.1371/journal.ppat.0020035. PubMed PMID: 16652171; PubMed Central PMCID: PMCPMC1447670.

17. Taylor PR, Brown GD, Reid DM, Willment JA, Martinez-Pomares L, Gordon S, et al. The beta-glucan receptor, dectin-1, is predominantly expressed on the surface of cells of the monocyte/macrophage and neutrophil lineages. J Immunol. 2002;169(7):3876-82. Epub 2002/09/24. doi: 10.4049/jimmunol.169.7.3876. PubMed PMID: 12244185.

18. Brown GD, Taylor PR, Reid DM, Willment JA, Williams DL, Martinez-Pomares L, et al. Dectin-1 is a major beta-glucan receptor on macrophages. J Exp Med. 2002;196(3):407-12. Epub 2002/08/07. doi: 10.1084/jem.20020470. PubMed PMID: 12163569; PubMed Central PMCID: PMCPMC2193936.

19. Brown GD, Gordon S. Immune recognition. A new receptor for beta-glucans. Nature. 2001;413(6851):36-7. Epub 2001/09/07. doi: 10.1038/35092620. PubMed PMID: 11544516.

20. Kennedy AD, Willment JA, Dorward DW, Williams DL, Brown GD, DeLeo FR. Dectin-1 promotes fungicidal activity of human neutrophils. Eur J Immunol. 2007;37(2):467-78. Epub 2007/01/19. doi: 10.1002/eji.200636653. PubMed PMID: 17230442.

21. Cohen-Kedar S, Baram L, Elad H, Brazowski E, Guzner-Gur H, Dotan I. Human intestinal epithelial cells respond to beta-glucans via Dectin-1 and Syk. Eur J Immunol. 2014;44(12):3729-40. Epub 2014/09/25. doi: 10.1002/eji.201444876. PubMed PMID: 25251945.

22. Gow NA, Netea MG, Munro CA, Ferwerda G, Bates S, Mora-Montes HM, et al. Immune recognition of Candida albicans beta-glucan by dectin-1. J Infect Dis. 2007;196(10):1565-71. Epub 2007/11/17. doi: 10.1086/523110. PubMed PMID: 18008237; PubMed Central PMCID: PMCPMC2655640.

23. Swidergall M, Solis NV, Wang Z, Phan QT, Marshall ME, Lionakis MS, et al. EphA2 Is a Neutrophil Receptor for Candida albicans that Stimulates Antifungal Activity during Oropharyngeal Infection. Cell Rep. 2019;28(2):423-33 e5. Epub 2019/07/11. doi:

10.1016/j.celrep.2019.06.020. PubMed PMID: 31291578; PubMed Central PMCID: PMCPMC6638578.

24. Swidergall M, Solis NV, Lionakis MS, Filler SG. EphA2 is an epithelial cell pattern recognition receptor for fungal beta-glucans. Nat Microbiol. 2018;3(1):53-61. Epub 2017/11/15. doi: 10.1038/s41564-017-0059-5. PubMed PMID: 29133884; PubMed Central PMCID: PMCPMC5736406.

25. Millet N, Solis NV, Aguilar D, Lionakis MS, Wheeler RT, Jendzjowsky N, et al. IL-23 signaling prevents ferroptosis-driven renal immunopathology during candidiasis. bioRxiv. 2021:2021.12.19.473386. doi: 10.1101/2021.12.19.473386.

26. van Bruggen R, Drewniak A, Jansen M, van Houdt M, Roos D, Chapel H, et al. Complement receptor 3, not Dectin-1, is the major receptor on human neutrophils for beta-glucan-bearing particles. Mol Immunol. 2009;47(2-3):575-81. Epub 2009/10/09. doi: 10.1016/j.molimm.2009.09.018. PubMed PMID: 19811837.

27. Li X, Utomo A, Cullere X, Choi MM, Milner DA, Jr., Venkatesh D, et al. The beta-glucan receptor Dectin-1 activates the integrin Mac-1 in neutrophils via Vav protein signaling to promote Candida albicans clearance. Cell Host Microbe. 2011;10(6):603-15. Epub 2011/12/20. doi: 10.1016/j.chom.2011.10.009. PubMed PMID: 22177564; PubMed Central PMCID: PMCPMC3244687.

28. Chen YL, Montedonico AE, Kauffman S, Dunlap JR, Menn FM, Reynolds TB. Phosphatidylserine synthase and phosphatidylserine decarboxylase are essential for cell wall integrity and virulence in Candida albicans. Mol Microbiol. 2010;75(5):1112-32. Epub 2010/02/06. doi: 10.1111/j.1365-2958.2009.07018.x. PubMed PMID: 20132453.

29. Davis SE, Hopke A, Minkin SC, Jr., Montedonico AE, Wheeler RT, Reynolds TB. Masking of beta(1-3)-glucan in the cell wall of Candida albicans from detection by innate immune cells depends on phosphatidylserine. Infect Immun. 2014;82(10):4405-13. Epub 2014/08/13. doi: 10.1128/IAI.01612-14. PubMed PMID: 25114110; PubMed Central PMCID: PMCPMC4187869.

30. Herrero AB, Magnelli P, Mansour MK, Levitz SM, Bussey H, Abeijon C. KRE5 gene null mutant strains of Candida albicans are avirulent and have altered cell wall composition and hypha formation properties. Eukaryot Cell. 2004;3(6):1423-32. Epub

2004/12/14. doi: 10.1128/EC.3.6.1423-1432.2004. PubMed PMID: 15590817; PubMed Central PMCID: PMCPMC539026.

31. Yang M, Solis NV, Marshall M, Garleb R, Zhou T, Wang D, et al. Control of beta-glucan exposure by the endo-1,3-glucanase Eng1 in Candida albicans modulates virulence. PLoS Pathog. 2022;18(1):e1010192. Epub 2022/01/08. doi: 10.1371/journal.ppat.1010192. PubMed PMID: 34995333; PubMed Central PMCID: PMCPMC8775328.

32. Chen T, Jackson JW, Tams RN, Davis SE, Sparer TE, Reynolds TB. Exposure of Candida albicans beta (1,3)-glucan is promoted by activation of the Cek1 pathway. PLoS Genet. 2019;15(1):e1007892. Epub 2019/02/01. doi: 10.1371/journal.pgen.1007892. PubMed PMID: 30703081; PubMed Central PMCID: PMCPMC6372213.

33. Chen T, Wagner AS, Tams RN, Eyer JE, Kauffman SJ, Gann ER, et al. Lrg1 Regulates beta (1,3)-Glucan Masking in Candida albicans through the Cek1 MAP Kinase Pathway. mBio. 2019;10(5). Epub 2019/09/19. doi: 10.1128/mBio.01767-19. PubMed PMID: 31530671; PubMed Central PMCID: PMCPMC6751057.

34. Wagner AS, Hancock TJ, Lumsdaine SW, Kauffman SJ, Mangrum MM, Phillips EK, et al. Activation of Cph1 causes ss(1,3)-glucan unmasking in Candida albicans and attenuates virulence in mice in a neutrophil-dependent manner. PLoS Pathog. 2021;17(8):e1009839. Epub 2021/08/26. doi: 10.1371/journal.ppat.1009839. PubMed PMID: 34432857.

35. Huppler AR, Conti HR, Hernandez-Santos N, Darville T, Biswas PS, Gaffen SL. Role of neutrophils in IL-17-dependent immunity to mucosal candidiasis. J Immunol. 2014;192(4):1745-52. Epub 2014/01/21. doi: 10.4049/jimmunol.1302265. PubMed PMID: 24442441; PubMed Central PMCID: PMCPMC3946223.

36. Altmeier S, Toska A, Sparber F, Teijeira A, Halin C, LeibundGut-Landmann S. IL-1 Coordinates the Neutrophil Response to C. albicans in the Oral Mucosa. PLoS Pathog. 2016;12(9):e1005882. Epub 2016/09/16. doi: 10.1371/journal.ppat.1005882. PubMed PMID: 27632536; PubMed Central PMCID: PMCPMC5025078.

37. Galan-Diez M, Arana DM, Serrano-Gomez D, Kremer L, Casasnovas JM, Ortega M, et al. Candida albicans beta-glucan exposure is controlled by the fungal CEK1-

mediated mitogen-activated protein kinase pathway that modulates immune responses triggered through dectin-1. Infect Immun. 2010;78(4):1426-36. Epub 2010/01/27. doi: 10.1128/IAI.00989-09. PubMed PMID: 20100861; PubMed Central PMCID: PMCPMC2849429.

38. Ramirez-Zavala B, Weyler M, Gildor T, Schmauch C, Kornitzer D, Arkowitz R, et al. Activation of the Cph1-dependent MAP kinase signaling pathway induces white-opaque switching in Candida albicans. PLoS Pathog. 2013;9(10):e1003696. Epub 2013/10/17. doi: 10.1371/journal.ppat.1003696. PubMed PMID: 24130492; PubMed Central PMCID: PMCPMC3795047.

39. Black CA, Eyers FM, Russell A, Dunkley ML, Clancy RL, Beagley KW. Acute neutropenia decreases inflammation associated with murine vaginal candidiasis but has no effect on the course of infection. Infect Immun. 1998;66(3):1273-5. Epub 1998/03/06. doi: 10.1128/IAI.66.3.1273-1275.1998. PubMed PMID: 9488427; PubMed Central PMCID: PMCPMC108047.

40. Peters BM, Palmer GE, Nash AK, Lilly EA, Fidel PL, Jr., Noverr MC. Fungal morphogenetic pathways are required for the hallmark inflammatory response during Candida albicans vaginitis. Infect Immun. 2014;82(2):532-43. Epub 2014/01/31. doi: 10.1128/IAI.01417-13. PubMed PMID: 24478069; PubMed Central PMCID: PMCPMC3911367.

41. Yano J, Noverr MC, Fidel PL, Jr. Vaginal Heparan Sulfate Linked to Neutrophil Dysfunction in the Acute Inflammatory Response Associated with Experimental Vulvovaginal Candidiasis. mBio. 2017;8(2). Epub 2017/03/16. doi: 10.1128/mBio.00211-17. PubMed PMID: 28292981; PubMed Central PMCID: PMCPMC5350465.

42. Verma AH, Richardson JP, Zhou C, Coleman BM, Moyes DL, Ho J, et al. Oral epithelial cells orchestrate innate type 17 responses to Candida albicans through the virulence factor candidalysin. Sci Immunol. 2017;2(17). Epub 2017/11/05. doi: 10.1126/sciimmunol.aam8834. PubMed PMID: 29101209; PubMed Central PMCID: PMCPMC5881387.

43. Klein SL, Flanagan KL. Sex differences in immune responses. Nat Rev Immunol. 2016;16(10):626-38. Epub 2016/08/23. doi: 10.1038/nri.2016.90. PubMed PMID: 27546235.

44. Barcena ML, Niehues MH, Christiansen C, Estepa M, Haritonow N, Sadighi AH, et al. Male Macrophages and Fibroblasts from C57/BL6J Mice Are More Susceptible to Inflammatory Stimuli. Front Immunol. 2021;12:758767. Epub 2021/12/07. doi: 10.3389/fimmu.2021.758767. PubMed PMID: 34867999; PubMed Central PMCID: PMCPMC8637417.

45. Chen KE, Lainez NM, Coss D. Sex Differences in Macrophage Responses to Obesity-Mediated Changes Determine Migratory and Inflammatory Traits. J Immunol. 2021;206(1):141-53. Epub 2020/12/04. doi: 10.4049/jimmunol.2000490. PubMed PMID: 33268480; PubMed Central PMCID: PMCPMC8903060.

46. Krieger S, Schwarz W, Ariyanayagam MR, Fairlamb AH, Krauth-Siegel RL, Clayton C. Trypanosomes lacking trypanothione reductase are avirulent and show increased sensitivity to oxidative stress. Mol Microbiol. 2000;35(3):542-52. Epub 2000/02/15. doi: 10.1046/j.1365-2958.2000.01721.x. PubMed PMID: 10672177.

47. Milne KG, Guther ML, Ferguson MA. Acyl-CoA binding protein is essential in bloodstream form Trypanosoma brucei. Mol Biochem Parasitol. 2001;112(2):301-4. Epub 2001/02/27. doi: 10.1016/s0166-6851(00)00369-8. PubMed PMID: 11223138.

48. Martin KL, Smith TK. The glycosylphosphatidylinositol (GPI) biosynthetic pathway of bloodstream-form Trypanosoma brucei is dependent on the de novo synthesis of inositol. Mol Microbiol. 2006;61(1):89-105. Epub 2006/07/11. doi: 10.1111/j.1365-2958.2006.05216.x. PubMed PMID: 16824097; PubMed Central PMCID: PMCPMC3793301.

49. Davis SE, Tams RN, Solis NV, Wagner AS, Chen T, Jackson JW, et al. Candida albicans Cannot Acquire Sufficient Ethanolamine from the Host To Support Virulence in the Absence of De Novo Phosphatidylethanolamine Synthesis. Infect Immun. 2018;86(8). Epub 2018/06/06. doi: 10.1128/IAI.00815-17. PubMed PMID: 29866908; PubMed Central PMCID: PMCPMC6056879.

50. Garcia-Rodas R, Labbaoui H, Orange F, Solis N, Zaragoza O, Filler SG, et al. Plasma Membrane Phosphatidylinositol-4-Phosphate Is Not Necessary for Candida albicans Viability yet Is Key for Cell Wall Integrity and Systemic Infection. mBio. 2022:e0387321. Epub 2022/02/16. doi: 10.1128/mbio.03873-21. PubMed PMID: 35164565; PubMed Central PMCID: PMCPMC8942462.

51. Vetvicka V, Thornton BP, Ross GD. Soluble beta-glucan polysaccharide binding to the lectin site of neutrophil or natural killer cell complement receptor type 3 (CD11b/CD18) generates a primed state of the receptor capable of mediating cytotoxicity of iC3b-opsonized target cells. J Clin Invest. 1996;98(1):50-61. Epub 1996/07/01. doi: 10.1172/JCI118777. PubMed PMID: 8690804; PubMed Central PMCID: PMCPMC507400.

52. Thornton BP, Vetvicka V, Pitman M, Goldman RC, Ross GD. Analysis of the sugar specificity and molecular location of the beta-glucan-binding lectin site of complement receptor type 3 (CD11b/CD18). J Immunol. 1996;156(3):1235-46. Epub 1996/02/01. PubMed PMID: 8558003.

53. Pericolini E, Perito S, Castagnoli A, Gabrielli E, Mencacci A, Blasi E, et al. Epitope unmasking in vulvovaginal candidiasis is associated with hyphal growth and neutrophilic infiltration. PLoS One. 2018;13(7):e0201436. Epub 2018/08/01. doi: 10.1371/journal.pone.0201436. PubMed PMID: 30063729; PubMed Central PMCID: PMCPMC6067721.

54. Gerwien F, Dunker C, Brandt P, Garbe E, Jacobsen ID, Vylkova S. Clinical Candida albicans Vaginal Isolates and a Laboratory Strain Show Divergent Behaviors during Macrophage Interactions. mSphere. 2020;5(4). Epub 2020/08/21. doi: 10.1128/mSphere.00393-20. PubMed PMID: 32817377; PubMed Central PMCID: PMCPMC7407065.

55. Styles C. How to set up a yeast laboratory. Methods Enzymol. 2002;350:42-71. Epub 2002/06/21. doi: 10.1016/s0076-6879(02)50955-1. PubMed PMID: 12073328.

56. Solis NV, Filler SG. Mouse model of oropharyngeal candidiasis. Nat Protoc. 2012;7(4):637-42. Epub 2012/03/10. doi: 10.1038/nprot.2012.011. PubMed PMID: 22402633; PubMed Central PMCID: PMCPMC3671943.

57. Yano J, Fidel PL, Jr. Protocols for vaginal inoculation and sample collection in the experimental mouse model of Candida vaginitis. J Vis Exp. 2011;(58). Epub 2012/01/05. doi: 10.3791/3382. PubMed PMID: 22215135; PubMed Central PMCID: PMCPMC3369659.

Appendix

S5.1 Table: Strains used in this study.

Strain	Genotype	Parent	Source or Reference
DAY286	*ura3::imm434/ura3::imm434, his1::hisG/his1::hisG, pARG4::URA3::arg4::hisG/arg4::hisG*)	SC5314	1
TC147	*STE11/*$P_{tet\text{-}off}$*-STE11*$^{\Delta N467}$	DAY286	2
SM3-1	*STE11/*$P_{tet\text{-}off}$*-STE11*$^{\Delta N467}$ 5 days post infection oral isolate #1 from male mouse #3	TC147	2
SM3-2	*STE11/*$P_{tet\text{-}off}$*-STE11*$^{\Delta N467}$ 5 days post infection oral isolate #2 from male mouse #3	TC147	2
SM3-3	*STE11/*$P_{tet\text{-}off}$*-STE11*$^{\Delta N467}$ 5 days post infection oral isolate #3 from male mouse #3	TC147	This study
SM3-4	*STE11/*$P_{tet\text{-}off}$*-STE11*$^{\Delta N467}$ 5 days post infection oral isolate #4 from male mouse #3	TC147	This study
SM3-5	*STE11/*$P_{tet\text{-}off}$*-STE11*$^{\Delta N467}$ 5 days post infection oral isolate #5 from male mouse #3	TC147	This study
SM4-1	*STE11/*$P_{tet\text{-}off}$*-STE11*$^{\Delta N467}$ 5 days post infection oral isolate #1 from male mouse #4	TC147	This study
SM4-2	*STE11/*$P_{tet\text{-}off}$*-STE11*$^{\Delta N467}$ 5 days post infection oral isolate #2 from male mouse #4	TC147	This study
SM4-3	*STE11/*$P_{tet\text{-}off}$*-STE11*$^{\Delta N467}$ 5 days post infection oral isolate #3 from male mouse #4	TC147	This study
SM4-4	*STE11/*$P_{tet\text{-}off}$*-STE11*$^{\Delta N467}$ 5 days post infection oral isolate #4 from male mouse #4	TC147	This study
SM4-5	*STE11/*$P_{tet\text{-}off}$*-STE11*$^{\Delta N467}$ 5 days post infection oral isolate #5 from male mouse #4	TC147	This study
SM5-1	*STE11/*$P_{tet\text{-}off}$*-STE11*$^{\Delta N467}$ 5 days post infection oral isolate #1 from male mouse #5	TC147	This study
SM5-2	*STE11/*$P_{tet\text{-}off}$*-STE11*$^{\Delta N467}$ 5 days post infection oral isolate #2 from male mouse #5	TC147	This study
SM5-3	*STE11/*$P_{tet\text{-}off}$*-STE11*$^{\Delta N467}$ 5 days post infection oral isolate #3 from male mouse #5	TC147	This study
SM5-4	*STE11/*$P_{tet\text{-}off}$*-STE11*$^{\Delta N467}$ 5 days post infection oral isolate #4 from male mouse #5	TC147	This study
SM5-5	*STE11/*$P_{tet\text{-}off}$*-STE11*$^{\Delta N467}$ 5 days post infection oral isolate #5 from male mouse #5	TC147	This study
SF3-1	*STE11/*$P_{tet\text{-}off}$*-STE11*$^{\Delta N467}$ 5 days post infection oral isolate #1 from female mouse #3	TC147	This study

S5.1 Table Continued

Strain	Genotype	Parent	Source or Reference
SF3-2	*STE11/P*$_{tet\text{-}off}$-*STE11*$^{\Delta N467}$ 5 days post infection oral isolate #2 from female mouse #3	TC147	This study
SF3-3	*STE11/P*$_{tet\text{-}off}$-*STE11*$^{\Delta N467}$ 5 days post infection oral isolate #3 from female mouse #3	TC147	This study
SF3-4	*STE11/P*$_{tet\text{-}off}$-*STE11*$^{\Delta N467}$ 5 days post infection oral isolate #4 from female mouse #3	TC147	This study
SF3-5	*STE11/P*$_{tet\text{-}off}$-*STE11*$^{\Delta N467}$ 5 days post infection oral isolate #5 from female mouse #3	TC147	This study
SF4-1	*STE11/P*$_{tet\text{-}off}$-*STE11*$^{\Delta N467}$ 5 days post infection oral isolate #1 from female mouse #4	TC147	This study
SF4-2	*STE11/P*$_{tet\text{-}off}$-*STE11*$^{\Delta N467}$ 5 days post infection oral isolate #2 from female mouse #4	TC147	This study
SF4-3	*STE11/P*$_{tet\text{-}off}$-*STE11*$^{\Delta N467}$ 5 days post infection oral isolate #3 from female mouse #4	TC147	This study
SF4-4	*STE11/P*$_{tet\text{-}off}$-*STE11*$^{\Delta N467}$ 5 days post infection oral isolate #4 from female mouse #4	TC147	This study
SF4-5	*STE11/P*$_{tet\text{-}off}$-*STE11*$^{\Delta N467}$ 5 days post infection oral isolate #5 from female mouse #4	TC147	This study
SF5-1	*STE11/P*$_{tet\text{-}off}$-*STE11*$^{\Delta N467}$ 5 days post infection oral isolate #1 from female mouse #5	TC147	This study
SF5-2	*STE11/P*$_{tet\text{-}off}$-*STE11*$^{\Delta N467}$ 5 days post infection oral isolate #2 from female mouse #5	TC147	This study
SF5-3	*STE11/P*$_{tet\text{-}off}$-*STE11*$^{\Delta N467}$ 5 days post infection oral isolate #3 from female mouse #5	TC147	This study
SF5-4	*STE11/P*$_{tet\text{-}off}$-*STE11*$^{\Delta N467}$ 5 days post infection oral isolate #4 from female mouse #5	TC147	This study
SF5-5	*STE11/P*$_{tet\text{-}off}$-*STE11*$^{\Delta N467}$ 5 days post infection oral isolate #5 from female mouse #5	TC147	This study
SM2-day2-1	*STE11/P*$_{tet\text{-}off}$-*STE11*$^{\Delta N467}$ 2 days post infection oral isolate #1 from male mouse #2	TC147	This study
SM2-day2-2	*STE11/P*$_{tet\text{-}off}$-*STE11*$^{\Delta N467}$ 2 days post infection oral isolate #2 from male mouse #2	TC147	This study
SM2-day2-3	*STE11/P*$_{tet\text{-}off}$-*STE11*$^{\Delta N467}$ 2 days post infection oral isolate #3 from male mouse #2	TC147	This study
SM2-day2-4	*STE11/P*$_{tet\text{-}off}$-*STE11*$^{\Delta N467}$ 2 days post infection oral isolate #4 from male mouse #2	TC147	This study
SM2-day4-3	*STE11/P*$_{tet\text{-}off}$-*STE11*$^{\Delta N467}$ 2 days post infection oral isolate #3 from male mouse #4	TC147	This study
SM2-day4-4	*STE11/P*$_{tet\text{-}off}$-*STE11*$^{\Delta N467}$ 2 days post infection oral isolate #4 from male mouse #4	TC147	This study

S5.1 Table Continued

Strain	Genotype	Parent	Source or Reference
SM2-day4-5	*STE11/P*$_{tet\text{-}off}$*-STE11*$^{\Delta N467}$ 2 days post infection oral isolate #5 from male mouse #4	TC147	This study
SM2-day5-1	*STE11/P*$_{tet\text{-}off}$*-STE11*$^{\Delta N467}$ 2 days post infection oral isolate #1 from male mouse #5	TC147	This study
SM2-day5-2	*STE11/P*$_{tet\text{-}off}$*-STE11*$^{\Delta N467}$ 2 days post infection oral isolate #2 from male mouse #5	TC147	This study
SM2-day5-3	*STE11/P*$_{tet\text{-}off}$*-STE11*$^{\Delta N467}$ 2 days post infection oral isolate #3 from male mouse #5	TC147	This study
SM2-day5-4	*STE11/P*$_{tet\text{-}off}$*-STE11*$^{\Delta N467}$ 2 days post infection oral isolate #4 from male mouse #5	TC147	This study
SM2-day5-5	*STE11/P*$_{tet\text{-}off}$*-STE11*$^{\Delta N467}$ 2 days post infection oral isolate #5 from male mouse #5	TC147	This study

References:

1. Davis DA, Bruno VM, Loza L, Filler SG, Mitchell AP. Candida albicans Mds3p, a conserved regulator of pH responses and virulence identified through insertional mutagenesis. Genetics. 2002;162(4):1573-81. Epub 2003/01/14. PubMed PMID: 12524333; PubMed Central PMCID: PMCPMC1462392.

2. Chen T, Wagner AS, Tams RN, Eyer JE, Kauffman SJ, Gann ER, et al. Lrg1 Regulates beta (1,3)-Glucan Masking in Candida albicans through the Cek1 MAP Kinase Pathway. mBio. 2019;10(5). Epub 2019/09/19. doi: 10.1128/mBio.01767-19. PubMed PMID: 31530671; PubMed Central PMCID: PMCPMC6751057.

CHAPTER 6 - CONCLUSIONS AND FUTURE DIRECTIONS

In this dissertation we have a shown a clear connection between altered ß(1,3)-glucan exposure and virulence. However, although we have begun to disentangle the signal transduction pathways that are important for mediating these changes and have shown preliminary evidence on the role that certain immune cells play *in vivo*, there remain significant questions in both cell physiology and immunology that must be addressed. In this chapter, we will break down the remaining questions into core components on physiology and immunology, highlighting areas where we have expanded the field, and the remaining paths of investigation that can be pursued.

Regulation of ß(1,3)-glucan exposure in *C. albicans*.

What are Cph1 effector proteins that mediate ß(1,3)-glucan unmasking?

In chapters 2 and 3 we showed that hyperactivation of the Cek1 MAPK pathway induces unmasking both directly and via stimulation of the calcineurin signal transduction pathway. Although we were able to utilize public datasets to identify effector proteins for unmasking within the calcineurin regulon, it is still unknown what genes within the direct control of Cph1 also impact this phenotype. Indeed, loss of Cph1 reveals that this transcription factor is the major driver of unmasking during hyperactivation of the Cek1 MAPK pathway (Fig. 2.4B), as calcineurin inhibition only modestly reduces the observed ß-glucan exposure (Fig. 3.1A-B). Therefore, further pursuit of these targets may highlight potent effector proteins of unmasking. One way to address this is to utilize the different hyperactive *STE11$^{\Delta N467}$* mutants that have been generated in our lab. The work done on signal transduction in this dissertation has been performed in the SC5314 laboratory strain, and during *STE11$^{\Delta N467}$* expression we see a specific hyperactivation of only the Cek1 MAPK pathway (Fig. 2.6). However, unmasking induced by *STE11$^{\Delta N467}$* expression was first performed in the Day286 laboratory strain. In this background, RNA sequencing identified 109 potential target genes that are differentially regulated during *STE11$^{\Delta N467}$* expression [1]. Yet, in addition to Cek1 hyperactivation, activation of the MAPK Mkc1 is also increased in this strain background. Therefore, repeating the RNA sequencing in the hyperactive *STE11$^{\Delta N467}$* mutants in these two strain backgrounds, along with the *STE11$^{\Delta N467}$cph1Δ/Δ* and *STE11$^{\Delta N467}$dfi1Δ/Δ* double mutants, should allow us to generate three regulons: one consisting of genes within the control of Cph1, another of genes downstream of Mkc1 and a third of genes within the calcineurin regulon. Given the role for each of these signal transduction pathways in mediating ß-glucan exposure in response to various stimuli, the newly generated datasets should not only refine the list of potential

effector proteins downstream of Cph1 but will also give important insights into the crosstalk between these pathways once one of them is perturbed.

How is signal transduction decision making achieved?

Possibly the most biologically significant question that can be asked from the work presented in this dissertation is how signal transduction through conserved nodes activates different downstream transcription factors to mediate specific stimulus dependent responses? In chapter 2, we showed that unmasking via hyperactive *STE11*$^{\Delta N467}$ functions through the transcription factor Cph1. However, the Cek1 MAPK pathway is also capable of activating Ace2, an alternative downstream transcription factor [2]. Furthermore, *ACE2* knockout mutants have been shown to display increased ß-glucan exposure [3], and preliminary results from our lab suggest that overexpression of *ACE2* in a hyperactive *STE11*$^{\Delta N467}$ background is also capable of partially reducing the unmasking induced by this mutant (data not shown). Collectively, this presents a model in which a conserved signal transduction pathway can either increase or decrease ß-glucan exposure by directed activation of an appropriate downstream transcription factor. Interestingly, previously reported ChIP-chip and transcriptomics analyses on both Cph1 and Ace2 have shown unique regulatory patterns for genes within the Cek1 MAPK pathway, with little overlap between them (with the exception of *CEK1*) (Fig. 6.1) [1, 2, 4]. We hypothesize that it is the overexpression of these nodes within the pathway that drive signal transduction to the appropriate transcription factor. Indeed, this is supported by observations made during response to α-pheromone presence in mating-competent *C. albicans* cells. *C. albicans* cells capable of responding to α-pheromone exhibit one of two phenotypes; sterile white cells or the mating-competent opaque morphology. Both cell types sense α-pheromone through the same G-coupled protein receptor that stimulates activation of the Cek1 MAPK pathway [5]. However, the transcription factor activated by α-pheromone binding differs between cell types, as white cells activate Tec1 to induce biofilm formation [6] and opaque cells activate Cph1 to promote mating [5]. Interestingly, Scaduto *et al.* have shown that simultaneous overexpression of specific components in the Cek1 MAPK pathway (*STE4*, *CST5*, and *CEK2*) is enough to make white locked cells mate at levels comparable to the mating-competent opaque cells, and suggests a bottleneck in which the expression levels of specific genes in the signal cascade can direct signal transduction through a specific transcription factor [7]. Given the

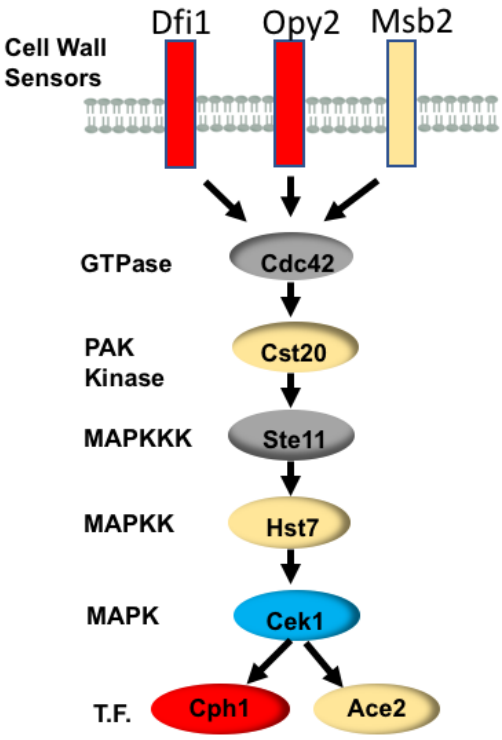


Fig 6.1: Cph1 and Ace2 regulate specific nodes within the Cek1 MAPK Pathway.
Proteins in yellow indicate genes within the Ace2 regulon. Proteins in red indicate genes within the Cph1 regulon. Blue proteins indicate shared genes in the pathway within both Ace2 and Cph1 regulons.

differential expression profiles of the various components in the Cek1 MAPK pathway that are regulated by either Cph1 or Ace2, we may be able to shuttle signal transduction toward a specific transcription factor by overexpression of these various upstream components. Overexpression of these genes should be assessed both individually and in combination, and transcription factor activation can be measured via fluorescent reporter strains for *CPH1* and *ACE2* or by tagging the proteins and assessing total levels and phosphorylation status.

In addition to the Cek1 MAPK pathway, the stimulus-dependent impact that calcineurin has on ß-glucan exposure may also serve as a model to begin to address this same question. Calcineurin either increases or decreases unmasking in response to 3 different stimuli (Chapter 3), and this is in part mediated by directed activation of the downstream transcription factor Crz1 to induce masking specifically (Fig. 3.2D-F). Although we do not currently know the transcription factors mediating calcineurin-induced unmasking, this begs the question as to how directed activation of Crz1 is achieved specifically in response to calcium. Interestingly, when hyperactive $STE11^{\Delta N467}$ cells are grown in the presence of exogenous calcium, the unmasking observed is reduced to only 40% of the ß-glucan exposure observed in $STE11^{\Delta N467}$ cells grown in YPD. This suggests a dominant role for calcium in directing calcineurin activity in these cells. It would therefore be interesting to see where calmodulin and calcineurin localize within the cytoplasm in response to these different stimuli. During $STE11^{\Delta N467}$ expression, we predict that calmodulin will be co-localized to the plasma membrane as it interacts with Dfi1 (which should be tagged as well). However, this interaction may be impaired during heavy influx of calcium into the cell, and calmodulin localization is directed elsewhere. If altered distribution of these proteins are indeed observed, then it may be possible to use proximity labeling to identify protein clusters with which calmodulin/calcineurin interact to activate alternative transcription factors and induce opposing phenotypes for ß-glucan exposure.

What directs chitin synthesis and unmasking in response to caspofungin exposure?

In chapter 4 we showed a strong correlation between calcineurin and Mkc1-mediated chitin synthesis and unmasking. However, several major questions remain about how these signal

cascades are coordinated in response to caspofungin to induce chitin synthesis, and presumably unmasking, at specific locations within the cell wall. A good place to begin is to investigate transcription factors that have been shown to be important for the cell wall damage response to caspofungin, and that putatively sit within the Mkc1 regulon. These include Rlm1, Sko1 and Cas5 [8]. Using knockout mutants for these genes, we can assess chitin and unmasking trends in response to caspofungin exposure. If any follow comparable trends seen in the *MKC1* knockout studies (Fig 4.4), we can then epistatically test if these proteins sit within the Mkc1 regulon to mediate the appropriate drug-induced cell wall changes. This can be done both genetically, by either knocking or overexpressing these transcription factors in a *MKC1* knockout, and by using qRT-PCR to assess the expression profiles of these targets during caspofungin exposure in the wild-type and *MKC1* knockout strains. Indeed, preliminary studies looking into this are already underway in our lab.

In addition to identifying downstream transcription factors that mediate caspofungin-induced chitin synthesis and unmasking, it is important to also beginning assessing how chitin synthesis is directed to specific foci within the cell wall to mediate these changes. Our data suggest that unmasking occurs at points of increased chitin synthesis at the poles of budding cells during caspofungin exposure (Fig. 5.1). Chitin is the last polymer deposited in the cell wall of budding daughter cells in *S. cerevisiae* [9, 10], and increased chitin synthesis is likely the consequence of a weakened cell wall at these points. Interestingly, phosphatidylinositol 4,5 biphosphate ($PI(4,5)P_2$), an important precursor of secondary messengers, has been shown to co-localize with areas of increased chitin within the cell wall in response to caspofungin [11]. $PI(4,5)P_2$ is a known regulator of Rho1 (the upstream GTPase of Mkc1) in *S. cerevisiae* [12], and we have shown that expression of a hyperactive allele of Rho1 is also capable of inducing unmasking in *C. albicans* [13]. Therefore, it may be that increased concentrations of $PI(4,5)P_2$ mediate Rho1 activation at weakened end points within the cell wall. Indeed, $PI(4,5)P_2$ accumulation has been postulated to then direct inappropriate localization of septins (known regulators of chitin synthesis) to these altered foci in response to caspofungin to induce these changes [11]. We have plasmid constructs that will allow us to assess the locations of $PI(4,5)P_2$ (by expression of a GFP protein bound to a tandem repeat of pleckstrin homology domains),

active Rho1(by expression of a GFP protein bound to a Rho1interactive domain (RID) that specifically binds active GTP-bound Rho1) and two septins (Cdc10-RFP and Sep7-GFP) that have been shown to colocalize with pockets of chitin in response to caspofungin [11]. We can therefore transform each of these into our wild-type background and look to see if they co-localize with areas of increased unmasking and chitin synthesis in our strains.

In addition to elucidating the regulatory mechanisms directing chitin synthesis to specific points within the cell wall, we must also further assess the impact that other chitin synthases play in this response. Chs3 is the major chitin synthase driving chitin synthesis in response to caspofungin treatment [14], and its cellular levels correspond nicely to cells with increased unmasking and chitin (Fig. 4.8). However, Chs3 is only one of four enzymes within this family that mediate chitin synthesis [15]. Indeed, both calcineurin and Mkc1 have been shown to regulate multiple chitin synthases in response to various stimuli [14, 16]. Therefore, these proteins should also be tagged, and their distribution and expression levels assessed in wild-type, calcineurin-inhibited and *mkc1Δ/Δ* cells exposed to caspofungin.

Host responses to infection with unmasked fungal cells.

What are the impacts that the various host PRRs have in response to infection?

In chapters 2, 3 and 5 we showed a clear connection between altered ß-glucan exposure and virulence. Importantly, we have shown that these responses are driven by the host immune system (Figs 2.2 and 3.6) and are not the consequence of *in vivo* fitness defects in the unmasked mutants. Given these observations, it is important to now start to assess how unmasked fungal cells are sensed by the host. Both hematopoietic and non-hematopoietic cells express pattern recognition receptors (PRRs) that are capable of sensing exposed ß(1,3)-glucan to initiate an immune response. These include dectin-1 [17-22], EphA2 [23, 24] and complement receptor 3 [25, 26], and loss of any of these host PRRs have been shown to impact disease progression in mice. Given these observations, a comprehensive examination on the role that these host PRRs play during infection with unmasked fungal cells is needed. Repeating systemic, oropharyngeal (OPC), and vulvovaginal (VVC) infections in knockout mice for each of these receptors would allow us to not only get an

idea of the role that these host PRRs have during infection with unmasked fungal cells, but would also give valuable insights into how they differ depending on the anatomical location in which the infection is occurring. This is significant, as a wholistic understanding of how these different receptors respond during infection within the various host tissues remains poorly understood. For example, although vaginal epithelia express EphA2, the impact that this host PRR has during VVC is unknown. Similarly, CR3 has only been assessed in the context of systemic infection, where it functions in the activation of neutrophils [25, 26]. Given the role that neutrophils play in both OPC and VVC [23, 27, 28], investigation into how disease progresses in CR3 knockout mice is needed for both infection models as well.

If knockout mice are obtained, several assays can be performed to assess their impact on disease progression. Along with the standard measures of virulence used in the Reynolds lab (fungal burden, survival curves for systemic infection, weight loss trends for OPC), it will be important to collect both serum and tissue homogenate for assessing local and global cytokine production. Cross comparison between the different knockout strains will therefore allow a more thorough understanding on how each of these receptors contribute to host signaling during disease progression with unmasked fungal cells. Furthermore, adoptive transfer assays may also be applicable to help discriminate between cell types in which these receptors may be contributing to infection (hematopoietic vs. non-hematopoietic). Finally, we are in the process of developing a panel to assess immune cell recruitment to the kidney. A similar assay may be performed for the oral model (tongue) to get an idea of how these receptors mediate immune cell recruitment to these different host niches. Given the selective pressure in the oral cavity for suppressed *STE11*$^{\Delta N467}$ mutants *in vivo* (Chapter 5), I would recommend doing preliminary infections using the *fgr41*Δ/Δ mutant, as this is more stable. However, our data suggest that much of the immune response is occurring early into the infection (Chapter 5). It would therefore be important to assess these changes at early timepoints (1- or 2-days post infection). Doing this may also help alleviate some of the issues of population shifts towards suppressed *STE11*$^{\Delta N467}$ cells *in vivo,* and would make it possible to assess more of our collection of unmasked mutants.

What are the roles of other myeloid derived immune cells?

In chapter 2, we showed that immunocompetent mice systemically infected with an unmasked *STE11$^{\Delta N467}$* mutant showed a 33-fold decrease in fungal burden when compared to mice infected with the wild-type control (Fig. 2.1). Importantly, broad-range immunosuppression induced by cyclophosphamide treatment restored the fungal burden difference to only a 2-fold reduction in *STE11$^{\Delta N467}$* infected mice (Fig. 2.2B). Neutrophil specific depletion was also able to recapitulate much of this phenotype (Fig. 2.2E). However, although 1A8 mediated neutrophil depletion showed only a 6-fold difference in fungal burden between wild-type and *STE11$^{\Delta N467}$* infected mice, it was unable to restore colonization trends to the 2-fold difference seen during cyclophosphamide-induced immunosuppression. This indicates a role for other immune cells in the clearance of unmasked *STE11$^{\Delta N467}$* cells during systemic infection. Macrophages and monocytes harbor receptors that are capable of recognizing ß(1,3)-glucan [22, 29, 30], and *in vivo* mouse model studies of disseminated candidiasis suggest an impact for both cell types on proper fungal clearance [30-33]. Therefore, it is likely that attenuation during systemic infection is also mediated by both tissue resident macrophages and infiltrating immune cells of the monocytic lineage, namely pro-inflammatory monocytes and monocyte-derived macrophages, when mice are infected with unmasked *C. albicans* cells.

C-C chemokine receptor 2 knockout (*Ccr2$^{-/-}$*) mice can be used to assess the impact that immune cells of the monocytic lineage have on mediating fungal clearance during systemic infection with an unmasked *STE11$^{\Delta N467}$* mutant. These mice are deficient in monocyte egress from the bone marrow and have served as a model to study the impact that recruited pro-inflammatory monocytes and downstream cell types within the monocytic lineage have on controlling *C. albicans* infection [30, 32-34]. Furthermore, these mice retain wild-type levels of tissue resident macrophages (TRMs) [32], and thus provide a means for separation of these macrophage lineages in understanding their role in mediating virulence attenuation. TRMs can be assessed by their additional depletion in *Ccr2$^{-/-}$* mice via the use of an anti-mouse colony stimulating factor 1 receptor (CSF-1R) monoclonal antibody (AFS98). CSF-1R is the receptor for macrophage-CSF and is present on macrophages as well as monocyte subsets within peripheral blood [35, 36]. AFS98

treatment will therefore target circulatory monocytes harboring CSF-1R (which are already deficient for tissue recruitment in *Ccr2*$^{-/-}$ mice) and has been extensively shown to induce successful depletion of TRM populations as well [35, 37-40]. Thus, *Ccr2*$^{-/-}$ mice treated with AFS98 will be deficient in both the recruitment of circulatory monocytes and in their ability to sense dissemination by TRMs. Assessing survival, fungal burden, tissue and peripheral cytokine levels, and immune cell recruitment into the kidney will therefore give valuable insights into the role that these immune cells play in the immune response to fungal infection during systemic infection.

What host responses are specific to ß(1,3)-glucan exposure?

This dissertation has shown a consistent impact that mutants with altered ß(1,3)-glucan exposure (specifically *STE11*$^{\Delta N467}$, *fgr41Δ/Δ* and *cwp419Δ/Δ*) have on levels of virulence during systemic infection in mice (Chapters 2 and 3). Importantly, the current collection of mutants also shows stepwise changes in the levels of unmasking observed, as *cwp419Δ/Δ* has the lowest levels of ß-glucan exposure, followed by *STE11*$^{\Delta N467}$, and then *fgr41Δ/Δ* cells. However, in addition to altered unmasking, each of these mutants also display unique profiles for changes in other cell wall components when compared to the wild-type (Figs. 2.4 and S3.2). For example, both the hyperactive *STE11*$^{\Delta N467}$ and *fgr41Δ/Δ* mutants have increased levels of total chitin (which is not seen in the *cwp419Δ/Δ* mutant), but only *STE11*$^{\Delta N467}$ cells also displays a robust increase in exposed chitin. Furthermore, the *fgr41Δ/Δ* strain is the only mutant to show increased levels of mannan within the cell wall. Each of these components within the cell wall have immunogenic properties that are capable of shaping the host immune response during infection [41]. Thus far in this dissertation, their contributions have been overlooked, and the role that they play in shaping the immune response must be accounted for.

Utilizing a combination of both *in vitro* and *in vivo* assays with each of these unmasked mutants may allow us to identify host responses that are specific to each cell wall component. As a proof of concept, we have performed *in vitro* tissue culture assays using wild-type, *STE11*$^{\Delta N467}$, *fgr41Δ/Δ* and *cwp419Δ/Δ* mutants co-incubated with macrophages to assess the impact that these various cell wall components have on cytokine

production. Interestingly, we observed a stepwise increase in only TNFα and CCL2 levels that corresponded linearly with unmasking specifically, where mutants that were more unmasked induced higher levels of production of both cytokines (data not shown). However, as this assay only includes one subset of immune cells, this data is limited on how it can be interpreted to translate to an *in vivo* setting. Therefore, it is necessary to repeat the systemic infections with each of these mutants and to assess the local inflammatory immune responses. Specifically, what does the cytokine profile within the kidney look like during infection (which can be measured via Luminex cytokine array kits) and how does influx of different immune cells change in response to altered levels of each of these cell wall components (which can be measured via flow cytometry)? Shared responses to each of the unmasked mutants (but not the wild-type) would be indicative of a conserved host immune response to exposed ß(1,3)-glucan, while unique responses to infection with *STE11*$^{\Delta N467}$ or *fgr41Δ/Δ* cells would be suggestive of a response to increases in exposed chitin and mannan, respectively. If changes are observed, this can then be verified by repeating these infections using mice harboring global knockouts for various PRRs that can recognize each of these cell wall epitopes. For example, does infection in dectin-1$^{-/-}$ mice ablate the conserved changes seen in response to infection with each of these mutants? Or, if a unique response to *STE11*$^{\Delta N467}$ is observed, does infection in a LYSMD3$^{-/-}$ (an epithelial chitin receptor) mouse block those changes as well? If this approach works, this will significantly increase our understanding of how the host responds to altered levels of specific cell wall components, as the methods often used to do so are confounded by pleiotropic changes to multiple cell wall epitopes or are limited to purified particles of the various cell wall constituents and do not reflect infection with an intact fungal cell. One important note on the design of this assay is that it appears that the host immune response is primarily occurring early into the infection period (Chapter 5). Therefore, harvesting the various tissues should be performed at early time points following intravenous injection.

References

1. Chen T, Wagner AS, Tams RN, Eyer JE, Kauffman SJ, Gann ER, et al. Lrg1 Regulates beta (1,3)-Glucan Masking in Candida albicans through the Cek1 MAP Kinase Pathway. mBio. 2019;10(5). Epub 2019/09/19. doi: 10.1128/mBio.01767-19. PubMed PMID: 31530671; PubMed Central PMCID: PMCPMC6751057.

2. van Wijlick L, Swidergall M, Brandt P, Ernst JF. Candida albicans responds to glycostructure damage by Ace2-mediated feedback regulation of Cek1 signaling. Mol Microbiol. 2016;102(5):827-49. Epub 2016/09/03. doi: 10.1111/mmi.13494. PubMed PMID: 27589033.

3. Ballou ER, Avelar GM, Childers DS, Mackie J, Bain JM, Wagener J, et al. Lactate signalling regulates fungal beta-glucan masking and immune evasion. Nat Microbiol. 2016;2:16238. Epub 2016/12/13. doi: 10.1038/nmicrobiol.2016.238. PubMed PMID: 27941860; PubMed Central PMCID: PMCPMC5704895.

4. Borneman AR, Gianoulis TA, Zhang ZD, Yu H, Rozowsky J, Seringhaus MR, et al. Divergence of transcription factor binding sites across related yeast species. Science. 2007;317(5839):815-9. Epub 2007/08/11. doi: 10.1126/science.1140748. PubMed PMID: 17690298.

5. Yi S, Sahni N, Daniels KJ, Pujol C, Srikantha T, Soll DR. The same receptor, G protein, and mitogen-activated protein kinase pathway activate different downstream regulators in the alternative white and opaque pheromone responses of Candida albicans. Mol Biol Cell. 2008;19(3):957-70. Epub 2007/12/29. doi: 10.1091/mbc.e07-07-0688. PubMed PMID: 18162580; PubMed Central PMCID: PMCPMC2262975.

6. Sahni N, Yi S, Daniels KJ, Huang G, Srikantha T, Soll DR. Tec1 mediates the pheromone response of the white phenotype of Candida albicans: insights into the evolution of new signal transduction pathways. PLoS Biol. 2010;8(5):e1000363. Epub 2010/05/11. doi: 10.1371/journal.pbio.1000363. PubMed PMID: 20454615; PubMed Central PMCID: PMCPMC2864266.

7. Scaduto CM, Kabrawala S, Thomson GJ, Scheving W, Ly A, Anderson MZ, et al. Epigenetic control of pheromone MAPK signaling determines sexual fecundity in Candida albicans. Proc Natl Acad Sci U S A. 2017;114(52):13780-5. Epub 2017/12/20.

doi: 10.1073/pnas.1711141115. PubMed PMID: 29255038; PubMed Central PMCID: PMCPMC5748179.

8. Heredia MY, Ikeh MAC, Gunasekaran D, Conrad KA, Filimonava S, Marotta DH, et al. An expanded cell wall damage signaling network is comprised of the transcription factors Rlm1 and Sko1 in Candida albicans. PLoS Genet. 2020;16(7):e1008908. Epub 2020/07/09. doi: 10.1371/journal.pgen.1008908. PubMed PMID: 32639995; PubMed Central PMCID: PMCPMC7371209.

9. Shaw JA, Mol PC, Bowers B, Silverman SJ, Valdivieso MH, Duran A, et al. The function of chitin synthases 2 and 3 in the Saccharomyces cerevisiae cell cycle. J Cell Biol. 1991;114(1):111-23. Epub 1991/07/01. doi: 10.1083/jcb.114.1.111. PubMed PMID: 2050738; PubMed Central PMCID: PMCPMC2289062.

10. Cabib E, Arroyo J. How carbohydrates sculpt cells: chemical control of morphogenesis in the yeast cell wall. Nat Rev Microbiol. 2013;11(9):648-55. Epub 2013/08/21. doi: 10.1038/nrmicro3090. PubMed PMID: 23949603.

11. Badrane H, Nguyen MH, Blankenship JR, Cheng S, Hao B, Mitchell AP, et al. Rapid redistribution of phosphatidylinositol-(4,5)-bisphosphate and septins during the Candida albicans response to caspofungin. Antimicrob Agents Chemother. 2012;56(9):4614-24. Epub 2012/06/13. doi: 10.1128/AAC.00112-12. PubMed PMID: 22687514; PubMed Central PMCID: PMCPMC3421880.

12. Audhya A, Emr SD. Stt4 PI 4-kinase localizes to the plasma membrane and functions in the Pkc1-mediated MAP kinase cascade. Dev Cell. 2002;2(5):593-605. Epub 2002/05/23. doi: 10.1016/s1534-5807(02)00168-5. PubMed PMID: 12015967.

13. Chen T, Jackson JW, Tams RN, Davis SE, Sparer TE, Reynolds TB. Exposure of Candida albicans beta (1,3)-glucan is promoted by activation of the Cek1 pathway. PLoS Genet. 2019;15(1):e1007892. Epub 2019/02/01. doi: 10.1371/journal.pgen.1007892. PubMed PMID: 30703081; PubMed Central PMCID: PMCPMC6372213.

14. Walker LA, Munro CA, de Bruijn I, Lenardon MD, McKinnon A, Gow NA. Stimulation of chitin synthesis rescues Candida albicans from echinocandins. PLoS Pathog. 2008;4(4):e1000040. Epub 2008/04/05. doi: 10.1371/journal.ppat.1000040. PubMed PMID: 18389063; PubMed Central PMCID: PMCPMC2271054.

15. Lenardon MD, Munro CA, Gow NA. Chitin synthesis and fungal pathogenesis. Curr Opin Microbiol. 2010;13(4):416-23. Epub 2010/06/22. doi: 10.1016/j.mib.2010.05.002. PubMed PMID: 20561815; PubMed Central PMCID: PMCPMC2923753.

16. Munro CA, Selvaggini S, de Bruijn I, Walker L, Lenardon MD, Gerssen B, et al. The PKC, HOG and Ca2+ signalling pathways co-ordinately regulate chitin synthesis in Candida albicans. Mol Microbiol. 2007;63(5):1399-413. Epub 2007/02/17. doi: 10.1111/j.1365-2958.2007.05588.x. PubMed PMID: 17302816; PubMed Central PMCID: PMCPMC2649417.

17. Taylor PR, Brown GD, Reid DM, Willment JA, Martinez-Pomares L, Gordon S, et al. The beta-glucan receptor, dectin-1, is predominantly expressed on the surface of cells of the monocyte/macrophage and neutrophil lineages. J Immunol. 2002;169(7):3876-82. Epub 2002/09/24. doi: 10.4049/jimmunol.169.7.3876. PubMed PMID: 12244185.

18. Brown GD, Taylor PR, Reid DM, Willment JA, Williams DL, Martinez-Pomares L, et al. Dectin-1 is a major beta-glucan receptor on macrophages. J Exp Med. 2002;196(3):407-12. Epub 2002/08/07. doi: 10.1084/jem.20020470. PubMed PMID: 12163569; PubMed Central PMCID: PMCPMC2193936.

19. Brown GD, Gordon S. Immune recognition. A new receptor for beta-glucans. Nature. 2001;413(6851):36-7. Epub 2001/09/07. doi: 10.1038/35092620. PubMed PMID: 11544516.

20. Kennedy AD, Willment JA, Dorward DW, Williams DL, Brown GD, DeLeo FR. Dectin-1 promotes fungicidal activity of human neutrophils. Eur J Immunol. 2007;37(2):467-78. Epub 2007/01/19. doi: 10.1002/eji.200636653. PubMed PMID: 17230442.

21. Cohen-Kedar S, Baram L, Elad H, Brazowski E, Guzner-Gur H, Dotan I. Human intestinal epithelial cells respond to beta-glucans via Dectin-1 and Syk. Eur J Immunol. 2014;44(12):3729-40. Epub 2014/09/25. doi: 10.1002/eji.201444876. PubMed PMID: 25251945.

22. Gow NA, Netea MG, Munro CA, Ferwerda G, Bates S, Mora-Montes HM, et al. Immune recognition of Candida albicans beta-glucan by dectin-1. J Infect Dis. 2007;196(10):1565-71. Epub 2007/11/17. doi: 10.1086/523110. PubMed PMID: 18008237; PubMed Central PMCID: PMCPMC2655640.
23. Swidergall M, Solis NV, Wang Z, Phan QT, Marshall ME, Lionakis MS, et al. EphA2 Is a Neutrophil Receptor for Candida albicans that Stimulates Antifungal Activity during Oropharyngeal Infection. Cell Rep. 2019;28(2):423-33 e5. Epub 2019/07/11. doi: 10.1016/j.celrep.2019.06.020. PubMed PMID: 31291578; PubMed Central PMCID: PMCPMC6638578.
24. Swidergall M, Solis NV, Lionakis MS, Filler SG. EphA2 is an epithelial cell pattern recognition receptor for fungal beta-glucans. Nat Microbiol. 2018;3(1):53-61. Epub 2017/11/15. doi: 10.1038/s41564-017-0059-5. PubMed PMID: 29133884; PubMed Central PMCID: PMCPMC5736406.
25. van Bruggen R, Drewniak A, Jansen M, van Houdt M, Roos D, Chapel H, et al. Complement receptor 3, not Dectin-1, is the major receptor on human neutrophils for beta-glucan-bearing particles. Mol Immunol. 2009;47(2-3):575-81. Epub 2009/10/09. doi: 10.1016/j.molimm.2009.09.018. PubMed PMID: 19811837.
26. Li X, Utomo A, Cullere X, Choi MM, Milner DA, Jr., Venkatesh D, et al. The beta-glucan receptor Dectin-1 activates the integrin Mac-1 in neutrophils via Vav protein signaling to promote Candida albicans clearance. Cell Host Microbe. 2011;10(6):603-15. Epub 2011/12/20. doi: 10.1016/j.chom.2011.10.009. PubMed PMID: 22177564; PubMed Central PMCID: PMCPMC3244687.
27. Black CA, Eyers FM, Russell A, Dunkley ML, Clancy RL, Beagley KW. Acute neutropenia decreases inflammation associated with murine vaginal candidiasis but has no effect on the course of infection. Infect Immun. 1998;66(3):1273-5. Epub 1998/03/06. doi: 10.1128/IAI.66.3.1273-1275.1998. PubMed PMID: 9488427; PubMed Central PMCID: PMCPMC108047.
28. Peters BM, Palmer GE, Nash AK, Lilly EA, Fidel PL, Jr., Noverr MC. Fungal morphogenetic pathways are required for the hallmark inflammatory response during Candida albicans vaginitis. Infect Immun. 2014;82(2):532-43. Epub 2014/01/31. doi:

10.1128/IAI.01417-13. PubMed PMID: 24478069; PubMed Central PMCID: PMCPMC3911367.

29. Galan-Diez M, Arana DM, Serrano-Gomez D, Kremer L, Casasnovas JM, Ortega M, et al. Candida albicans beta-glucan exposure is controlled by the fungal CEK1-mediated mitogen-activated protein kinase pathway that modulates immune responses triggered through dectin-1. Infect Immun. 2010;78(4):1426-36. Epub 2010/01/27. doi: 10.1128/IAI.00989-09. PubMed PMID: 20100861; PubMed Central PMCID: PMCPMC2849429.

30. Thompson A, Davies LC, Liao CT, da Fonseca DM, Griffiths JS, Andrews R, et al. The protective effect of inflammatory monocytes during systemic C. albicans infection is dependent on collaboration between C-type lectin-like receptors. PLoS Pathog. 2019;15(6):e1007850. Epub 2019/06/27. doi: 10.1371/journal.ppat.1007850. PubMed PMID: 31242262; PubMed Central PMCID: PMCPMC6594653.

31. Qian Q, Jutila MA, Van Rooijen N, Cutler JE. Elimination of mouse splenic macrophages correlates with increased susceptibility to experimental disseminated candidiasis. J Immunol. 1994;152(10):5000-8. Epub 1994/05/15. PubMed PMID: 8176217.

32. Dominguez-Andres J, Feo-Lucas L, Minguito de la Escalera M, Gonzalez L, Lopez-Bravo M, Ardavin C. Inflammatory Ly6C(high) Monocytes Protect against Candidiasis through IL-15-Driven NK Cell/Neutrophil Activation. Immunity. 2017;46(6):1059-72 e4. Epub 2017/06/22. doi: 10.1016/j.immuni.2017.05.009. PubMed PMID: 28636955.

33. Ngo LY, Kasahara S, Kumasaka DK, Knoblaugh SE, Jhingran A, Hohl TM. Inflammatory monocytes mediate early and organ-specific innate defense during systemic candidiasis. J Infect Dis. 2014;209(1):109-19. Epub 2013/08/08. doi: 10.1093/infdis/jit413. PubMed PMID: 23922372; PubMed Central PMCID: PMCPMC3864383.

34. Shi C, Pamer EG. Monocyte recruitment during infection and inflammation. Nat Rev Immunol. 2011;11(11):762-74. Epub 2011/10/11. doi: 10.1038/nri3070. PubMed PMID: 21984070; PubMed Central PMCID: PMCPMC3947780.

35. MacDonald KP, Palmer JS, Cronau S, Seppanen E, Olver S, Raffelt NC, et al. An antibody against the colony-stimulating factor 1 receptor depletes the resident subset of monocytes and tissue- and tumor-associated macrophages but does not inhibit inflammation. Blood. 2010;116(19):3955-63. Epub 2010/08/05. doi: 10.1182/blood-2010-02-266296. PubMed PMID: 20682855.

36. Rojo R, Raper A, Ozdemir DD, Lefevre L, Grabert K, Wollscheid-Lengeling E, et al. Deletion of a Csf1r enhancer selectively impacts CSF1R expression and development of tissue macrophage populations. Nat Commun. 2019;10(1):3215. Epub 2019/07/22. doi: 10.1038/s41467-019-11053-8. PubMed PMID: 31324781; PubMed Central PMCID: PMCPMC6642117.

37. Arnold IC, Mathisen S, Schulthess J, Danne C, Hegazy AN, Powrie F. CD11c(+) monocyte/macrophages promote chronic Helicobacter hepaticus-induced intestinal inflammation through the production of IL-23. Mucosal Immunol. 2016;9(2):352-63. Epub 2015/08/06. doi: 10.1038/mi.2015.65. PubMed PMID: 26242598; PubMed Central PMCID: PMCPMC4650208.

38. Carrero JA, McCarthy DP, Ferris ST, Wan X, Hu H, Zinselmeyer BH, et al. Resident macrophages of pancreatic islets have a seminal role in the initiation of autoimmune diabetes of NOD mice. Proc Natl Acad Sci U S A. 2017;114(48):E10418-E27. Epub 2017/11/15. doi: 10.1073/pnas.1713543114. PubMed PMID: 29133420; PubMed Central PMCID: PMCPMC5715775.

39. Bauche D, Joyce-Shaikh B, Jain R, Grein J, Ku KS, Blumenschein WM, et al. LAG3(+) Regulatory T Cells Restrain Interleukin-23-Producing CX3CR1(+) Gut-Resident Macrophages during Group 3 Innate Lymphoid Cell-Driven Colitis. Immunity. 2018;49(2):342-52 e5. Epub 2018/08/12. doi: 10.1016/j.immuni.2018.07.007. PubMed PMID: 30097293.

40. Hashimoto D, Chow A, Noizat C, Teo P, Beasley MB, Leboeuf M, et al. Tissue-resident macrophages self-maintain locally throughout adult life with minimal contribution from circulating monocytes. Immunity. 2013;38(4):792-804. Epub 2013/04/23. doi: 10.1016/j.immuni.2013.04.004. PubMed PMID: 23601688; PubMed Central PMCID: PMCPMC3853406.

41. Netea MG, Joosten LA, van der Meer JW, Kullberg BJ, van de Veerdonk FL. Immune defence against Candida fungal infections. Nat Rev Immunol. 2015;15(10):630-42. Epub 2015/09/22. doi: 10.1038/nri3897. PubMed PMID: 26388329.

VITA

Andy Wagner was born in Bowling Green, OH to Mark and Amy Wagner. Andy spent most of his childhood pursuing sports and outdoor recreational activities, and his passion for nature is where his interest in the biological sciences started to form. After graduating from Perrysburg High School, Andy went on to attend Bowling Green State University (BGSU), where he became excited about science and lab work. After obtaining an B.S. in Biology from BGSU, Andy moved to Knoxville, TN. He started his Tennessee journey as a janitor in the Walters Life Science building at the University of Tennessee, Knoxville (UTK), where he was discovered after hours solving a previously considered impossible genetics problem known as the "Reynolds conundrum" that had been left on the board earlier that day. Upon this discovery, Andy was offered an acceptance letter to the UTK microbiology Ph.D. program. After discussing it, at length, with his best friend Ben Affleck, Andy accepted the offer and pursued his doctorate in Dr. Todd Reynolds lab.